The Neuronal Basis of Zebrafish Olfactory Imprinting: Evaluation of Activity Markers and Characterization of the Primary Olfactory System with Calcium-binding Protein Expression

Sigrid Kress

Dissertation

an der Fakultät für Biologie

der Ludwig - Maximilians - Universität München

München 2014

Diese Dissertation wurde angefertigt unter der Leitung von

PD Dr. Mario Wullimann in der Abteilung Neurobiologie der

Ludwig – Maximilians – Universität in München

1. Gutachter: PD Dr. Mario Wullimann

2. Gutachter: Prof. Dr. Benedikt Grothe

Mündliche Prüfung am 15.04.2014

Acknowledgements

The completion of my thesis was merely possible due to the invaluable help, advice and friendship of many people:

First, I would like to thank PD Dr. Mario Wullimann for being my doctoral advisor and the opportunity to work on my thesis in his research group. Dear Mario, thank you for our valuable discussions and good advice and for sharing your vast knowledge of the zebrafish brain. I would also like to thank you for your patience, encouragement and great support during the last years – and your swiss chocolate.

I would also like to thank Prof. Dr. Benedikt Grothe for being my secondary supervisor and his support during my doctoral thesis. I spent a wonderful time in the division of Neurobiology at the LMU. Thus, I would like to thank you for creating a great research environment and I am very happy that I had the opportunity to be a part of your group.

I thank GSN for funding they provided during parts of my doctoral thesis.

Especially, I would like to thank Bea Stiening and Dani Biechl for their practical assistance, knowledge, helpful suggestions and the great support during the last years.

Very special thanks to all of my dear colleagues from the division of Neurobiology. Many thanks for the great time in Munich.

Furthermore, I thank Prof. Dr. Gabriele Gerlach and Dr. Cornelia Hinz for their great support and helpful suggestions during my experimental work at the University of Oldenburg.

I would also like to thank Prof. Dr. Rainer Friedrich and Dr. Iori Namekawa, the two other members of our SPP tandem group, for their support and helpful suggestions during my doctoral thesis.

Special thanks to my twin sister Ulrika and my partner Stefan for giving me the best assistance and personal reflection. Thanks for your loving support.

Table of Contents

List of Figures and Tables

Figures:

Tables:

Abbreviations

A	axon
ac	anterior commissure
AP	area postrema
ATN	anterior tuberal nucleus
c	cilia
Cantd	commissura anterior, pars dorsalis
Cantv	commissura anterior, pars ventralis
CB(ir)	calbindin (immunoreactive)
CBP(s)	calcium binding protein(s)
CC	crista cerebellaris
CCe	corpus cerebelli
CeP	cerebellar plate (larvae)
Ch	chorda dorsalis (notochord)
CIL	central nucleus of hypothalamic inferior lobe
CM	corpus mamillare
CR(ir)	calretinin (immunoreactive)
CZ	central zone
D/d	dendrite
D	dorsal telencephalic area
Dc	central zone of dorsal telencephalic area
di	diencephalon
DIL	diffuse nucleus of hypothalamic inferior lobe
Dl	lateral zone of dorsal telencephalic area
Dm	medial zone of dorsal telencephalic area
Dp	posterior zone of dorsal telencephalic area
DT	dorsal thalamus (thalamus)
DZ	dorsal zone
EG	eminentia granularis
EmT	eminentia thalami
GC	griseum centrale
gl, Gl	glomerular layer of olfactory bulb
Glo	glomeruli
GPCR	G-protein-coupled receptor
H	hypothalamus
Ha	habenula
Had	dorsal habenular nucleus
Hav	ventral habenular nucleus
Hc	caudal zone of periventricular hypothalamus
Hd	dorsal zone of periventricular hypothalamus
Hv	ventral zone of periventricular hyypothalamus
Hy	hypophysis (pituitary)
icl	internal cellular layer of olfactory bulb
IRF	inferior reticular formation
LC	locus coeruleus
LCa	lobus caudalis cerebelli
lfb	lateral forebrain bundle
LG1-4	lateral glomeruli1 – 4 (larvae)

LOT	lateral olfactory tract
LVII	lobus facialis
LX	lobus vagus
m	microvilli
MC	mitral cell
mes	mesencephalon
MG1-4	medial glomeruli1 – 4 (larvae)
mlf	medial longitudinal fascicle
MO	medulla oblongata
MOE	main olfactory epithelium
MON	medial octavolateralis nucleus
MOS	main olfactory system
MOT	medial olfactory tract
N	region of the nucleus of medial longitudinal fascicle
OB	olfactory bulb
OC	otic capsule
oc	optic chiasma
OE	olfactory epithelium
OG	octaval ganglion
on	optic nerve
ON	olfactory nerve
OSN(s)	olfactory sensory neuron(s)
OR	olfactory receptor
P	pallium
pc	posterior commissure
PGZ	periventricular gray zone of optic tectum
PLLG	posterior lateral line ganglion
PM	magnocellular preoptic nucleus
Po	preoptic region
poc	postoptic commissure
PPa	anterior parvocellular preoptic nucleus
PPp	posterior parvocellular preoptic nucleus
PPr	periventricular pretectum (adult)
Pr	pretectum (larvae)
PR	posterior recess of diencephalic ventricle
PT	posterior tuberculum
PTd	dorsal part of posterior tuberculum
PTv	ventral part of posterior tuberculum
PTN	posterior tuberal nucleus
PVO	paraventricular organ
rhom	rhombencephalon
RMS	rostral migratory stream
S	subpallium
sc	spinal cord
SC	suprachiasmatic nucleus
SD	saccus dorsalis
Sd	dorsal division of subpallium (larvae)
SRF	superior reticular formation
Sv	ventral division of subpallium (larvae)
T	midbrain tegmentum
tel	telencephalon

TeO	optic tectum
TeVe	tectal ventricle
TG	trigeminal ganglion
TH	tyrosine hydroxylase
TLa	torus lateralis
TL(o)	torus longitudinalis
TN cells	terminal nerve cells
TPm	migrated nucleus of posterior tuberculum
TPp	periventricular nucleus of posterior tuberculum
TS	torus semicircularis
TSc	central nucleus of torus semicircularis
TVe	telencephalic ventricle
Va	valvula cerebelli
Val	lateral division of valvula cerebelli
Vam	medial division of valvula cerebelli
Vc	central nucleus of ventral telencephalic area
Vd	dorsal nucleus of ventral telencephalic area
Vl	lateral nucleus of ventral telencephalic area
VNO	vomeronasal organ
Vs	supracommissural nucleus of ventral telencephalic area
VT	ventral thalamus (prethalamus)
Vv	ventral nucleus of ventral telencephalic area

Abbreviations for identified glomeruli in adult zebrafish (adapted from Baier & Korsching, 1994)

a-e	dorsal – cluster – associated glomeruli 1 – 5
ap	anterior plexus
dc	glomeruli of the dorsal cluster
k	medial elongated glomerulus
l	glomerulus of the lateral chain 1
lc	lateral chain
m	glomerulus of the lateral chain 2
$mdpG_{1-2}$	mediodorsal posterior glomeruli 1 – 2
n	glomerulus of the lateral chain 3
p	glomerulus of the lateral chain 5
q	lateroventral posterior glomerulus
u-w	glomeruli of the ventral triplet 1 – 3
vpG	ventroposterior glomerulus

Abstract

The sense of smell is an important window for the perception of the environment in all vertebrates, including teleost fish such as the zebrafish. Using olfaction, fish detect compounds dissolved in the surrounding water and these odorants affect behaviours, involving feeding, reproduction, migration, predator avoidance and kin recognition. Although teleosts do not have a separate vomeronasal organ as most mammals do, the fish olfactory system is also able to detect pheromones and to mediate pheromone effects. For example, kin recognition in juvenile zebrafish, *Danio rerio*, is based on phenotype matching and larvae imprint on olfactory cues of the urinary odor on the 6th day of development. Kin recognition is used by zebrafish larvae for aggregating (shoaling) and by adult females for inbreeding avoidance.

My thesis focusses on the identification of zebrafish olfactory system structures involved in olfactory imprinting and, thus, kin recognition. I tried to mark neuronal activity in differently treated zebrafish larvae and adults in various olfactory test procedures. To this aim I used the Erk / MAPK (Mitogen – Activated Protein Kinase) signaling pathway and associated immediate early gene expression and as a target gene tyrosine hydroxylase. I visualized for the first time in the entire zebrafish larval and adult primary olfactory system the basal expression of the three activity markers *egr1*, *cfos* and pErk previously shown to be useful in mammals in similar experiments. Furthermore, I demonstrated activity dependent downregulation of *egr1*/TH expressing periglomerular olfactory bulb dopaminergic cells after ipsilateral deprivation. Additionally, I laid groundwork for continuing experiments using imprinted and non-imprinted larval and adult zebrafish to test for upregulation of activity markers (in particular pErk and *cfos*) after exposure to imprinting or kin cues (MHC peptides, kin water).

A second aim of my thesis is to provide new insight about differential olfactory zebrafish subsystems characterized by different calcium binding proteins (CBPs). My characterization of the zebrafish olfactory epithelium using CBP immunohistochemistry showed differential

expression of calretinin, calbindin1, parvalbumin and S100 in the three olfactory sensory neuronal cell types (OSNs). While calretinin and calbindin1 are predominantly, if not exclusively, expressed in adult ciliated OSNs, parvalbumin is expressed equally abundantly in microvillous and ciliated OSNs. Whereas these three CBPs are absent in crypt cells, S100 is strongly expressed in crypt cells and weakly in a subpopulation of microvillous cells. During larval development, calbindin1 and calretinin are also expressed in microvillous cells, but become increasingly restricted to ciliated cells in the adult. Primary projections of OSNs were also revealed in CBP immunohistochemistry and show calretinin/calbindin1 positive fibers in dorsolateral and ventrolateral glomeruli. Parvalbumin positive fibers are present in various additional mediodorsal, lateral and ventroposterior glomeruli, consistent with the expression of this CBP in microvillous cells in addition. Only one mediodorsal glomerulus ($mdpG_2$) exhibits S100 positive fibers, indicating that it contains all crypt cell plus the S100 positive microvillous OSN projections. The study of the temporal development of projections in larvae indicates a retardation of S100 positive projections compared to parvalbumin and a peak of crypt cell numbers around 6 dpf. Whether or not this correlation with the known imprinting process has a functional context must be further investigated.

1. Introduction

1.1. Zebrafish Imprint on Kin Through Olfactory Signals

Zebrafish (*Danio rerio*) are able to recognize their siblings using olfactory cues (Gerlach and Lysiak, 2006; Mann et al., 2003), that is, they can discern kin from non – kin. Larvae imprint on an olfactory template of their kin during a 24h time window from day 6 to day 7 post fertilization (Gerlach et al., 2008) and can later use this template to recognize even unfamiliar kin. Larvae prefer to associate with kin (Mann et al., 2003) and grow significantly more (33%) in kin groups (Gerlach et al., 2007). It has been supposed that improved growth rates in larvae or juvenile fish may correlate with increased fitness (Gerlach et al., 2007). Faster – growing larvae, especially females, reach sexual maturity earlier and thus show increased levels of reproductive output (Gerlach et al., 2007). The preference for kin changes with sexual maturity (Gerlach and Lysiak, 2006). Adult females prefer the odor of unfamiliar, unrelated males to that of unfamiliar brothers, indicating inbreeding avoidance, whereas adult males show no preference for the odor of related or unrelated females (Gerlach and Lysiak, 2006).

Several mechanisms of kin recognition have been identified (Tang-Martinez, 2001) and in zebrafish kin recognition is based on phenotype matching of olfactory cues which is caused by imprinted effects on urinary odor during development (Gerlach and Lysiak, 2006). This sensitive imprinting phase on 6 days post fertilization (dpf) is necessary but not sufficient (see below) for imprinting (Gerlach et al., 2008). It has been demonstrated that larvae exposed to kin odor before or after - but not on 6 dpf - did not recognize kin (Gerlach et al., 2008). Gerlach and colleagues supposed that imprinting may be delayed by an inability to receive the signal until specific olfactory receptors are expressed at 6 dpf or the signal itself is not released before 6 dpf (Gerlach et al., 2008). Additionally, there is no kin recognition through self – matching revealed by larvae that were isolated from all contact with conspecifics, and which did not imprint on their own chemical cues (Gerlach et al., 2008).

Furthermore exposure to non – kin odor during the imprinting phase did not result in imprinting on the odor cues of unrelated individuals (Gerlach et al., 2008). Thus a genetic predisposition to kin odor in zebrafish has been presumed (Gerlach et al., 2008). Gerlach and colleagues hypothesized that the chemical cue (ligand) involved in olfactory imprinting process has to closely match the receptor system of the recipient and suggested a genetic component similar to the innate immune system where cell – cell recognition and rejection of non – self ligands are based on the similarity of the major histocompatibility complex (MHC) – derived surface proteins (Gerlach et al., 2008).

Due to its immunological function of self / non – self discrimination MHC has been recognized as a possible source of individual specific body odors (Ferstl et al., 1998) and thus, MHC peptides are excellent candidates for social recognition signals that convey information about genetic individuality (Leinders-Zufall et al., 2004). It is assumed that MHC molecules as transmembrane molecules are shed from the cell surface and appear in body fluids such as sweat and urine (Gerlach et al., 2008). In mammals these molecules can be assessed via the olfactory system and are used as signals of genetic relatedness and health (Leinders-Zufall et al., 2004). In zebrafish it has been revealed that imprinting on olfactory signals depends on MHC class II similarity and only larvae that share MHC class II alleles can imprint on each other (Hinz et al., 2012).

Most recent studies revealed that kin recognition in zebrafish depends in fact on a two – step imprinting process involving olfactory as well as visual cues of kin (Hinz et al., 2013). It has been demonstrated in detailed flume choice tests that larvae have to perceive visual cues of kin on 5 dpf and olfactory cues of kin on 6 dpf (Hinz et al., 2013). Zebrafish larvae differ in their visual appearance, such as body and iris pigmentation as well as morphometry, according to their relatedness. and 5 days old larvae are able to recognize those fine differences (Hinz et al., 2012). Moreover larvae do not imprint on visual cues of non – kin and thus they can visually differentiate between kin and non – kin during the visual imprinting phase (Hinz et al., 2012). Furthermore, zebrafish larvae that share the same MHC class II alleles share a more similar morphometry

and iris pigmentation than those did not share the alleles (Hinz et al., 2012). Thus, Gerlach and colleagues revealed in zebrafish larvae that MHC genes do not only influence the chemical signature but also the visual appearance and proposed a possible basis for predisposition for the visual cues of kin (Hinz et al., 2012).

Thus, olfactory or visual cues alone are not sufficient for successful imprinting and through this combined, two – step imprinting process larvae can avoid false imprinting on unrelated individuals (Hinz et al., 2013). Therefore zebrafish have evolved a very effective method to discriminate even unfamiliar kin from non – kin (Hinz et al., 2013). However, the present thesis has been undertaken in order to elucidate only the involvement of olfactory neural structures in zebrafish imprinting.

1.2. Olfaction: Overview

The olfactory system is an important window for perception of the environment. It is important for interaction of an organism with its surrounding world, because it detects and discriminates among a large number of structurally different odor molecules that carry information about the environment (Menini et al., 2004). These odorous cues significantly contribute to the identification and evaluation of food, predators, territories and reproductive partners (Breer, 2001) and therefore they are clearly important for animal survival.

The olfactory system enables an organism to detect and discriminate between thousands of odorous molecules. The odorants are classified into two major categories, on the one hand general odors, which signal potential food and environmental warnings and on the other hand pheromones, which signal social or sexual status among individuals of the same species (Ma, 2012).

An odorant is a volatile chemical compound with a molecular weight of lower than ~300 Daltons, which can vary in size, shape and functional groups, and the detection of an odorant leads to perception of smells (Touhara and Vosshall, 2009). Odorants include various alcohols, ketones, acids, esters and aldehydes; organic chemicals with aromatic, alicyclic, polycyclic or heterocyclic ring structures; and a lot of substituted chemicals

of each of these types, as well as combinations of them (Gaillard et al., 2004). Natural odors often comprise complex mixtures of odorants and odor clusters can be defined qualitatively (e.g. from aromatic to minty to spearmint) or quantitatively (e.g. concentration changes) (Laurent, 2002).

In contrast to general odorants, pheromones often do not lead to perception of smells and they range from small organic molecules to large peptides (Touhara and Vosshall, 2009). Pheromones are used by most species, from bacteria (e.g. “quorum sensing”, i.e. chemical determination of population density) to mammals and the study of chemical communication within insect societies has revealed the complexity of pheromone – evoked behavioral responses (Dulac and Torello, 2003). Thus, all vertebrate taxa use pheromones, but the evidence in birds is still somewhat circumstantial (Eisthen and Wyatt, 2006). Pheromones can elicit stereotyped behaviors or endocrinological changes in the conspecific receivers in vertebrates and different pheromone effects can be provoked by urine or other bodily secretions (Buck, 2000). Pheromones are divided into their function as primer and releaser. Primers produce physiological effects in receivers over time, for instance, by stimulating the release of hormones that in turn affect the endocrine system of the receiver (Bradbury and Vehrencamp, 2011). In contrast, releasers produce immediate effects on the behavior of the receiver.

An example for pheromone effects in rodents is the Bruce Effect. This effect is also known as the pregnancy block effect, where exposure of newly mated female mice to males, different from the mating partner, causes a high rate of pregnancy failure (Brennan and Keverne, 1997). The Bruce Effect is mediated by pheromones and presumably coupled with the detection of “individuality cues” that result from genetic variation within a species, like different MHC loci (Buck, 2000).

However, the distinction between odorants and pheromones is sometimes ambiguous since some compounds can serve as both pheromones and odorants (Ma, 2012).

In terrestrial vertebrates, odorants and pheromones have traditionally been considered to be detected by two functionally and anatomically distinct olfactory systems and processed through two

anatomically segregated neural pathways: The main olfactory system (MOS) with the main olfactory epithelium (MOE) lining the nasal cavity deals with general environmental odors whereas pheromone signaling is characterized by the vomeronasal system (VNS) which includes a special chemosensory organ, the vomeronasal organ (VNO) at the base of the nasal cavity (Dulac and Torello, 2003; Eisthen, 1992; Halpern, 1987). The VNS is a tetrapod – specific accessory olfactory system that is present in most mammals, amphibians and reptiles (Grus and Zhang, 2006). In terrestrial environments, chemical cues can be volatile or non – volatile. The volatile cues are perceived by the MOS and non – volatile pheromones are mostly processed by the VNS (Dulac and Torello, 2003). Therefore, the VNS is used for nasal chemoreception, but in its size and evolutionary origin it is secondary to the MOS (Grus and Zhang, 2006). In the MOS, odorants are carried by the airstream, making it more suitable for detection of volatile compounds, whereas in the VNO there is a large influx of mucus into the organ carrying with it the non – volatile pheromonal components (Brennan and Keverne, 1997). It is commonly believed, that the flehmen behavior of many mammals, especially felids and ungulates, is a performance to transfer fluid – borne chemical stimuli, such as sex pheromones, from the oral cavity into the VNO (Doving and Trotier, 1998). After the physical contact with a conspecific or with scents emanating from its excrements (urine or feces), animals lift the head, draw back their lips, and push the tongue towards the anterior region of the palate, which allow a faster transfer of pheromones into the VNO (Tirindelli et al., 2009). The vomeronasal organ (VNO) is a blind – ending epithelial tube found bilaterally at the base of the nasal septum in most mammals (Doving and Trotier, 1998). It is blind posteriorly, and depending on the species, opens anteriorly into the nasal cavity or the oral cavity to permit entry of non – volatile chemical cues after direct physical contact of the snout with pheromone sources (Dulac and Torello, 2003).

However, although predominantly pheromones are detected via the vomeronasal system, this system also responds to some chemicals that are not pheromones, and on the other hand some pheromone effects are mediated by the main olfactory system (Baxi et al., 2006; Eisthen, 1997;

Eisthen and Wyatt, 2006). Therefore, the two systems are not absolutely different in this respect because, apparently it cannot be argued that the MOS is merely used to detect environmental chemical cues while the VNS is a terrestrial adaptation for detecting volatile pheromones (Grus and Zhang, 2006). For example, in rabbits, a pheromone produced on the ventrum of lactating rabbits provokes a highly specific and stereotyped nipple search behaviour in young rabbit pups that enables them to locate the nipples during suckling. Lesioning the VNO does not disrupt the pheromonal effects, which are, thus, mediated by the main olfactory system (Brennan, 2001). One hypothesis suggests, that the VNS responds to non – volatile molecules that are too large to reach the dorsally located olfactory epithelium, and that the olfactory system detects lighter, more volatile molecules (Eisthen and Wyatt, 2006). Another hypothesis is that the VNS mediates unlearned responses to odorants, and that the olfactory system mediates learned responses (Eisthen and Wyatt, 2006). However, either the hypotheses have been hard to test in part because it is not enough known about how chemical stimuli move around and gain access to the separated organs or the hypotheses have received little experimental attention (Eisthen and Wyatt, 2006). In addition to pheromones, vertebrates have individual or ‘fingerprint odors’ that reflect genetic factors, such as the MHC type, as well as hormonal state, diet and bacterial flora (Eisthen and Wyatt, 2006).

The processes of odor detection and pheromonal chemical communication in vertebrates depend on the nature of the environment. Accordingly, separate olfactory and vomeronasal systems are present only in tetrapod vertebrates living in terrestrial environments. A VNS is absent in fish, crocodilians, marine turtles and exclusively marine mammals including porpoises, dolphins, whales and manatees, but present in most terrestrial mammals, amphibia and reptiles (Brennan, 2001; Doving and Trotier, 1998; Eisthen and Wyatt, 2006). It is suggested, that chemical communication using the vomeronasal organ is of little use in the marine environment. It would also appear that the VNS is of little use for airborne vertebrates and, accordingly, the VNS it is absent in birds and many bats (Brennan, 2001). In aquatic environment, the odorants are waterborne

and, thus, maybe easier to employ and less susceptible to non - receptor - mediated interactions than airborne stimuli which may bypass the receptor and thereby directly activate second messengers (Korsching et al., 1997a). However, it could be shown that a VNS develops during the aquatic larval stage of amphibians and it was, thus, hypothesized that the VNS is apparently important in both aquatic and terrestrial stages in amphibians (Eisthen, 1992; Grus and Zhang, 2006).

Moreover, it was shown that teleost fish can detect and discriminate several structurally different classes of odorants, such as amino acids, nucleotides, bile acids, and hormones like gonadal steroids and prostaglandins (Sorensen and Caprio, 1998; Hansen et al, 2003, Sorensen and Sato, 2005). Odorants play different roles in fish behavior involving feeding, migration, predator avoidance, reproduction and kin recognition (Laberge & Hara, 2001). Therefore, although teleost fish lack a morphologically separate VNS and display only a main olfactory epithelium, different classes of odorants activate different behavioral and physiological responses. For example, amino acids and nucleotides trigger arousal and feeding behaviors, whereas, prostaglandins, steroids and possibly bile acids elicit unique social behaviors and / or endocrine responses (Sorensen and Caprio, 1998). Previous studies in the goldfish, *Carassius auratus*, showed that an oocyte maturation – inducing steroid (MIS), released by female goldfish, induced in males strong behavioral and endocrinological (i.e., pheromonal) effects (Stacey and Sorensen, 2005). In zebrafish the females can use waterborne pheromones to suppress reproduction by other females and male pheromones stimulate female reproduction (Gerlach, 2006). Therefore, the olfactory system of teleost is able to detect pheromones and to mediate pheromone effects.

These and other studies allowed rejecting the hypothesis that a functional VNS emerged as a terrestrial adaptation was rejected (Eisthen, 1992; Grus and Zhang, 2006), and it was hypothesized that a precursor system exists in teleost fish (Grus and Zhang, 2006). A morphologically separate VNS is absent in fishes, but despite this, teleost homologs of VNS – specific genes have been identified and therefore, it has been

suggested that the VNS – specific signal transduction pathway existed in the common ancestor of teleosts and tetrapods (Grus and Zhang, 2006).

1.3. Primary Olfactory Pathway and Signal Transduction

Olfaction begins with the transduction of information carried by odor molecules into electrical signals in the olfactory sensory neurons (OSNs). The bipolar OSNs possess a thin and long axon and a relatively short and thick dendrite with either microvilli or cilia, which contain receptors and associated signal transduction cascades (Ma, 2012). The OSNs send their axons to the olfactory bulb (OB), the first relay station for odor processing in the brain (Friedrich and Korsching, 1997b). Olfactory transduction and neural processing in the primary olfactory pathway involve basic mechanisms that are universal across most species in most phyla (Hildebrand and Shepherd, 1997). The organization of the primary olfactory pathway is similar for all animals, vertebrates and invertebrates, with modifications between divergent species (Farbman, 1994). Thus, olfaction occurs when an odor molecule binds to an odorant receptor in the microvilli or cilia of OSN dendrites whose axons forward the information to the brain.

Chemosensory signal transduction in the olfactory sensory neurons (OSNs) is distinct from that in vomeronasal sensory neurons (VSNs), because it was shown, that major components of the signal transduction cascade in OSNs are not expressed by VSNs (Berghard and Buck, 1996). Futhermore, the principle that different transduction cascades involving G - protein coupled receptors (GPCRs) are utilized by microvillous VSNs and ciliated OSNs appears to be conserved through much of vertebrate evolution (Hansen et al., 2004).

Upon olfactory transduction in the cilia of the OSNs, the binding of an odorant to an olfactory receptor (OR) converts the G protein α – subunit, $G\alpha_{olf}$, from GDP – bound state to a GTP – bound state. The $G\alpha_{olf}$ in turn activates adenylyl cyclase type III (ACIII). ACIII catalyzes the conversion of ATP to cyclic AMP (cAMP) and pyrophosphate. The second messenger cAMP opens the cyclic nucleotide – gated Na^+/Ca^+ channels (CNC) and then the CNC channel, together with the chloride (Cl^-) channels, induces

the depolarization of membrane potentials (Imai and Sakano, 2008; Mombaerts, 2004).

In cilia of OSNs of the MOE three channel subunits are expressed including the olfactory – specific cyclic nucleotide – gated channel subunits 1 (CNC1) and 2 (CNC2), as well as an olfactory – specific splice variant of the rod photoreceptor *β* subunit (Baker et al., 1999; Liman and Buck, 1994).

In microvilli of VSNs the binding of a pheromone or an odorant to a GPCR activates the G – protein subunits $G\alpha_o$ or $G\alpha_i$ which leads to a signal transduction cascade. This G protein activation by vomeronasal GPCRs triggers a phospholipase C – dependent cascade, which in turn directly activates either the transient receptor potential channel C2 (TRPC2) or another associated conductance (Dulac and Torello, 2003). Phospholipase C activity results in the cleavage of the phospholipid phosphatidylinositol - 4,5 - bisphosphate (PIP_2), leading to an increase in the intracellular concentrations of the second messengers inositol trisphosphate (IP3) and diacylglycerol DAG, both of which have been implicated in TRPC activation (Dulac and Torello, 2003; Harteneck et al., 2000). The DAG gates TRPC2 channels, whereas IP3 may a play a role in stimulating the release of calcium from the endoplasmic reticulum store (Lucas et al., 2003).

Thus, unlike ciliated OSNs, microvillous VSNs do not express cAMP and CNCs, but apparently IP3 and DAG are involved in the transduction process (Doving and Trotier, 1998; Rodriguez and Boehm, 2008; Spehr et al., 2002) as well as a DAG – activated cation channel, which partially depends on the TRPC2, a VNO – specific member of the transient receptor potential family of calcium channels (Lucas et al., 2003; Rodriguez and Boehm, 2008; Zufall, 2005).

Functionally interesting is that electrophysiological responses to urine and pheromones are strongly reduced in *Trp2* – knockout mice, which also show corresponding abnormal behaviour (Leypold et al., 2002; Mombaerts, 2004; Stowers et al., 2002).

Within the VNO, there are two GPCR types: the V1Rs are coexpressed with the G protein $G\alpha_{i2}$ in the apical zone of the VNO and the

V2Rs are coexpressed with the G protein $G\alpha_o$ in the basal zone of the VNO (Halpern et al., 1995; Thompson et al., 2006). Several studies have shown that there are three G proteins on the microvillar surface of the VNO, $G\alpha_{i2}$, $G\alpha_o$ and $G\alpha_{q/11}$, and that these G proteins mediate increase of IP3 (Berghard and Buck, 1996; Luo et al., 1994). The functions of $G\alpha_o$ seem to be inhibition of neuronal calcium channels (Linder et al., 1990; Thompson et al., 2006) and activation of potassium channels (Van Dongen et al, 1988; reviewed in Thompson et al, 2006), whereas $G\alpha_q$ and $G\alpha_{11}$ ($G\alpha_{q/11}$) activate phospholipase C (Taylor et al., 1991; Thompson et al., 2006).

In addition, it was demonstrated in the VNO, that the V2R pheromone receptors are functionally associated with the M10 and M1 families of non – classical MHC molecules, and β2 – microglobulin (β2m), a component of MHC class I molecules (Dulac and Torello, 2003; Loconto et al., 2003). M10, V2R and β2m form a multimolecular complex that is localized to the dendritic tips of VNO neurons at the site of pheromone detection and thus M10 might be involved either in receptor localization or more directly in the process of pheromone detection (Dulac and Torello, 2003; Loconto et al., 2003). MHC molecules play an important role in the immune system by presenting intracellular peptides to T cells and furthermore their function in neuronal networks was shown, where they are involved in plasticity and development (Huh et al., 2000; Rodriguez and Boehm, 2008). Apparently, MHC molecules are also involved in olfaction (Boehm and Zufall, 2006; Chamero et al., 2012; Leinders-Zufall et al., 2009). In conclusion, mammals use two different transduction pathways in ciliated OSNs and microvillous VSNs. As will be discussed below, teleosts, such as the zebrafish, do not have a VNO separate from an MOE, but they do have ciliated and microvillous sensory neurons in a unified olfactory epithelium the two types of sensory neurons share molecular similarities regarding their transduction pathways with corresponding sensory neurons in mammals (see below).

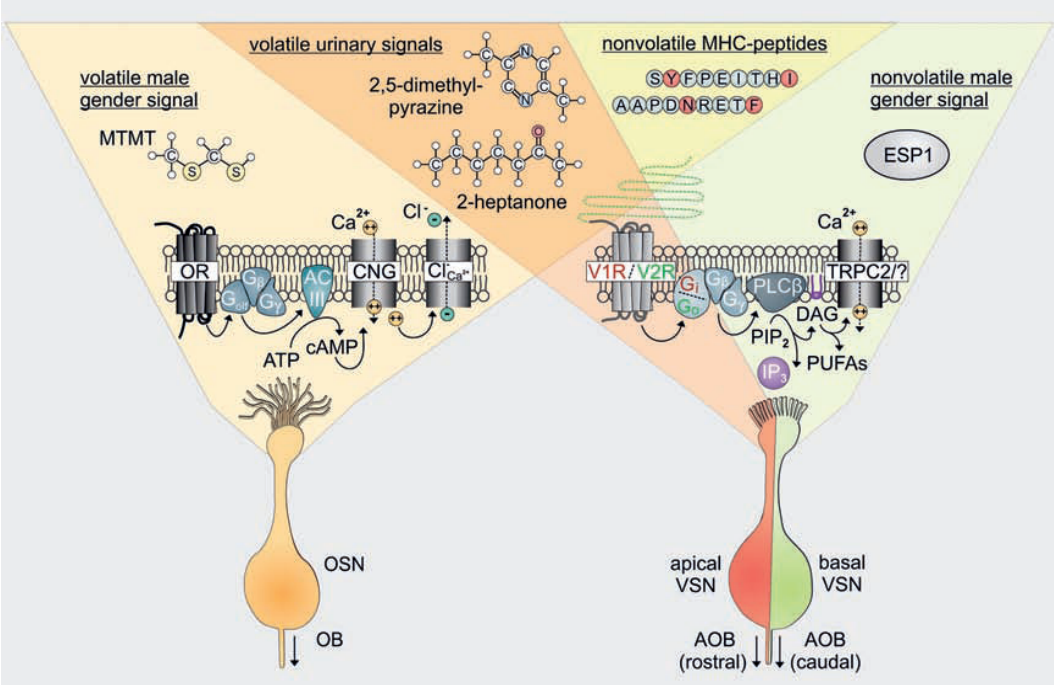

Fig.1. Signal transduction pathways. Left: ciliated OSNs of mammalian main olfactory epithelium, right: apical and basal microvillous OSNs of vomeronasal organ (see text for details). Note that various chemicals are known to bind to receptors of both ciliated and microvillous OSNs (from Spehr et al., 2006).

1.4. Olfactory Epithelia

1.4.1. Olfactory Epithelia in Mammals

In mammals, the MOE covers cartilaginous lamellae, called turbinates, in the posterior nasal cavity, comprising a few million OSNs (Breer et al., 2006). The MOE was subdivided in four OSN zones of equal surface area expressing different ORs (Gaillard et al., 2004), but recent studies demonstrated that OSNs expressing particular ORs are rather organized in overlapping zonal positions which are continuously arrayed along the central to peripheral axis of the MOE (Breer et al., 2006; Iwema et al., 2004; Miyamichi et al., 2005; Murthy, 2011) (see Fig. 2).

Moreover, topographic expression patterns for defined groups of receptor types, demonstrated by cells expressing the same OR, appear to be randomly distributed within a designated area, but, concerning their projection into the bulb, they can be grouped into a medial and a lateral subpopulation, which converge separately onto medial and lateral glomeruli, respectively (Breer et al., 2006; Levai et al., 2003; Mori and Sakano, 2011; Schoenfeld et al., 1994) (see Fig. 3). The ORs expressed in the dorsal MOE zone (DI domain) include all of the phylogenetically

class I receptors that are most related to those found in aquatic vertebrates, such as fish and amphibians (Breer et al., 2006; Freitag et al., 1995), and which are expected to be particularly tuned to hydrophilic odorants (Breer et al., 2006; Mezler et al., 2001). As the airflow will first approach the dorsal region containing fish – like class I receptors, this area will preferentially encounter the most adsorptive hydrophilic odorous compounds (Breer et al., 2006). Recent studies suggest that this arrangement may match the OR types with the physicochemical features of the odorants (stability, volatility and water solubility) that each region tends to encounter during odor sampling (Kent et al., 1996; Ma, 2012). Thus, the disproportional expression of distinct OR types along the inspiratory airstream may have functional implications for efficiently matching the physicochemical features of odor molecules and the relevant receptor types (Breer et al., 2006).

The epithelium consists of a limited number of cell types and the cell somata are arranged in a roughly laminar pattern (Schwob, 2002). From the apical surface to the basal lamina, they are mature and immature OSNs, globose and horizontal basal cells and Bowman's glands extend from the lamina propria through the epithelium to discharge contents at the apical surface (Schwob, 2002). Furthermore, glia – like supporting cells provide metabolic and physical support in the olfactory epithelium (Ma, 2012). The mature OSNs in the MOE are bipolar neurons with a single dendrite that ends in a knob – like swelling from which project some 20–30 very fine cilia (Firestein, 2001) into the nasal cavity and a central projection axon. OSNs express the olfactory marker protein (OMP) (Schwob, 2002).

The basal cells are a type of stem cells and undergo continuous division and differentiation to replace OSNs and supporting cells throughout life or after injury (Schwob, 2002). The destruction and reconstruction of the epithelium was demonstrated after irrigation with toxic zinc sulfate (ZnSO4) (Schwob, 2002; Thompson et al., 2000). The small basal cells with their large oval or round nuclei, lie between the basal parts of the supporting cells and the axons of the receptor cells adjacent to the basal lamina (Schwob, 2002).

Vertebrate OSN have a short lifetime (30 – 90 days) and are continually replaced from the basal cells. One function for this ongoing neurogenesis is to replace cells that have been damaged by toxic dust or external pathogens (Bradbury and Vehrencamp, 2011).

The second major chemosensory organ in rodents, the VNO, is separated into apical and basal compartments expressing two classes of vomeronasal receptors V1Rs and V2Rs, respectively (Dulac and Torello, 2003). Each bipolar vomeronasal sensory neuron (VSN) extends a single apical dendrite towards the vomeronasal cavity covered by microvilli, not cilia, which are bathed in fluid that is secreted by the vomeronasal glands at the dorsal and ventral tips of the lumen (Dulac and Torello, 2003).

Like OSNs in the MOE, the VSNs have a limited life span and are continually being replaced from basal stem cells. These new neurons are particularly concentrated at the margins of the receptor epithelium where it borders the sensory epithelium (Weiler et al., 1999).

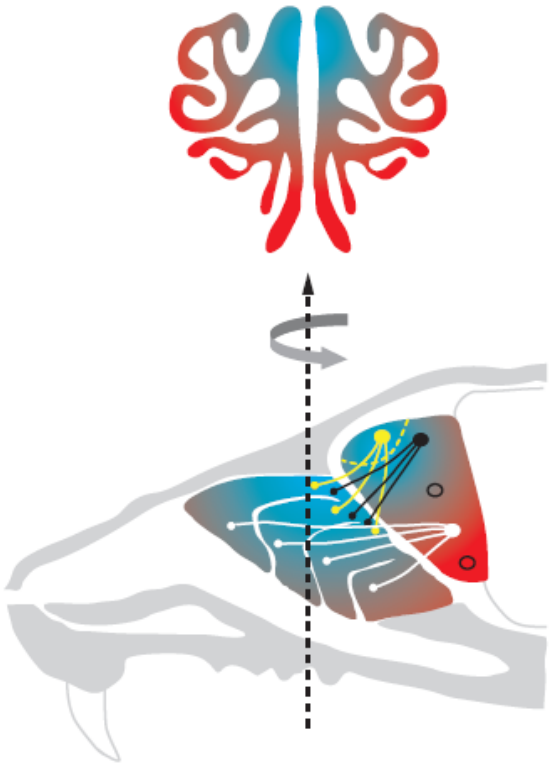

Fig. 2. Olfactory receptor expression in OSNs and converging projection to olfactory bulb glomeruli (adapted from Murthy, 2011).

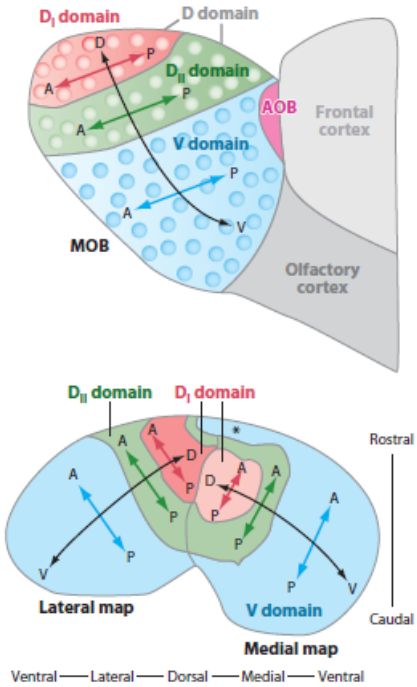

Fig. 3. Lateral (B) and dorsal view (C) of one unrolled olfactory bulb (adapted from Mori & Sakano 2011).

In addition to the MOE and VNO, there are two small chemosensory organs in the nasal cavity, i.e., the Grüneberg Ganglion (containing V2R and TAAR expressing OSNs) and the septal organ (containing OR and GD-D expressing OSNs) (Fleischer et al., 2006).

1.4.2. Olfactory Epithelium in Teleosts

In most teleosts, such as the zebrafish, the nostrils of the paired olfactory organ lie on the dorsal side of the head close to the eyes and the mouth and water enters the nasal cavity through an inlet and exits through a posterior outlet (Hansen and Zeiske, 1998). The rosette - shaped olfactory organs are bilaterally symmetric covered by sensory and non – sensory epithelium (Hansen and Zielinski, 2005). The sensory epithelium is a pseudostratified, columnar epithelium and quite thin (4 - 5 cells thick), and the nonsensory epithelium is columnar (Byrd and Brunjes, 1995). The morphology of the rosette and the number of lamellae vary interspecifically (Laberge and Hara, 2001b). In zebrafish, the old animals (2 - 2.5 years) have a total of 19 - 21 lamellae and younger animals 12 -15 lamellae (Hansen and Zeiske, 1998). Thus, 6 – 12 lamellae ascend from the bottom of a median raphe on each side of an olfactory organ (Byrd and Brunjes, 1995; Korsching et al., 1997a). The central part of each lamella contains the sensory epithelium which extends over the ridge onto both sides (see Fig. 4). The sensory epithelium on each lamella is surrounded by a non – sensory epithelium with kinocilia that ensure adequate movements of mucus or water through the nose (Hansen and Zielinski, 2005; Korsching et al., 1997a; Zeiske et al., 1992). The cilia are long, regular, and dense, but sometimes patchy (Weth et al., 1996). These special types of ciliated cells in the non – sensory part of the epithelium are present in all teleosts (Hansen and Zeiske, 1998; Hansen and Zielinski, 2005). In some species these cells are only present in the non – sensory part of the epithelium, whereas in other species, as in goldfish, these cells are also scattered across the sensory areas (Hansen and Zielinski, 2005; Hansen et al., 1999).

The olfactory epithelium in fish is organized far simpler than that of mammals (Ngai et al., 1993), as it is less well stratified than that of

mammals (Korsching et al., 1997a). Furthermore, teleosts are equipped with only one olfactory organ (not divided into MOE and VNO). However, this epithelium consists of the two distinct types of OSNs also seen in mammals (microvillous and ciliated OSNs; see Fig. 4), supporting cells and small, roundish basal cells. As a special feature, a third type of OSNs was found in fish which is absent in mammals. These crypt cells contain microvilli and cilia and comprise only a minor population in the OE (Hansen et al., 2004; Hansen and Zeiske, 1998; Sato et al., 2005). Crypt cells are present already in cartilaginous fish, primitive bony fish (e.g., skate, sturgeon) and also many modern teleost fish species (e.g. zebrafish) (Hansen and Zielinski, 2005). Based on their morphology the identification of the crypt cells is quite feasible, because they have a typical ovoid shape, rounded apical pole and an eccentric basal nucleus (Braubach et al., 2012) and they are located in the upper third of the olfactory epithelium (Hansen and Zielinski, 2005). The microvillous OSNs with short and relatively thick dendrites are located in the superficial to intermediate layers of the OE (Hansen and Zielinski, 2005), whereas the ciliated OSNs with long dendrites are situated in the deep layer of the OE (Sato et al., 2005; see Fig. 4).

Ciliated and microvillous OSN cell bodies are spindle-shaped and their dendrite ends apically in a so – called olfactory knob from which either cilia or microvilli extend into the lumen of the nasal cavity (Hansen and Zielinski, 2005). Ciliated OSNs have a pronounced olfactory knob, which projects into the lumen of the olfactory cavity and bears 3 – 7 cilia whereas the olfactory knobs of the microvillous OSNs are less pronounced than those of the ciliated OSNs and bear 10 to 30 short microvilli (Hansen and Zeiske, 1998). The crypt cells have no olfactory knob but bear microvilli as well as submerged cilia at their apical end. Crypt cell bodies are egg – shaped and appear only in the upper quarter of the epithelium (Hansen and Zeiske, 1998). Therefore, although the morphologically distinct types of OSNs are not distributed in differential patterns within the whole OE (Hansen and Zeiske, 1998), they are easily distinguishable by overall morphology and relative basal to apical position in the OE (Hansen et al., 2004). The total number of OSNs per epithelium is about 40,000

(Barth et al., 1996), and the receptor neuron somata measure about 5 X 10 µm (reviewed in Korsching et al., 1997a).

The supporting cells are more or less cylindrical and their apical surface has small irregular protrusions that reach into the lumen and separate the dendrites of the OSNs (Hansen and Zeiske, 1998). They are restricted to the sensory areas of the olfactory cavity (Hansen and Zielinski, 2005). In contrast to supporting cells in mammals, the nuclei of supporting cells in all fish are located beneath the layer of OSNs nuclei and are less electron – dense (Zeiske et al., 1992; reviewed in Hansen and Zielinski, 2005).

The small basal cells (stem cells) lie basal between the cell bodies of the supporting cells and the axons of the OSNs and have the same regenerative function as in mammals. Basal cells are small cells of different shape and their nuclei are large in relation to their cell size (Hansen and Zielinski, 2005). There is no distinction between globose and horizontal basal cells as in mammals (Hansen and Zielinski, 2005).

Additionally, Bowman's glands, the mucous secreting glands present beneath the epithelium in most mammals, are lacking, but numerous goblet cells, which fulfill the same role, are scattered throughout the epithelium (Byrd and Brunjes, 1995). Goblet cells are restricted to the non – sensory areas and they are surrounded by ciliated non – sensory cells or epidermal cells bearing microridges (Hansen and Zeiske, 1998). Mature goblet cells secrete large granules into the lumen of the olfactory cavity (Hansen and Zeiske, 1998).

Furthermore the teleost olfactory epithelium contains rodlet cells. These cells have a thick cuticula – like wall and are filled with abundant electron – lucent vesicles (Hansen and Zeiske, 1998). Rodlet cells are most probably parasitic organisms rather than part of the fish olfactory epithelium (Hansen and Zielinski, 2005).

As discussed above, the expression of ORs is overlapping, but not random. In goldfish and catfish, the OR gene expression patterns has first been interpreted to be random (Cao et al., 1998; Laberge and Hara, 2001a; Ngai et al., 1993). However, analysis of 10 very divergent OR molecules in the zebrafish and an exact comparison of four of those

regarding their spatial expression patterns revealed different concentric rings with some overlap within the entire epithelium in very sparse cell populations (Weth et al., 1996). Thus, the OR genes in fish are not entirely randomly expressed, although they occur in spatial expression domains that are broader and overlap more than the mammalian expression zones (Korsching, 2008).

In conclusion, differing from the situation in mammals, the fish OE contains three, not two, different types of OSNs (ciliated and microvillous OSNs and crypt cells) and these three types of OSNs are intermingled in one epithelium (Hansen and Zeiske, 1998). As discussed above, these teleost ONSs are characterized by different receptor molecules G protein *α* – subunits and second messenger activation (Hansen and Zielinski, 2005).

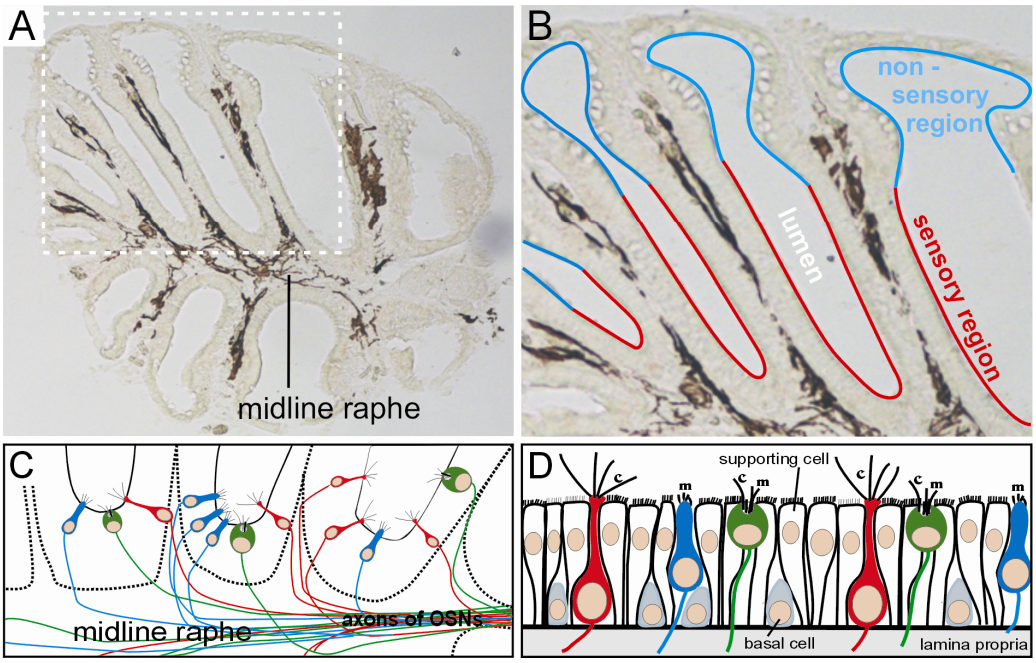

Fig. 4. Unstained olfactory epithelium (OE) of adult zebrafish. (A) Coronal section of one OE shows midline raphe and lamellae with melanophores. White dashed box marks area magnified in (B). In (B) blue line outlines non – sensory OE and red line the sensory OE. (C) The three types of olfactory sensory neurons (OSNs) intermingled in sensory OE and their axons in the median raphe. (D) Detail of OE shows three different types of OSNs embedded by supporting cells and the small, roundish basal cells. Ciliated OSNs: red, microvillous OSNs: blue, crypt cells: green. c = cilia; m = microvilli.

1.4.3. Olfactory Receptor Genes/Proteins and G proteins: Overview

In 1991, Linda Buck and Richard Axel started the characterization of olfactory receptors (ORs) by cloning of 18 different members of a

multigene family that encodes ORs in olfactory epithelium of rats (Buck and Axel, 1991). The OR gene family is known to be the largest gene family in the vertebrate genome and since its original discovery, OR genes have been partially cloned from many vertebrates (Ma, 2012). The complexity of the OR repertoire is evident in mouse and rat with more than 1000 genes, or 1 percent of the genome (Mombaerts, 1999). In the mouse, the OR repertoire consists of 1,391 genes and about 75% (~1,000) of the OR genes are potentially functional genes, whereas 25% seem to be pseudogenes (Shi and Zhang, 2007). Therefore more than 1,000 functional OR genes, comprising approximately 4% of all protein – coding genes in the mouse genome, are dedicated to olfaction (Zhang and Firestein, 2002).

It is not always easy to determine whether a gene is functional and therefore three criteria were used to recognize a gene as a pseudogene: two or more disruptions in a full – length gene, fewer than two disruptions and the absence of any of the highly conserved motifs found in OR genes, or partial sequence with one or more disruption (Zhang and Firestein, 2002).

Moreover, the high percentage of pseudogenes suggests that OR genes are one of the fastest – evolving gene families (Zhang and Firestein, 2002). In mammals, the number of OR genes (including pseudogenes) ranges between ~800 to ~1700. In detail, the mouse and rat genome contains 1391 and 1767 OR genes, respectively, while the human genome contains 802 OR genes (Shi and Zhang, 2008). The fraction of pseudogenes increases from ~25% in rodents to >50% in humans, consistent with the fact that humans rely more on other senses (Ma, 2012).

Furthermore, mammalian OR genes are classified into two groups, class I and class II, based on their sequences. Sequence analysis in fish revealed the existence of an unambiguous division (class I ORs) which represents an OR repertoire that is ~10% of that of mammalian species, whereas class II genes comprise the majority of mammalian OR genes (Ngai et al., 1993 reviewed in Gaillard et al, 2004). It has been hypothesized that class I ORs could recognize relatively hydrophilic

volatile odorants, whereas class II ORs would be dedicated to hydrophobic compounds (Niimura, 2009). For example in *Xenopus laevis*, class I and class II ORs were shown to be expressed differentially in water or air – accessible areas, respectively (Ngai et al, 1993 reviewed in Gaillard et al, 2004). Therefore they are also called fish – like class I genes and mammalian – like class II genes. However, the functional difference between class I and class II genes is still unclear (Niimura, 2009). The class I receptors resemble the family that was first found in fish and frog, but had been regarded as an evolutionary relic in mammals (Zhang and Firestein, 2008).

All in all, mammals have both class I and class II ORs, whereas all ORs in fish belong to class I and the insect ORs are quite different from each other and also different from fish and mammalian ORs (Zhang and Firestein, 2008). Teleost fish (zebrafish, medaka, stickleback, fugu and spotted green pufferfish) generally have much smaller numbers of OR genes than mammals, but the number of functional OR genes varies among species, as it was observed in mammals (Niimura, 2009). Zebrafish have the largest known functional OR gene repertoire in fish, with at least 102 genes (reviewed in Shi and Zhang, 2008).

Olfactory Receptors. Olfactory signal transduction involves G proteins and G protein – coupled receptors (GPCR) (Buck and Axel, 1991), shortly called olfactory receptors (ORs). These receptor proteins belongs to the same general protein class as the visual pigment rhodopsin and, like opsins, the chemosensory receptor proteins consists of seven transmembrane helices with a binding pocket in the center (Bradbury and Vehrencamp, 2011). Variations in amino acid sequences in the pocket region determine the structure of ligands that can bind to the receptor protein (Bradbury and Vehrencamp, 2011), which initiates signal transduction (see above). OR genes have no introns and the coding region of each gene has about 1,000 nucleotides (Shi and Zhang, 2008). The coding region of OR gene sequences is encoded by a single exon with conserved amino acid motifs that distinguish them from other non OR seven – transmembrane proteins (Buck and Axel, 1991). The size of OR

repertoire varies dramatically among different species (Zhang and Firestein, 2008).

Furthermore, it was hypothesized that an individual OSN expresses only a single OR, known as the one receptor – one neuron rule (Mombaerts, 2004). This idea has served as the basis for models of olfactory coding and is established in mammalian olfactory systems (Imai and Sakano, 2008).

In mice, it was supposed that out of ~1000 potential candidates, only one OR gene is monoallelically expressed in a given OSN (Serizawa et al., 2004). In spite of findings in mammals, recent studies in insects have found exceptions to the rule and demonstrate that the one receptor – one neuron rule is not always applicable to other species, but should be modified to multiple receptors – one neuron rule (Spehr and Leinders-Zufall, 2005). Studies in teleost fish showed that OR genes follow the one receptor – one neuron rule, even though closely related subfamily members may be coexpressed (Oka et al., 2012; Sato et al., 2007). However, both, one receptor – one neuron rule and multiple receptors – one neuron rule, were demonstrated in zebrafish depending on the different families of ORs and the divergence of functions in distinct types of OSNs (Yoshihara, 2008).

Each OR interacts with a broad range of chemical compounds, although with different affinities (Breer, 2001). Accordingly, one OR recognizes multiple odorants, and an odorant is recognized by various OR types. This combinatorial receptor strategy is used to encode odor qualities (Breer, 2001).

G Proteins. In tetrapods, in both chemosensory systems, that is, main olfactory system (MOS) and vomeronasal systems (VNS), initiation of odor sensing is mediated by distinct families of receptors, which are all members of the G protein – coupled receptor family (Breer, 2001). When a ligand binds to a receptor, a G protein complex coupled to the receptor protein is activated and this activation triggers the function of the above mentioned adenylyl cyclase which leads to a cascade of transduction events that open ion channels in the membrane (Bradbury and

Vehrencamp, 2011). The neuron becomes depolarized and action potentials are transmitted down the axon of the neuron. The first evidence for the involvement of G proteins in odorant transduction was obtained through biochemical experiments in which investigators demonstrated that the odorant – induced stimulation of olfactory sensory cilia was dependent upon the presence of GTP (Rhein and Cagan, 1980; Ronnett and Moon, 2002). G proteins are heterotrimers composed of α, β and γ subunits. Extracellular stimuli activate G protein – coupled receptors, which then catalyse GTP – GDP exchange on the G protein α – subunit. The α – subunit is a GTPase and when the receptor stimulates the G protein, the α – subunit release GDP and binds GTP (Downes and Gautam, 1999). Therefore, the α – subunits interact with GPCRs directly (Oka et al., 2009). The multigene family of G protein α – subunits, which interact with receptors and effectors, exhibit a high level of sequence diversity and thus, all members of the Gα proteins belong to 4 major classes on the basis of their sequence homologies: Gs , Gi, Gq, and G12 (Wilkie et al., 1992). Additionally in 2009, a fifth class of Gα proteins was found, the Gv class (Oka et al., 2009). Each class can be subdivided into 2 – 4 families: the Gs class comprises $G\alpha_s$ and $G\alpha_{olf}$, whereas Gi contains $G\alpha_t$, $G\alpha_o$, $G\alpha_i$ and $G\alpha_z$; the Gq comprises $G\alpha_q$, $G\alpha_{11}$, $G\alpha_{14}$ and $G\alpha_{15/16}$; and G12 encompasses $G\alpha_{12}$ and $G\alpha_{13}$ (Downes & Gautam, 1999 reviewed in Oka et al., 2009). The Gv proteins segregate into 2 families, $G\alpha_{v1}$ and $G\alpha_{v2}$ (Oka et al., 2009).

Some α - subunits show specificity for effectors (Downes and Gautam, 1999). The $G\alpha_s$ as well as the $G\alpha_i$ activates adenylate cyclases, and $G\alpha_q$ activates phospholipase C isozymes (reviewed in Downes and Gautam, 1999). Thus each G protein family possesses a particular set of interaction partners, respectively to both GPCRs and effector proteins, but there is considerable overlap and also crosstalk between different pathways (Oka et al., 2009).

1.4.4. Olfactory Receptor Gene Families in Mammals

In the main olfactory epithelium (MOE), sensory transduction occurs in specialized cilia that extend into the nasal lumen from the OSNs,

whereas sensory neurons in the vomeronasal organ (VNO) extend microvilli instead of cilia into the VNO lumen (Berghard and Buck, 1996). Vertebrate ciliated and microvillous cells have different protein receptors in their cell membranes, and the G proteins to which they are coupled lead to different second – messenger cascades (Bradbury and Vehrencamp, 2011; Dulac and Wagner, 2006; Touhara and Vosshall, 2009).

Most sensory neurons in the MOE are ciliated OSNs, which express G protein coupled ORs and utilize the cAMP cascade to transform chemical energy into electrical signals (Ma, 2012). The ORs are coupled to the Gs class G protein *α* – subunit, $G\alpha_{olf}$ (Matsunami and Buck, 1997).

Moreover, in the MOE, a second class of chemosensory receptors was identified in a small subpopulation of neurons and these receptors are called trace amine – associated receptors (TAARs) (Liberles and Buck, 2006). ORs and TAARs, both, belong to the rhodopsin – like subclass of GPCRs, class A, with short N – and C – termini outside the seven – transmembrane domain (Korsching, 2008). Therefore, these receptor proteins share many features, such as gene structure. Nevertheless, the two receptor types are not coexpressed in any sensory neuron, and their expression profile is similar, because different TAARs are expressed in different neurons, and those with the same TAAR are scattered in selected olfactory epithelial regions (Liberles and Buck, 2006). Additionally, The TAARs are also coupled to the G protein *α* – subunit, $G\alpha_{olf}$ and the subset of OSNs expressing TAARs responds to amines and urine (Liberles and Buck, 2006).

Another subset of OSNs in the MOE expresses guanylyl cyclase-type D (GC-D) (Fülle et al, 1995), which were revealed to be extremely sensitive chemodetectors (Leinders-Zufall et al., 2007). GC-D – expressing OSNs do not express components of the canonical OSN odor transduction cascade and are therefore not GPCRs (Juilfs et al., 1997; Zufall and Munger, 2010). Stimulus encoding by GC-D cells differs sharply from that of canonical OSNs, where a given molecular cue stimulates only a small fraction of the entire population (Firestein, 2001), because of the expression of large numbers of receptors with different receptive properties (Mombaerts, 2004 reviewed in Leinder-Zufall et al., 2007).

OSNs expressing GC-D detects ambient CO2 (Hu et al., 2007; Ma, 2012) and natriuretic peptides (uroguanylin and guanylin) (Leinder-Zufall et al, 2007). Because of the sensitive and selective detection of uroguanylin and guanylin by the GC-D neurons the possibility has been suggested that these cells contribute to the maintenance of salt and water homeostasis or the detection of cues related to hunger, satiety, or thirst (Leinders-Zufall et al., 2007).

Also two distinct superfamilies of GPCRs have been identified as vomeronasal receptors (V1Rs and V2Rs), because they are expressed in microvillous neurons within the VNO and not observed in sensory neurons of the MOE (Dulac and Axel, 1995; Matsunami and Buck, 1997). These receptors are unrelated to their counterparts in the MOE (Tirindelli et al., 1998). Like ORs and TAARs, V1R genes have an intronless coding region, whereas V2Rs are characterized by the presence of a long, highly variable N – terminal domain (Matsunami and Buck, 1997; reviewed in Shi and Zhang, 2008). V2Rs belong to class C GPCRs, with the ligand binding pocket in the large N – terminal extracellular domain, which is similar in structure to the metabotropic glutamate receptor, whereas V1Rs have not been formally classified, but are closest to class A receptors (Korsching, 2008).

Of seven Gα subunits identified as being expressed in the VNO, it was demonstrated that mRNAs encoding only two, $G\alpha_o$ and $G\alpha_i$ are highly expressed in VNO neurons by separate subsets of neurons in different regions of the VNO neuroepithelium (Berghard and Buck, 1996). V1R genes are coexpressed with the G – protein subunit $G\alpha_i$ in sensory neurons located in the apical part of the vomeronasal epithelium, whereas V2R genes are expressed in $G\alpha_o$ – positive neurons in the basal part of the vomeronasal epithelium (Dulac and Torello, 2003).

In 2009, the existence of a third family of candidate chemosensory receptors in the VNO of mice and rat was demonstrated (Riviere et al., 2009). Thus, 5 of 7 members of the formyl peptide receptor (FPR) family are expressed by VNO neurons, whereas the other 2 FPRs are instead expressed in the immune system, where they are believed to stimulate chemotaxis to sites of infection or tissue damage upon recognition of their

ligands, such as formylated pepides from bacteria or mitochondria (reviewed in Liberles et al, 2009). Similar to expression patterns of V1Rs and V2Rs, FPRs are selectively expressed in the VNO and each FPR is expressed in a different small subset of neurons that are highly dipersed.

Furthermore, it could be demonstrated that V1Rs and all FPRs, except FPR receptor 1, couple to $G\alpha_{i2}$, whereas V2Rs and FPR receptor 1 couple to $G\alpha_{o.}$ (Liberles et al., 2009). Therefore, FPRs consistently express $G\alpha_{i}$ or $G\alpha_{o}$ and appear to lack other chemoreceptor proteins.

Table1: OSNs, ORs and G proteins in mammals

OSN:	**OR + G protein:**	
Ciliated ORs in MOE:	ORs + $G\alpha_{olf}$	TAARs + $G\alpha_{olf}$
Microvillous ORs in VNO:	V1Rs / FPRs (2-5) + $G\alpha_{i2}$	V2Rs / FPR (1) + $G\alpha_{o}$

1.4.5. Olfactory Receptor Gene Families in Teleosts

Teleosts are equipped with only one olfactory organ containing three morphologically distinct types of OSNs: microvillous and ciliated OSNs, and a third type, which comprise only a minor population in the olfactory epithelium (OE), the crypt cells, with both microvilli and cilia (Hansen et al., 2004; Hansen and Zeiske, 1998; Sato et al., 2005). The morphologically different types of OSNs utilize different families of olfactory receptors (ORs) coupled to different G protein α – subunits (Hansen et al., 2004). Thus, expression of ORs is observed in ciliated OSNs in teleosts, while V2R – type ORs are found in microvillous OSNs and therefore, the ciliated and microvillous OSNs likely detect distinct types of chemosensory signals through different families of ORs (Hansen et al., 2004; Sato et al., 2005 reviewed in Yoshihara, 2008).

In zebrafish, 102 intact OR genes and 35 pseudogenes were identified and subdivided by phylogeny into 9 groups (Niimura and Nei, 2005). The OR repertoire in zebrafish is twice as large than that of pufferfish with <50 OR genes (Alioto and Ngai, 2005; Korsching, 2008).

Furthermore, another family of chemosensory receptors were identified in zebrafish, the TAARs. At first 57 intact TAAR genes were identified in zebrafish (Gloriam et al., 2005), but the number of putatively functional TAAR genes found in zebrafish increased by using different analysis up to 109 genes (Hashiguchi and Nishida, 2007). The evidence that TAARs are also expressed in the teleost OE (probably ciliated cells) (Hussain et al., 2009) suggests that TAARs are likely to serve as ORs in fishes as well as in mammals (Liberles and Buck, 2006). In contrast to the OR gene family, which is larger in tetrapods than in fishes, the TAAR gene family is smaller in tetrapods (Shi and Zhang, 2008).

In teleosts, a third receptor family was identified and characterized as “V2R – like” olfactory C family GPCRs (Alioto and Ngai, 2006). In zebrafish, 44 intact genes and 8 disrupted genes were found (Shi and Zhang, 2007). Mammalian V2Rs are the closest relatives of the teleost olfC receptors because the V2Rs, as well as teleosts olfC receptors, belong to the class C of GPCRs (Korsching, 2008). Furthermore teleost olfC GPCRs are expressed by microvillous, but not ciliated OSNs (Alioto and Ngai, 2006), and maybe crypt cells (Cao et al, 1998).

A fourth teleost olfactory receptor family is represented by the olfactory receptor genes related to class A GPCRs (*ora*), which were identified as the teleost homologs of the mammalian V1R genes (Saraiva and Korsching, 2007). With only 6 members compared to over 100 genes in the corresponding rodent V1R gene family, the *ora* receptor gene family is very small (Korsching, 2008). It was shown that all 6 *ora* genes are expressed specifically in the olfactory organ of zebrafish, in sparse cells within the sensory surface, probably including microvillous cells (Pfister and Rodriguez, 2005; Saraiva and Korsching, 2007) and *ora4* expressed only in crypt cells (Oka and Korsching, 2011).

Thus, the teleost olfactory receptor gene repertoires are smaller in size (OR and *ora*), comparable (olfC), or even larger (TAAR) than the corresponding mammalian gene repertoire (Korsching, 2008). Therefore, although fish show no spatial segregation in epithelial subsystems, the fish olfactory system is no less complex (Oka et al., 2012).

In contrast to ORs, little is known about the G protein *α* – subunit in fish species (Oka and Korsching, 2011). Via immunohistochemical studies that used antibodies raised against mammalian G protein *α* – subunit, expression patterns could be visualized in teleosts (Braubach et al., 2012; Hansen et al., 2004; Hansen et al., 2003; Hansen and Zielinski, 2005). In goldfish, the ciliated OSNs utilize OR – type receptors along with $G\alpha_{olf}$, whereas microvillous OSNs express V2R – type receptors with either $G\alpha_o$, $G\alpha_i$ or $G\alpha_q$. Furthermore, the crypt cells utilize $G\alpha_q$ and $G\alpha_o$ (Hansen et al., 2004). Whereas in catfish, ciliated OSNs also express OR – type receptors along with $G\alpha_{olf}$, the microvillous OSNs are heterogeneous, with many expressing $G\alpha_{q/11}$, and the crypt cells express $G\alpha_o$ (Hansen et al., 2003). Although, in catfish, $G\alpha_o$ is expressed in crypt cells, and in goldfish, $G\alpha_o$ is mainly expressed in microvillous OSNs (Hansen et al., 2003, 2004), ciliated OSNs always express the G protein subunit $G\alpha_{olf}$. Apparently, localization of G protein subunits $G\alpha_o$, $G\alpha_i$ and $G\alpha_q$ to microvillous OSNs or crypt cells varies among different species (Oka et al., 2012).

In zebrafish, ciliated OSNs were identified with antibodies against various G protein α and calcium – binding proteins demonstrating some differential expression in OSNs of zebrafish and other teleosts (Braubach et al., 2012; Castro et al., 2006; Gayoso et al., 2011; Germana et al., 2004; Germana et al., 2007). It could be demonstrated that the calcium – binding protein calretinin is exclusively or mainly expressed in ciliated neurons and also labels their axonal projections in the olfactory bulb (Castro et al., 2006; Gayoso et al., 2011; Braubach et al., 2012). Furthermore, G protein subunit $G\alpha_{olf}$ – immunoreactivity in zebrafish ciliated OSNs was confirmed by an anti – calretinin antibody double labeling (Braubach et al., 2012). Furthermore, the calcium – binding protein S100 is reported to be expressed in zebrafish crypt cells (Germana et al., 2004, 2007), and presumably additionally in microvillous OSNs (Gayoso et. al., 2011; Braubach et al., 2012). The identification of the crypt cells is also quite feasible based on their typical morphology (Braubach et al., 2012). Thus, it was demonstrated, that some $G\alpha_o$ – immunoreactive cells in the zebrafish OE are crypt cells, because they are also labeled by anti – S100 antibody and they displayed the crypt cell morphotype

(Braubach et al., 2012). .Most $G\alpha_o$ (and calretinin or S100) positive cells, appeared to be in intermediate position (likely microvillous cells). However, antibodies against G protein α subunits $G\alpha_{q/11}$ and $G\alpha_{i-3}$ showed no unambiguous or reproducible labeling in zebrafish (Braubach et al., 2012).

In 2009, the Gα gene family has been characterized in 5 teleost fish with a total of 26 genes in zebrafish, 27 genes in stickleback and 25 genes each in medaka, tetradon and fugu (Oka et al, 2009). Therefore the teleost Gα gene family is larger than the mammalian family size of 16 functional genes (Birnbaumer, 2007; Oka and Korsching, 2011).

The expression of 4 genes was demonstrated in the OE in adult zebrafish, $G\alpha_{olf2}$, $G\alpha_{i1b}$, $G\alpha_{o1}$ and $G\alpha_{o2}$ (Oka and Korsching, 2011). The $G\alpha_{olf2}$ is the direct ortholog of the mammalian $G\alpha_{olf}$ (Oka and Korsching, 2011) and as in mammals, the ciliated OSNs of teleost fishes express OR – type odorant receptors and transduce signals through a cAMP cascade that includes the G protein $G\alpha_{olf}$ (Ngai et al., 1993; Vielma et al., 2008).

Both zebrafish $G\alpha_{o1}$ and $G\alpha_{o2}$ genes are expressed in the OE, presumably in microvillous neurons expressing the V2R – like olfC genes, exactly as the single mammalian $G\alpha_o$ gene, which is co – expressed with V2R genes (Oka and Korsching, 2011). Moreover, ORs of the *ora* / V1R – family are coupled to $G\alpha_{i1b}$. Although $G\alpha_{i1b}$ is not ortholog of the mammalian $G\alpha_{i2}$, it is associated with members of the same olfactory receptor family (Oka and Korsching, 2011).

Lastly, it was revealed that the crypt cells in zebrafish express a single V1R – like gene, *ora*4, and no evidence for expression of other V1R – like *ora* genes, V2R – like olfC or *taar* genes in crypt cells was found (Oka et al., 2012). In the *ora*4 – positive crypt cells the inhibitory Gα protein $G\alpha_{i1b}$ is co – expressed (Oka et al., 2012). It was shown that the G α – subunit $G\alpha_i$ inhibits adenylate cyclases (Downes and Gautam, 1999). In the mammalian VNO the situation is similar but not identical, because the V1R genes are co – expressed also with a class Gi protein, the inhibitory G protein α – subunit $G\alpha_{i2}$ (Mombaerts, 2004; Oka et al., 2012). The signal transduction steps in crypt neurons and their subsequent neuronal network are not known so far (Oka et al., 2012).

Table 2: OSNs, ORs and G proteins in zebrafish

OSN:	**OR + G protein:**	
Ciliated ORs	ORs + $G\alpha_{olf2}$	TAARs + $G\alpha_{olf2}$
Microvillous ORs	V1R – like *ora* + $G\alpha_{i1b}$	V2R – like olfC + $G\alpha_{o1}$ / $G\alpha_{o2}$
Crypt Cells	V1R – like *ora*4 + $G\alpha_{i1b}$	

In conclusion, via immunohistohistochemistry using antibodies against mammalian G-proteins and other analysis, the G protein subunits $G\alpha_{olf}$ and $G\alpha_{i1b}$/$G\alpha_{o}$ were identified in teleost ciliated OSNs and crypt/ microvillous cells, respectively.

Furthermore, via RT – PCR and gene expression analysis the expression of receptors and corresponding G protein subunits in different zebrafish OSNs revealed the expression of G protein subunit $G\alpha_{olf2}$ with zebrafish ORs and TAARs in ciliated ORs, the expression of G protein subunits $G\alpha_{o1}$ and $G\alpha_{o2}$ with V2R – like olfC in microvillous ORs and the subunit $G\alpha_{i1b}$ expression with V1R – like *oras* and V1R – like *ora*4 in crypt cells, respectively. Therefore, the identification of receptors and corresponding G protein subunits in the different zebrafish OSNs is not yet complete and also shows discrepancies between different analytical methods.

1.5. Olfactory Bulb (OB)

1.5.1. Olfactory Bulb in Mammals

General. Olfactory stimuli are transduced in the apical dendrite of OSNs into electrical activity which ultimately leads to action potentials propagating along a single, unbranched axon towards the olfactory bulb (OB), the first relay station for odor processing in the brain (Friedrich and Korsching, 1997a). In the OB, OSN axons make synapses with the dendrites of projection and other neurons within discrete neuropil structures known as glomeruli (Buck and Axel, 1991) which represent globular conglomerates of neuropil (axons/dendrites).

The synaptic interactions within OB glomeruli are considered modules for representing and processing sensory features (Araneda et al., 2000; Breer et al., 2006; Mori et al., 1999). Interaction of olfactory nerve terminals, different types of projection neurons and various interneurons is fundamental for the fine tuning of the output from each glomerulus. Additionally interneurons that make synapses outside the glomeruli are involved in this processing (Kosaka and Kosaka, 2003; 2004; 2005b).

In mouse and rat, OSNs expressing the same OR converge their axons to two glomeruli located in stereotyped positions on the OB, one on the medial and the other on the lateral surface (Imai et al., 2010; Mombaerts et al., 1996; Ressler et al., 1994; Vassar et al., 1994). Since the OSNs expressing the same OR are widely scattered in the OE (see above), topographic reorganization must occur during the process of axonal projection to the OB (Imai and Sakano, 2008). By using transgenic mice in which the expression of a given OR gene was linked to the expression of the green fluorescent protein (GFP), this convergence of axons of OSNs expressing a given OR has been experimentally visualized at single – axon resolution and it has been shown that all and only the axons of neurons expressing that particular OR, were converging to their target glomeruli (Menini et al., 2004; Mombaerts, 1999; Treloar et al., 2002). Thus, odorous molecules which stimulate different receptor subtypes will activate a characteristic pattern of glomeruli, which may be used by the brain to encode the quality of a particular odor (Strotmann, 2001). Convergence becomes obvious by consideration of the number of the OSN (millions in mouse and rat), glomeruli (thousands), and OB projection neurons, (tens to hundreds of thousands of mitral and tufted cells) that make synaptic contacts with OSN in glomeruli (Shepherd et al., 2004; Shipley et al., 2004; Toida, 2008).

Thus, the convergence of receptor – specific neuron populations onto mutually exclusive glomeruli generates a chemospecific (odotopic) map which is regarded as the basis for a combinatorial processing of molecular entities, leading to the identification of odors (Malnic et al., 1999; Schoenfeld and Cleland, 2005; Zou et al., 2001).

Laminar Organization. The rodent OB has a multi – layered (laminar) cellular architecture exhibiting six layers. As the axons of the OSNs in the OE accumulate and penetrate the basal lamina in bundles which exit the olfactory organ, these bundles form the nervus olfactorius, i.e., the cranial nerve I (Korsching et al., 1997b). As the nerve reaches the OB, a complex process of defasciculation begins and the olfactory nerve layer (ONL) is formed as the outermost layer of the OB (Firestein and Beauchamp, 2008). The glomeruli form the next layer below the surface of the bulb, the so – called glomerular layer (GL) (Ma, 2012). In this layer the glomeruli are encapsulated by glia cells, some of which extend processes into the neuropil. The glomeruli are furthermore surrounded and delineated by a large population of juxtaglomerular neuronal cells (Wachowiak and Shipley, 2006).

The external plexiform layer (EPL) is predominantly an area of complex neuropil, but contains also scattered populations of cell bodies, including tufted cells and short axon cells (Firestein and Beauchamp, 2008). The tufted cells are one of two populations of projection neurons in the OB and their apical dendritic processes arborize within the glomerulus, whereas the secondary dendrites are restricted to the EPL (Firestein and Beauchamp, 2008). The single apical dendritic processes of mitral cells, the primary projection neurons, extend unbranched through the EPL as they target one glomerulus each, whereas the secondary dendritic processes of these projection neurons also extend laterally into the EPL (Firestein and Beauchamp, 2008). Thus, mitral cells and tufted cells send their primary dendrites into glomeruli where they form a highly branched tuft (Egger and Urban, 2006) and secondary dendrites into the EPL (Kosaka et al., 1998). Mitral cells also have long lateral dendrites in the deeper half of the EPL, whereas tufted cells project their secondary (lateral) dendrites to the superficial half of the EPL and both types have dendrodendritic reciprocal connections with a different subset of granule cells (Mori and Sakano, 2011). Furthermore, the dendritic processes of deep lying interneurons, the granule cells, branch peripherally and establish reciprocal dendrodendritic synapses with the secondary dendrites of projection neurons in the EPL (Firestein and Beauchamp,

2008). The next layer, called mitral cell layer (MCL), is a monolayer that includes the somata of the primary population of projection neurons in the OB, the mitral cells.

The olfactory information processed by this complex neuronal network of the OB is relayed by the mitral and tufted cells to higher brain regions for the perception of smell (Breer et al., 2006; Zou et al., 2005). The axons of mitral cells extend from the basal pole and join other axons in the deeper internal plexiform layer (IPL) where myelination is present (Firestein and Beauchamp, 2008). The IPL includes axons of projection neurons which coalesce to form the lateral olfactory tract projecting to higher centers of the brain and axons of intrabulbar cells from the juxtaglomerular region that appear to contact homotypic regions on the opposite side of the OB (Belluscio et al., 2002; Firestein and Beauchamp, 2008; Liu and Shipley, 1994).

Finally, the granule cell layer (GCL) includes somata of granule cells, the main population of interneurons in the OB. The granule cell somata are organized in islets and the granule cell dendrites project into the EPL (Firestein and Beauchamp, 2008). Between the somata islets, axons from the projection neurons extend through the GCL to form later the lateral olfactory tract (Firestein and Beauchamp, 2008).

Additionally, the innermost region of the OB is the terminal region of the rostral migratory stream, the path of migrating neuroblasts forming new OB interneurons in the adult (Firestein and Beauchamp, 2008).

Cell Populations. Mitral and tufted cells are both excitatory projection neurons of the OB, using glutamate as their primary neurotransmitter (Egger and Urban, 2006). While the numbers of mitral and tufted cells are comparable in the OB, they differ in many respects, such as their axonal and dendritic projection patterns and their immunoreactivity for different markers (Allison, 1953; Egger and Urban, 2006; Schneider and Scott, 1983). Furthermore, there is communication within and between glomerular units via reciprocal dendrodendritic synapses and the mitral and tufted cells excite local interneurons which in turn inhibit the same and other mitral and tufted cells (Ma. 2012). Thus in addition to the excitatory

neurons, there are several types of inhibitory interneurons (Wilson and Mainen, 2006).

Although evidence for monosynaptic excitatory connections between mitral cells is lacking (Pinching and Powell, 1971; Schoppa and Urban, 2003), it is supposed that glomerulus – specific mitral cells are electrically coupled (Schoppa and Urban, 2003; Schoppa and Westbrook, 2002). Moreover, according to the laminar segregation of mitral and tufted cell secondary dendrites within the EPL, it has been suggested that both projection neurons preferentially interact via dendrodendritic synapses with various subtypes of inhibitory granule cells (Mori, 1987; reviewed in Mori & Sakano, 2011). Additionally, mitral cells also display auto – excitatory responses to glutamate released from their own dendrites (Aroniadou-Anderjaska et al., 1999; Friedman and Strowbridge, 2000; Nicoll and Jahr, 1982; Salin et al., 2001; Schoppa and Westbrook, 2001) and they can undergo self – inhibition in response to depolarization (Margrie et al., 2001; Nowycky et al., 1981; Schoppa and Urban, 2003).

The granule cells are small interneurons without an axon and, thus, all synaptic input and output occurs via dendrites (Firestein and Beauchamp, 2008; Price and Powell, 1970a). Granule cells are exclusively GABA (Gamma-amino-butyric acid) ergic and form reciprocal dendrodendritic contacts with mitral cell and tufted cell dendrites (Didier et al., 2001; Schoppa and Urban, 2003). Granule cells are the most numerous type of neuron in the OB and form the most central layer of the OB, the GCL, where the granular cell bodies are seen in tightly packed groups of 2 – 10 cells (Egger and Urban, 2006; Price and Powell, 1970b). They have a distinct apical dendrite which arborizes in the EPL and is heavily covered with dendritic spines; furthermore, a basally (centrally) extended dendrite remains restricted to the GCL (Firestein and Beauchamp, 2008). Moreover, the dendritic spines of granule cell dendrites, also known as gemmules, carry pre- or postsynaptic regions, whereby contiguous compartments within the spines are specialized for efferent or afferent function (Firestein and Beauchamp, 2008; Price and Powell, 1970c). There are three subpopulations of granule cells, including (1) those with cell bodies located deep within the GCL and with an apical

dendrite limited to the deep EPL; (2) granule cells with cell bodies located more superficially in the GCL and dendrites arborizing extensively in the superficial EPL; and (3) the granule cells whose apical dendrites arborize within the superficial and deep EPL (Firestein and Beauchamp, 2008; Greer, 1987; Imamura et al., 2006; Mori et al., 1983; Orona et al., 1983).

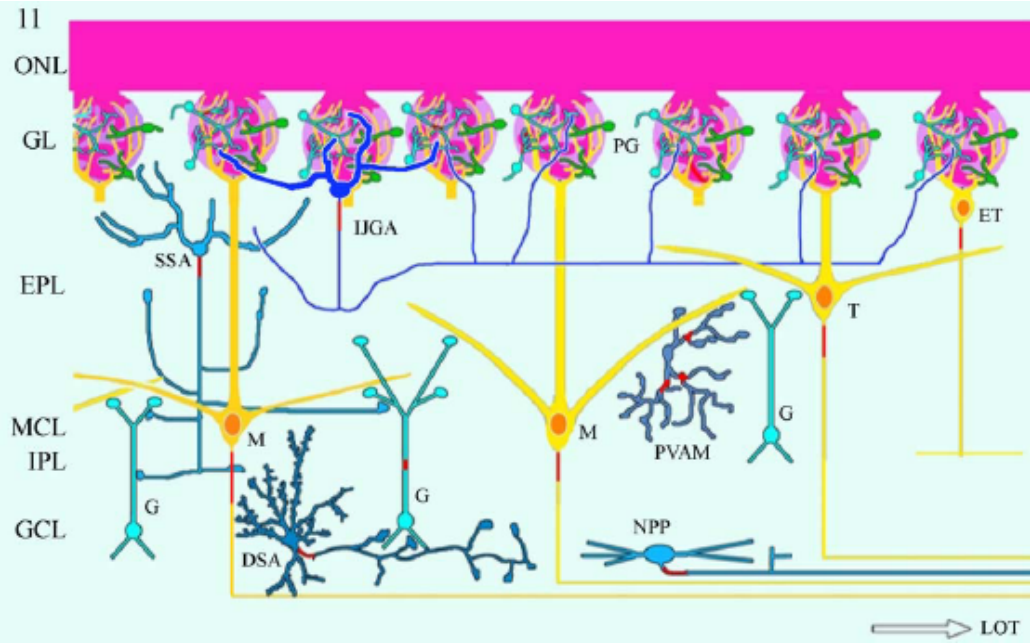

Fig. 5. Organization of rodent olfactory bulb. DSA deep short axon cell, EPL external plexiform layer, ET external tufted cell, G granule cell, GCL granule cell layer, GL glomerular layer, IJGA inhibitory juxtaglomerlar association system, IPL inner plexiform layer, M mitral cell, MCL mitral cell layer, NPP nonprincipal projection neuron, ONL olfactory nerve layer, PVAM parvalbumin anaxonic multipolar EPL cell, SSA superficial short axon cell, T tufted cell. Adapted from Kosaka and Kosaka 2011

The granule cells are inhibitory (GABAergic) interneurons which control the activity of glutamatergic mitral and tufted cells (Shepherd et al., 2007). It has been suggested that the organization of the granule cell dendrites is associated with the differential distribution of the secondary dendrites of the two projection neuron types; and, thus, the deep granule cells may interact preferentially with mitral cell dendrites, whereas the superficial granule cells interact preferentially with tufted cell dendrites (Firestein and Beauchamp, 2008). The granule cell has been revealed as an extraordinarily complex cell, which occupies a key role in processes of olfactory perception including processing of odor maps in the glomeruli, and formatting the result for output to the olfactory cortex (Shepherd et al., 2007). The granule cells in the OB outnumber mitral cells by a factor of

approximately 50 – 100 (Egger and Urban, 2006; Shepherd and Greer, 2004). Moreover, because granule cells (as periglomerular cells, see below) are continuously replaced throughout adulthood (Bayer, 1983; Egger and Urban, 2006), different cellular stages of maturation coexist in the bulb (Carleton et al., 2003; Egger and Urban, 2006).

The interneurons associated with the glomerular layer (GL) may collectively be referred to as juxtaglomerular neurons whose cell bodies are located around glomeruli and represent various types of neurons. Juxtaglomerular cells form local circuits that make dendrodendritic synaptic connections with each other and with apical dendrites of mitral and tufted cells (Liu and Shipley, 2008b). They are morphologically classified into periglomerular cells (PG), (superficial) short axon cells (SSA) and external tufted cells (ET) (see Fig. 5) (Kosaka et al., 1997; Kosaka and Kosaka, 2011; Shipley and Ennis, 1996). Periglomerular cells and external tufted cells send dendrites into glomeruli, whereas the superficial short axon cells are described to send dendrites into the juxtaglomerular region but not into glomeruli (Kosaka et al., 1997).

The majority of interneurons in the GL are the periglomerular neurons whose cell bodies surround and define individual glomeruli in the GL (Firestein and Beauchamp, 2008). These interneurons extend their dendrites into glomeruli and make synapses with the OSN axon terminals, and / or the mitral and tufted cell dendrites (Toida, 2008). Kosaka and colleagues proposed that the periglomerular cells include two different types that can be distinguished based on the intraglomerular dendritic arborization which correlates with their chemical properties (Kosaka et al., 1997). Each glomerulus is composed of two zones, the olfactory nerve (ON) zone where OSNs make synapses on their targets and the non – ON zone where dendrodendritic interactions between intrinsic neurons mainly occur (Kosaka et al., 1997). Accordingly, the ON zone corresponds to sensory/axonal - and the non-ON zones to the centralsynaptic/dendritic subcompartments (Chao et al., 1997; Kasowski et al., 1999; Kosaka et al., 2001). The periglomerular cells differ in their synaptic organization and were classified into type 1 periglomerular cells and type 2 periglomerular cells. In rat, type 1 periglomerular cells, i.e., TH/GABA positive neurons

(see below), send their dendrites into both the glomerular ON zone and non – ON zones and receive asymmetrical synapses from olfactory nerve terminals and mitral cell dendrites and make symmetrical synapses on mitral cell dendrites (Kosaka et al., 2001; Kosaka and Kosaka, 2005a; Toida et al., 2000). Additionally, there are no reciprocal synapses between TH/GABA positive dendrites and mitral cell dendrites. In contrast, type 2 periglomerular cells send their intraglomerular dendrites only into the non-ON zone where they receive no or few, if any, synapses from olfactory nerve terminals (Kosaka et al., 2001; Toida et al., 2000; Toida et al., 1998). However, calbindin – immunoreactive (see below) dendrites of type 2 cells make symmetrical synapses on mitral cell dendrites and receive asymmetrical synapses from them (Toida et al., 2000).

Additionally, chemical heterogeneity of periglomerular cells was revealed by immunocytochemical studies in rodents with markers for neurotransmitter and / or calcium – binding proteins (Kosaka et al., 1998; Kosaka et al., 1997; Toida et al., 2000; Toida et al., 1998). Type 1 periglomerular cells include GABA– immunoreactive neurons and neurons which are immunoreactive for TH (the dopamine – synthesizing enzyme tyrosine hydroxylase). In contrast, type 2 periglomerular cells include neurons immunoreactive for calcium – binding proteins calbindin D28k (CB) or calretinin (CR) (Toida et al., 1998, 2000; Kosaka et al., 2001). Further studies demonstrated that GABA, and calretinin and calbindin characterize three largely separate groups of periglomerular cells in the rat OB, while in the mouse, separate CB and CR cell populations both largely overlap with GABA positive cells (Kosaka and Kosaka, 2005a; 2007a; Kosaka et al., 1998; Kosaka and Kosaka, 2005c). In both rat and mouse, TH is always (mouse) or predominantly (rat) present in GABA – positive cells (Kosaka et al., 1998; Kosaka and Kosaka, 2005, 2007). Thus, colocalization relationships are different in mouse and rat periglomerular OB cells (Kosaka and Kosaka, 2005, 2007).

Recently, the cytologigal analysis of the rodent MOB has been challenged by new findings (Kosaka and Kosaka, 2011). Immunohistochemical analyses revealed characteristic chemical markers for “axon initial segments” (AIS), such as sodium channel clusters,

ankyrinG, βIV – spectrin and phosphor – IκBα. This work suggested that there are two functionally different types of periglomerular cells: Axon – bearing periglomerular cells with axons extending to distant glomeruli which presumably participate in the interglomerular lateral inhibition. In contrast, the second group of periglomerular cells, so – called anaxonic periglomerular cells, demonstrate no axon or a short axon extending very close to their somata and rather participate in the intraglomerular self – inhibition or self – modulation (Kosaka and Kosaka, 2011). The external tufted cells were identified at the GL and EPL border and demonstrate a generally elliptical and slightly larger cell body than the periglomerular neurons (Firestein and Beauchamp, 2008).

They extend an apical dendrite into a single glomerulus and receive monosynaptic input from OSNs, provide monosynaptic glutamatergic input in turn and receive inhibitory synaptic feedback from their postsynaptic targets in the GL including GABAergic periglomerular cells (Hayar et al., 2004; Liu and Shipley, 2008a; Wachowiak and Shipley, 2006). Therefore, external tufted cells play a critical role in the glomerular network because they receive monosynaptic ON input and provide the major excitatory drive on intra – and interglomerular inhibitory circuits (Liu and Shipley, 2008). Furthermore, external tufted cells extend axons into the IPL where they course to terminate in the IPL on the opposite side of the same olfactory bulb (Liu and Shipley, 1994; Shipley and Ennis, 1996).

The short axon cells are the rarest interneurons in the GL and their cell bodies are slightly larger than those of periglomerular neurons (Firestein and Beauchamp, 2008). They were classified based on their position of somata (superficial and deep short axon cells; SSA and DSA, respectively), structural features uncovered via classical Golgi – impregnation methods (Blanes cell, Golgi cell, Cajal cell, etc.) and their chemical properties concerning neuroactive substances and / or their synthesizing enzymes, calcium binding proteins, receptors and channels (Kosaka and Kosaka, 2011). Short axon cell bodies extend the axon along the periphery of up to 2-4 glomeruli (Shipley and Ennis, 1996). Because these cells have a dendritic arbor that seems to surround the glomeruli and their axons remain restricted to the GL, it has been suggested that the

short axon cells form circuits with the external tufted cells and periglomerular neurons (Firestein and Beauchamp, 2008). Moreover, several physiological and morphological analyses demonstrated that short axon cells, particularly DSA cells, made synaptic contacts selectively on GABAergic local circuit neurons (Eyre et al., 2008; Gracia-Llanes et al., 2003; Kosaka and Kosaka, 2011; Pressler and Strowbridge, 2006).

Additionally, large TH positive neurons had been considered as external tufted cells but later revealed to be also GABAergic, are a particular type of juxtaglomerular neurons (Kosaka and Kosaka, 2011). There are two types of TH positive juxtaglomerular neurons with different size of soma (Halasz et al., 1981; Kosaka and Kosaka, 2007a; Kosaka and Kosaka, 2008b; 2011). The larger type had been regarded as dopaminergic external tufted cells and the smaller type as periglomerular cells but both types were revealed to be GABAergic (Kosaka and Kosaka, 2011). Therefore, both types have been regarded as DA – GABAergic juxtaglomerular (JG) neurons (Kosaka and Kosaka, 2008a) and it was shown that those neurons with the long interglomerular connections are large in soma size and extend at least some dendrites into glomeruli also located distantly (Kosaka and Kosaka, 2011). Furthermore, the DA – GABAergic JG neurons are known to be the major groups of adult generated JG neurons (De Marchis et al., 2007; Kosaka and Kosaka, 2011; Merkle et al., 2007; Whitman and Greer, 2007). The large DA – GABAergic JG neurons participating in the interglomerular connection are different from the adult – generated DA – GABAergic JG neurons, which are the small type of DA – GABAergic JG neurons (Kosaka and Kosaka, 2009; 2011).

Moreover, Michael Shipley's group analyzed the physiological and structural properties of DA – GABAergic JG neurons and also revealed the interglomerular connections of DA – GABAergic JG neurons (Kiyokage et al., 2010). However, they supposed that these DA – GABAergic JG neurons are short axon cells rather than periglomerular cells, because these cells extended their processes from several (oligoglomerular) to many (polyglomerular) glomeruli. In contrast, Kosaka's group argued that JG neurons with intraglomerular dendrites (other than tufted cells) should

be considered as periglomerular cells rather than short axon cells disregarding of their mono – or oligoglomerular dendritic branches, and that short axon cells are generally considered to have no intraglomerular dendritic branches. Moreover, Shipley's group did not differentiate dendrites and axons in their oligo – and polyglomerular DA – GABAergic short axon cells types (Kiyokage et al., 2010; reviewed in Kosaka and Kosaka, 2011). Therefore, definitions of the Kosaka group of DA – GABAergic juxtaglomerular cells are not consistent with that of short axon polyglomerular cells in the mouse MOB of Kiyokage et al (2010; reviewed in Kosaka and Kosaka, 2011). In addition, Kosaka & Kosaka (2011) added some particular features of DA – GABAergic neurons by using retrograde tracing in the GL. They demonstrated that a few DA – GABAergic cells with relatively large somata are scattered in the EPL and extend some dendritic processes into glomeruli and these TH positive cells, although not located in a juxtaglomerular position, are "displaced DA – GABAergic JG neurons". Also there are large DA – GABAergic JG neurons extending axons which descended in the EPL, then branched and extended laterally in the EPL and some collaterals ascended toward the GL (Kosaka and Kosaka, 2011).

Thus, Kosaka's group assumes that DA – GABAergic JG neurons are heterogeneous, consisting of a small type ("conventional periglomerular cells") and large type DA – GABAergic JG neurons (rather than short axon cells) which extend dendrites into several glomeruli close to their somata but also far from their somata (Kosaka and Kosaka, 2011). However, the situation is not definitely resolved and more detailed analyses are needed.

Furthermore, previous studies in the mouse MOB revealed that nitric oxide synthase (NOS) positive neurons project to higher olfactory related regions (Kosaka and Kosaka, 2007b) and via retrograde tracing and intracellular labeling experiments it was shown that deep short axon cells or interneurons project to higher olfactory areas (Eyre et al., 2008; Kosaka and Kosaka, 2011). Additionally, some calbindin positive short axon cells in the IPL extend their axons into the lateral olfactory tract (Kosaka and Kosaka, 2010) and cells located in the IPL and GCL were

retrogradely labeled when tracers were injected into higher olfactory related regions (Kosaka and Kosaka, 2011).

Thus, the rodent MOB might have more types of cells than the principal projection neurons that project to higher olfactory related regions, (analogoug to glutamatergic principal projection neurons and other nonprincipal GABAergic projection neurons in other brain regions; Kosaka and Kosaka, 2011) which were suggested to be called “nonprincipal projection (NPP) neurons” rather than “short axon cells” (Kosaka and Kosaka, 2011).

Moreover, interneurons in the EPL, like Van Gehuchten cells, satellite cells or pyriform cells might not be different cell types, but should rather be summarized as “anaxonic multipolar EPL neurons” (Kosaka and Kosaka, 2011). These parvalbumin positive medium – sized anaxonic multipolar EPL (PVAM) neurons may display some particular patch – like portions with AIS – characteristics on their dendritic processes, so – called “dendritic hot spots” (Kosaka and Kosaka, 2011). Additionally, some NOS positive periglomerular cells and a few calretinin positive granule cells also displayed similar dendritic hot spots (Kosaka et al, 2008a; reviewed in Kosaka and Kosaka, 2011).

There is an intrabulbar association system linking reciprocally the mirror – symmetric isofunctional odor columns (Lodovichi et al., 2003). As mentioned above, OSNs expressing the same receptor project into glomeruli located on both the medial and lateral aspects of each bulb, and the spatial relationships between glomeruli on one side of the bulb are reflected on the other side. Anatomical tracer studies have also revealed that the bilateral olfactory maps are connected through a set of intrabulbar projections mediated through excitatory external tufted cells that specifically link the odor column circuitry of glomeruli that receive input from the same OR (Ludovichi et al., 2003). This system was also called the excitatory juxtaglomerular association (EJGA) system, which is present in addition to the above discussed inhibitory juxtaglomerular association (IJGA) system connecting glomeruli mainly on one side of the glomerulus trough large type of DA – GABAergic JG neurons (Kosaka and Kosaka, 2011).

1.5.2. Olfactory Bulb in Teleosts

Laminar Organization and Cell Populations. As in all vertebrates, the olfactory bulb (OB) in teleosts is the first brain center where odor information is processed. Each glomerulus receives convergent input from sensory neurons expressing the same OR, resulting in the formation of combinatorial topologic maps upon ligand binding (Bally-Cuif and Vernier, 2010). While the general anatomical organization of the olfactory system is similar across vertebrates, the finer organization and neural connections within and outside of the OB may differ in detail between teleosts and mammals (Dryer and Graziadei, 1994; Firestein and Beauchamp, 2008).

In contrast to the mammalian OB, the teleostean OB is more diffusely organized in that it is composed of only 3 distinguishable layers: the outermost layer of the OB is the olfactory nerve layer (onl), the glomeruli (Glo) are embedded in the glomerular layer (gl) at the surface of the OB followed centrally by the granule cell layer called internal cell layer (icl) (Byrd, 2000; Fuller et al., 2006). However, there is no recognizable separate mitral cell layer between gl and icl as in mammals. In zebrafish, neuronal tracing using DiI and biocytin demonstrated that efferent cells (mitral cells/ruffed cells, see below) are located primarily in the gl and superficial icl, instead of forming a well – defined monolayer in the OB, (Fuller et al., 2006; Rink and Wullimann, 2004). Therefore, multi – layered cellular architecture in the OB is less complex in teleosts compared to mammals.

In addition to mitral cells, another type of OB output neuron not described in tetrapods, the so – called ruffed cells were observed in teleosts in the gl, which are possibly homologous to tufted cells (Firestein and Beauchamp, 2008; Kosaka and Hama, 1979; 1981; Rink and Wullimann, 2004; Satou, 1990). Ruffed cells have the distinctive characteristic that the initial portion of the axon carries a series of protrusions with a ruff – like appearance around the shaft (Kosaka and Hama, 1979). The ruffed cells, although similar in size and localization to mitral cells (MCs), constitute only a minor population (~5%) of total OB output neurons in zebrafish (Fuller and Byrd, 2005; Miyasaka et al., 2009) and receive no OSN innervation (Edwards and Michel, 2002).

The zebrafish OB has been described to have overall five neuronal phenotypes: MCs and ruffed cells (projection neurons), two types of local circuit inhibitory neurons, i.e. juxtaglomerular/periglomerular GABAergic and combined GABA/TH positive cells, plus the inhibitory (solely GABAergic) granule cell interneurons (Edwards and Michel, 2002; Rink and Wullimann, 2004; Fuller and Byrd, 2005; Fuller et al., 2006; Miyasaka et al., 2009).

Like in tetrapods, zebrafish MCs are also glutamatergic and represent the main type of OB output neurons, which also receive excitatory input from glutamatergic OSNs (Friedrich and Laurent, 2001). Zebrafish MC somata are ovoid, spherical, fusiform or elongated and therefore similar in their shapes to that of other teleosts, but they differ in their dendritic morphology (Fuller et al., 2006). In the zebrafish there are two mitral cell subtypes (Fuller et al., 2006). One population has a single primary dendrite, typically with a single dendritic tuft (unidendritic cells) and the other population has several dendrites arising from the cell body (multidendritic) with several dendritic tufts located near each other (Fuller et al., 2006). Unidendritic MCs make up ~69% of the total population, whereas multidendritic MCs comprise ~31% of the total population (Fuller et al., 2006). However, both types of MCs innervate only a single glomerulus rather than multiple glomeruli (Fuller et al., 2006).

Furthermore, by using genetic labeling techniques it has been demonstrated that MCs in zebrafish are heterogeneous in relation to transgene expression profiles and spatial distribution in the OB, for example dorsomedial and ventrolateral ones (Miyasaka et al., 2009).

This paper visualized the trajectories of MC axons in zebrafish at both single – cell and population levels and demonstrated that individual MCs project axons to multiple target regions in the telencephalon and MCs which relate to the same glomerulus do not necessarily display the same axon trajectory.

It has been shown that glutamate is the principal excitatory neurotransmitter in the zebrafish olfactory system as in tetrapods (Edwards and Michel, 2002). Thus, the excitatory synaptology of cells in the teleostean OB appears to be similar to mammals. Mitral cells receive

excitatory input from OSNs and communicate with granule cells at dendrodendritic synapses (Baier et al., 1994; Edwards and Michel, 2002; Friedrich and Laurent, 2001; Hansen and Zeiske, 1993; Satou, 1990).

However, as usual most neurons in the OB are inhibitory interneurons and express GABA. An estimate of 20'000 interneurons is given for adult zebrafish, compared to 1500 mitral cells (Wiechert et al., 2010). GABAergic interneurons play an important role in neuronal computations in the OB and they have a strong inhibitory influence on odor – evoked activity patterns already at early developmental stages (Friedrich and Laurent, 2001; Miyasaka et al., 2013; Niessing and Friedrich, 2010; Tabor and Friedrich, 2008; Wiechert et al., 2010). Moreover, interneurons mediate intraglomerular and interglomerular neuronal circuits in the OB that are thought to preprocess odor representations for higher – order computations (Bundschuh et al., 2012).

In zebrafish, at least three types of GABA – positive interneurons were visualized via immunocytochemistry (Edwards and Michel, 2002). The most abundant are the granule cells in the icl. The remaining GABAergic interneurons are divided in two groups based on tyrosine hydroxylase (TH) – immunoreactivity (Edwards and Michel, 2002). In the gl, local circuit inhibitory neurons are either GABA – positive and TH – negative ($GABA^+/TH^-$) or both GABA – positive / TH – positive ($GABA^+/TH^+$) (Edwards and Michel, 2002). Moreover, these TH – positive cells in the adult zebrafish gl were also described before to have extensive processes into glomeruli (Byrd and Brunjes, 1995). Thus, the modulatory neurotransmitter dopamine (DA) is coexpressed with GABA by a subpopulation of local interneurons indicated by the expression of TH, the rate – limiting enzyme in DA synthesis in mammals and zebrafish (Baker, 1990; Bundschuh et al., 2012; Parrish-Aungst et al., 2011).

The DA – interneurons in the OB are a large population of DA neurons conserved in all vertebrates, but the role of DA in olfaction is still unclear (Bundschuh et al., 2012). In the zebrafish OB, DA hyperpolarizes MCs, decreases their input resistance and reduces spontaneous firing (Bundschuh et al., 2012). GABA and DA are both released from DA – interneurons by electrical activity and inhibit MCs, but on different

timescales (Bundschuh et al., 2012). Bundschuh and colleagues suggested that GABAergic transmission is involved in dynamic odor processing and hypothesized that function of DA may be an “additive adaptation” that filters out slow variations in background odors without compromising sensitivity in other stimuli (Bundschuh et al., 2012).

Thus, the zebrafish olfactory bulb at least contains two types of excitatory projection (mitral/ruffed) cells and two types of juxtaglomerular cells: GABA+/TH+ interneurons and solely GABA+ interneurons, in addition to the centrally located (GABAergic) granule cells. However, it remains unclear in comparison to rodents (see above) whether there is a second, smaller type of GABA+/TH+ cells. Also the (glutamatergic) so – called external tufted cells, as well as various types of (presumably GABAergic) small axon cells (see above, after Kosaka and Kosaka, 2011) have not been identified in teleosts.

Furthermore, astroglial fibers have also been identified in the zebrafish OB on the basis of glial fibrillary acidic protein (GFAP) - immunoreactivity, a marker for astrocytes (Byrd and Brunjes, 1995). Edwards and Michel (2002) identified on the basis of sensitivity to glutamate analogs tentatively two small populations of glial cells.

Teleost Olfactory Bulb Primary Input and Glomerular Organization. Unlike rodents, teleosts have more than one OSN type in the main olfactory epithelium (see above). Since this thesis is concerned with identifying the pathway involved in imprinting, the organization of the zebrafish olfactory bulb with respect to its primary input shall be considered here.

One adult zebrafish OB was initially described to contain about 80 glomeruli and all glomeruli exhibit bilateral symmetry (Baier and Korsching, 1994). Of these ~80 glomeruli, 22 were identified to have the same position and morphology in different animals (classified glomeruli), whereas less than 10 of the remaining glomeruli were unclassified (not present in all animals) and around 49 glomeruli were diffusely organized in a dorsal cluster in the dorsal group (Baier and Korsching, 1994). Other bulbar glomerular groups are the medial, anterior, lateral and ventral

groups. Except for the anterior group, all other groups include classified glomeruli, and all but the dorsal group have unclassified ones. In addition, an “anterior plexus” (in anterior group) and “plexus of the lateral chain” (in lateral group) is present, which is a special feature of teleosts (Baier and Korsching, 1994; Kosaka and Hama, 1982).

Other researchers detected these glomeruli and glomerular fields in zebrafish described by Baier and Korsching with different labeling methods and used the nomenclature of individual glomeruli (Friedrich and Korsching, 1998; Gayoso et al., 2011; Koide et al., 2009; Sato et al., 2005) Braubach and colleagues (2012) used whole – mount immunocytochemistry to study the neurochemistry and anatomical organization of adult zebrafish OB glomeruli. They analyzed the distributions of G – protein α subunits, calcium binding proteins (Calretinin, S100) and general axonal markers to visualize selectively labeled OSNs, their axonal projections in the glomeruli and the detailed anatomical distribution of the glomeruli in the OB. They identified 27 classified glomeruli (within a total of ~140) in each OB, with most of the classified ones identified by Baier and Korsching (1994), but apparently showing many more unclassified glomeruli. For example, they identified ~15 glomeruli in the anterodorsal region, which was previously described as a fibrous, aglomerular nerve plexus (Baier & Korsching, 1994; Gayoso et al., 2011; reviewed in Braubach et al., 2012).

Therefore they suggested a revision of the glomerular nomenclature:

1. Dorsal groups: dorsolateral glomeruli (dlG)
   dorsal glomeruli (dG)
2. Ventral groups: ventromedial glomeruli (vmG)
   ventroposterior glomeruli (vpG)
   ventroanterior glomeruli (vaG)
3. Lateral group: lateral glomeruli (lG)
4. Medial groups: mediodorsal glomeruli (mdG)
   medial anterior glomeruli (maG)
   medial posterior glomeruli (mpG)

Unlike Baier and Korsching (1994), the bulbar glomerular fields are separated in dorsal, medial, lateral and ventral groups without further recognition of an anterior group. Moreover, Braubach and colleagues classified the glomeruli into two different types (Braubach et al., 2012). One type includes 27 large glomeruli distinguishable by their selective labeling with antibodies raised against calcium binding proteins or G – protein α subunits. These glomeruli are nearly invariant in number and arrangement and therefore individually identifiable glomeruli. The other type includes the remaining glomeruli of 82% of total glomeruli number. They are smaller on average and are located in units which cannot be distinguished from one another and were labeled with both anti – calretinin and anti - $G\alpha_{s/olf}$ antibodies (Braubach et al., 2012). However, despite the different number of identified glomeruli by different methods (~ 80 glomeruli by Baier and Korsching, 1994; ~ 140 glomeruli by Braubach et al., 2012) many of these glomeruli are arranged in a stereotyped pattern that is conserved between individuals of the same species.

Subregions of the zebrafish OB are innervated by distinct types of OSNs that differ in their morphology, their expression of defined OR families, and their signal transduction components (Baier and Korsching, 1994; Sato et al., 2005; Koide et al., 2009; Braubach et al., 2012; reviewed in Miyasaka et al., 2013). Thus, odors are represented in the OB by a distributed code across the glomeruli (Friedrich and Korsching, 1997) innervated by different OSN types with various ORs that bind particular ligands.

In zebrafish the presynaptic activity in glomerular fields has been shown via labeling of primary afferents with calcium – sensitive dye and postsynaptic activity via electrophysiological studies and two – photon Ca^{2+} imaging (Friedrich et al., 2004; Friedrich and Korsching, 1997b; 1998; Friedrich and Laurent, 2001; 2004; Yaksi et al., 2007; Yaksi et al., 2009). Visualization of axonal projections in transgenic zebrafish revealed that ciliated OSNs project their axons to almost all over the dorsal region (dG) and the ventromedial portion (vmG) of the OB, whereas microvillous OSNs projected their axons exclusively to the ventrolateral region (lG) (Koide et al., 2009; Sato et al., 2005).

Amino acids and nucleotides, as food odors in teleosts, are bound mostly by microvillous OSNs expressing V2R – type ORs and transient receptor channel C2 (TrpC2) (Hansen et al., 2003; Luu et al., 2004; Sato et al., 2005; Speca et al., 1999; Yoshihara, 2008) and activate a chain of glomeruli located on the ventrolateral side of the OB (Friedrich and Korsching, 1997; reviewed in Yoshihara, 2008; Sato et al., 2005; Koide et al,. 2009; Yaksi et al., 2009). In contrast, bile acids, regarded as sex or migratory pheromones in sea lamprey (Li et al., 2002; Sorensen et al., 2005; Yoshihara, 2008), activate a cluster of glomeruli in the dorsomedial part of the zebrafish OB (Friedrich and Korsching, 1998; reviewed in Yoshihara, 2008). This dorsomedial cluster represents the target glomeruli of ciliated OSNs (Sato et al., 2005) expressing $G\alpha_{olf2}$ and probably ORs. These correlations were also revealed by demonstrating in transgenic zebrafish that tetanus neurotoxin (blocks synaptic transmission) selectively expressed in microvillous OSNs blocks attraction to amino acids while in ciliated OSNs it blocks bile acid response (Koide et al., 2009).

Thus, these data strongly suggest that microvillous OSNs innervating the lateral chain glomeruli are important for perception of amino acids, probably leading to feeding behaviors in zebrafish (Koide et al., 2009). Although it is not entirely clear what type of behavioral responses are caused by bile acids in teleosts, they are potent odorants that activate ciliated OSNs in zebrafish (Yoshihara, 2008).

The coarse organization of the glomerular fields is present already in early larvae and maintained through adulthood (Sato et al., 2005; Braubach et al., 2012; reviewed in Miyasaka et al., 2013).

Friedrich and colleagues visualized activity patterns across thousands of individual neurons in the intact OB of zebrafish over time using two-photon calcium imaging (Friedrich and Laurent, 2001, 2004; Yaksi et al., 2007; Bundschuh et al., 2012). They could demonstrate that mitral cells responding to amino acids are located predominantly in a ventrolateral subregion of the OB that contains probably ~200 MCs (Edwards and Michel 2002; Friedrich and Korsching 1997, 1998; reviewed in Friedrich and Laurent, 2004; Yaksi et al., 2009). They found that the slow temporal change of activity patterns across MCs during odor

presentation results in a decorrelation of initially similar activity patterns, thereby enhancing their discriminability (Friedrich and Laurent, 2001). Furthermore, bile acids activate MCs mainly in the medial OB, along with some MCs in the posterior – lateral OB. Thus MCs responses to amino acids and bile acids are clearly segregated and these response patterns are consistent with the distributions of activated glomeruli (Yaksi et al., 2009).

However, although the axonal projections of microvillous OSNs and ciliated OSNs in the zebrafish OB and the presynaptic activity in glomerular fields and the nearby output neurons (MCs) by amino acid stimuli or putative social pheromones emerge from these OSNs has been revealed, the situation in the specific third type of OSNs, the crypt cells, has not yet been resolved.

Recent studies used the expression of different calcium – binding proteins visualized the three types of OSNs in the epithelium and additional application of fluorescent tracing substance DiI to characterize axonal projections to the OB and its telencephalic targets in zebrafish (Braubach et al., 2012; Gayoso et al., 2012; Gayoso et al., 2011). Double immunofluorescence for calretinin (CR) and $G\alpha_{olf}$ indicated that most CR – immunoreactive cells are ciliated OSNs (Braubach et al., 2012; Gayoso et al., 2011; Germana et al., 2007), and it has been shown that S100 is highly expressed in the crypt cells (Gayoso et al., 2012; Gayoso et al., 2011; Germana et al., 2004; Germana et al., 2007; Sandulescu et al., 2011).

Another report from the Anadón lab demonstrated in zebrafish via application of DiI that the only bulbar region that received afferents from the crypt cells (and scant bipolar OSNs) are glomeruli in the dorsomedial field (Gayoso et al., 2012). Whereas mainly slender bipolar cells (presumably ciliated OSNs) innervate glomeruli in the dorsolateral field (Gayoso et al., 2012) and in the ventromedial field (Gayoso et al., 2011). Furthermore, mainly plump, short bipolar OSNs (presumably microvillous OSNs) innervate glomeruli in the ventrolateral field (Gayoso et al., 2011).

Olfactory Bulb Projections. As in all vertebrates, olfactory information enters the teleostean telencephalon via OB projections, arising from the projection neurons and are generally indicated as the secondary olfactory pathway.

However, the topology of the teleostean telencephalon differs from all other vertebrate groups (Nieuwenhuys and Meek, 1998; Wullimann, 1997). Whereas in other vertebrate groups the telencephalic hemispheres develop by paired evagination and thickening of the most rostral embryonic neural tube, in ray – finned fish (including teleosts) the telencephalic hemispheres develop by eversion (Wullimann, 1997). During this process, the roof plate of the embryonic telencephalon extends laterally and causes the paired alar plates which form the hemispheric walls to roll out lateroventrally (Wullimann et al., 1996). Later, in teleosts a new developmental model, the so – called Partial Eversion Model, has been generated (Wullimann and Mueller, 2004).

In teleosts the most rostral telencephalic divisions are the paired OBs and the remaining telencephalic hemispheres are subdivided into the dorsal telencephalic area (D) which is homologous to cortical structures of land vertebrates (pallium) and the ventral telencephalic area (V) corresponding to the subpallium (Mueller and Wullimann, 2009; Wullimann and Mueller, 2004). It has been demonstrated in various teleostean species that the dorsal subpallial nuclei (Vd, Vc), represent the striatal formation whereas the ventral subpallial nuclei (Vv, Vl) correspond to the septal formation (Wullimann and Mueller, 2004).

The secondary olfactory projections reach most nuclei in the ventral telencephalic area (V, includes Vv, Vs, Vd and Vl) but only selected zones (Dp, Dlv) of the dorsal telencephalic area (D) and the preoptic (PO) and posterior tubercular regions (PT) in the diencephalon (Nieuwenhuys and Meek, 1998; Mueller and Wullimann, 2004, see Fig. 6.). Moreover, a large subpopulation of MCs innervating the medial glomerular cluster project axons directly and asymmetrically to the right habenula (Ha) (Miyasaka et al., 2009; see Fig. 6).

Another notable difference between mammalian and teleostean olfactory systems is that mammals have a single olfactory tract per main

OB, whereas fish have both a lateral and a medial olfactory tract (LOT and MOT, respectively) (Fuller et al., 2006). The MOT projects predominantly to the ventral telencephalic area and the LOT to the dorsal telencephalic area (Nieuwenhuys and Meek, 1998). Several studies in fish suggested that the MOT plays a significant role in processing of pheromonal information, thus mediates reproductive behavior, while the LOT conveys information about food and processes other kinds of odorants (Demski and Dulka, 1984; Fuller et al., 2006; Hamdani et al., 2001; Sorensen et al., 1991; Stacey and Kyle, 1983; Weltzien et al., 2003). Axons of MCs project to either the MOT or LOT, due to the location of the cell on the medial or lateral side of the OB, respectively (Fuller et al., 2006). Moreover, it has been demonstrated that the medial OB has a larger number of multidendritic MCs than the lateral OB (Fuller et al., 2006).

Gene expression analyses and adult connectional (hodological) data of brain regions have established tentative homologies between a variety of forebrain areas in teleosts and mammals (Northcutt, 2006; Wullimann and Mueller, 2004). They are consistent with Dp being homologous with the olfactory (lateral) pallium (piriform cortex), with Dl being homologous to the hippocampus, and Dm being homologous to the pallial amygdala (Wullimann, 2009).

In mammals, the map of OR expression in the OB is not preserved by the secondary olfactory projection to piriform cortex (Miyasaka et al., 2013; Stettler and Axel, 2009; Yaksi et al., 2009). It has been suggested that neurons in piriform cortex integrate inputs from topographically and functionally different MCs and respond to odors with widespread, stimulus – specific activity patterns (Friedrich et al., 2010; Poo and Isaacson, 2009; Stettler and Axel, 2009).

In adult zebrafish, bulbar projections to Dp run in both the LOT and MOT (Miyasaka et al. 2009; Gayoso et al. 2011, reviewed in Gayoso et al., 2012). No clear segregation between fibers arising from the different glomerular fields of the OB exist in Dp and, thus, pathways conducting different olfactory information converge in this area (Gayoso et al., 2012). Functional analysis by optical imaging of the neurons in Dp reveal that Dp integrates synaptic input from functionally diverse MCs via excitatory and

inhibitory synaptic pathways (Yaksi et al., 2009). Therefore, the lack of chemotopy and powerful inhibition has been observed in zebrafish Dp, which is consistent with recent observations in mammalian olfactory cortex (Friedrich et al., 2010; Poo and Isaacson, 2009; Stettler and Axel, 2009).

Moreover, Anadón and colleagues described the secondary olfactory projections arising from the dorsomedial and dorsolateral glomerular fields to Dp and Vv (Gayoso et al., 2012) whereby bulbar efferent neurons (MCs) project bilaterally to Dp (Gayoso et al., 2012). In contrast, only projections from MCs in the dorsomedial glomerular field (bulbar region that mainly receives afferents from the crypt cells) were shown lateral to the supracommissural nucleus of the ventral telecephalic area (Vs). It has been hypothesized that Vs represent part of the subpallial (medial) amygdala (Northcutt, 2006; Northcutt and Braford, 1980; Wullimann and Mueller, 2004).

In a functional context, the olfactory pallium (Dp) is responsible for general odor analyses, while the medial amygdala (Vs) is related to socially relevant olfactory signals (Northcutt, 2006; Northcutt and Braford, 1980; Wullimann and Mueller, 2004). In mammals the amygdala is recipient of vomeronasal information, often involved with processing of pheromones (Martinez-Garcia et al., 2009). Although teleosts do not have a separate vomeronasal organ in addition to the MOE (Eisthen, 1997; 2004), they do have OSNs carrying the corresponding class of receptors (Hansen et al., 2004; Hansen et al., 2003). Therefore, the olfactory system of teleost is able to detect pheromones and to mediate pheromone effects and likely involves the medial amygdala (Vs).

Additionally, in teleosts some primary olfactory fibers from the MOE project beyond the OB, so – called extrabulbar primary olfactory projections (EBOPs) (Anadon et al., 1995; Hofmann and Meyer, 1995; Honkanen and Ekstrom, 1990; Huesa et al., 2000). Tracing experiments indicate that the EBOPs of the zebrafish are largely bilateral and run through the ventral region of the OB towards the ventral telencephalic area (subpallium) into the neuropil of the ventral nucleus (Vv) and dorsolaterally to the anterior commissure (Gayoso et al., 2011).

Table 3: OSN characterization

Microvillous OSNs (=plump, short bipolar OSNs")

Receptors: V2R – like olfC + $G\alpha_o$, V1R – like ora + $G\alpha_i$, , TrpC,2

Ligands: amino acids / nucleotides

Primary projection in OB: ventrolateral region

Secondary (telencephalic) targets: Dp, Vv

Ciliated OSNs (="slender bipolar OSNs")

Receptors: ORs and TAARs + $G\alpha_{olf}$

Ligands: bile acids

Pimary projection in OB: ventromedial and most of dorsal region

Secondary (telencephalic) targets: Dp, Vv

Crypt cells

Receptors: V1R – like ora4, $G\alpha_i$

Ligands: ?

Primary projection in OB: one dorsomedial glomerulus

Secondary (telencephalic) targets: Dp, Vv + Vs

The teleostean OB receives not only primary olfactory input, but also input from telencephalic regions through the lateral part of the MOT (Nieuwenhuys and Meek, 1998). This input originates from ipsilateral neurons in the ventral and dorsal posterior (Dp) telencephalon and from neuron subpopulations in the dorsal telencephalic area, plus from the preoptic region (Po), the nucleus posterior tuberis (TP), a preglomerular nucleus, the locus coeruleus (LC) and the raphe nuclei (Nieuwenhuys and Meek, 1998).

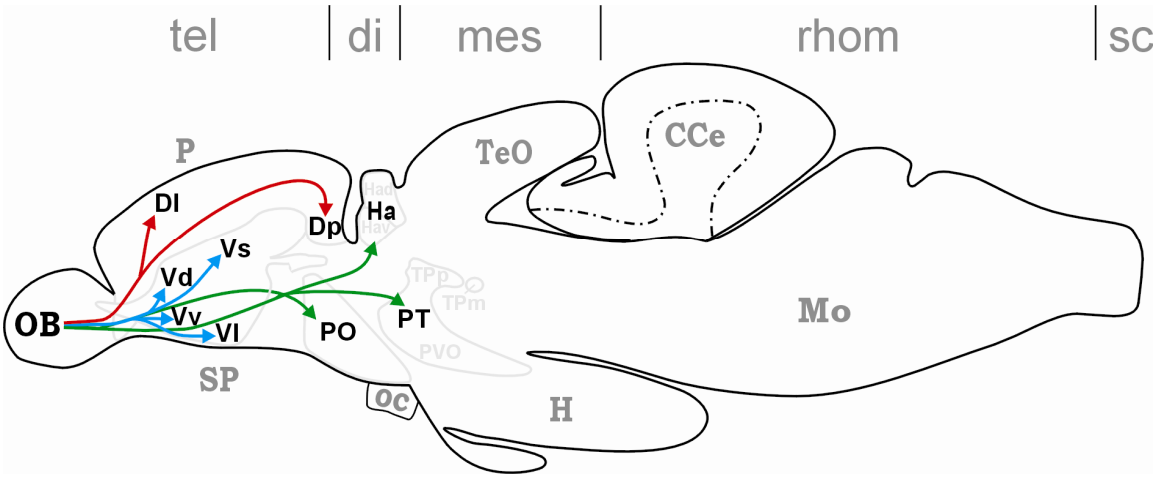

Fig. 6. Secondary olfactory pathways in zebrafish. Red: input to pallial area (Dlv and Dp). Blue: input to subpallial areas (Vd, Vv, Vl, Vs). Green: input to diencephalon (PO, PT and Ha). See text for details and list for abbreviations.

2. Aims of the Thesis

This thesis' focus is on the zebrafish olfactory system to identify brain areas involved in olfactory imprinting related to kin recognition. Olfactory imprinting is a special form of unconditioned learning in which olfactory information is acquired during a defined developmental time window and then used in specific behavioral contexts later in life. The induction of gene expression is generally regarded as one of the key steps underlying long – lasting forms of memory which rely on changes in the strength and structure of synaptic connections (Hawkins et al., 2006). Immediate early genes (IEGs) are a class of genes that are rapidly (within minutes) and transiently activated in response to neuronal activity and thereby identified as a part of the transcriptional regulation that accompanies long – lasting forms of synaptic plasticity (Pinaud and Tremere, 2006).

(1) One aim of my thesis is to use IEG expression as a marker for neuronal activation in the zebrafish brain and to study these expression patterns to reveal the activation of neuronal circuitry involved in the processing of olfactory imprinting signals. In many groups of vertebrates IEGs such as *cfos* and *egr1* (early growth response gene-1) have proven to be useful markers in the context of long term potentiation (LTP) and memory (Pinaud and Tremere, 2006). Therefore, I analyze in my thesis for the first time the basal expression of *cfos* and *egr1* in larval and adult zebrafish brains to provide background information for experiments involving olfactory activation or deprivation.

(2) A second aim of my thesis is to investigate the correlated expression of IEGs and tyrosine hydoxylase as a marker for dopaminergic neurons. In rodents, *egr1* mediated tyrosine hydroxylase (TH) expression has been shown (periglomerular cells of OB and medial amygdale) (Akiba et al., 2009; Northcutt and Lonstein, 2009). Therefore, I will survey co – expression of these two markers in adult zebrafish brains with emphasis on the OB and medial amygdala, as these two areas are candidates for being activated in kin recognition in zebrafish. In this context, a new fluorescent *in situ* hybridization (FISH) protocol on zebrafish sections has

to be established which allows for unambiguous identification of double – labeled cells. This is the appropriate methodological tool to determine the potential role of IEGs in odor perception and kin recognition by analyzing *egr1* and *cfos* gene expression in dopaminergic neurons of imprinted and non – imprinted larval or adult zebrafish brains.

(3) A third aim is to demonstrate down – and up - regulation of IEG expression via odor – deprivation or via odor – stimulation using various olfactory test procedures (including tests for kin water recognition). I will test odor – deprivation through temporary knockout of olfactory receptor cells using a lesion – solution in order to show a selective down – regulation of *egr1* and TH co – expression in the same periglomerular cells in OB. Furthermore, I will develop different olfactory test procedures to generate up – regulation of IEG expression and thus to determine the central olfactory system activity triggered by olfactory (including kin water) clues in larvae and adult imprinted females.

(4) Moreover, I will expand the study of neuronal activity marker by demonstrating phosphorylated extracellular signal – regulated kinase (pErk), another part of the neuronal response mechanism accompanying long – lasting forms of synaptic plasticity that underlies learning and memory (Zhang et al., 2003). In neurons, binding of signaling molecules or synaptic release of a transmitter to receptors of a dendrite activate the mitogen – activated protein kinase (MAPK) signaling pathway which leads to Erk/MAPK phosphorylation and translocation into the nucleus where the Erk/MAPK activation promotes immediate early gene expression. The IEG proteins promote or inhibit transcription of other genes (for example TH), which leads to long lasting functional changes in the neuron (see Fig.7). Thus, my thesis looks at functionally related markers in the neuronal activation pathway: the expression of phosphorylated Erk, the immediate early genes *egr1* and *cfos* and as a target gene TH.

(5) A final aim of my thesis is to provide new insight about differential olfactory zebrafish subsystems characterized by different calcium binding proteins (CBPs). Therefore I visualize expression patterns of CBPs calretinin -, calbindin -, parvalbumin - and S100 – immunoreactive cells and fibers in epithelium and OB of larvae and adult zebrafish.

3. Materials and Methods

3.1. Study Animals

3.1.1. Animals and Rearing Conditions

In this study, wild type zebrafish from the Gerlach lab (Carl von Ossietzky University Oldenburg, Department of Biology and Environmental Sciences, Animal Biodiversity and Evolutionary Biology, Oldenburg, Germany) and from our own facility were used. In Oldenburg, zebrafish were kept in mixed-sex groups of 8-15 animals in 9 Liter aquariums in Aquatic Habitats (ZF0601 Zebrafish stand-alone system, USA) at Oldenburg University. Conditions were maintained at 26°C water temperature and an 11:13h light/dark cycle. Animals were fed twice daily with live brine shrimps (*Artemia*), dried blood worms or standard fish food flakes.

For breeding, each female was housed with one male in a 3 Liter tank. In the afternoon, egg dishes covered with a mesh were put into the tanks and examined at the following morning.Embryos and larvae originating from a clutch of a single pair of adult fish were reared together in glass dishes. They were kept under the same light and temperature regime as the adults but in an incubator (SANYO MIR, 553 Incubator). After hatching and depletion of the yolk (on 5 days postfertilization, dpf) larvae were fed daily with live paramecia *ad libitum*.

In Munich, zebrafish were kept in mixed-sex groups of 5-15 animals in 8 Liter aquariums in Aquatic Habitats (Zeb TEC, Standalone Aquatic System, Techniplast, Deutschland) at Ludwig Maximilians-Universität (LMU). Animals were kept at 28°C water temperature and an 14:10h light/dark cycle and fed twice daily with standard fish food flakes. Animals used in this study were treated according to the German regulations on Animal Protection (Deutsche Tierschutzgesetz).

3.1.2. Animal Preparation

Adult zebrafish were anesthetized in tricaine methanesulfonate (MS222; Sigma-Aldrich; 500 mg/l) in tank water. They lost control over balance after around 15 s, and did not react to tail pinching with forceps after around 40

s. The animals were then immediately killed by decapitation. Brains were exposed dorsally by removing the skull and fixed with 4% paraformaldehyd (PFA) in Sörensen phosphate buffer at 4°C overnight before being removed from the skull.

Larvae were killed with an overdose of MS222 and fixed with cold 4% PFA overnight. Following cryoprotection in 30% sucrose solution overnight, adult brains and whole larvae were embedded in TissueTek (A. Hartenstein GmbH, Germany). Adult brains were cut into 30 µm sections for expression analyses of *egr1*, *cfos*, pErk and calcium binding proteins (CBPs). For comparison of CBP expressions the olfactory bulb and olfactory epithelium of adult zebrafish were cut in 14 µm sections, while larvae were only cut into 14 µm sections on a freezing microtome.

3.2. *In Situ* Hybridization and Immunohistochemistry

3.2.1. Digoxigenin Labeled Riboprobe Synthesis for *In Situ* Hybridization

Plasmids providing the template for riboprobe synthesis were donated to us (see below) on Whatman paper and recovered in 10mM Tris (pH8). Transformation of plasmid in *Escherichia coli* bacteria (DH5α strain), was done via heat shock transformation at 42°C, before amplification of bacteria on ampicillin plates (100 µg/ml) overnight at 37°C. We lysed bacteria under alkaline conditions and used small-scale isolation of plasmid DNA from bacteria (minipreparation). Afterwards, plasmid DNA was purified with phenol – chloroform extraction and concentrated via ethanol precipitation. Concentration of DNA was determined using a NanoDrop Spectrophotometer and in addition with an agarose gel.

Plasmids were linearized by restriction digest and sense and antisense RNA probes were then synthesized and labeled with digoxigenin (DIG)-UTP by *in vitro* transcription according to the manufacturer's instructions (DIG RNA Labeling Kit; # 11175025910, Roche Diagnostics).

Riboprobe Synthesis of egr1. Full-length *egr1* cDNA, inserted into pGEM-T Easy Vector (Promega), was kindly donated to us by Prof. H.-J.

Tsai, National Taiwan University (see Hu et al, 2006). The plasmid was digested with SacII and the DIG labeled riboprobe was synthesized by *in vitro* transcription with SP6 RNA polymerase for *egr1* antisense and digested with SalI and synthesized by *in vitro* transcription with T7 for sense as control.

Riboprobe Synthesis of cfos. Prof. Dr. Reinhard Köster, Technische Universität Braunschweig kindly sent to us *cfos* cDNA, inserted into pCR II Vector (Invitrogen) (Kuhn and Koster, 2010). The plasmid was digested with NotI and the DIG labeled riboprobe was synthesized by *in vitro* transcription with SP6 for *cfos* antisense. The sense control was digested with BamHI and synthesized by *in vitro* transcription with T7.

3.2.2 *In Situ* Hybridization (ISH)

Cryosections were washed in phosphate buffered saline (PBS), rinsed in 50% ethanol and dried for 30 minutes under the hood. Then the sections were incubated with the respective digoxigenin (DIG)-labeled RNA probe (riboprobe) in hybridization solution (5× SSC, 50% formamide, 0.5 mg/ml yeast tRNA, 50 µg/ml heparin, and 0.1% Tween 20, 9.2mM citric acid at pH 6.0 in DEPC-H_2O) at 68°C overnight. After stringent washes in HYB/SSC wash buffer (32.5% formamide, 6.5x SSC, 0.05% Tween 20 in dH_2O) for 1h at 68°C, in 2x SSC (2 times 30 min each) at 68°C, in 0.5x SSC (2 times 30 min each) at room temperature and in PBT (PBS + 0.1% Tween 20) (2 times 30 min each) at room temperature, the sections were incubated in blocking buffer (2% normal goat serum, 2% bovine serum albumine in PBT) for 1h, and incubated with anti-DIG-alkaline phosphatase (anti-DIG-AP ab; Roche Diagnostics) diluted 1:2000 in blocking buffer at 4°C overnight. After washing in PBT, the sections were equilibrated in NTMT buffer (100mM NaCl, 0.1% Tween 20, 50 mM $MgCl_2$ 100mM Tris [pH 9.5]) for 10 min at room temperature and then stained with nitroblue tetrazolium chloride (NBT; 225 µg/ml) and 5-bromo-4-chloro-3-indolyl-phosphate (BCIP; 175 µg/ml) in NTMT in darkness to visualize the anti-DIG-AP. The staining reaction was stopped by washing sections in PBT when good signal to background ratio was achieved.

3.2.3. Immunohistochemistry (IHC)

Incubations were all done in a humid chamber. After washing off TissueTek in cryosections in PBS, the endogenous peroxidase activity was first blocked with 0.3% H_2O_2 in PBS for 30 min at room temperature and the sections were washed again in PBT (PBS + 0.1% Tween 20). The sections were then incubated with blocking buffer (2% normal goat serum, 2% bovine serum albumine, 0.2% Tween 20, 0.2% Triton X-100 in PBS) for 1h at room temperature before exposition to a primary antibody diluted in blocking buffer at 4°C for 1 - 3 days (dilution and incubation time see table 1). After washing, the sections were again incubated with blocking buffer for 1h at room temperature before the secondary antibody was applied at 4°C overnight.

DAB Staining. For immunohistochemistry with 3,3`- diaminobenzidine (DAB) a biotinylated secondary antibody (see Table 2) was used at 4°C overnight. Sections were washed and incubated in avidin–biotin–peroxidase complex (ABC Kit; Vector Laboratories Inc.) for 1h at room temperature. After pre-incubation in DAB solution (SIGMA*FAST*™ 3,3`-Diaminobenzidine tablets; Sigma-Aldrich, #D4418, diluted in PBS) for 20 min, the immunolabeling was visualized by adding 1µl H_2O_2. The reaction was stopped by transferring the sections into PBT. After washing in PBT, sections were mounted on the glass slides with Aqua-Poly / Mount (APM; Polysciences, Inc.)

Immunofluorescence. Endogenous peroxidase activity was blocked with 0.3% H_2O_2 in PBS for 30 min at room temperature and afterwards washed in PBT. Sections were blocked with blocking buffer (2% normal goat serum, 2% bovine serum albumine, 0.2% Tween 20, 0.2% Triton X-100 in PBS) for 45-60 min at room temperature in a humid chamber and incubated with the primary antibody (Table 1) diluted in blocking buffer at 4°C 1 – 3 x overnight.

Sections were washed again in PBT and blocked with the same blocking buffer as for the primary antibody. Afterwards they were incubated with secondary antibody (Table 2) diluted in blocking buffer at

4°C overnight. Finally sections were washed in PBT and counterstained with DAPI (4'- 6- Diamidino-2-phenylindole; Carl Roth) for 3 min at room temperature and washed in PBT. Slides were mounted with Vectashield (Vectorlabs).

3.2.4. Fluorescence *In Situ* Hybridization (FISH) /Immunofluorescence Double (Triple) Labeling

Riboprobe was prepared under the same conditions as with conventional *in situ* hybridization (ISH). For FISH we used the fluorophore-labeled Tyramide Signal Amplification System (TSA Plus Cyanine 3 System, Perkin Elmer). After incubation of the sections with DIG-labeled cRNA probe in hybridization solution at 68°C overnight, stringent washing in HYB / SSC wash buffer for 1h at 68°C, in 2x SSC (2 times 30 min each) at 68°C, in 0.5x SSC (2 times 30 min each) at room temperature and in PBT (2 times 30 min each) at room temperature followed (see above).

Then, non-specific binding sites were blocked with TNB (100mM Tris [pH 7.5], 150 mM NaCl and 0.5% blocking reagent (PerkinElmer) for 1h at room temperature in humid chamber and then incubated with anti-DIG-horseradish peroxidase (anti-DIG-POD ab; Roche Diagnostics) at a concentration of 1:1000 in TNB blocking buffer overnight at 4°C in humid chamber. After washing in TNT (100 mM Tris [pH 7.5], 150 mM NaCl and 0.05% Tween20) sections were equilibrated in Amp Dil buffer (Perkin Elmer) for 5 min at room temperature in darkness. The following steps were performed in darkness. Sections were incubated with TSA solution (Amp Dil buffer with Tyramide (1:50; Perkin Elmer) for 1h at room temperature and afterwards washed in TNT.

Sections were post-fixed in 4 % PFA for 20 min at room temperature and washed in PBT at room temperature.

For double (or triple) -labeling, endogenous peroxidase activity was blocked with 0.3% H_2O_2 in PBS for 30 min at room temperature, followed by washes in PBT. Sections were blocked with blocking buffer (2% normal goat serum, 2% bovine serum albumine, 0.2% Tween 20, 0.2% Triton X-100 in PBS) for 45-60 min at room temperature in a humid chamber and

incubated with the primary antibody (or two antibodies; see table 1) diluted in blocking buffer at 4°C three times overnight.

After washing in PBT, sections were blocked with the same blocking buffer as for the primary antibody and afterwards incubated with secondary antibody (see table 2) diluted in blocking buffer at 4°C overnight. The next day, sections were washed in PBT and counterstained with DAPI (4'- 6- Diamidino-2-phenylindole; Carl Roth) for 3 min at room temperature. In a final step, sections were washed in PBT and slides were mounted with Vectashield (Vectorlabs).

3.2.5. Characterization of the Antibodies

During this study, various antibodies were used. The following table provides the total list of used primary (1st), antibodies and lists in detail the antigen and species in which the antibody was raised, the manufacturer, the catalog number (cat. no.) and the used concentration. Additionally, particular applications of some antibodies were described.

Table 4: Overview of 1st antibodies used in this study

Antigen	Species antibody was raised in, manufacturer, cat. no	Dilution	Particular application
Phospho – p44/42 MAPK (Erk1/2)	Rabbit monoclonal, NEB (Cell Signaling), # 4370S	1:200	Permeablized sections with 100 % methanol at – 20°C for 10 min
Tyrosine hydroxylase (TH)	Mouse monoclonal, AbCys (Millipore), # VMA318	1:300	
S100	Rabbit polyclonal, DAKO, # Z0311	1:400	
Calbindin1	Mouse monoclonal, SYSY, # 214011	1:200	
Calretinin	Rabbit polyclonal, SWANT, # 7699/3H	1:500	
GFAP	Rabbit polyclonal, ABCAM, # 7260	1:500	
Parvalbumin	Mouse monoclonal, Millipore, # MAB1572	1:2000	
Phospho – histone H3 (PH3)	Rabbit polyclonal, Millipore, # 06-570	1:250	

Various secondary (2nd) antibodies used to determine the location of the 1st antibodies (or digoxigenin) in the sections generated through different methods like *in situ* hybridization (ISH), fluorescence *in situ* hybridization (FISH), immunohistochemistry (IHC) and immunofluorescence (IF) with specific corresponding conjugates were used. In Table 2, the different conjugates, antibodies and species in which antibody was raised, the manufacturer, the catalog number (cat. no.) and used concentration of the antibody is shown. Particular applications and the methods secondary antibodies were used for are listed on the right.

Table 5: Overview of 2nd antibodies used in this study

Conjugate	Species antibody was raised in, manufacturer, cat. no	Dilution	Particular application and applied method
Biotinylated IgG	Goat anti - mouse, Vector Laboratories Inc., # BA-9200	1:200	Visualized by DAB and H_2O_2 in IHC
Alexa 488	Donkey anti - mouse, Mol Probes, # A21202	1:200	Immunofluorescence (IF)
Alexa 488	Donkey anti - rabbit, Mol Probes, # 21206	1:200	IF
DyLight 488	Donkey anti - rabbit, Dianova, # 711-486-152	1:400	IF
Cy3	Donkey anti - rabbit, Dianova, # 711-165-152	1:200	IF
Cy3	Donkey anti - mouse, Dianova # 711-166-151	1:200	IF
DyLight 649	Donkey anti - rabbit, Dianova, # 711-496-152	1:100	IF
DIG-horseradish peroxidase (DIG - POD	Anti – DIG – POD ab, Roche Diagnostics, # 11207733910	1:1000	used for digoxigenin labeled riboprobe in FISH
DIG-alkaline phosphatase (DIG - AP	Anti – DIG – AP ab, Roche Diagnostics, # 11093274910	1:2000	used for digoxigenin labeled riboprobe in ISH

3.3. Experimental Setups and Equipment

All experiments involving imprinted/versus non-imprinted larvae, tests using olfactory stimuli or Triton X-100 treatment were performed in Oldenburg in Prof. G. Gerlach's laboratory.

3.3.1. Imprinted and Non – Imprinted Larvae

The imprinted larvae were reared with their siblings in kin groups up to at least 8dpf when the imprinting phase is completed (see Introduction). Thus, they were exposed to physical, visual and olfactory cues of their siblings.

Additionally, larvae from the same clutch were isolated directly after fertilization by placing them each separately into glass-beakers (diameter: 3 cm) filled with 10 ml plain tank water, without any physical, visual or olfactory cues of their sibling. Furthermore, the same amount of food (*Paramecium caudata*) was added to both test and control larva. Both kinds of larvae were kept under identical conditions in an incubator (SANYO MIR, 553 Incubator) at 26°C.

3.3.2. Preparations of Odor Stimuli

Odorless Water. Odorless water, as basis for dilution of odor stimulus and as control during experiments, was created by freshwater staled for at least 3 days in a reservoir and afterwards placed in an incubator to warm up to 26°C overnight.

Kin Water. Larvae, used for this study, were full siblings from different pairs, and were tested for kin recognition in previous olfactory flume choice tests (see above) and showed preference for kin water.

By using full-siblings of the test larvae, kin – conditioned water was prepared by placing 20 larvae per 120 ml odorless water in an incubator at 26°C for at least 24 hours. Thereby it was assumed that stimulus water contained a high concentration of urinary odor cues of kin.

Non – kin water was prepared by using larvae of unrelated non – kin group from same day of fertilization as test larvae from kin group. Apart from that, they were treated under same conditions and also 20 larvae per 120 ml odorless water were placed together for at least 24 hours in an incubator at 26°C.

MHC Peptide Mix. The MHC peptide mix was kindly donated to us by Prof. Gabriele Gerlach, Carl – von – Ossietzky Universität Oldenburg,

Germany, and MHC peptide mix water (1.25 nM / liter in odorless water) was prepared freshly before tests started.

Larvae were isolated and imprinted on this MHC peptide mix during imprinting phase (6 – 7 dpf). Afterwards larvae were tested for preference for MHC peptide mix in olfactory flume choice tests (see above) and showed preference for the peptide mix compared to odorless water.

Adult zebrafish used in this study were offspring of the first generation of these MHC peptide mix imprinted zebrafish and also tested as larvae in olfactory flume choice tests showing preference for MHC peptide mix in comparison to odorless water. Thus we have verified whether such test fish are able to recognize MHC peptide mix and thus are suitable for odor stimulation treatment with MHC peptide mix.

Amino Acid L – Alanine. In fish amino acids are have been identified as a class of natural odorants and it was shown that amino acids induced glomerular activity patterns in the olfactory bulb by repeated application of amino acids (Friedrich and Korsching, 1998 and Rainer Friedrich, pers. comm). Therefore, we used 10µM L – alanine (Sigma, # A7627) diluted in odorless plain water to provide odor stimulation with an amino acid for adult zebrafish.

3.4. Test Procedure

To identify the brain areas involved in olfactory imprinting I tried to mark neuronal activity in differently treated zebrafish larvae and adults. Therefore I used the Erk / MAPK (Mitogen – Activated Protein Kinase) signaling pathway and associated immediate early gene (IEG) expression and as a target gene tyrosine hydroxylase (TH) (Fig. 7). One aim of my thesis is to visualize neuronal activity by up – and downregulation of expression of IEGs *egr1* and *cfos* and phosphorylated Extra cellular – signal regulated kinase (pErk) expression via odor stimulation or odor deprivation.

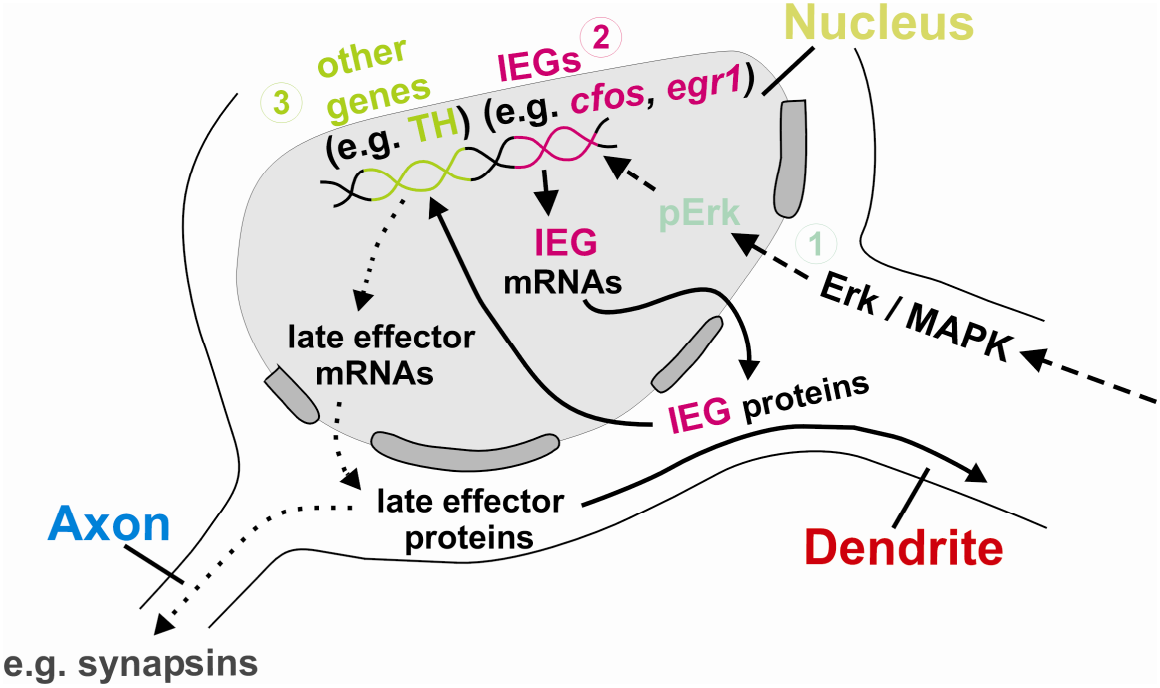

Fig. 7. The Erk / MAPK signaling pathway in neurons. The phosphorylated Extra cellular – signal regulated kinase (pErk) is one of four MAPK (Mitogen – Activated Protein Kinase) groups differentiated by their structure and function.The MAPK/Erk pathway is activated by ligand or transmitter binding to receptors (e.g. GPCRs) of the neuron dendrite. Activation occurs through a cascade of upstream kinases; (which finally leads to phosphorylation of Erk. (1) Activated (p)Erk translocates to the nucleus and (2) promotes the expression of immediate early genes (IEGs; e.g. *cfos* and *egr1*). The IEG messenger RNAs (mRNAs) move out of the nucleus into the cytoplasm in which cellular ribosomes produce IEG proteins (translation). The proteins of IEGs *cfos* and *egr1* are transcription factors which turn back into the nucleus and bind to specific DNA sequences (3), thereby promote or inhibit transcription of other genes (e.g. TH). The mRNAs of these late effectors again move out of the nucleus into the cytoplasm, but after translation the late effector proteins implement cellular functions which lead to long lasting functional changes in the neuron (e.g. synapsins in axons). Modified from (Moorman et al., 2011).

It was shown in mice, that sexual odor stimulation increased pErk – positive cells in the male mouse brain within 10 minutes (Taziaux et al., 2011). Therefore, for olfactory stimulation treatment to visualize pErk – positive cells in the zebrafish brain, duration of 7 minutes (called short stimulation treatment) was taken in this study.

Expression of IEGs like *cfos* or *egr1* is downstream of pErk and it was shown that it takes at least 60 min to obtain sufficient IEG mRNA induction and 90 min to visualize IEG protein induction for immunohistochemical detection (Chaudhuri, 1997; Watts et al., 2006).

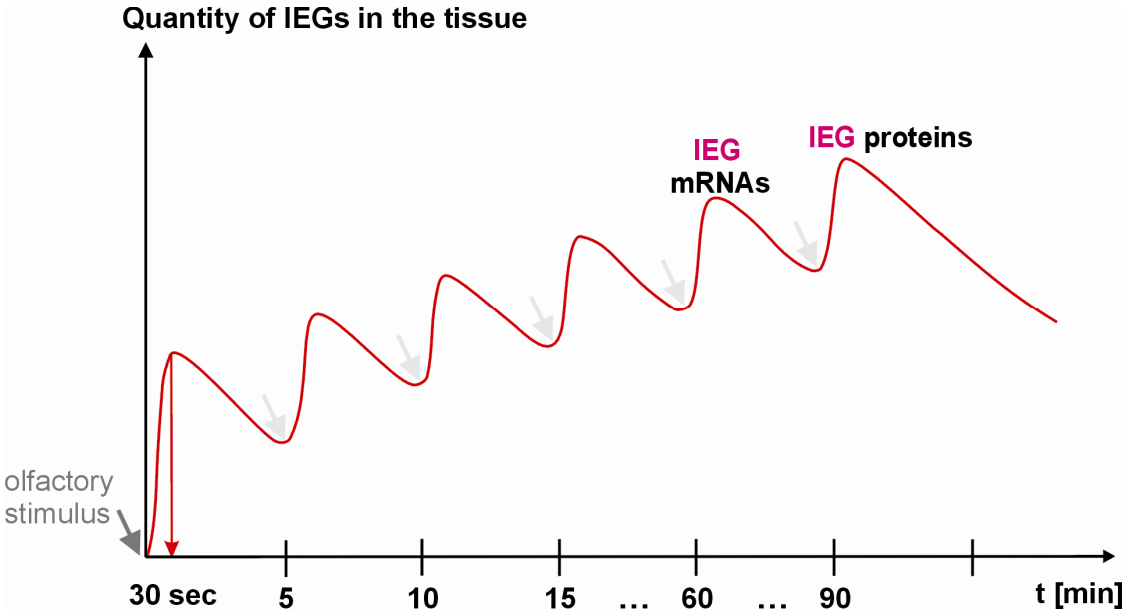

Fig. 8. Main principles of olfactory test procedures. The graph gives a general idea how the stimulation treatments should be performed to achieve high quantity of immediate early genes (IEGs) in the tissue (see Y-axis). The IEGs are activated as response to a sensory stimulus. Repetitive stimulation over time is needed to reach enough detectable amounts of IEGs in the tissue (red line). Test procedure takes 60 minutes to reach high quantity of detectable IEG mRNAs in the tissue via *in situ* hybridization and 90 minutes to detect a high quantity of detectable protein via immunohistochemistry. In my experiments, the following was done: After presenting olfactory stimulus (grey arrow) to the test fish, odor was immediately replaced by odorless water. Replacement lasted 30 seconds in the Mini – flume (red arrow) and each cycle started with inflow of odor stimulus (light grey arrows) followed by 5 minutes of odorless water.

IEG expression is activated transiently and rapidly in response to a wide variety of stimuli. Therefore, the input of external stimuli such as light and noise was minimized during test procedure. Each test fish was accustomed to the surrounding before test procedure started. This ensures that possible neuronal activity induced by changing environment had decreased to its baseline level by the time the experiment started. This stimulation paradigm was called long stimulation treatment (See Fig. 8 and text below).

3.4.1. Long Stimulation Treatment

Mini – Flume. Olfactory stimulation tests were conducted in a mini – flume (overall 10 cm long x 4.5 cm wide, and test area 5 cm long; see Fig. 9) with steady flow generated by a peristaltic pump (pump generator MCP Ismatec) 40 ml per minute (rpm). In front of the flume was a T – piece with an entrance into the flume and two flexible tubes attached to the other side

to present separately odorless water or olfactory stimulus. Inflow of stimulus and non – stimulus water could be regulated by an on / off function of the T – piece. This mini – flume ensured a fast replacement of stimulus and odorless water, which was calculated with regular food dye and lasted 30 seconds. Additionally, little free moving space and performance of stimulation treatment in darkness and silence ensured decrease of external stimuli.

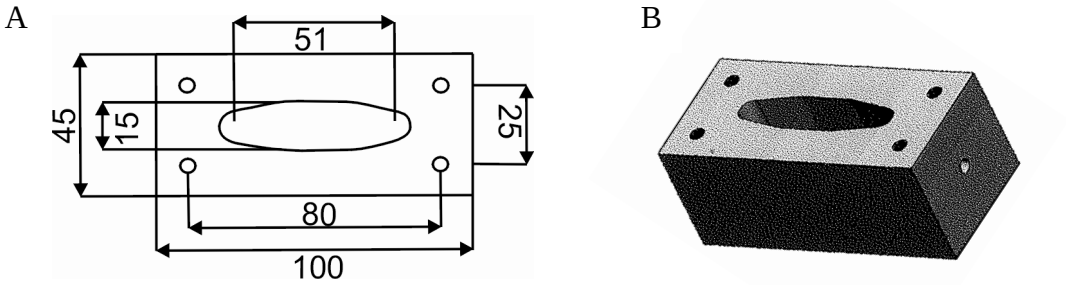

Fig. 9. Schematic drawing of the Mini – flume. (A) Dimensions of the Mini – flume pictured in (B) are given in millimeter (mm). Oval area in the middle of the flume (51mm long) demonstrates placement of the test fish with head to the left. Size of the oval area is adapted to the size of adult zebrafish preventing swimming motions of the fish. Water inflow on the left side and outflow on the right side of the flume ensured bathing of the test fish with odor stimulus.

Olfactory Stimulation With a Mini – Flume. Adult zebrafish were used for short stimulation treatment with amino acid L – alanine. Test fish (stimulated) and control fish (non – stimulated) were both kept in 1 Liter tanks individually one night before test procedure. Experiments started with presenting odorless water to the fish in experimental setup as an adaptation phase of 10 minutes. Afterwards test fish received 20 ml of odor stimulus and control fish 20 ml of odorless water added by injection in flexible tube in front of the mini flume. Odor stimulus was directly replaced by odorless water entered in the flume by the other flexible tube (replacement lasted 30 seconds; see Fig. 10). Test fish were exposed to odor stimulus in repetitive cycles, because immediate early genes are activated transiently and rapidly in response to a stimulus. Each cycle started with inflow of odor stimulus followed by 5 minutes of odorless water as cleaning – part. Therefore, according to theory, expression of immediate early genes was repetitive refreshed and each adjacent cycle summate the previous cycle (Fig. 8). Test procedure lasted 60 minutes to reach high quantity of detectable immediate early gene mRNA in the

tissue and 90 minutes to detect a high quantity of detectable protein. Test fish and control fish were treated under same conditions except for the stimulus during experiments in the Mini – flume.

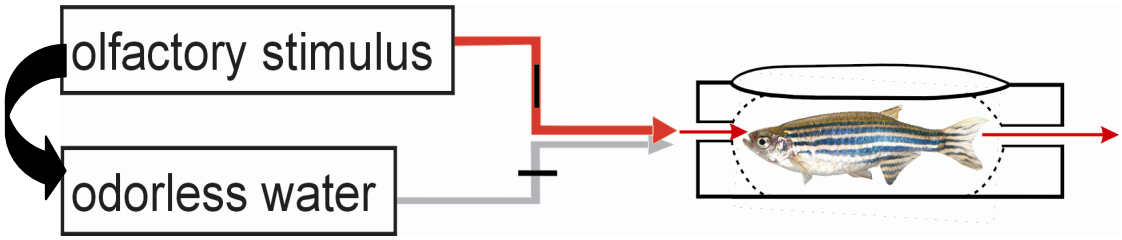

Fig. 10. Odor stimulation treatment in the Mini – flume. On the left side switch between olfactory stimulus and odorless water is demonstrated (black arrow) with inflow into the Mini – flume (red arrow and grey arrow, respectively). Test fish is placed in oval area in the middle of the flume and olfactory stimulus reaches nostrils in front of the head at first. Outflow is shown on the opposite side (red arrow on the right side). Replacement of olfactory stimulus lasted 30 seconds which was tested with colored waterflow beforehand.

3.4.2. Short Stimulation Treatment

Imprinted and non – imprinted larvae (see Results 3.2) were used for short stimulation treatment with kin water at day 8, 10 and 12 post – fertilization. Test larvae were transferred separately into small glass-beakers (diameter: 3 cm) filled with 5 ml odorless plain water one day before tests started and furthermore kept under identical conditions in an incubator at 26°C.

Before testing, the water – level was reduced to 1 ml odorless plain water in small glass beaker and larvae acclimated for 10 min. Thereafter, 1 ml odor stimulus was added for 7 minutes. Acclimation and test procedure was performed with reduced light and noise to minimize external stimuli.

Larvae were killed by an overdose of MS222 and immediately transferred into 4% PFA for 24 hours.

Adult zebrafish were used for short stimulation treatment with MHC peptide mix. Fish were separated in 1 liter tanks filled with odorless water, one day before tests started. Additionally, water – level was reduced before tests started to approximately 200 ml in 1 liter tanks and adult zebrafish acclimated for 10 minutes. Afterwards adult test fish received the odor stimulus for 7 minutes. Adult zebrafish were anesthetized in MS222 then immediately killed by decapitation.

3.5. Olfactory deprivation treatment

3.5.1. Unilateral Chemical Lesion With Triton X-100

Adult fish used for the Triton X-100 experiments were put individually into 3 l tanks the day before the deprivation treatment started and kept there for the following 10 days during experiments. Fish were anesthetized with 0.03% tricaine methanesulfonate (MS222; Sigma-Aldrich) in tank water. Immediately after losing control over upright body position and no longer responding to tail pinching, zebrafish were wrapped in a wet paper towel and removed from water during the chemical application period. Petroleum jelly was placed between the two nares to ensure that there would be no leakage of the chemical to the control naris. Then, 1-2 µl of lesion-solution (0.7% Triton X-100 and 0.15% methylene blue in water) was slowly injected with a gel-loading tip (neoLab, Germany) under the skin flap covering the nasal opening into the left nasal cavity and the fish were kept in this position for 5-6 min. The methylene blue allowed to visually confirming that the lesion-solution did not enter the contralateral naris. Afterwards, fish were moved to the recovery 3 l tank where lesion-solution and anesthesia were quickly washed away as the fish began swimming. Experimental procedure was repeated every day at the same time for 10 days.

3.5.2. Quantification of Labeled Neurons in the OB After Triton X-100 Treatment

Transverse fluorescent triple labeled sections (*egr1*/TH/DAPI) were used for the analysis of TH and *egr1* downregulation. Three sections from each olfactory bulb (7 treated, 7 control bulbs; n = 7) in the center of the bulb were taken for confocal photography (using 25 x objective, see below) in order to contain all histological layers. This is important, because a section at the anterior or posterior end of the bulb would only contain the glomerular layer and not give representative results. One olfactory bulb yields around only 6 sections (30 µm each). Thus, three centered sections contain most of the volume of each investigated bulb. Using TH single or TH/*egr1* double labeled signal, individual cells were counted manually using ImageJ 1.37k plugin Cell Counter software which did result in

absolute cell numbers. For TH/*egr1* double labeled cells, only the enlarged area shown (see Results, Fig. 19N) was counted (6 treated, 6 control bulbs; n = 6) using 25 x objective and zoom factor 3. Using the ImageJ 1.37k plugin Cell Counter software routine, one goes through each optical section level (RGB stacks) of one physical section. This allows to manually counting all cells singly within a physical section, thus, omitting double counts. Since tyrosine hydroxylase IHC visualizes the extent of somata as well as neurites, individual TH (and TH/*egr1*) positive cells could be easily distinguished from other cells. Thus, we counted all cells in each section, and the mean cell number per section is plotted on the y-axis in (see Results, Fig. 19O).

For *egr1* and DAPI single labeling, the y-axis indicates in a non-logarithmic scale the counted thresholded voxels in entire stacks of these three consecutive, confocally photographed sections of all 7 treated and 7 control bulbs (see Results, Fig. 19A-I). This was done because the scattered *egr1 in situ* signal is almost impossible to allocate to a particular cell. Therefore, we did not count cell numbers for *egr1* and DAPI, but volumes, using ImageJ 1.37k plugin Voxel Counter to count the thresholded voxels in each stack for red or blue dye. While not yielding cell numbers, the results reflect the amount of *egr1* or DAPI positive neurons, respectively.

Table 6: Overview of animal consumption in different experiments

	Short stimulation treatments	Long stimulation treatments	Odor deprivation treatment	Dynamics of developmental expression
Adults	12 (pErk)	20 (cfos)	10	
Larvae	24 (pErk) 20 (cfos)	-	-	8 (parvalbumin) 8 (S100)

Table 7: Overview of animal consumption for basal expression studies

	egr1 + (TH)	*c fos* + (TH)	pE rk (TH)	parvalbumin	calretinin	calbindin1	S100
Adults	20	18	11	8	7	4	8
Larvae	98	44	32	17	9	8	20

3.6. Photomicrography

Photomicrographs of adult brain sections singly labeled for *egr1* or double labeled with conventional ISH/IHC for *egr1*/TH were taken with a research microscope (Olympus BX51 upright microscope) equipped with a universal camera (Olympus XC10). Optical sections were analyzed with OlyVia 2.1 (Olympus Soft Imaging Solutions GmbH) and transformed in PDFs with PDF Converter Professional 7.0 (Nuance Communications, Inc.). After conversion in Tagged Image File Format (TIFF), images were exported to Adobe Photoshop 8.0.1 (Adobe Systems, San Jose, CA) software and the brightness and contrast were slightly modified when needed.

Furthermore, the FISH - and immunofluorescence double labeled (*egr1*/TH) adult zebrafish brain sections were captured with a confocal microscope. Confocal optical sections were acquired with a Leica TCS SP-5 confocal laser-scanning microscope (Leica Microsystems, Mannheim, Germany) equipped with Plan Fl25x/0.75 NA and Plan 63x/1.32 NA oil immersion objectives. Fluorochromes were visualized by using an argon laser with excitation wavelengths of 488 nm, emission 510–540 nm for Alexa 488 and a DPSS laser with a laser line of 561 nm, emission 565-600 nm for Cy3 and a diode laser with a laser line of 405 nm, emission 420-470 nm for DAPI. Stacks of eight-bit grayscale images were obtained with axial distances of 0.3 – 1 µm between optical sections and pixel sizes of 0.12 – 1.2µm depending on the selected zoom factor and objective. After stack acquisition, Z chromatic shift between color channels was corrected.

The RGB stacks, montages of RGB optical sections, and maximum – intensity projections were assembled into tables by using ImageJ 1.37k plugins and Adobe Photoshop 8.0.1 (Adobe Systems, San Jose, CA) software.

Photomicrographs of larval brain sections were taken with a light microscope (Nikon Eclipse 80i; Nikon Instruments Inc.) equipped with Nikon Plan Fluor 10x/0.30 and Plan Fluor 20x/0.50, a Nikon Digital Sight DS-U1 Photomicrographic Camera (Nikon Instruments Inc.) and LUCIA-G5 software. The same microscope was used with fluorescence equipment for triple labeled sections of olfactory bulb of adult zebrafish.

All microscopic images used in this study were slightly adapted for brightness and contrast with Adobe Photoshop 8.0.1 (Adobe Systems, San Jose, CA) software and photographic plates were mounted and further processed with CorelDraw 9.532 (Corel Corporation).

3.7. Terminology

Neuroanatomical designations for larval and adult zebrafish brain are taken from the respective atlases (Mueller and Wullimann, 2005; Wullimann et al., 1996), unless otherwise noted.

4. Results

4.1. Experiments Involving the IEG *egr1*

4.1.1. Developmental Basal *egr1* Zebrafish Brain Expression Profile

Analysis of *egr1* activity in the larval zebrafish brain shows that this IEG gene maintains its expression within the forebrain and alar plate mesencephalon beyond the previously described similar embryonic pattern of basal *egr1* expression (Close et al., 2002). In my expression study I confirm essentially the reported embryonic domains (retina, telencephalon, hypothalamus, preoptic region, diencephalon, optic tectum), except for the (probably erroneously) reported embryonic midbrain tegmental domain. I did not see *egr1* expression in the basal plate midbrain at any larval stage investigated (Figs. 11, 12) and also not at adult stages (Fig. 14). In fact, a comparison of early differentiated Hu - positive cells (Mueller and Wullimann, 2005) with *egr1* ISH sections shows that the midbrain tegmental cell masses are free of *egr1* expression (Fig. 12D-F).

The olfactory bulb (OB) lights up as a new major *egr1* positive domain at early larval stages starting with 3 dpf likely reflecting a correlation with onset of olfactory function (Figs. 11 - 14). Domains of *egr1* are present also at day 3, in pallial (P) and subpallial (stronger in dorsal, Sd, than ventral, Sv, subpallial) regions (Fig. 11B). In the OB and telencephalon it is particularly evident that *egr1* is never expressed in periventricular mitotic cells, but this applies to other sites as well. Mitotic cells show a somewhat elongated morphology compared to the more migrated *egr1*-positive, differentiating cells (see subpallial proliferative zone (S) in Fig. 13.) At the boundary zone of dorsal and ventral (pre-) thalamus a horizontal stripe of *egr1* positive cells is visualized (Fig. 11C). Some scattered cells remote from the ventricle are seen more caudally in the preoptic region and in the dorsal and ventral thalamus (Fig. 11D). The hypothalamus also shows *egr1* domains as well as the periventricular gray zone of the optic tectum (Fig. 11E). In contrast, expression in the medulla oblongata and early cerebellar plate is absent (Fig. 11F, G).

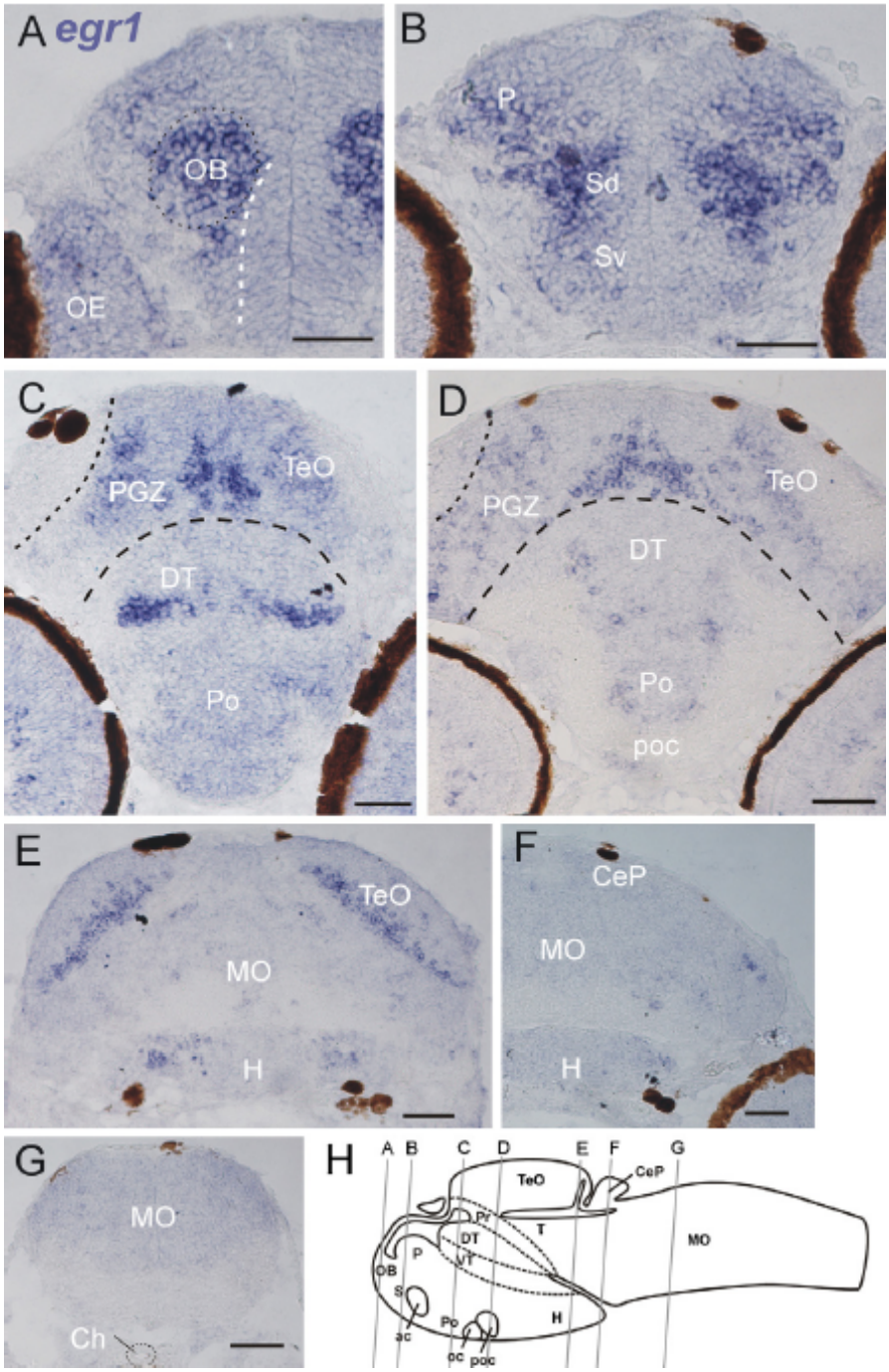

Fig. 11: Early larval basal *egr1* expression. A series of transverse zebrafish brain sections from rostral (A) to caudal (G) showing early larval (3 dpf) *egr1* expression. Abundant *egr1* expressing neurons are present in the olfactory bulb (A), pallial and subpallial regions of telencephalon (B), boundary region between ventral and dorsal thalamus (C), preoptic region (D), and hypothalamus (E), as well as in the periventricular gray zone of optic tectum (PGZ; between two dashed lines in (C and D). No *egr1* expression is seen in the olfactory epithelium (A) the cerebellar plate and at posterior hindbrain levels (F and G). Note also that no *egr1* expression is seen in subpallial proliferative zone (right to dashed line in A). (H) Schematic sagittal view of larval brain shows section levels. See list for abbreviations. Scale bars: 50 µm (from Kress and Wullimann, 2012).

Later larval (6 dpf - 8dpf) *egr1* expression reveals a more mature larval situation emerging with increasing neural differentiation. Domains of

egr1 in the forebrain have extended (Fig. 12). In the optic tectum, there is now additional expression in more superficial tectal layers. Also the torus semicircularis, which represents the posterior part of the alar plate mesencephalon, is discernible as *egr1* positive (Fig. 12E). However, the midbrain tegmentum remains negative (Fig. 12 E, F), as do medullary cell masses and the cerebellar plate (Fig. 12 G, H).

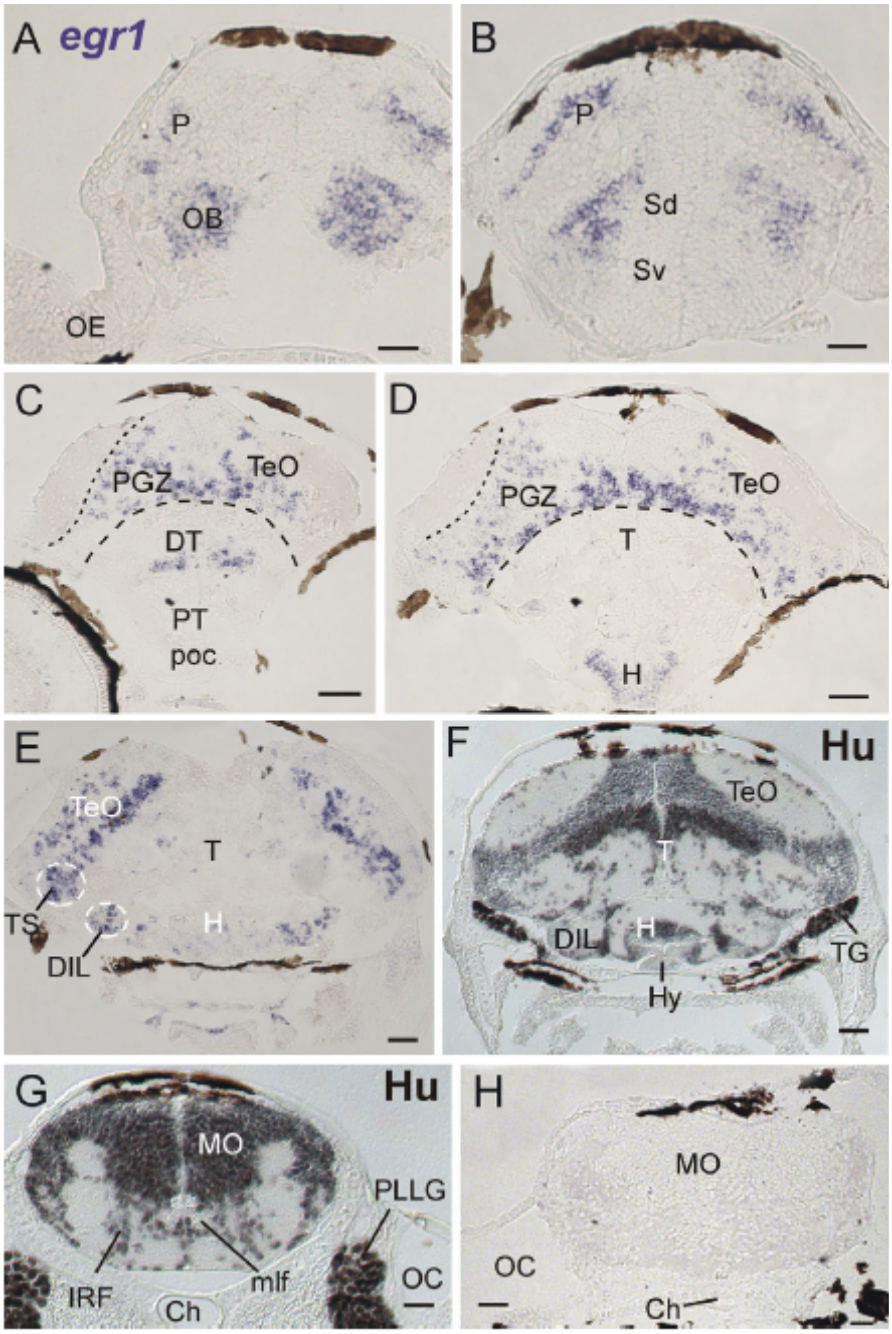

Fig. 12: Late larval basal *egr1* expression. A series of transverse zebrafish brain sections from rostral to caudal (A–E and H) showing later larval (6 dpf) *egr1* expression. (F) and (G) Hu-protein immunostains in transverse section to demonstrate, respectively, differentiating neuronal cells at the level between (D) and (E) and at the level of (H) (as reported previously; Mueller and Wullimann, 2005). Many *egr1* positive cells are present

in olfactory bulb, but none in olfactory epithelium (A). Strong *egr1* expression is visualized in telencephalic pallium and subpallium (B), in diencephalic boundary region between ventral and dorsal thalamus and in hypothalamus, as well as in the (mesencephalic) periventricular gray zone of optic tectum (PGZ; between two dashed lines in C and D). Note that no *egr1* positive neurons are seen in the mesencephalic tegmentum (D and E). In the hindbrain, expression of *egr1* is also absent. Note extent of *egr1* negative cells by comparing Hu-protein with *egr1* stained sections. See list for abbreviations. Scale bars: 50 µm (from Kress and Wullimann, 2012).

4.1.2. Comparison of egr1 Expression: Untreated, Imprinted and Non-Imprinted Larvae

A comparison of *egr1* basal expression (untreated larvae) versus *egr1* expression in imprinted and non – imprinted larvae visualized strong *egr1* expression in olfactory bulb and telencephalic pallium (P), and posterior subpallium (S; expression only seen in Fig. 13A'). In the anterior subpallium, no *egr1* expression is seen in sections B, B' - C, C' because of different section plane. Also, the subpallial proliferative zone close to the ventricle (Fig. 13) is always free of *egr1* expression. Imprinted larvae were tested in flume choice tests and showed preference for kin water. Non – imprinted larvae grew up isolated and showed no preference neither for kin odor nor non – kin odor also tested in flume choice tests. Untreated larvae grew up in larval groups with siblings and non - sibling larvae and were not tested in flume choice tests. However, all three types of zebrafish larvae revealed no qualitative differences in *egr1* expression domains in the olfactory bulb (Fig. 13).

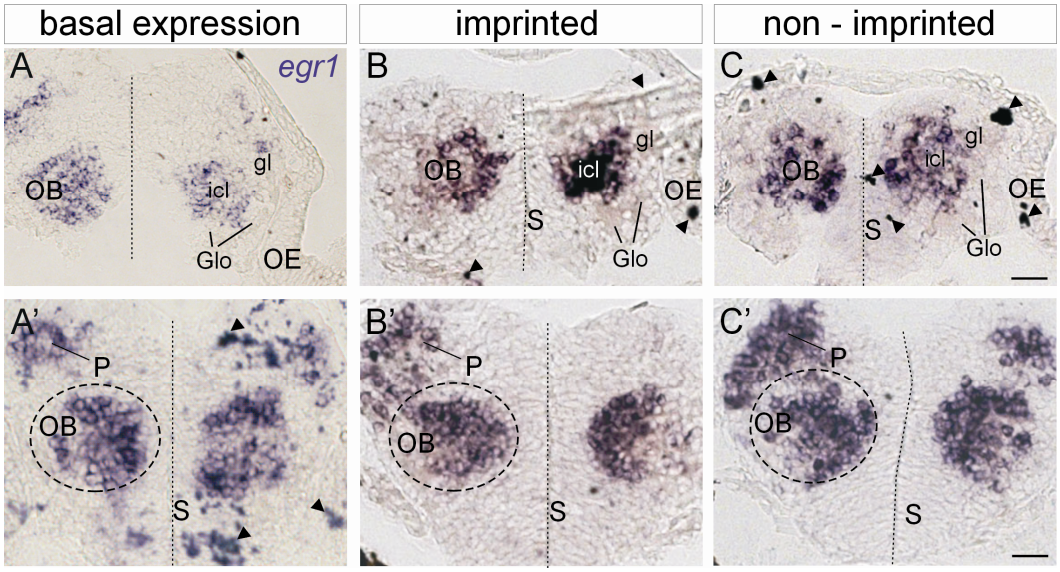

Fig. 13: Comparison of *egr1* expression in imprinted and non-imprinted larvae. Transverse zebrafish brain sections from rostral (A, B, C) to caudal (A', B', C') of larval (A and A': 6dpf; B, C and B' and C': 7dpf) basal *egr1* expression (A and A') and *egr1* expression in imprinted (B and B') and non – imprinted (C and C') larvae. (A), (B) and (C) visualize strong *egr1* expression in the icl and scattered *egr1* expressing neurons in gl of

the olfactory bulb (OB), but none *egr1* – immunoreactive neurons in the olfactory epithelium (OE). Strong *egr1* expression is shown in the pallium (P). Dashed circles reveal the boundary of OB and dashed lines visualize midline of the brain. Note also that no *egr1* expression is seen in subpallial proliferative zone (S). Black arrowheads mark artifacts. See list for abbreviations. Scale bars: 50 µm.

4.1.3. Adult Basal *egr1* Expression Domains in the Zebrafish Brain

In the adult zebrafish brain expression domains of *egr1* are qualitatively very similar to the late larval situation (Figs. 14 - 16). Extensive *egr1* expression is present in forebrain and alar plate midbrain (Fig. 14C), but very restricted to absent *egr1* expression is seen in basal plate midbrain and hindbrain (medulla oblongata, Fig. 14D). There is the notable exception of the *egr1* positive domain in the facial lobe (Fig. 16D) and, more weakly, in the vagal lobe (Fig. 14A). These general relationships are nicely demonstrated in a comparison of an *egr1* stained sagittal section with a combined Bodian – silver / Cresyl stained sagittal section (Fig. 14A, E). The majority of adult forebrain cell groups show basal *egr1* expression (see also Figs. 15, 16), with negative cells only in some areas, for example the posterior zone of area dorsalis (Fig. 15C; Dp, the presumed homologue of the mammalian olfactory cortex), the periventricular pretectum (Fig. 15F, I, J), or the ventrolateral thalamus (Fig. 15D, G). New *egr1* expression domains in comparison to the larval situation arise in the adult brain in the cerebellar granular layer of corpus and valvula cerebelli, caudal lobe, and eminentia granularis (Figs. 14A, D; 16A - C).

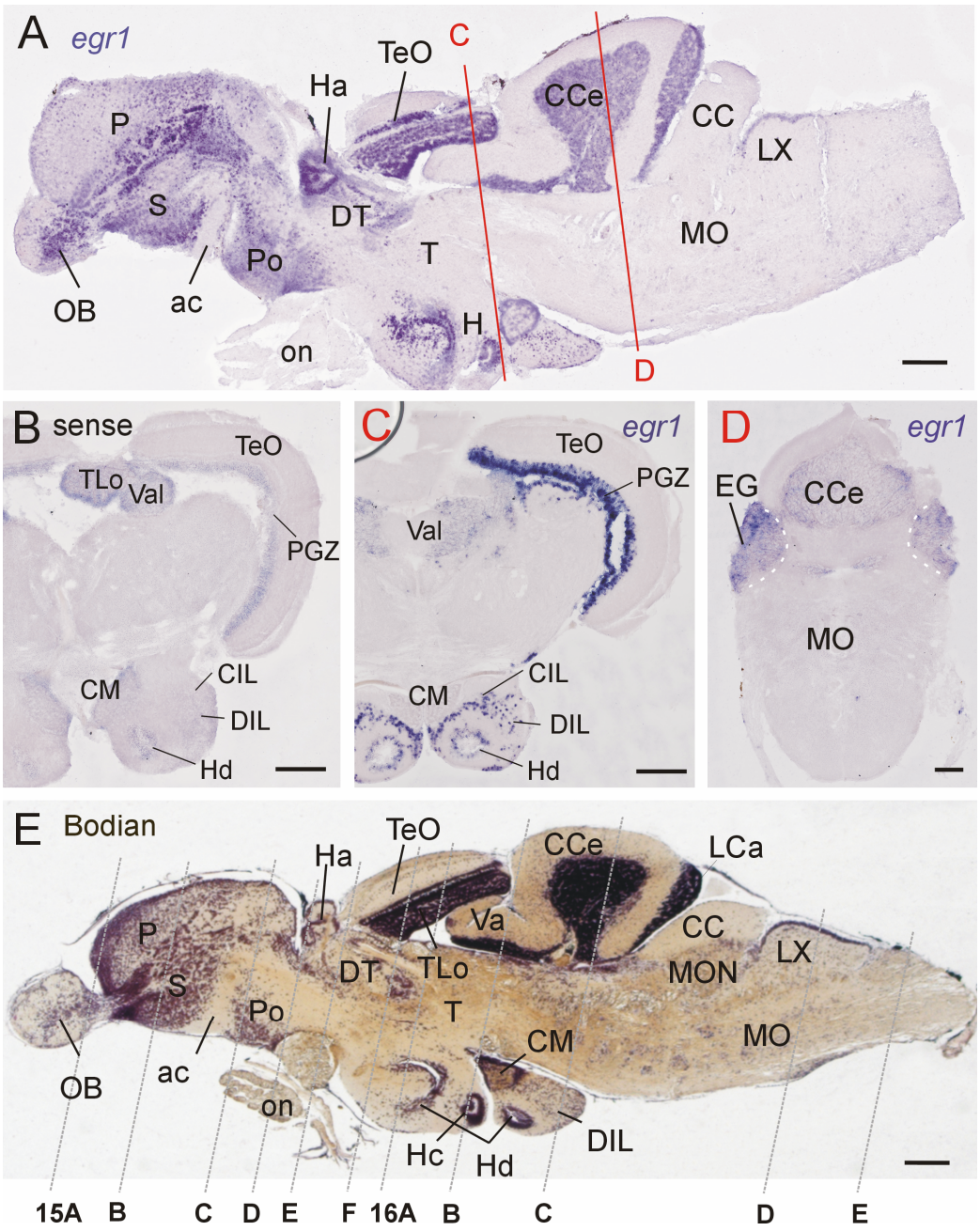

Fig. 14. Adult basal expression of *egr1* shown in a sagittal zebrafish brain section (A) and transverse sections (B-D), including a sense / antisense comparison. (E) Bodian-silver–Cresyl stained sagittal section visualizing normal zebrafish brain neuroanatomy at the same level as (A). Section levels (C and D) are indicated in (A) and reveal highly restricted to absent *egr1* expression in hindbrain. Section levels for Figs. 15 and 16 are shown basally in (E). See list for abbreviations. Scale bars: 200 µm (Kress and Wullimann, 2012).

4.1.4. Co – Localization of Tyrosine Hydroxylase and *egr1* in the Adult Zebrafish Brain

The proximal promoter of tyrosine hydroxylase (TH) contains immediate early gene (IEG) – transcription factor binding sites necessary for activity – dependent TH expression in the OB (Liu et al., 1999) (see

Fig. 7 in Materials & Methods). In mammals, the IEG *egr1* appears to mediate activity-dependent TH – expression in OB dopaminergic periglomerular neurons (Akiba et al., 2009). Thus I analyzed adult zebrafish brain sections for *egr1* and TH double labeling in order to establish possible co – localization of *egr1* and TH in particular in olfactory related areas (Figs. 15, 16). Fortunately, in the zebrafish brain the distribution of TH is well established (Kaslin and Panula, 2001; Rink and Wullimann, 2001; Yamamoto et al., 2011) and these TH positive cell groups will be examined one by one regarding co – localization with *egr1* transcripts. The olfactory bulb shows TH positive periglomerular cells with their dendrites seemingly extending into the glomeruli, as seen typically in all vertebrates. Interestingly, some TH positive cells were always additionally seen in the internal cellular layer and they may represent displaced periglomerular cells. Some TH positive cells both in the glomerular layer as well as in the internal cellular layer appear to be double labeled (white and black arrows in Fig. 15A). Additionally, many singly *egr1* positive cells are seen in the internal cellular layer.

The telencephalic population of TH positive cells extends throughout the subpallium from anteroventral to posterodorsal levels (Fig. 15B, C). Particulary in the supracommissural nucleus of ventral telencephalic area (Vs), a large proportion of TH/*egr1* positive cells is apparent (Fig. 15B, C; red arrowheads). There is only occasional co-localization in various preoptic nuclei, most obvious in the suprachiasmatic nucleus (Fig. 15C - E, G, H). Both in the periventricular pretectum and the lateral prethalamus (former ventral thalamus), co-localization of *egr1*/TH seems absent (Fig. 15D - F, I, J). In contrast, there is clear co – localization of TH/*egr1* in the periventricular posterior tubercular nucleus and the paraventricular organ (Figs. 15E, H; 16A, G). The posterior tuberal nucleus and the caudal hypothalamus also show partial co – localization of the two markers (Fig. 16B, H). In most TH positive forebrain areas, single labeled TH cells always also occur, but apparently not in the pear-shaped posterior tubercular cells, where TH cells seem always double labeled with *egr1* (Fig. 16G). The midbrain does not contain TH cell bodies, but a peculiar pattern of TH positive axonal terminations is seen in two broad

layers in the optic tectum, one in the central zone and one in the superficial white and gray zone, as previously reported by (Kaslin and Panula, 2001). These axons originate presumably from periventricular pretectal neurons (see their axons extending into optic tectum in Fig. 15E). The TH positive nuclei of the hindbrain, i.e., locus coeruleus, reticular formation (interfascicular and vagal groups of (Ma, 1997), and area postrema seem to be free of basal *egr1* expression (Fig. 16 C - F, I, J).

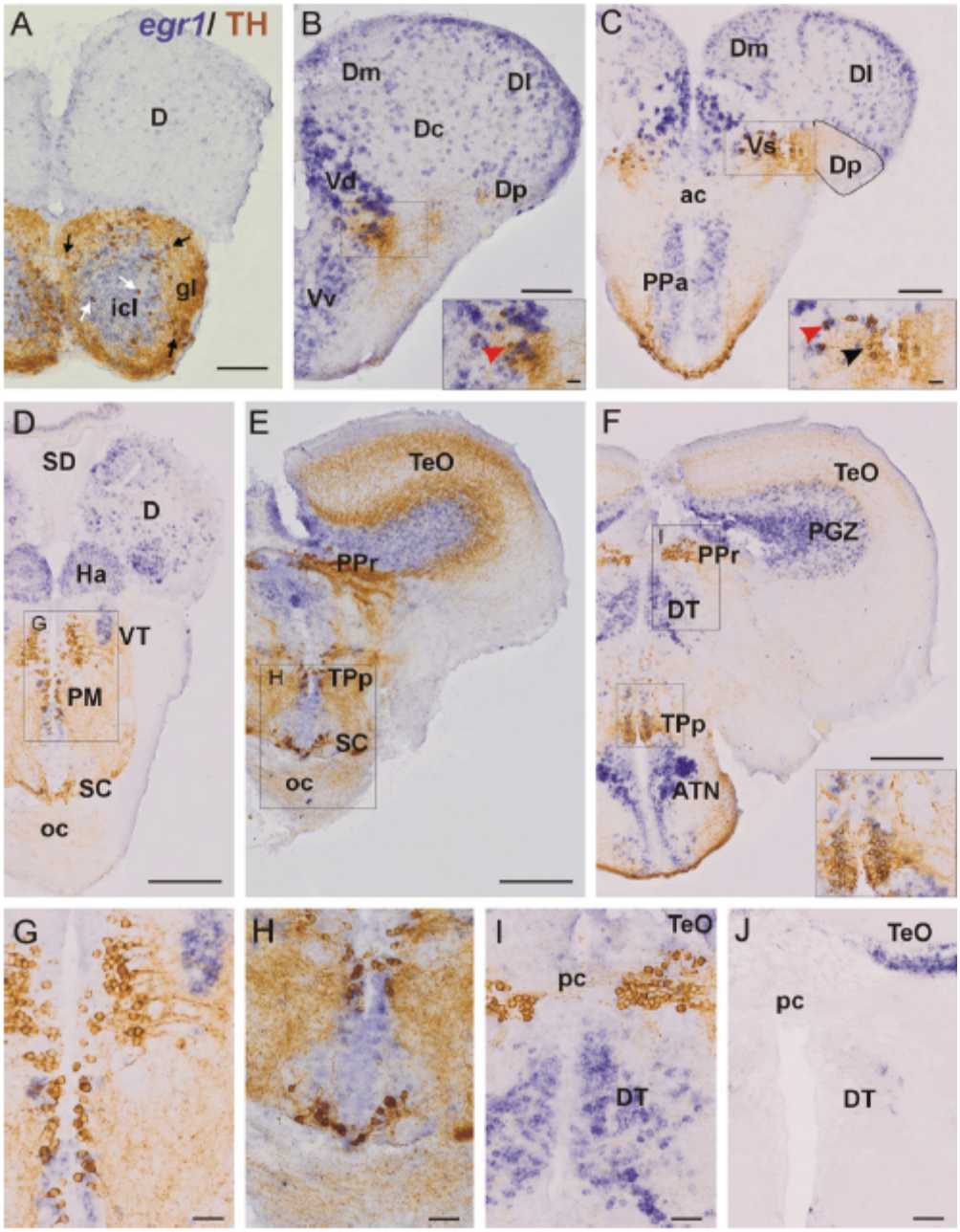

Fig. 15: Adult double label of *egr1* and TH (forebrain/midbrain). Transverse zebrafish brain sections show adult expression of *egr1* via ISH (purple) and TH via IHC (brown) from olfactory bulb (A) to anterior diencephalon and midbrain (F). White and black arrows in (A) point out TH immunoreactive (THir) cell bodies in olfactory bulb internal cellular layer (icl) and glomerular layer (gl), respectively. Insets in (B) and (C) show magnified

subpallial telencephalic area with red arrowheads pointing out dark gray-colored double labeled *egr1* and TH co-expressing cells. Black arrowhead in inset in (C) marks light brown colored TH single labeled cell. Magnified details of sections (D)–(F) highlight double labeling of *egr1* and TH in magnocellular preoptic nucleus and medial ventral thalamus (G), suprachiasmatic and posterior tubercular area (H), as well as the absence of TH cells in lateral part of ventral thalamus (G). Sections (I and J) show expression of *egr1* in dorsal thalamus (DT) and optic tectum (TeO), but absence of *egr1* positive neurons in TH positive pretectal area, which is anatomically marked by the posterior commissure (pc). See list for abbreviations. Scale bars in (A–C): 100 µm, in (D–F): 200 µm and in (G–J): 20 µm (from Kress and Wullimann, 2012).

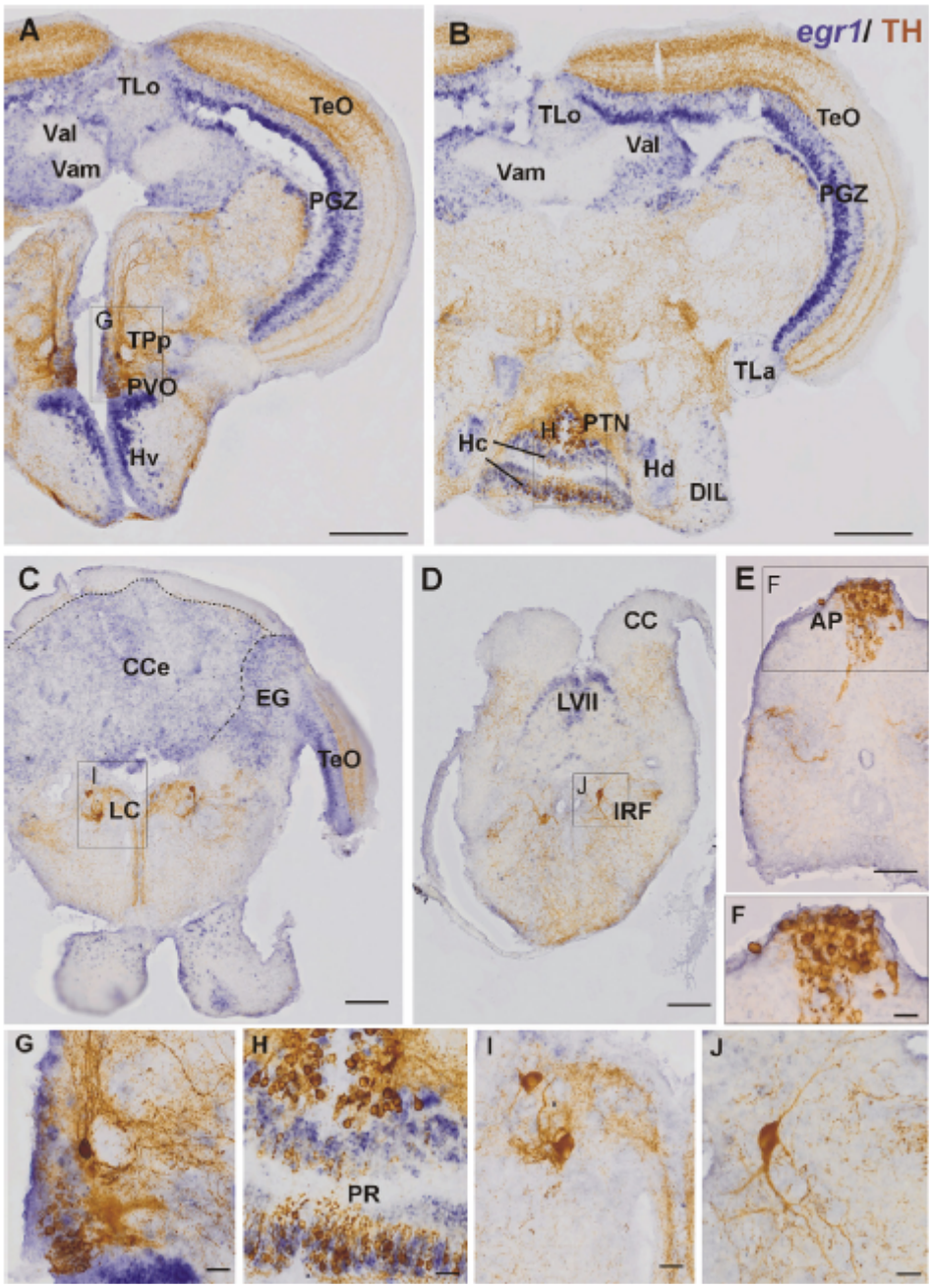

Fig. 16: Adult double label of *egr1* and TH (midbrain/hindbrain). Transverse zebrafish brain sections show adult expression of *egr1* via ISH (purple) and TH via IHC (brown) from midbrain (A) to hindbrain (E). Note absence of TH positive cell somata in optic tectum and cerebellum. (F) to (J) show magnified details of sections shown in (A) to (E). Double labeling of *egr1* and TH is seen in diencephalic areas, such as posterior tuberculum (TPp / PTN: G and H) and hypothalamus (Hc: H). Sole expression of TH is seen in area postrema (AP: F), locus coeruleus (LC: I), and inferior reticular formation

(IRF: J). See list for abbreviations. Scale bars in (A–E): 200 µm, in (F–J): 20 µm (from Kress and Wullimann, 2012).

For further analysis of *egr1*/TH co – localization, I focused on the olfactory bulb (OB) and the supracommissural nucleus of ventral telencephalic area (Vs), the hypothesized medial amygdala of teleosts. As shown for the example for the olfactory bulb (Fig. 17), light microscopical views may visualize double label nicely, but on the single cell level, the demonstration remains in many cases questionable.

Thus, I had to develop a protocol for fluorescent *in situ* hybridization (FISH) for *egr1* combined with immunohistochemical double labeling for TH for a quantitative analysis of cell numbers in this primary (OB) and secondary (Vs) olfactory target of interest (Figs. 17, 18; see Materials and Methods). This allows for confocal microscopical analysis and clear demonstration of double label on the single cell level in OB and Vs (arrows in Fig. 18) and a quantitative analysis of cell numbers of different phenotypes, i.e., double labeled cells, as well as single labeled TH and *egr1* positive cells in a defined area.

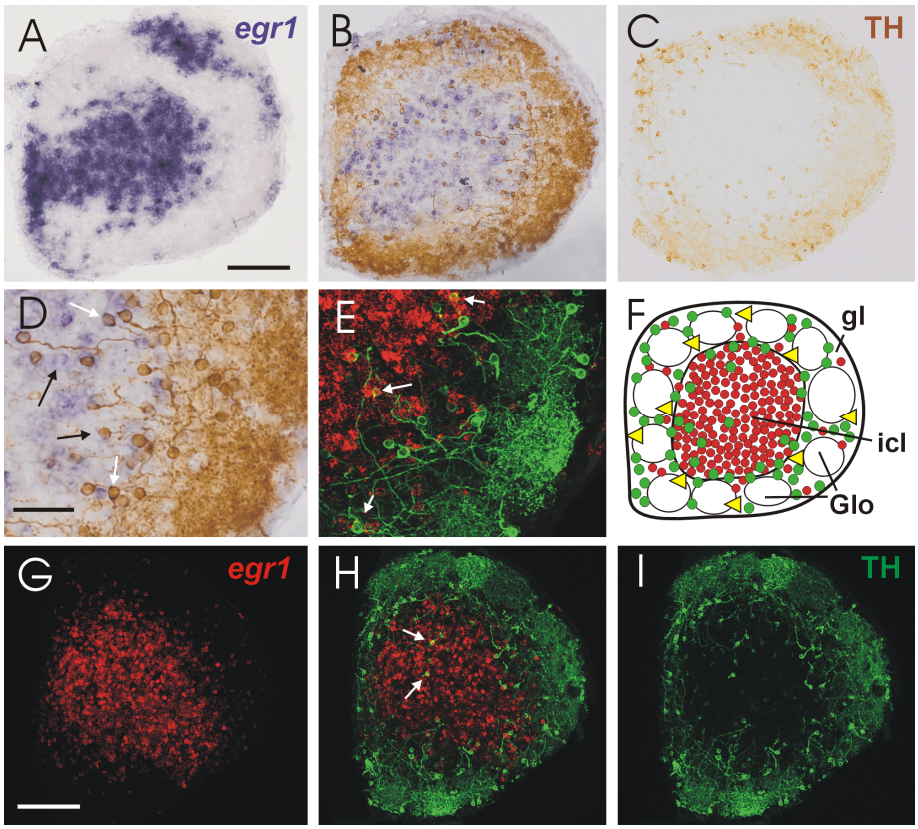

Fig. 17: Comparison of conventional ISH and fluorescent ISH. Transverse sections of adult zebrafish olfactory bulb. (A) and (C) show light-microscopical adult

egr1 or TH expression, respectively, and (B) a double labeling of *egr1* and TH. (D) shows a detail of (B) at higher magnification to point out *egr1*- and TH single labeled (black arrows) and co-expressing cells (white arrows). Transverse sections in (E), and (G)-(I) demonstrate *egr1* and TH expression with fluorescent double labeling using normal fluorescence (E) or confocal microscopy, with (G) showing *egr1* expression (FISH) and (I) TH expression (IHC), and (H) showing merged pictures. White arrows point out co-expressing cells, which are much better defined in confocal microscopy. (F) Schematic drawing of the olfactory bulb outlines cell types and layers in adult zebrafish olfactory bulb. Green dots are dopaminergic periglomerular cells, red dots are *egr1* expressing cells, mostly granular cells in the internal cellular layer (icl) and scattered cells in the glomerular layer (gl). Yellow triangles represent the mitral cells (not visualized in photomicrographs). See list for abbreviations. Scale bar in (A and G): 100 µm; scale bar in (D): 50 µm. (from Kress and Wullimann, 2012).

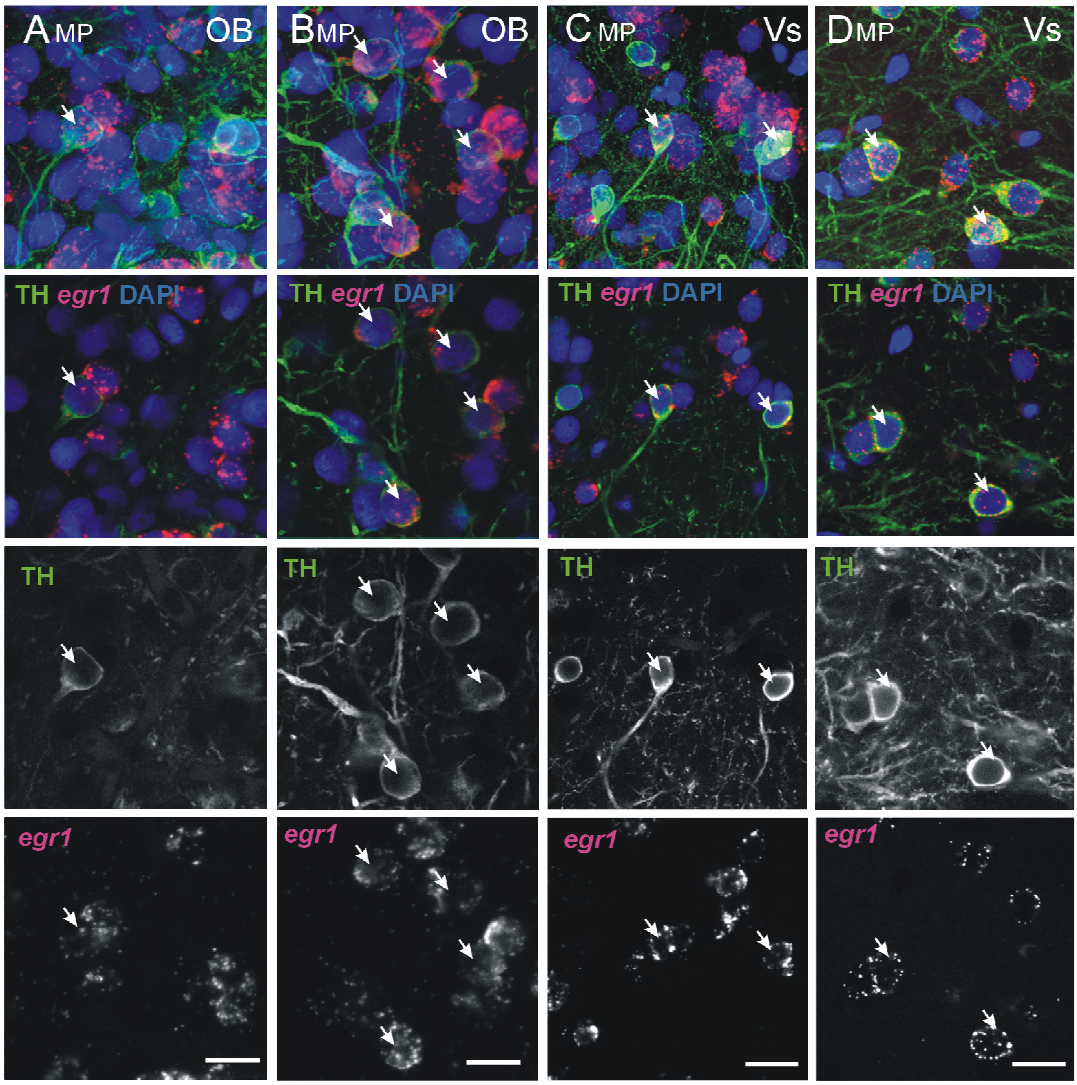

Fig. 18: Confocal double label analysis of TH/*egr1* in OB and Vs. Confocal images (using 64x objective) of fluorescent triple label in glomerular cell layer of adult zebrafish olfactory bulb (OB; two left vertical columns) and telencephalic supracommissural nucleus of area ventralis (Vs, suspected homologue of medial amygdala; two right vertical columns). (A/B) and (C/D) show two examples of *egr1*- (magenta) and TH- (green) expressing neurons counterstained with DAPI (blue) in OB and Vs, respectively. Upper row demonstrates maximum projections (MP) and subjacent three pictures present the overlays of optical sections for triple staining. Last two rows are monochromatic images of TH and *egr1*, respectively. White arrows point to triple labeled cells. See list for abbreviations. Scale bars: 10 µm (from Kress and Wullimann, 2012).

4.1.5. Downregulation of egr1 and TH After Triton X-100 Application to Olfactory Epithelium

This work aims to demonstrate in the zebrafish brain that *egr1* and TH expression are susceptible to olfactory activity levels. Thus, I tested whether olfactory deprivation through temporary loss of cilia / microvilli using the detergent Triton X-100 as lesion solution leads to downregulated expression of *egr1* and TH, as is the case in rodents (Akiba et al., 2009; see discussion). It had previously been shown that in zebrafish such treatment leads to temporary loss of cilia / microvilli without long – lasting effects on the olfactory epithelium (Friedrich and Korsching, 1997b) and that the olfactory epithelium recovers fully within 2 to 5 days (Iqbal & Byrd-Jabobs, 2010). Thus, I applied Triton X-100 over a period of 10 days once daily into one olfactory epithelium of adult zebrafish, killed the fish on the eleventh day and looked for differences in expression levels of *egr1* and TH as well as for morphological appearance of the olfactory bulb. Counterstaining with DAPI, a marker for cell nuclei, shows that the OB ipsilateral to the Triton X-100 application does not significantly differ in terms of size and morphological appearance from the (untreated) contralalateral side (Fig. 19C, F, I). Clearly, glomerular and internal cellular layers can be seen to be very similar to the untreated side in relative extent and histology. However, both *egr1* expressing cells (Fig. 19B, E, H) and TH positive cells (Fig. 19A, D, G) were far less in numbers on the ipsilateral side. This together indicates that *egr1* / TH expression was downregulated without great cell loss in the OB on the treated side. Interestingly, *egr1* was also downregulated in the internal cellular layer.

Quantification (see Materials and Methods) using RGB stacks of optical sections (3 each in seven treated and seven control olfactory bulbs) revealed that significantly more neurons were TH singly and TH / *egr1* doubly positive in the OB corresponding to the untreated olfactory epithelium (TH**:** paired *t*-test, p=0.001; t value: -6.542; Fig. 19J; TH/*egr1*: Wilcoxon test, p=0.028; Z value: -2,201; Fig. 19O) in comparison to the OB corresponding to the olfactory epithelium treated with Triton X-100. Furthermore, values of tresholded voxel counting for red dye (representing *egr1*) also resulted in apparent differences of treated versus control bulbs

seen as a clear tendency in the histogram, although missing significance (*egr1*: Wilcoxon test, p=0.128; Z value: -1.521; Fig. 19K). In contrast, no significant difference was observed between OBs of untreated and treated olfactory epithelia when the same voxel counting method was used for blue dye (representing DAPI; paired *t*-test, p=0.576; t-value: -0.591; Fig. 19L). This together indicates that *egr1* and TH positive cells as well as *egr1* / TH doubly positive cells were diminished in the treated bulbs, whereas DAPI positive cells (i.e., total cells present) were not.

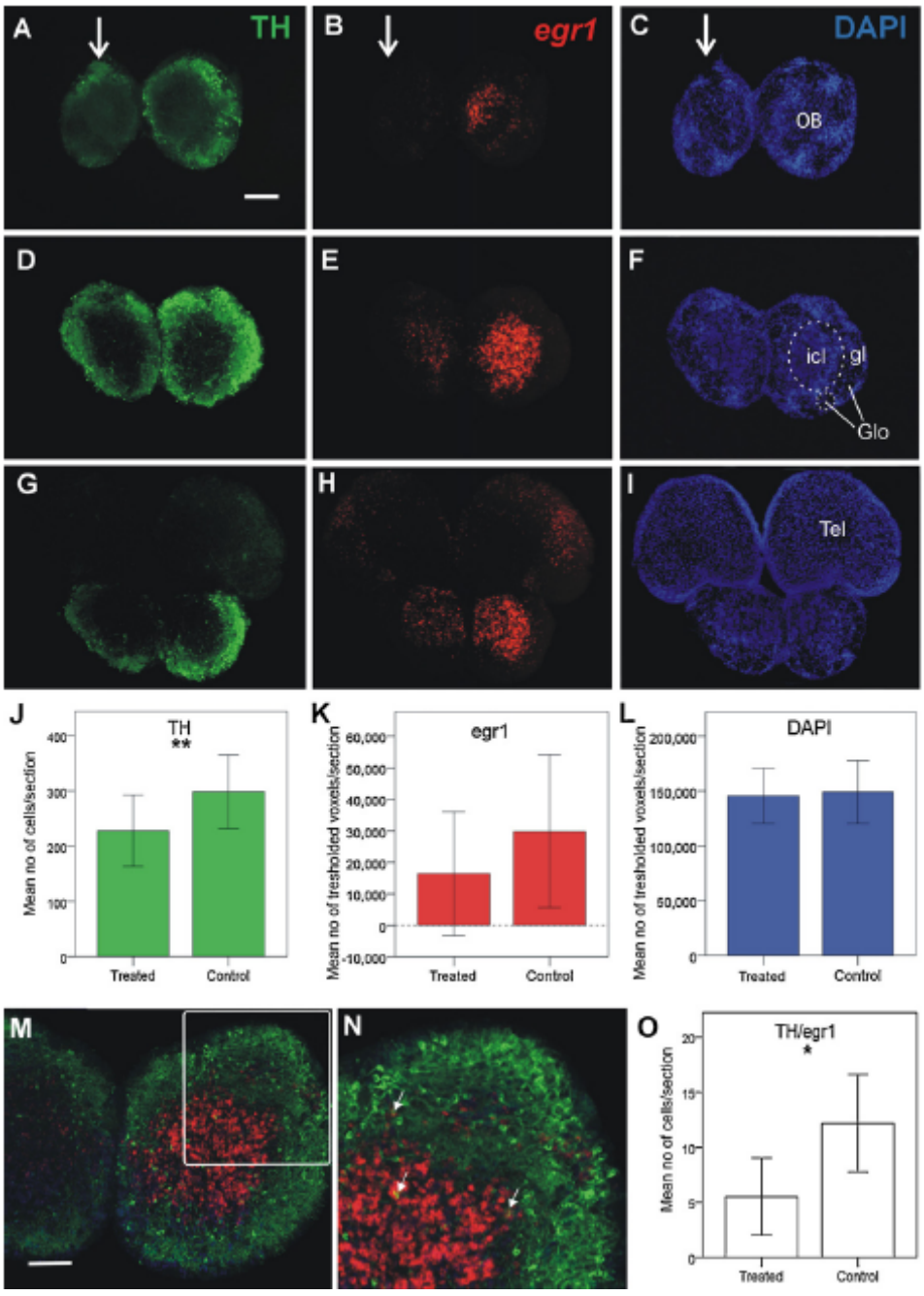

Fig. 19: Deprivation treatment of one olfactory epithelium and effect on ipsilateral adult olfactory bulb. Transverse sections of zebrafish olfactory bulb in a series from rostral (A–C) to caudal (G–I) show the expression of TH (green), *egr1* (red) and DAPI

(blue). Large white arrows in A, B and C mark the olfactory bulb on the treated side. (J, K, L and O) Quantification of TH, *egr1*, DAPI and TH/*egr1* expression in the ipsilateral olfactory bulb after Triton X-100 application in the corresponding olfactory epithelium compared to the contralateral olfactory bulb (untreated control side). Three confocally photographed brain sections per olfactory bulb and brain side were analyzed with ImageJ 1.37 (7 animals; n = 7; except in O: 6 animals; n = 6; see text for details). Mean number of TH (J) or TH/*egr1* (O) expressing cells per section is shown on the y-axis. Mean number of thresholded voxels of red or blue dye, representing respectively the expression of *egr1* (K) or DAPI (L) per section is shown on the y-axis. Note strong tendency for *egr1* reduction on the treated side, whereas no difference is seen for DAPI. (M and N) show example of area quantified for TH/*egr1* cells. Small white arrows point to double labeled cells. Error bars in histograms show standard deviation. *P < 0.05, **P < 0.01. icl internal cellular layer, gl glomerular layer, Glo glomeruli. Scale bar in (A): 200 µm; in (M): 100 µm (from Kress and Wullimann, 2012).

To ensure that *egr1* / TH expression was downregulated without great cell loss in the OB on the treated side, I investigated adult neurogenesis in the Triton X-100 treated zebrafish. Under the assumption that great cell loss in the OB would cause faster turnover in the OB on the treated side, I visualized progenitor cells with the mitosis marker PH3 and checked for migrating cells along the rostral migratory stream (RMS) to the OB where they are known to differentiate into interneurons (Marz et al., 2010) (Fig. 20A). Comparison of PH3 positive cells on the RMS in each telencephalic brain hemisphere of treated and control side demonstrated no quantitative differences (Fig. 20) indicating that no increased cell replacement via the RMS was initiated by the lesion experiment.

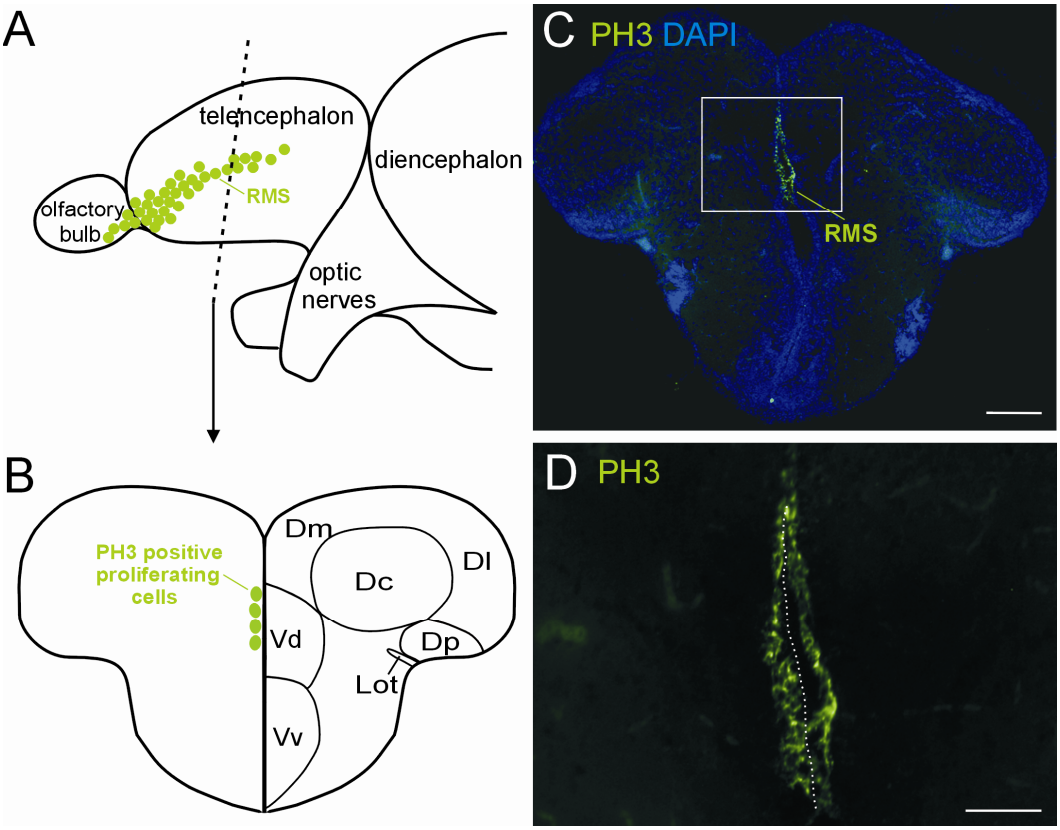

Fig. 20. No effect of deprivation treatment on rostral migratory stream (RMS). RMS visualized via PH3 – immunoreactive cells and DAPI as nuclear counterstain in transverse brain section (C and D) of TritonX-100 treated adult zebrafish. (A) Schematic sagittal view of RMS in adult zebrafish brain. Dashed line demonstrate sectional plane of (B). (B) schematic telencephalic transverse section of (A) visualize PH3 positive proliferating cells of RMS in ventricular zone adjacent to dorsal zone of ventral telencephalic area (Vd) of adult zebrafish brain described by März et al. (2010). Schematic drawings modified from März *et al.,* 2010. (C) Transverse zebrafish brain section of telencephalon visualizes PH3 expression and nuclear marker DAPI. PH3 positive cells are shown in ventricular zone adjacent to Vd representing RMS. (D) Higher magnification of (C; white box) demonstrate comparison of PH3 positive proliferating cells of RMS in treated versus control brain hemisphere. No difference is seen. Dashed line visualizes midline of the brain. See list for abbreviations. Scale bars: in (C) 100 µm; in (D) 50 µm.

4.2. Experiments Involving the IEG *cfos*

4.2.1. Basal Expression of *cfos* in Larval and Adult Zebrafish Brains

Although I could demonstrate downregulation of *egr1* expression in single labeled and *egr1* / TH co – expressing cells via odor deprivation (Fig. 19), upreglation through odor stimulation turned out to be difficult because of the strong basal expression of *egr1* (Figs. 11 - 18).

Therefore I decided to use the IEG *cfos* as an alternative. Basal expression studies of *cfos* in larval (Fig. 21) and adult zebrafish brains (Figs. 22 – 24) revealed some overlapping expression domains of *cfos* and *egr1*, but also significant differences. A particulary notable difference is the generally weaker basal expression of *cfos* in comparison to *egr1* in both zebrafish larvae (Fig. 21) and adults (Fig. 22).

Starting with the telencephalon, the OB in larvae (Fig.21) and adult zebrafish (Figs. 22B, D; 23A) shows basal *cfos* expression in GABAergic granule cells in the icl (Figs.22B; 23A'), and also in periglomerular cells in the gl (Figs. 21A; 23A). Regions with ongoing strong proliferation show lateral to the proliferation zones less, more weakly stained Hu positive cells compared with more mature regions (Mueller and Wullimann, 2005). Thus, comparison of early differentiated Hu – positive cells (Mueller and Wullimann, 2005) with *cfos* FISH section shows that the ventricularly located proliferation zone remain Hu free and the *cfos* positive cells lie ventrolaterally to this proliferation zone (Fig. 21A, B). Domains of *cfos* are also present in telencephalic pallial regions and scattered c*fos* expressing cells are present in the preoptic region (Fig. 21C). Furthermore, in the diencephalon weak *cfos* expression is seen in the epiphysis, and not in the

habenula (Fig. 21D). In the adult brain, the habenula is definitely *cfos* positive (Fig. 22). Strong larval *cfos* expression is visualized in the ventral (pre-) thalamus (Fig. 21D), and in the dorsal thalamus (Fig. 21E, F) which can be seen also in adult sagittal sections (Fig. 22). Strong *cfos* expression is observed in larval periventricular posterior tuberculum (Fig. 21E, F). Also the posterior part of the alar plate mesencephalon, the torus semicircularis, is *cfos* positive (Fig. 21H). A notable difference to *egr1* expression is that in adult zebrafish, *cfos* expression is absent in the diencephalic posterior tuberal nucleus (Fig. 24H), whereas in adult zebrafish double labeling of *egr1* and TH expressing cells was demonstrated (see Figs. 15H; 16G, H). The periventricular gray zone of optic tectum shows less and weaker *cfos* expression in comparison to expression of *egr1* (Fig. 22) Additional imortant differences to *egr1* expression are *cfos* positive cells in larval midbrain tegmentum (Fig. 21H; T within dashed white line) which is *egr1* free (see above). However, *cfos* is absent in adult zebrafish sagittal brain sections (Fig 22). In the hindbrain *cfos* positive cells are shown in medulla oblongata (Fig. 21I), while *egr1* expression is absent in the hindbrain. The cerebellum is *cfos* free in larvae (as for *egr1*), and has only some expression of *cfos* in the adult caudal cerebellar lobe (while all adult cerebellar parts are *egr1* positive).

Lau et al. (2011; their Fig. S3*A*) compared *cfos* expression in the hypothalamus between untreated adult zebrafish and stressed testfish and implicate strong upregulation of *cfos* expressing hypothalamic cells after intense handling stress (Lau et al., 2011). Addtionally, untreated animals were habituated to their environment for at least 24h and directly killed for comparison analysis. These animals appear to express no *cfos* positive cells in the hypothalamus whereas the testfish subjected to intense handling stress demonstrate strong and widespread *cfos* expression in the hypothalamus (Lau et al., 2011).

In contrast, my extensive study of *cfos* basal expression visualizes strong basal *cfos* expression in hypothalamus (H) of untreated larvae (Fig. 21G - I) and adult zebrafish (Fig. 22B; Fig. 24D, D'). These untreated adult zebrafish and larvae were also habituated to their environment for at least

24h and directly killed for comparison analysis without intense handling stress.

In summary, a comparison of adult zebrafish c*fos* and *egr1* basal expression reveals extensive expression domains in the forebrain for both genes. In the diencephalon, weak *cfos* expression is shown in the preoptic region and habenula, whereas strong expression of *egr1* is seen there. In dorsal thalamus, the reverse is true, i.e. strong basal *cfos* expression, but only weak basal *egr1* expression. The mesencephalic periventricular gray zone of optic tectum shows strong *egr1* expression (Fig. 14C), but less *cfos* expression (see also Fig. 24D, E). Only in the adult zebrafish brain is basal *egr1* and *cfos* expression visualized in the granular layer of the cerebellum (Fig. 22), with *cfos* expression restricted to the caudal cerebellar lobe. While *cfos* positive cells are present in the medulla oblongata of the hindbrain, *egr1* expression is absent there (Fig. 22).

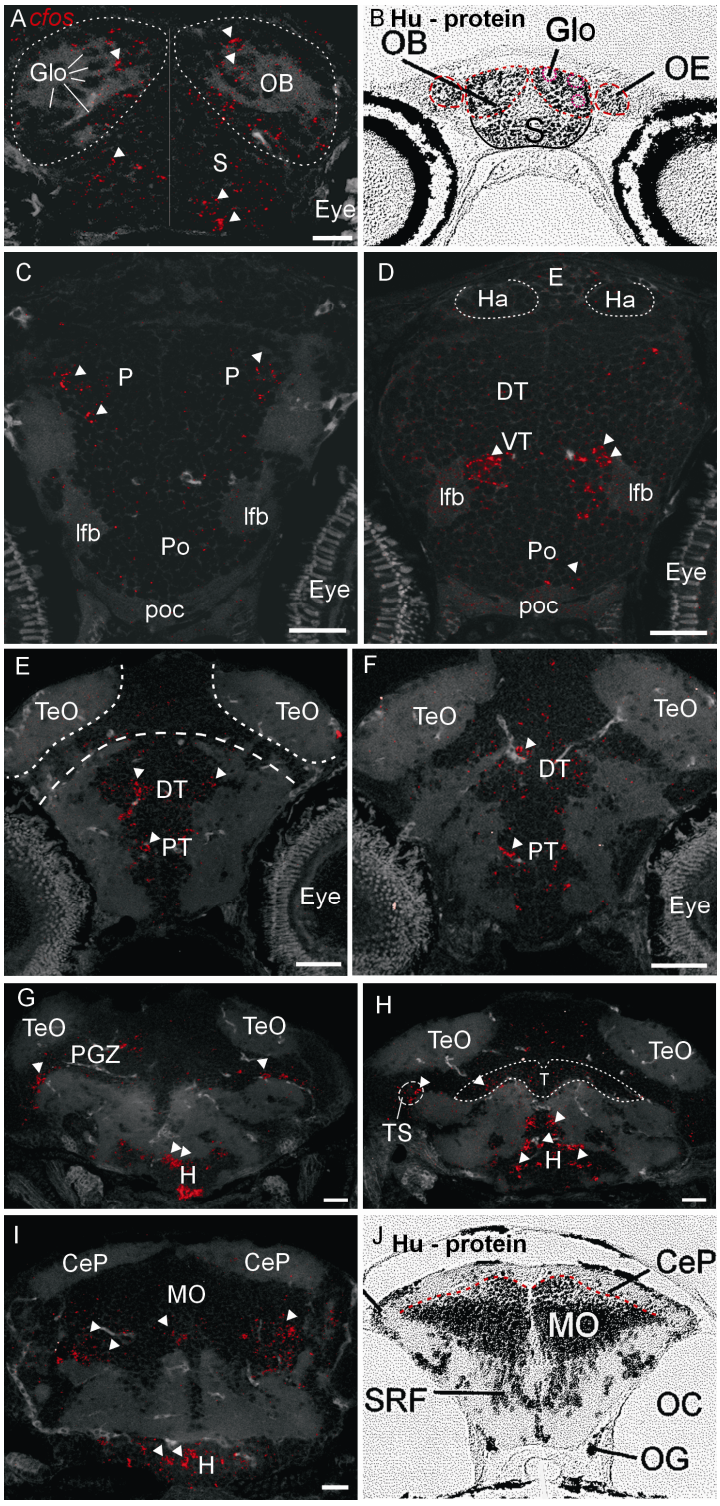

Fig. 21. Developmental basal *cfos* expression. A series of transverse zebrafish brain sections from rostral (A) to caudal (I) shows larval (9dpf) basal *cfos* expression. (B) and (J) Hu – protein immunostains in transverse section show differentiating neuronal cells at the level of (A) and (I) (both modified from Mueller and Wullimann, 2005). (A) *cfos* positive cells (arrowheads) are present in the glomerular layer of olfactory bulb (and in icl, not shown) as well as in telencephalic subpallium (S). Dashed line around olfactory bulb and olfactory epithelium. (C) *cfos* positive cells are also visualized in the telencephalic pallium (P) and weakly in the preoptic region (PO) (D-E). Strong *cfos* expression is present in diencephalic ventral (pre-) and dorsal thalamus (VT and DT, respectively) and the posterior tuberculum (PT).No *cfos* positive cells are seen in the habenula (Ha). (F-I) In the mesencephalon, *cfos* expression is visualized in the periventricular gray zone of optic tectum (PGZ; between two dashed lines in E), in the torus semicircularis (TS) and the

tegmentum (T; dashed line in H). Note that strong *cfos* expression is also visualized in (diencephalic) hypothalamus (H) as well as in medulla oblongata of the hindbrain, but not cerebellum (I). Arrowheads point to cfos positive cells See list for abbreviations. Scale bars: 50 µm.

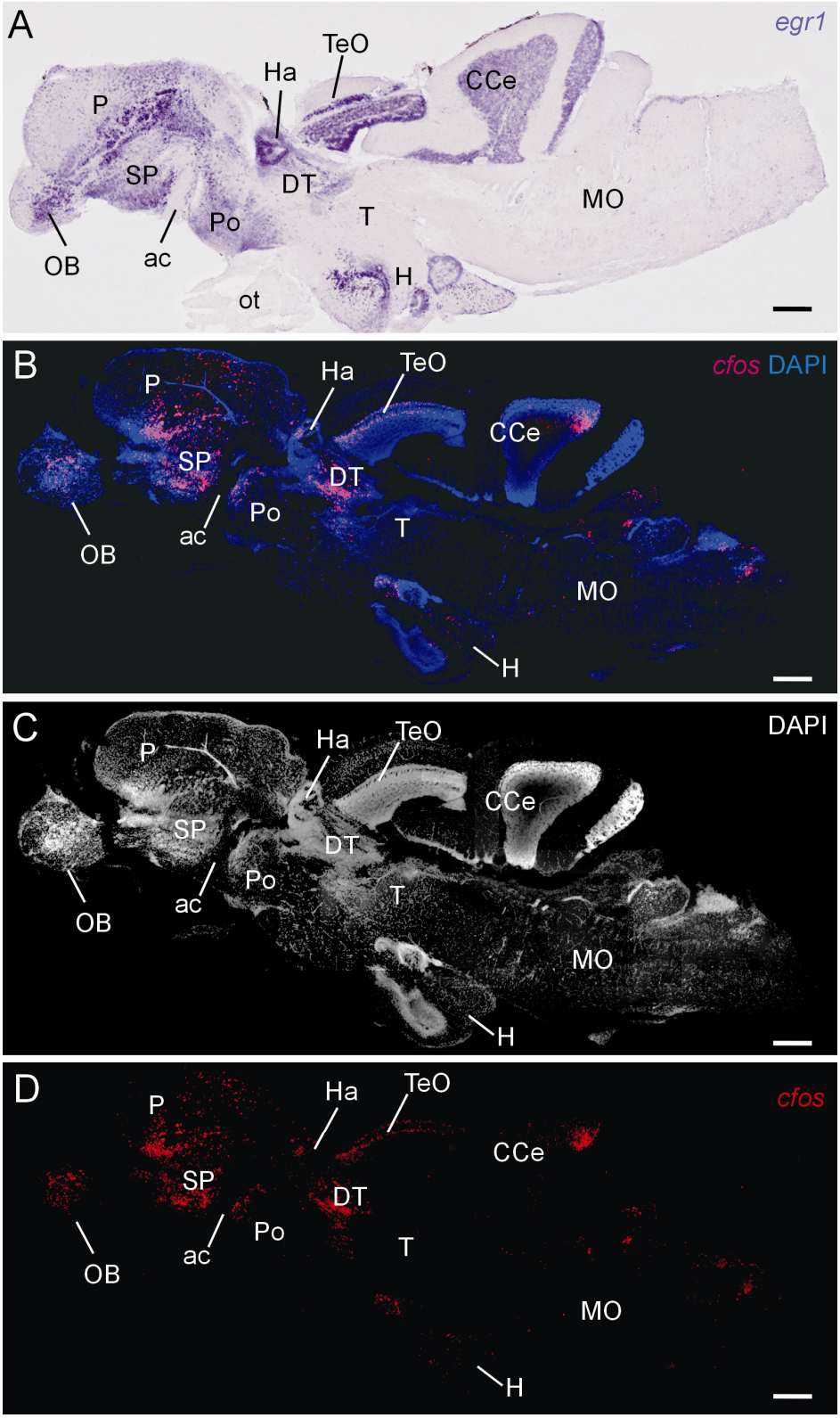

Fig. 22. Comparison of adult basal *egr1* and *cfos* expression. (A) Sagittal zebrafish brain section reveals strong basal *egr1* expression in forebrain and midbrain, but highly restricted to absent in hindbrain. Sagittal zebrafish section (B-D) visualizes *cfos* basal

expression. In (B) *cfos* expression is counterstained with the nuclear marker DAPI and show qualitative similar expression domains, but less immunoreactive cells in comparison to *egr1* expression. For differences see text. In (C), DAPI nuclear counterstain is visualized for morphologically comparison of (A) and (B). (D) monochromatic image of *cfos* presents distribution of *cfos* – immunoreactive neurons. See list for abbreviations. Scale bars: 200 µm.

4.2.2. Co – Localization of Tyrosine Hydroxylase and *cfos* in Adult Zebrafish Brain Olfactory Areas

For future experiments involving olfactory stimulation, it seems important to know which olfactory areas show basal co – localization of *cfos* and TH. Therefore, I analyzed (adult zebrafish brain sections for *cfos* (FISH) and TH (fluorescent IHC) by double labeling (Figs. 23, 24). In the OB confocal analysis (using 64x objective) of fluorescent triple label in gl and icl reveals very restricted to absent *cfos*/TH double labeling (Fig. 23A, A', A''). In the pallial telencephalic area Dp, the presumed homologue of mammalian olfactory cortex, weak basal *cfos* expression is shown and no TH positive cells are present (Fig. 23C'). In the subpallial telencephalic area Vs, the presumed homologue of mammalian medial amygdala, many *cfos* and TH single labeled cells and scattered *cfos*/TH double labeled cells (Fig. 23C'; white arrows) are visualized. To analyze basal expression of *cfos* in hypothalamus in detail, *cfos*/TH double labeling in optical transverse sections is analyzed (Fig. 24D, D'). The TH positive posterior tuberal nucleus shows no *cfos* cells (Fig. 24D, D'). In contrast the caudal zone of periventricular hypothalamus displays many TH or cfos expressing cells (with few if any double labeled cells). Many cfos positive cells are present in corpus mamillare and dorsal zone of periventricular hypothalamus, but no TH cells were seen.

Another TH positive area is the locus coeruleus (LC) in the hindbrain and it represents the noradrenergic ascending activating system (Kress and Wullimann, 2012). The large cells of the TH positive LC show triple labeling of *cfos*, TH and DAPI (Fig. 24E'; white arrows). Interestingly, some TH positive cells show up in the central gray (Fig. 24E).

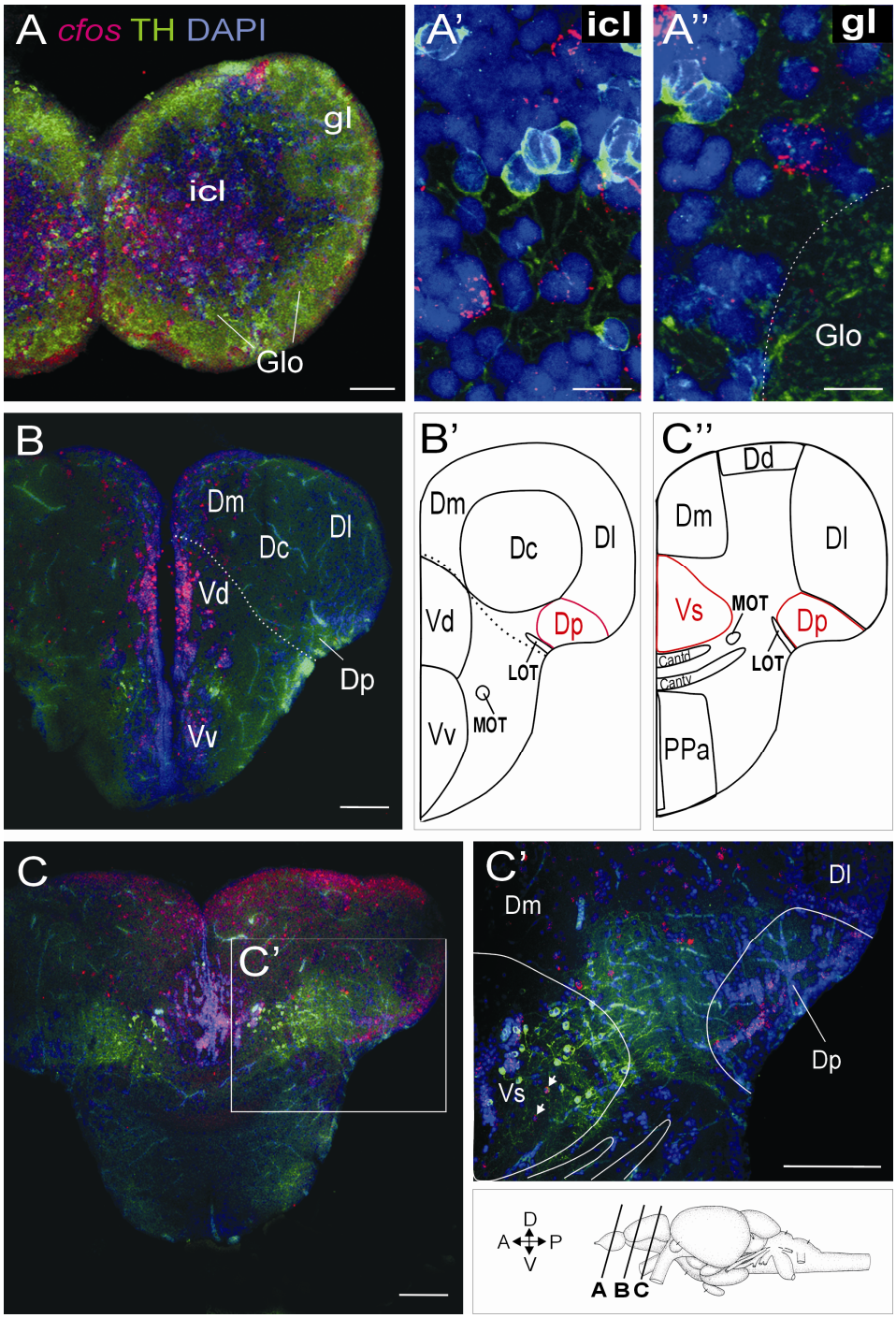

Fig. 23. Double labeling of *cfos* and TH (forebrain). Transverse zebrafish brain sections show adult expression of *cfos* via FISH (magenta) and TH via IHC (green) counterstained with nuclear marker DAPI (blue) in olfactory bulb (A) and telencephalon (B,C). (A) Strong TH expression (cell bodies and fibers) is visualized in glomerular layer of olfactory bulb (gl) with scattered TH – immunoreactive cell bodies in the internal cellular layer (icl). *cfos* positive neurons are visualized in icl and gl. (A') and (A'') show magnified icl and gl of olfactory bulb, respectively, in confocal images (using 64x objective). Note that no TH/cfos double labeled cells are visualized. White dashed line in (A'') marks boundary of a glomerulus (Glo) in gl. (B) Strong *cfos* expression is visualized in subpallial telencephalic areas Vd and less in Vv plus scattered *cfos* positive neurons in pallial telencephalic areas Dm, Dc and Dp**.** TH – immunoreactive cells are shown at the boundary of Vd and Vv. White dashed line shows the border of dorsal (pallial) and ventral (subpallial) telencephalon. (B') Schematic drawing at the same level of (B) highlighting posterior zone of dorsal telencephalic area (Dp) in red. (C) Strong *cfos* expression is shown in pallial telencephalic areas (Dm, Dd, Dl and Dp) and scattered *cfos* -

immunoreactive neurons in subpallial Vs. TH positive neurons are demonstrated in Vs and in the ventral area of the anterior part of the parvocellular preoptic nucleus (PPa). (C') shows magnified telencephalic area at the boundary of pallium and subpallium including Dl, Dm, Dp and Vs (see white box in C. White lines mark the borders of Dp and Vs and the anterior commissure is indicated separaterly for ventral (Cantv) and dorsal parts (Cantd). TH - immunoreactive cells are shown in Vs and *cfos* positive cells are visualized in Dl, Dm, Dp and Vs. White arrows mark *cfos*/TH double labeled cells. (C'') is a schematic drawing at the same level of (C) highlighting Dp and Vs in red. Schematic sagittal view of adult brain shows section levels in A, B and C. See list for abbreviations. Scale bars in (A): 50 µm; in (A') and (A''): 10µm; in (B), (C) and (C'): 100 µm.

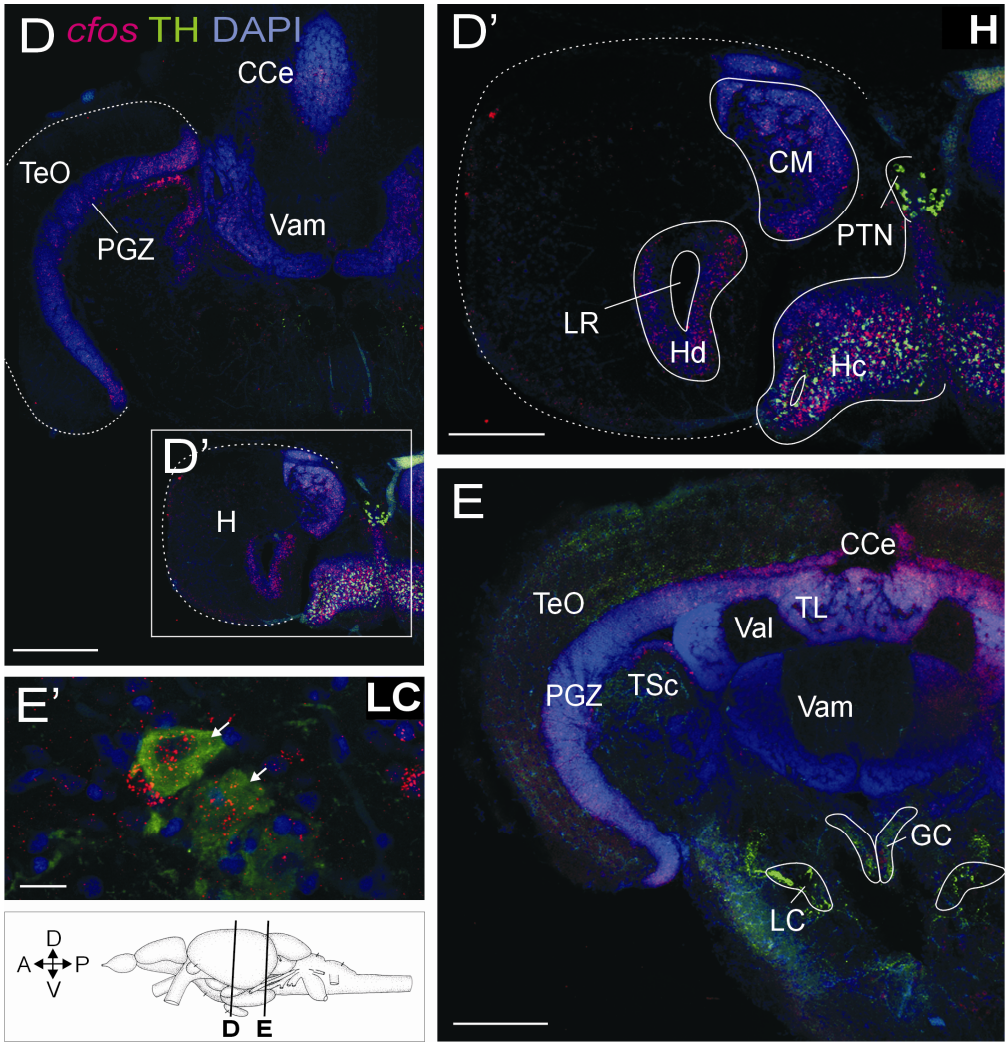

Fig. 24. Double labeling of *cfos* and TH (mid-/hindbrain).Transverse zebrafish brain sections show adult expression of *cfos* via FISH (magenta) and TH via IHC (green) counterstained with nuclear marker DAPI (blue) in the mid- and hindbrain from rostral (D) to caudal (E), incl. parts of hypothalamus also. (D) Strong *cfos* expression is visualized in diencephalic hypothalamus (H) and also in the mesencephalic periventricular gray zone of optic tectum (PGZ). TH immunoreactive cells are shown in the diencephalic posterior tuberal nucleus (PTN). Note absence of TH positive cell somata in optic tectum (TeO). (D') shows magnified hypothalamus (see white box in D). *cfos* positive cells are demonstrated in caudal zone (Hc) and dorsal zone (Hd) of periventricular hypothalamus and in corpus mamillare (CM). (E) *cfos* expression is shown in mesencephalic PGZ, in the cerebellum (CCe) in the hindbrain and in the locus coeruleus (LC) as part of the brainstem. TH expression is visualized in LC and griseum centrale (GC). (E') show magnified the locus coeruleus (LC). The large cells of LC show triple – labeling of *cfos*, TH and DAPI (white arrows). Schematic sagittal view of adult brain shows section levels in D and E. See list for abbreviations. Scale bars in (D) and (E): 200 µm; in (D'): 100 µm in (E'): 10 µm.

4.2.3. Stimulation Experiments Using *cfos* as Marker

The basal expression studies described above (*cfos* - FISH and cfos/TH double fluorescent labeling) demonstrated a generally weaker basal expression of *cfos* in comparison to *egr1* in larvae and adult zebrafish. Based on these results, I decided to measure upreglation through odor stimulation in larvae (Fig. 25) and adults (Fig. 26) using *cfos* expression as activity marker.

Short Stimulation Treatment With Kin Odor. I first compared cfos expression between imprinted larvae and non – imprinted larvae (12 dpf) after short stimulation treatment with kin odor (see Materials and Methods). The comparison is based on quantitative analysis of cfos single labeled cell counting in OB, in comparison of cfos/TH double labeled cells (Fig. 25C, D; white arrows mark cfos/TH double labeled cells) and qualitative analysis of cfos expression patterns in comparable section levels in OB (Fig. 25C', D').

Surprisingly, larvae showed always double labeled cfos/TH positive cells unlike the adults. However, no differences between *cfos* positive cells or *cfos*/TH double labeled cells could be shown in imprinted versus non – imprinted larvae. Both types of larvae were short stimulated with kin odor under same conditions, but no quantitative differences to basal *cfos* expression could be demonstrated (Fig. 21A; Fig.25).

Qualitative analysis focused on *cfos* positive cells in specific parts of larval OB. Comparison of comparable section levels from rostral to caudal visualize evenly distributed *cfos* immunoreactive cells surrounding glomeruli in glomerular layer (gl) (Fig. 25C', D'; medial: MG1-2, lateral: LG1, 3, 4;central zone CZ) without presenting obvious differences in expression patterns between imprinted and non-imprinted larval brains.

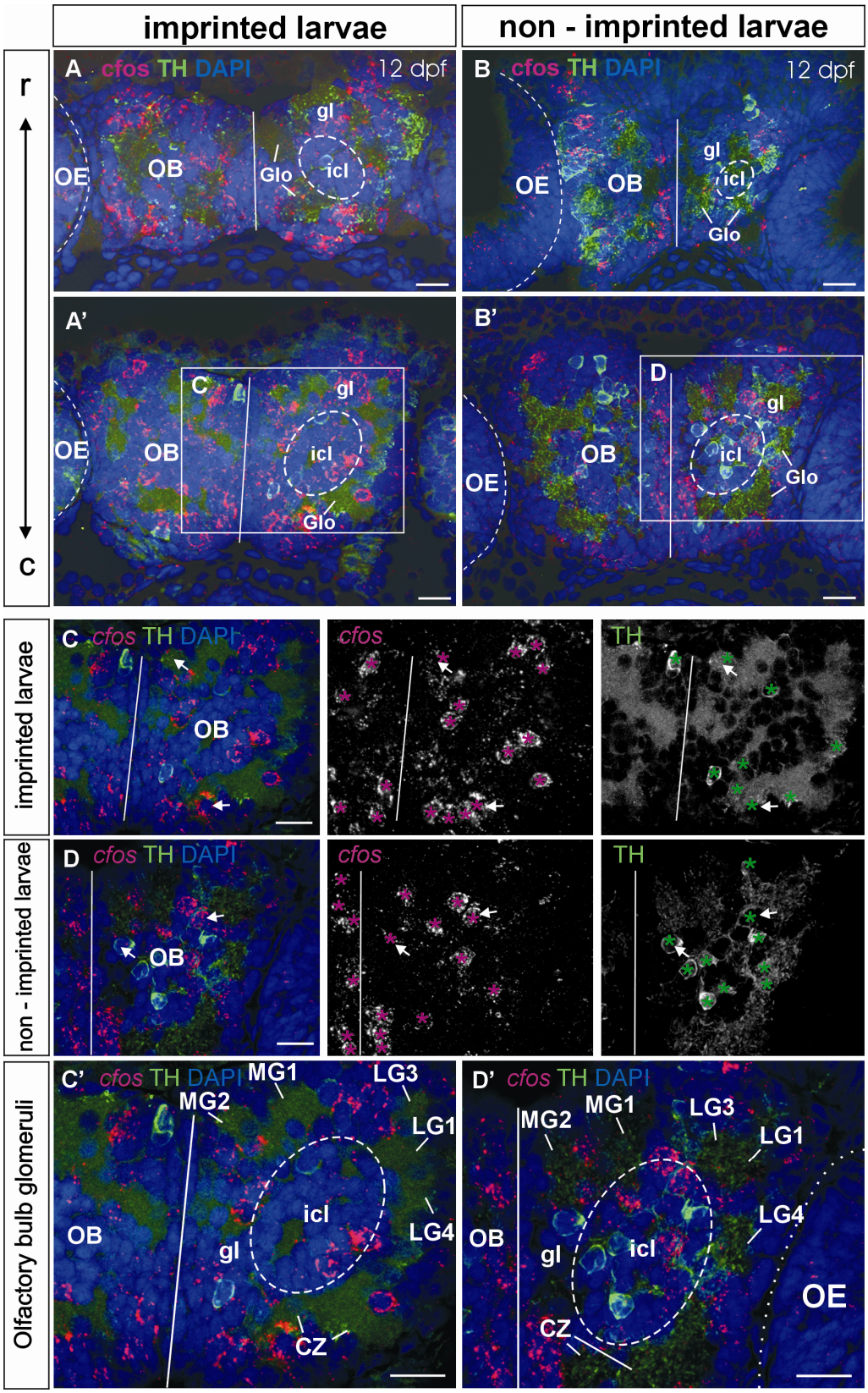

Fig. 25. *cfos* and TH expression in imprinted and non-imprinted larvae after kin odor stimulation.Transverse larval zebrafish brain sections show expression of *cfos* (magenta) and TH (green) counterstained with nuclear marker DAPI (blue) in the olfactory bulb (OB) after short stimulation treatment with kin odor in imprinted and non – imprinted larvae (12dpf). Expression of *cfos*, TH and DAPI is visualized in transverse brain sections of OB from rostral to caudal in imprinted (A, A') and non – imprinted (B, B') larvae. White dashed line encircles the internal cellular layer (icl). Glomeruli (Glo) are visualized via TH

immunoreactive fibers (green) in the glomerular layer (gl). White lines mark the midline of larval brain and white dashed lines visualize the border of the olfactory epithelium (OE). Note the absence of *cfos* or TH positive cells in OE. (C) and (D) show magnifications of OB in imprinted (A') and non – imprinted larva (B') (white boxes C and D, respectively). The *cfos*, TH and DAPI expression is visualized in optical sections and monochromatic images of *cfos* and TH in particular. Red and green stars mark *cfos* and TH positive cells, respectively. White arrows mark triple – labeled neurons and white lines show the midline of the larval brain. (C') and (D') demonstrate *cfos*, TH and DAPI expression in optical sections with specified and labeled OB glomeruli (MG1, 2; LG1, 3, 4; CZ after Baier and Korsching, 1994). See list for abbreviations. Scale bars: 20 µm.

Long Stimulation Treatment With L-Alanine. In zebrafish the labeling of primary afferents using calcium – sensitive dye in conjunction with odor stimulation has previously shown that amino acids activate a chain of glomeruli located on the lateral side of the OB (Friedrich and Korsching, 1997). Therefore, I used amino acid L – alanine in the same concentration used for visualizing activation in lateral OB to show *cfos* upregulation after odor long stimulation treatment in a Mini – flume (see Figs. 9, 10 in Materials & Methods).

In my analysis of L – alanine, as a class of natural odorants, the focus was directed to two olfactory related areas: (1) odor information is conveyed to the OB as first central processing center and (2) from there to the posterior zone of area dorsalis in the telencephalic pallium (Dp), the presumed homologue of the mammalian olfactory cortex. The comparison involved analysis of 10 adult L – alanine stimulated zebrafish versus 10 non – stimulated adult zebrafish in a Mini – flume. The data revealed no obvious quantitative differences neither in *cfos* single labeled neurons nor *cfos*/TH double labeled cells (Fig. 26). Additionally, *cfos* immunoreactive neurons restricted to a particular glomerular field in OB (e.g. the expected lateral side of OB) were not observed. In fact, the *cfos* expression seemed to be distributed over the entire glomerular layer (gl) as well as the internal cellular layer (icl) and, without difference of stimulated and non – stimulated fish compared to basal *cfos* expression patterns.

In Dp scattered *cfos* immunoreactive cells are visualized without differing in cell count from *cfos* basal expression as well as between stimulated and non – stimulated zebrafish.

Thus, in both olfactory related areas (OB and Dp) in adult zebrafish forebrain no quantitative or qualitative differences could be shown in

comparison to basal *cfos* expression or between L-alanine stimulated and non-stimulated fish.

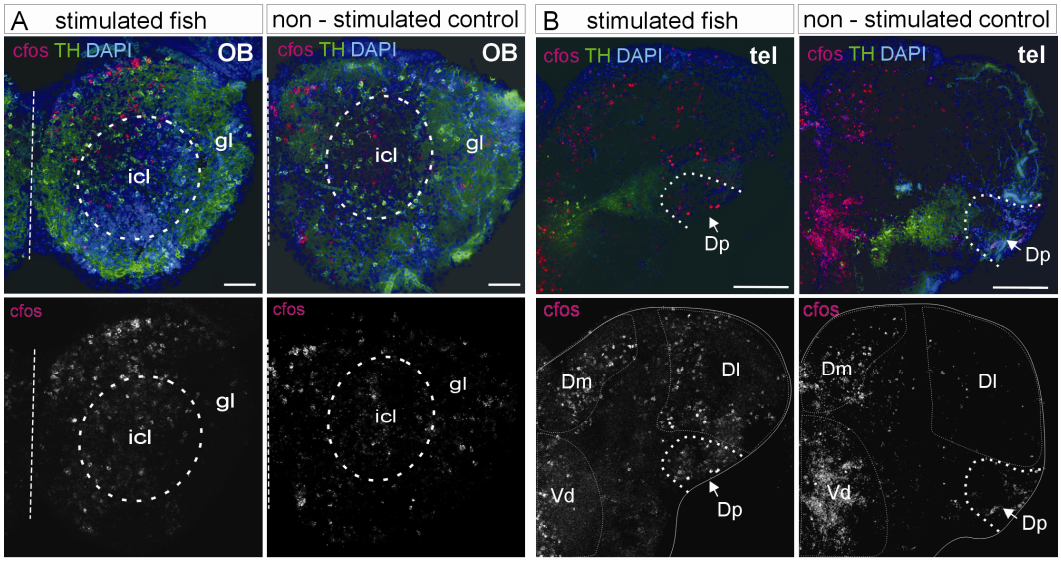

Fig. 26: *cfos* and TH expression in adults after amino acid stimulation. Transverse brain sections show adult *cfos* and TH expression in the olfactory bulb (A) and telencephalon (B) of L – alanine long stimulated zebrafish in comparison to non - stimulated control zebrafish. Upper rows in (A) and (B) demonstrate *cfos* (magenta) and TH (green) expression counterstained with DAPI (blue) in confocal optical sections and the subjacent rows present corresponding monochromatic images of *cfos*. (A) White dashed circles mark the boundary of internal cellular layer (icl) in olfactory bulb and white dashed lines demonstrate the midline of adult brain. *cfos* immunoreactive neurons are visualized in the glomerular layer (gl) and in the icl in stimulated and unstimulated fish. Strong TH expression is shown in gl. See Fig. 13(A) for comparison with basal *cfos* and TH expression. (B) White lines mark the boundary of telencephalon and telencephalic areas inside. White dashed lines demonstrate the midline of adult brain and white dotted lines point out the posterior zone of dorsal telencephalic area (Dp; see white arrows). *cfos* immunoreactive neurons are visualized in pallial telencephalic areas Dm, Dl and Dp and in subpallial Vd (see white lines). TH expressing cells are shown in Vd. See Fig. 13(B, B') for comparison with basal *cfos* and TH expression. See list for abbreviations. Scale bars in (A): 50 µm and in (B): 100 µm.

4.3. Experiments Involving pErk

4.3.1. Olfactory Stimulation Using pErk as Activity Marker

An alternative neuronal activity marker, i.e. the phosphorylated form of the mitogen – activated protein kinase (MAPK – also known as Extra cellular signal Regulated Kinase; ERK1/2) - was used in further experiments in order to possibly visualize differences in expression patterns after olfactory stimulation in larval and adult zebrafish.

It is known that the timeline of kinase – dependent protein phosphorylation is much shorter in comparison to IEG expression (Murphy and Blenis, 2006; Taziaux et al., 2011). Phosphorylation of MAPK/Erk (referred to as pErk in my thesis) occurs upstream of the IEGs and

involves only one enzymatic activity in contrast to the induction of genomic transcription and translation of IEG products (see Fig. 7 in Materials & Methods). Therefore using pErk as a tool for mapping neuronal activity allows much shorter stimulation periods in comparison to those needed for reaching high quantity of detectable IEG products in brain tissue. Zebrafish larvae are physically unable for stimulation treatments in the Mini – flume over a period of 60 to 90 minutes (personal observation). However, the shorter timeline of pErk activation allows for stimulation treatment of larvae.

4.3.2. Larvae

Triple labeling of pErk, *cfos* and TH demonstrates basal expression of all three markers for neuronal activity at the same time in OB of untreated zebrafish larva (9dpf) (Fig. 27). Basal expression of pErk revealed numerous pErk immunoreactive neurons and fibers in the telencephalon including OB and terminal nerve (TN) cells (Fig. 27). In OB expression of pErk is shown in neurons and fibers in the glomerular layer which is demonstrated by pErk/TH double labeling (white arrowheads in Fig. 27C, D, F). Moreover, scattered pErk positive cells are visualized in the icl. Expression of *cfos* is difficult to assign to specific cells but *cfos* /pErk double labeled cells could be demonstrated in OB and telencephalon (white arrows in Fig. 27C, D, E). Triple labeling also revealed numerous unlabeled cell bodies enclosed by pErk and TH immunoreactive fibers in OB (Fig. 27C, D, F). These may represent (glutamatergic) projection cells.

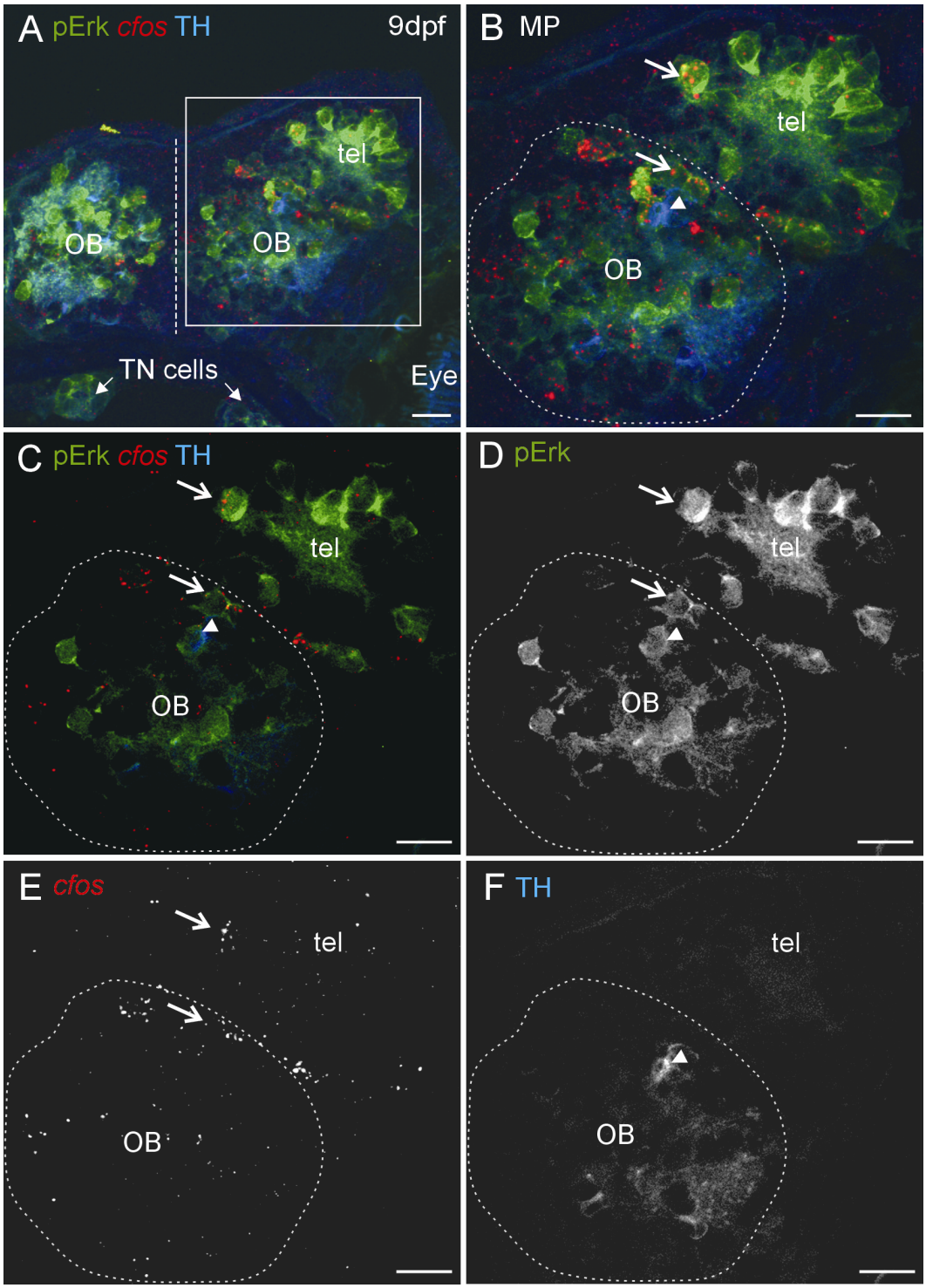

Fig. 27. Larval basal pErk, cfos, and TH expression. Transverse zebrafish brain sections show basal expression of pErk (green), *cfos* (red) and TH (blue) in the olfactory bulb (OB) and rostral telencephalon (tel) of larvae (9dpf). (A) Transverse section of left and right OB and rostral telencephalon of the right side visualize strong expression of pErk in cell somata and fibers. In ventral part of the larval head, pErk immunoreactivity is shown in terminal nerve cells (TN cells; white arrows). Scattered *cfos* expressing neurons are demonstrated in OB and tel. TH positive neurons and fibers are visualized in OB. White dashed line indicates midline of larval head and white box shows region magnified in (B). (B) Magnification of right OB and rostral tel (see white box in A) shows maximum projection (MP) of confocal image. White dashed circle marks the border of OB. (C) demonstrates pErk, *cfos* and TH expression in optical section. (D), (E) and (F) visualize pErk, *cfos* and TH expression, respectively, in monochromatic images. White arrows in (B) – (E) mark pErk / *cfos* double – labeled neurons in OB and rostral telencephalon.

White arrowheads in (B), (C), (D) and (F) mark pErk / TH double – labeled neuron in OB. Note the absence of *cfos* / TH double – labeled neurons. See list for abbreviations. Scale bars: 20 µm.

Next, I analyzed pErk expression of imprinted and non – imprinted larvae (10 dpf) after short stimulation with kin odor (Fig. 28). Double labeling with TH visualized strong pErk expression in neuronal cell bodies and fibers in OB in addition to singly pErk positive cells**.** Additional analysis of pErk expression in olfactory epithelium (OE) revealed pErk immunoreactive olfactory sensory neurons (OSNs) in imprinted and non – imprinted larvae. In comparison to pErk expression in the forebrain, there are less and more weakly stained pErk immunoreactive cells in the OE. Most pErk positive OSNs are slender cells with the somata in basal position and long dendrites extending into lumen (presumably ciliated OSN), but also some pErk positive neurons are visualized as plump – shaped cells which have shorter apical processes (presumably microvillous OSN) (Fig. 28 C, C').

Qualitative analyses of pErk expression in OB and OE of 12 imprinted and 12 non – imprinted larvae revealed no dramatic differences but show a tendency of pErk upregulation in OB and OE in imprinted larvae (10 dpf).

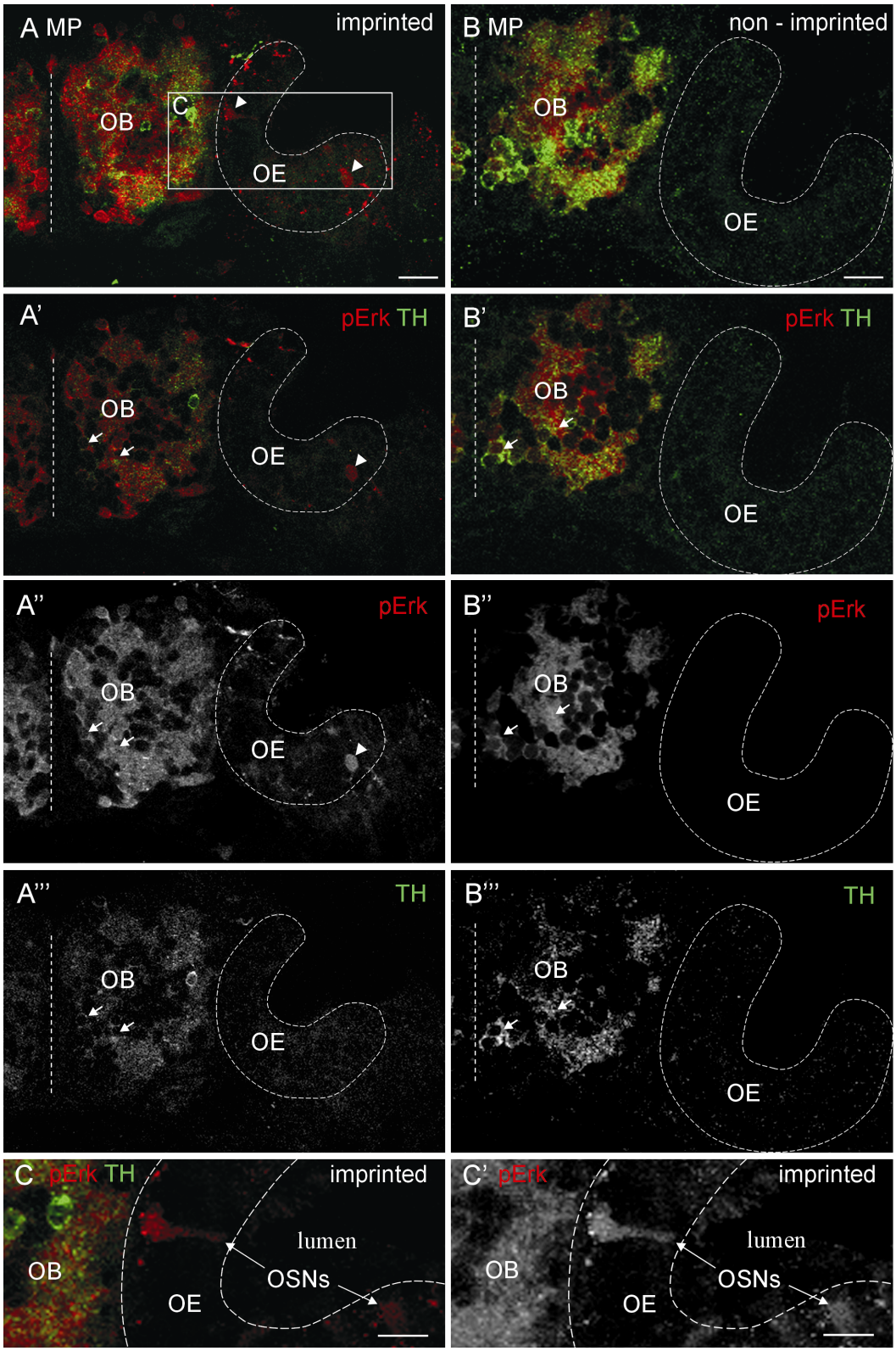

Fig. 28. pErk and TH expression in imprinted and non-imprinted larvae after kin odor stimulation. Transverse zebrafish brain sections show expression of pErk (red) and TH (green) in the olfactory bulb (OB) and olfactory epithelium (OE) in imprinted and non – imprinted larvae (10 dpf) after short stimulation with kin odor. In (A) maximum projection (MP) visualizes pErk expressing neurons in OB and OE in imprinted larva. White arrowheads mark pErk immunoreactive olfactory sensory neurons (OSNs) in OE. White dashed lines visualize boundary of OE. TH expressing neurons are shown in OB, but not in OE. White box marks area magnified in (C). In non-imprinted larvae (B) pErk and TH expressing neurons are visualized in OB. In the OE, no TH cells are seen, but pErk

immunoreactive neurons may occur in the OE (not shown here)**.** In (A') and (B') optical sections demonstrate pErk and TH expression in OB. White arrows mark pErk/TH double labeled cells. In (A') white arrowhead labels pErk immunoreactive OSN in OE. No pErk immunoreactive neurons are visualized in OE of non-imprinted larvae (B'). pErk (A''; B'') and TH expression (A'''; B''') is visualized and in monochromatic images, respectively. In (C) magnified image of (A; see white box) shows pErk and TH expression in OE of imprinted larva. White dashed lines visualize boundary of OE; white arrows visualize OSNs in OE. White dashed lines mark the midline of larval brain. See list for abbreviations. Scale bars in (A) and (B): 20 µm; in (C) and (C'): 10 µm.

4.3.3. Adults

Basal expression of pErk in adult zebrafish revealed immunoreactive neurons and fibers surrounding glomeruli (Glo) in glomerular layer (gl) of OB (Fig. 29 A). Scattered pErk positive cells are also shown in internal cellular layer (icl) of OB.

Secondary olfactory neurons (mitral cells/ruffed cells) in OB project via the medial and lateral olfactory tract into higher centers of the brain. I focused on two olfactory related telencephalic areas: (1) the posterior zone of the dorsal telencephalon (Dp; Fig. 29B), which is considered as the pallial homologue of the mammalian olfactory cortex and (2) the supracommissural nucleus of the ventral telencephalon (Vs; Fig. 29C), the hypothetical medial amygdala in zebrafish. Interestingly basal expression of pErk revealed that pErk immunoreactive cells are absent or very sparsely expressed in Dp (Fig. 29B, C). Also, little to no basal pErk expression is seen in the dorsal and central zones of the dorsal telencephalon (Dd, Dc). In contrast, other telencephalic areas, in particular the like medial and lateral dorsal telencephalic zones (Fig. 29B; Dm and Dl, the homologues of pallial amygdala and hippocampus, respectively), as well as ventral and dorsal ventral telencephalic nuclei (Fig. 29B; Vv and Vd, respectively) demonstrate strong pErk expression in neurons and fibers. Basal pErk expression is also visualized in Vs where clearly defined scattered pErk immunoreactive neurons, but no pErk immunoreactive fibers are present in Vs (Fig. 29C).

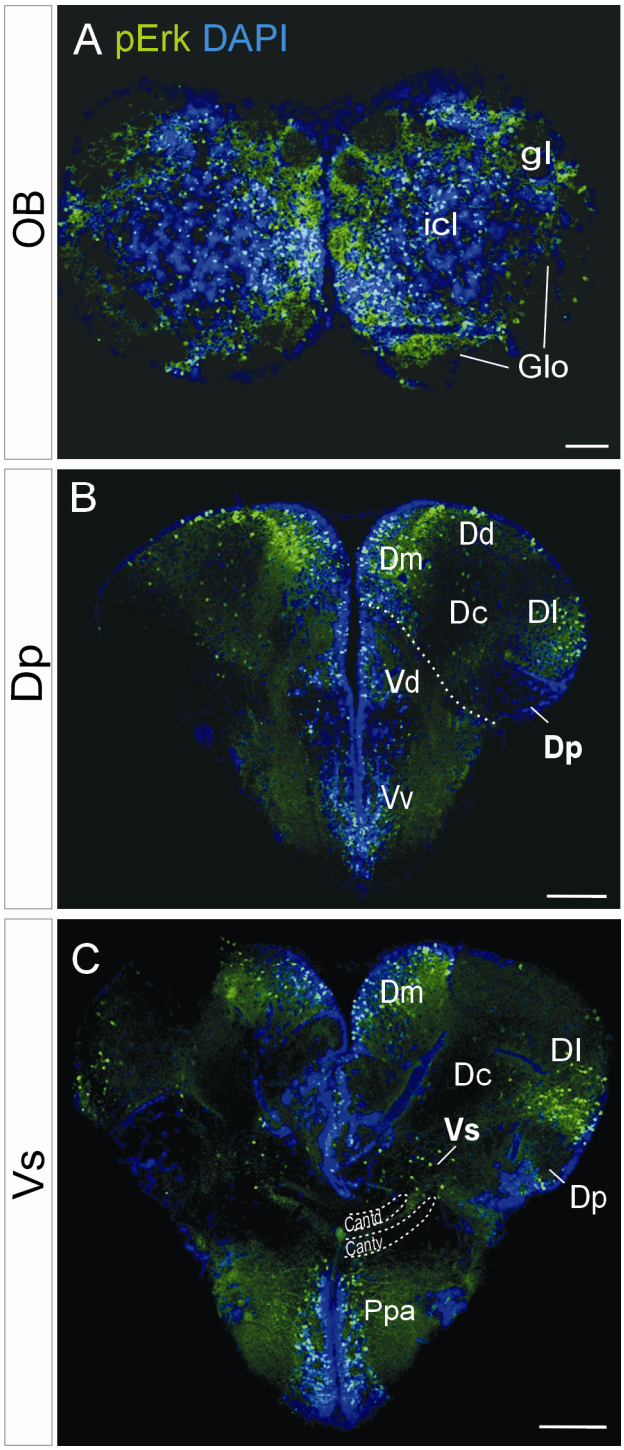

Fig. 29. Adult basal pErk expression. Transverse zebrafish brain sections show adult expression of pErk (green) counterstained with nuclear marker DAPI (blue) in olfactory related areas OB, Dp and Vs in the forebrain. (A) in the olfactory bulb (OB) pErk positive neurons are visualized in glomerular layer (gl) and in the internal cellular layer (icl). Strong pErk immunoreactive fibers are shown in gl surrounding glomruli (Glo). (B) pErk expression is visualized in subpallial telencephalic areas Vd and Vv and in pallial telencephalic areas Dm and Dl. pErk positive fibers are also demonstrated in pallial and subpallial regions. Scattered pErk immunoreactive neurons and fibers are shown in Dc and Dd, but are absent in Dp. White dashed line show the border of dorsal (pallial) and ventral (subpallial) telencephalon. (C) pErk immunoreactive cells and fibers are shown in pallial telencephalic areas Dm and Dl and scattered pErk - immunoreactive neurons are seen in Dc. In subpallial Vs, pErk expressing cells are visualized and pErk - immunoreactive neurons and fibers are seen in the anterior part of the parvocellular preoptic nucleus (PPa). White dashed lines mark the border of the anterior commissure separated in a ventral (Cantv) and dorsal part (Cantd). See list for abbreviations. Scale bar in (A): 50 µm; in (B) and (C): 100 µm.

Based on these results of pErk basal expression in adult zebrafish olfactory areas, I aimed to visualize pErk expression after olfactory test procedure. Adult zebrafish used in this experiment were offspring of the first generation of MHC peptide mix imprinted zebrafish (Hinz et al., 2012; Ma, 1997) and tested as larvae in olfactory flume choice tests showing preference for MHC peptide mix in comparison to odorless water. In short stimulation treatments, 12 MHC peptide mix imprinted adult zebrafish were

used and half of them stimulated with MHC peptide mix for 7 minutes and the other half were stimulated with odorless water under same conditions.

Triple labeling of pErk, TH and the nuclear marker DAPI in transverse brain sections of stimulated versus non – stimulated adult fish revealed no difference in expression patterns in olfactory related areas OB, Dp and Vs (Fig. 30). Strong pErk expression is shown in neurons and fibers in OB without obvious differences to pErk basal expression (Fig. 29A; Fig. 30A, A'). Scattered pErk positive cells are visualized in Dp in both testfish groups (Fig. 30B, B', D, D'). In Vs pErk single labeled neurons and pErk/TH double labeled neurons (white arrows in Fig. 30D, D') are visualized, but no differences could be shown between MHC peptide mix stimulated fish and non – stimulated control fish. Expression of pErk in Vs of both testfish groups shows also no differences to pErk basal expression (Fig. 29C; Fig. 30D, D').

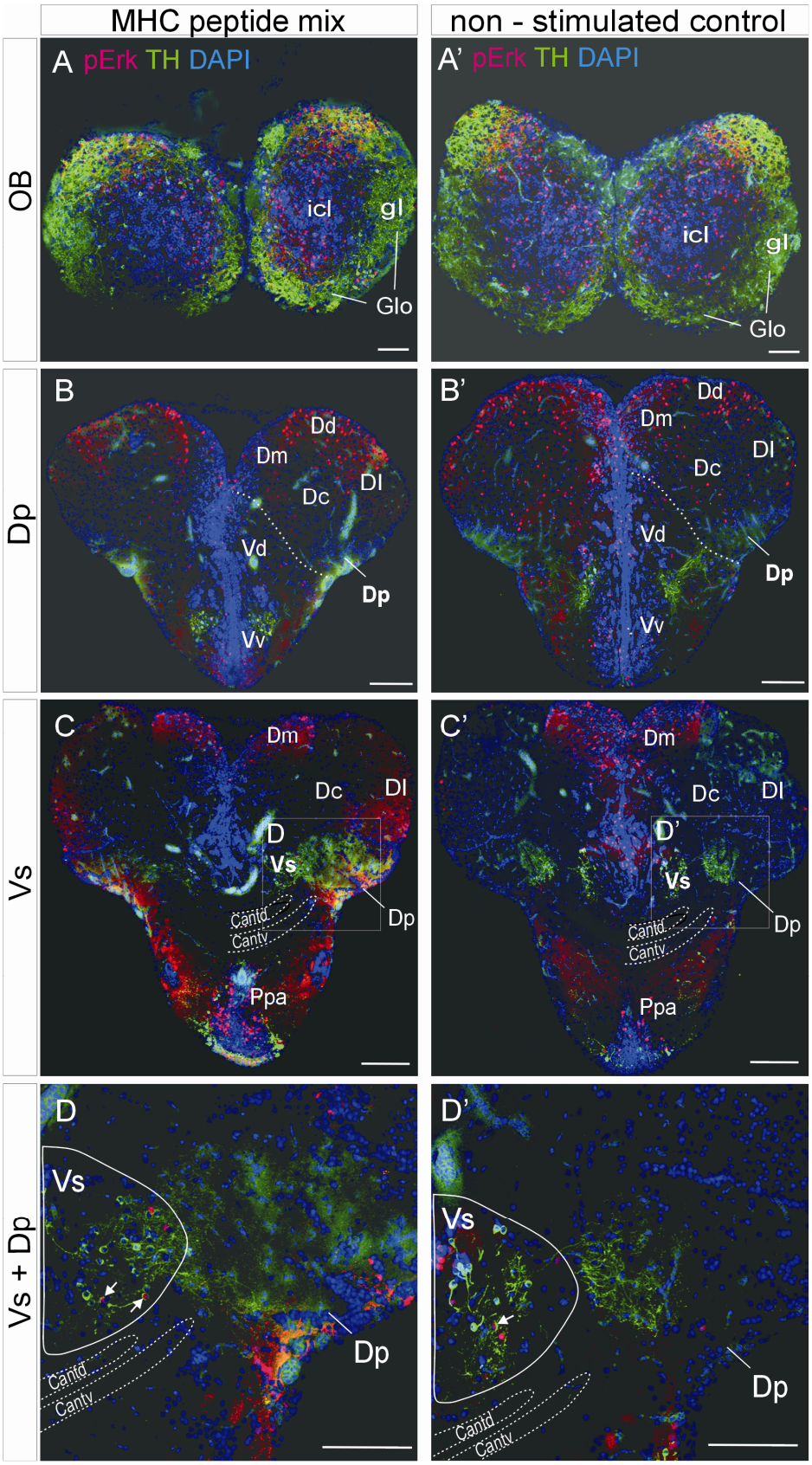

Fig. 30. Comparison of adult pErk/TH double labeling in MHC stimulated and control fish. Transverse brain sections show adult pErk (magenta) and TH (green) expression counterstained with nuclear marker DAPI (blue) from rostral (OB) to caudal forebrain (telencephalon) in MHC peptide mix stimulated zebrafish in comparison to non - stimulated control zebrafish. (A) Strong TH expression is visualized in glomerular layer of

olfactory bulb (gl) with scattered TH – immunoreactive cells in the internal cellular layer (icl). pErk positive neurons are visualized in icl and gl.
(B) pErk expression is visualized in subpallial telencephalic areas Vd and Vv and pErk positive neurons in pallial telencephalic areas Dm, Dd, Dc and Dp. TH – immunoreactive cells are shown in Vv. White dashed line show the border of dorsal (pallial) and ventral (subpallial) telencephalon. In (C) pErk expression is shown in pallial telencephalic areas (Dm, Dc, Dl and Dp) and scattered pErk - immunoreactive neurons in subpallial Vs and the anterior part of the parvocellular preoptic nucleus (PPa). TH positive neurons are demonstrated in Vs and in the ventral area of PPa. White boxes outline areas magnified in (D) and (D'). White dashed lines mark the border of the anterior commissure separated in a ventral (Cantv) and dorsal part (Cantd). In (D) and (D') magnified telencephalic area at the boundary of pallium and subpallium including Dp and Vs (see white boxes in (C) and (C') visualize pErk expressing cells and TH expressing cells and pErk / TH double – labeled cells (white arrows) in Vs. Scattered pErk immunoreactive neurons are visualized in Dp. White lines mark the border Vs and white dashed lines mark the borders of Cantv and Cantd. See list for abbreviations. Scale bars in (A) and (A'): 50 µm; in (B) and (B'), (C) and (C') and (D) and (D'): 100 µm.

Based on pErk expression in olfactory sensory neurons (OSNs) in olfactory epithelium (OE) of larvae, pErk expression, I also visualized in transverse sections of adult olfactory epithelium in zebrafish (Fig. 31). In the sensory region, only a few pErk positive slender cells are found with somata in basal position and long dendrites extending into lumen which possess ciliary knobs (Fig. 31B, B'). This morphology of OSNs indicates that adult pErk positive cells represent ciliated OSNs.

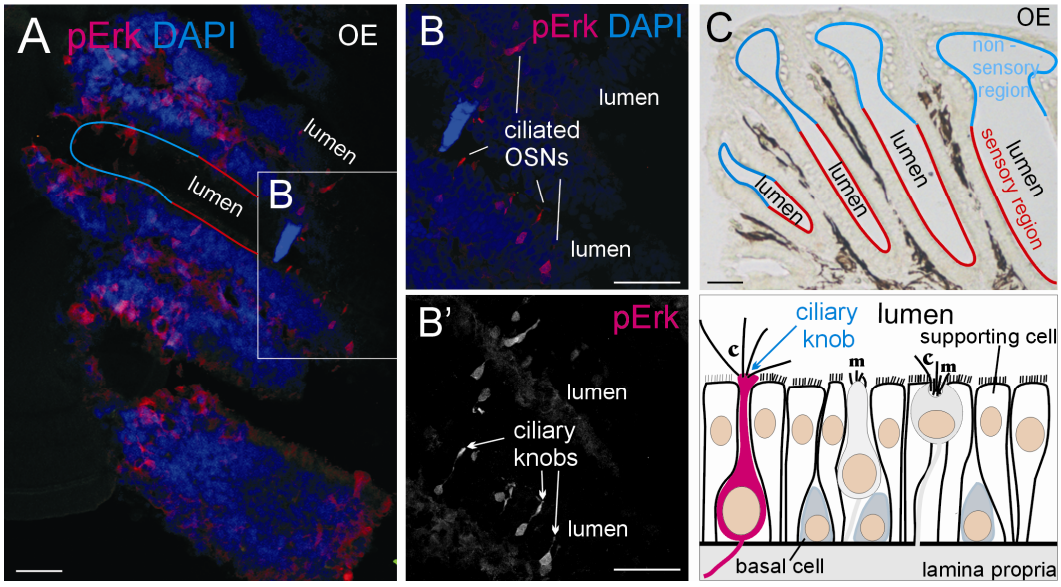

Fig. 31. pErk expression in adult olfactory epithelium (OE). Transverse section of adult OE visualizes pErk expression counterstained with nuclear marker DAPI. In (A) pErk immunoreactive cells are visualized in sensory region (red line) and non – sensory region (blue line in C) of OE. White box marks region magnified in (B) and (B'). Magnified image in (B) reveals pErk immunoreactivity in olfactory sensory neurons (OSNs) with long dendrites extending into the lumen and featuring cilia. (B') monochromatic image of pErk point out ciliary knobs (white arrows; see schematic drawing). (C) transverse section demonstrates non – sensory region and sensory region of OE highlighted in blue and red, respectively. The subjacent schematic drawing visualizes different cell types in OE and in magenta highlighting ciliated OSN. See list for abbreviations. Scale bars: 20 µm

4.4. Calcium-Binding Proteins in the Zebrafish Primary Olfactory System

4.4.1. Olfactory Sensory Neurons

As in other vertebrates odor information in teleosts is conveyed to the OB, the first central olfactory processing region. A final aim of my thesis is to provide new insight about differential primary olfactory zebrafish subsystems using calcium binding proteins (CBPs). These often characterize different neuron types and I aimed to accomplish a combinatorial analysis of subtypes of olfactory sensory neurons in the OE and their differential axonal projections into the OB in larval and adult zebrafish.

The OE of fish contains three different types of olfactory sensory neurons (OSNs), which are ciliated OSNs, microvillous OSNs and crypt cells (Fig. 32 I, II, III, respectively). In zebrafish, the CBPs calretinin (Castro et al. 2006; Gayoso et al. 2011, Braubach et al. 2012) and S100 (Germana et al. 2004, 2007, Gayoso et al. 2011, Sandulescu et al. 2011, Braubach et al. 2012) are mainly expressed in ciliated OSNs or crypt cells, respectively. In contrast, parvalbumin and calbindin1 have not been investigated in the zebrafish OE.

Combinatorial analysis of the CBPs calretinin, S100, parvalbumin and calbindin1 in larval and adult zebrafish OE revealed that calretinin and calbindin1 are strongly expressed in ciliated and microvillous OSNs in larvae (Fig. 34C-C''), but both appear to become restricted to ciliated cells in adult zebrafish (Fig. 33A, D). Parvalbumin is strongly expressed in ciliated and microvillous OSNs. All three CBPs are not present in crypt cells (Fig. 32A, B; Fig. 33). Additionally, my analysis confirms a major expression of S100 in larval and adult crypt cells, but shows also limited expression of S100 in some microvillous OSNs (Fig. 32C, D, E; Fig. 33 C). Extension of the analysis by parvalbumin/S100 double labeling revealed that microvillous cells are divided at least in solely parvalbumin positive and parvalbumin/S100 double - positive subpopulations (Fig. 32C, D, E; Fig. 33B, C).

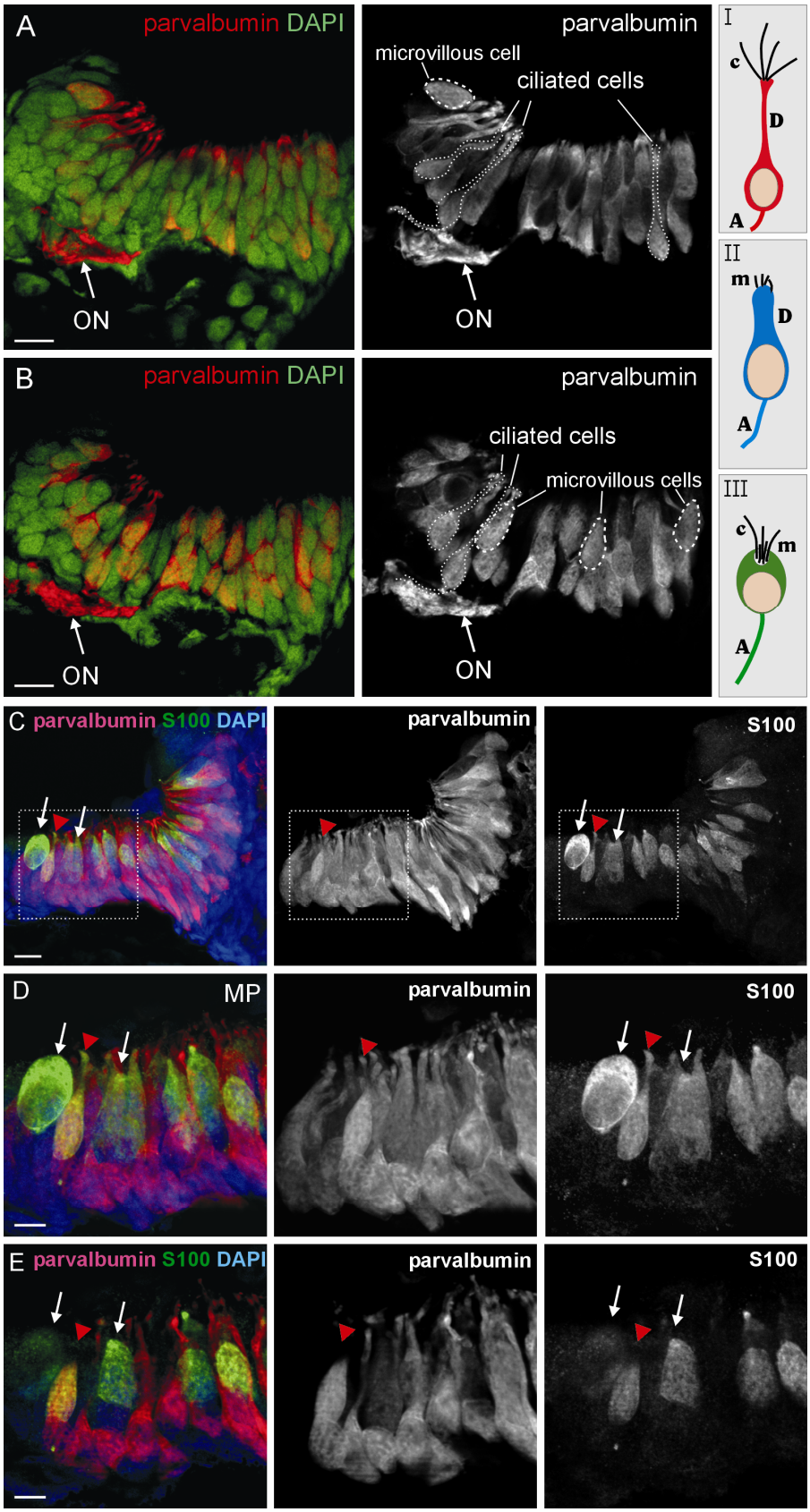

Fig. 32. Ca-binding proteins in larval crypt cells and microvillous OSNs. Transverse sections visualize expression of parvalbumin and S100 counterstained with nuclear marker DAPI in olfactory epithelium of larval zebrafish (9 dpf). Optical sections in (A) and (B) demonstrate parvalbumin immunoreactive olfactory sensory neurons (OSNs) and parvalbumin positive olfactory nerve (ON) in the same OE rostrally (A) and more caudally (B). Panels to the right show parvalbumin expression in monochromatic images.

Schematic drawings show ciliated OSN in red (I), microvillous OSN in blue (II) and crypt cells in green (III) with dendrites (D), axons (A), microvilli (m) and cilia (c). Transverse sections in (C; maximum projection), (D; maximum projection) and (E; optical section) visualize parvalbumin and S100 expression counterstained with nuclear marker DAPI. White box in (C) marks area magnified in (D) and (E). On the right, parvalbumin and S100 immunoreactive OSNs are visualized in monochromatic images. White arrows point out S100 immunoreactive crypt cells and red arrowheads show parvalbumin and S100 double labeled microvillous cells. See list for abbreviations. MP = maximum projection. Scale bars in (A), (B), (C): 20 µm and in (D) and (E): 10 µm.

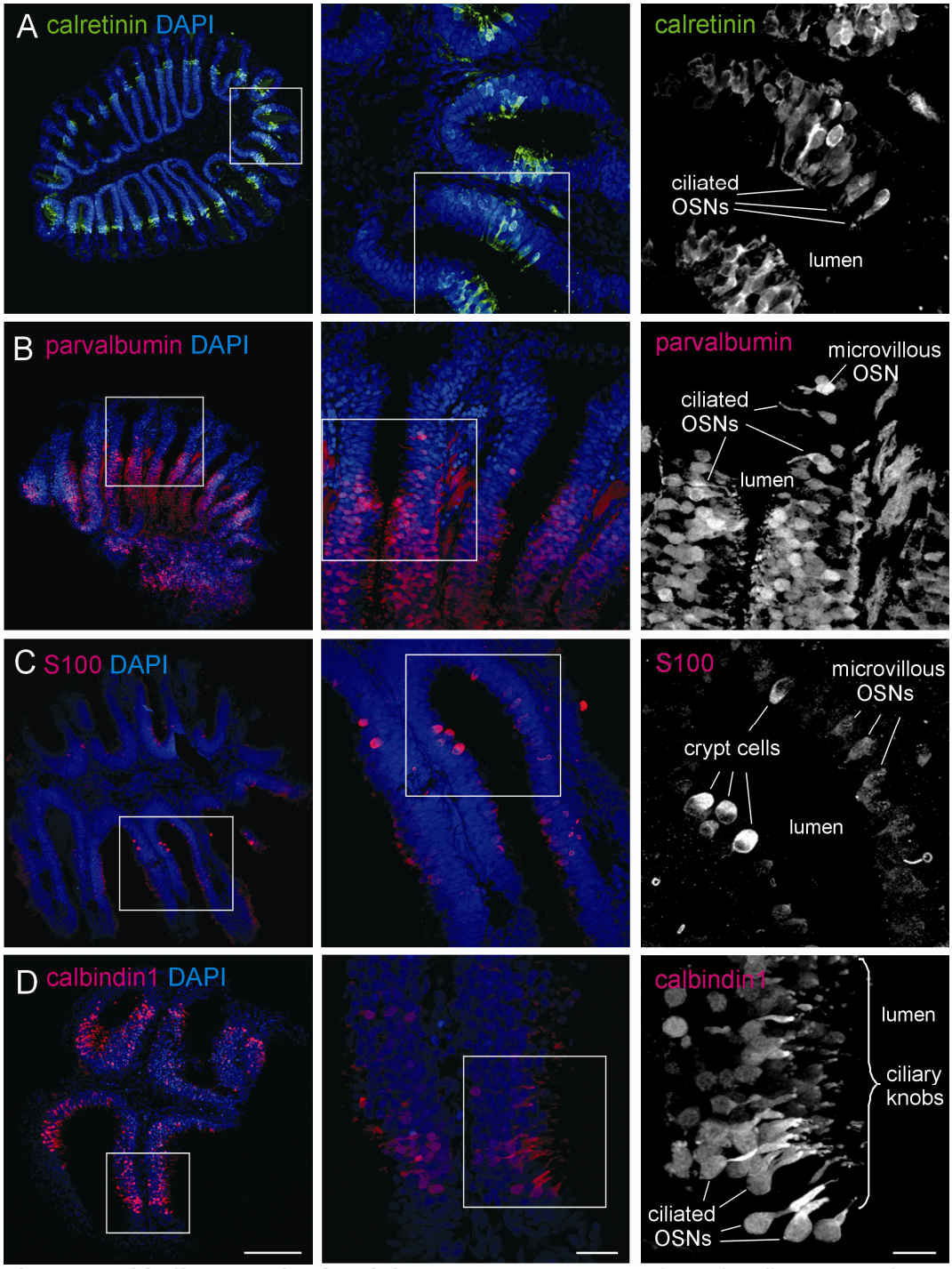

Fig. 33. Ca-binding proteins in adult OSNs. Transverse sections visualize expression of calcium binding proteins calretinin (A), parvalbumin (B), S100 (C) and calbindin1 (D) counterstained with nuclear marker DAPI in olfactory epithelium of adult zebrafish. White boxes mark areas magnified in images on the right. Right panels: magnified optical sections of area in boxed in middle panels visualize monochromatic images. See list for

abbreviations. Scale bar in (D) and middle panel right of (D): 100 µm; 20 µm and in right panels: 10 µm.

4.4.2. Larval Olfactory Bulb Projections

CBP immunohistochemistry was also used to visualize primary projections of different OSNs into the OB of larval and adult zebrafish.

Combinatorial analysis of axonal projections in the larval OB reveals different bulbar targets of CBP - immunoreactive axons correlated with different expression patterns of corresponding CBP expression in OSNs (Fig. 34). Consistent with strong expression of parvalbumin in ciliated and microvillous OSNs, parvalbumin positive axons also show numerous glomerular targets in OB (Fig. 34A, A', B). A detailed analysis demonstrates that almost all larval glomeruli are innervated by parvalbumin positive axonal projections.

In contrast, double labeling of parvalbumin and S100 reveals that S100 immunopositive projections only innervate a defined glomerulus in the medial region (medial glomerulus2 = MG2) in the OB which is also innervated by parvalbumin positive projections (Fig. 34B. B').

Double labeling of calretinin and calbindin1 visualize that both CBPs are expressed in many larval ciliated and microvillous OSNs in OE and largely overlap in bulbar targets in OB (Fig. 34C-C''). But in comparison, calbindin1 is less strongly expressed than calretinin in OE (white arrows in Fig. 34C-C'') and OB. However, calretinin and calbindin1 immunopositive fibers appear not to project to the MG2.

Calretinin immunopositive projections innervate lateral glomeruli (LG) and glomeruli of the central zone (CZ) in OB (Fig. 34C''). Expression of calbindin1 is only visualized in lateral glomerli (LG) (Fig. 34C'), not in CZ.

Thus, these investigations of calretinin and calbindin1 immunopositive projections indicate that calbindin1 is less strongly expressed than calretinin in OE and this is reflected in the extent of bulbar targets of CBP immunopositive axons. For a more detailed description of the projection differences of calbindin1 and calretinin, analyses using confocal microscopy are necessary.

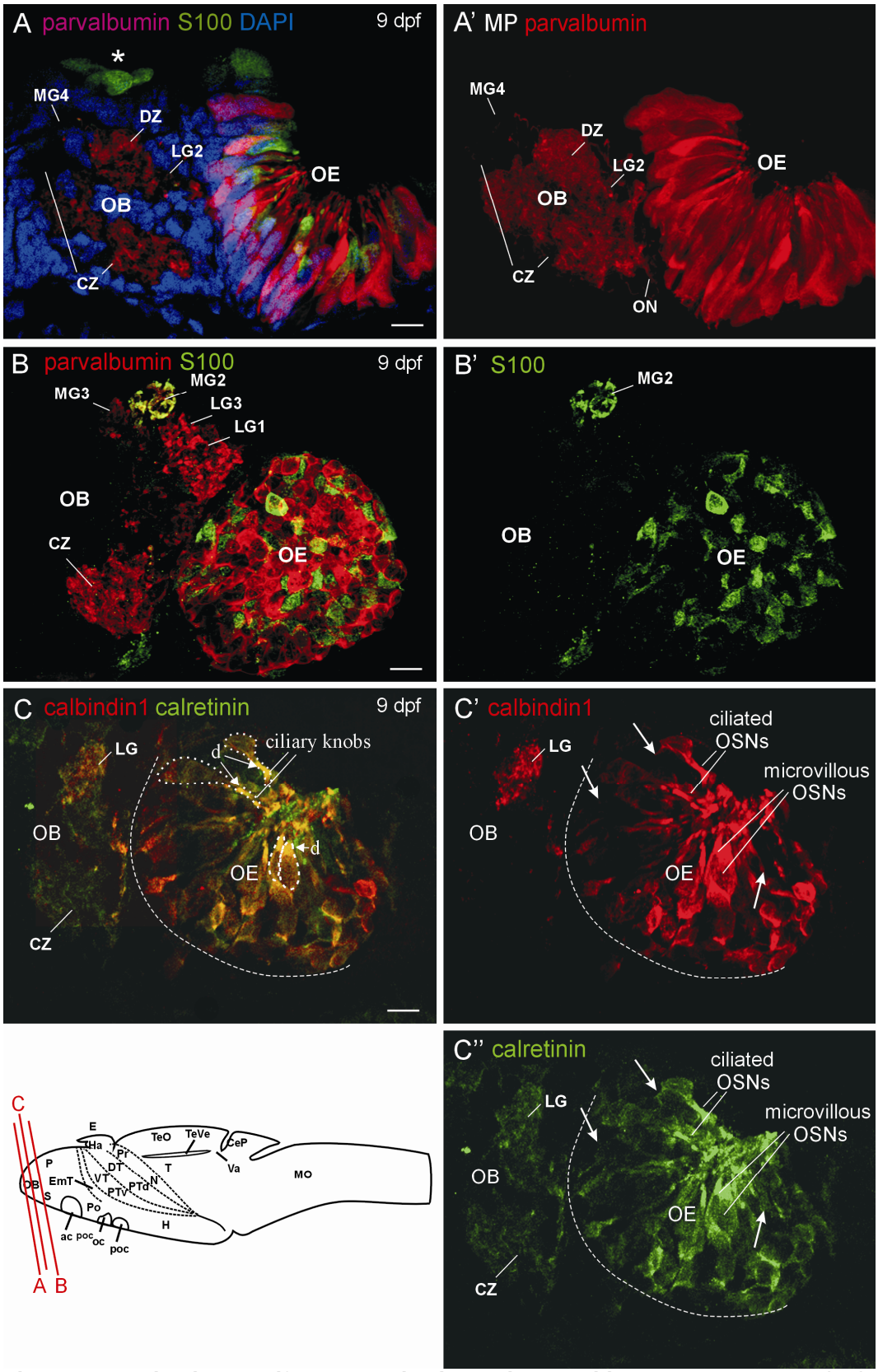

Fig. 34. Larval primary olfactory projections shown with CBPs. Transverse brain sections visualize expression of parvalbumin, S100, calretinin and calbindin1 in olfactory sensory neurons in the olfactory epithelium (OE) and their projections into the olfactory bulb (OB) in zebrafish larvae (9 dpf). (A) Double – labeling of parvalbumin and S100 counterstained with nuclear marker DAPI visualizes larval OB. White star marks S100 immunoreactive neuromast. Strong expression of parvalbumin in OSNs and their extensive projections to the glomeruli in the OB is shown. Scattered S100

immunopositive cells are seen in OE. Note the absence of S100 positive projections at this level in OB. (A') Monochromatic image of parvalbumin demonstrates strong expression of parvalbumin in OSNs and their axonal projections. (B) Double labeling of parvalbumin and S100 at a more caudal level of the larval brain (see schematic sagittal view of larval brain). Strong expression of parvalbumin in OSNs and their extensive projections to the glomeruli in the OB is demonstrated. Scattered S100 immunoreactive OSNs and their S100 immunopositive projections to the medial glomerulus2 (MG2) in the dorsomedial region of OB are shown. Parvalbumin positive projections are also present in medial glomerulus2 (MG2) and medial glomerulus3 (MG3) right next to MG2, but no S100 positive projections are shown in medial glomerulus3 (MG3). Note that no other glomeruli except for MG2 show S100 positive projections. Note that the S100/parvalbumin co – expressing OSNs and the double labeling of projections to MG2 in the OB are shown. (B') Monochromatic image shows S100 expression in OE and projection to MG2. (C) Double labeling of calretinin and calbindin1 reveals co – expressing neurons in OE and double labeling of projections to lateral glomeruli (LG) in OB. (C', C'') Monochromatic images of calbindin1 (C') and calretinin (C'') visualize double labeled OSNs with long dendrites (d) and ciliary knobs and microvillous OSNs in OE and double labeled projections to LG. White arrows label calretinin positive OSNs, which are not visualized by calbindin1expression. Note that calbindin1 (C') immunopositive projections only reach lateral glomeruli (LG), but that calretinin (C'') has projections to central zone (CZ) and lateral (LG) glomeruli. White dashed lines indicate boundary of OE. Schematic sagittal view of larval brain shows section levels in A, B and C. See list for abbreviations. Scale bars: 20 µm

Analysis of parvalbumin/S100 positive axonal projections in the developing OB reveals differing time course of different primary projections between 3 to 9dpf (Fig. 35). At day 3, parvalbumin positive projections are already seen to invade the OB, but S100 positive terminals are completely absent at this early larval stage (Fig. 35A) despite the fact that both immunoreactive parvalbumin and S100 OSNs are present at this age (Fig. 35A, middle and right panel). From day 6 on, the S100 positive terminals can be visualized in the medial glomerulus2 (MG2) and increase to day 9 (Fig. 35B-D; see above). In contrast, parvalbumin positive terminals appear not to increase during this time frame, but are present from 6 to 9 dpf at similar strength, apparently reaching the MG2 and many other glomeruli much earlier (Fig. 35A-D).

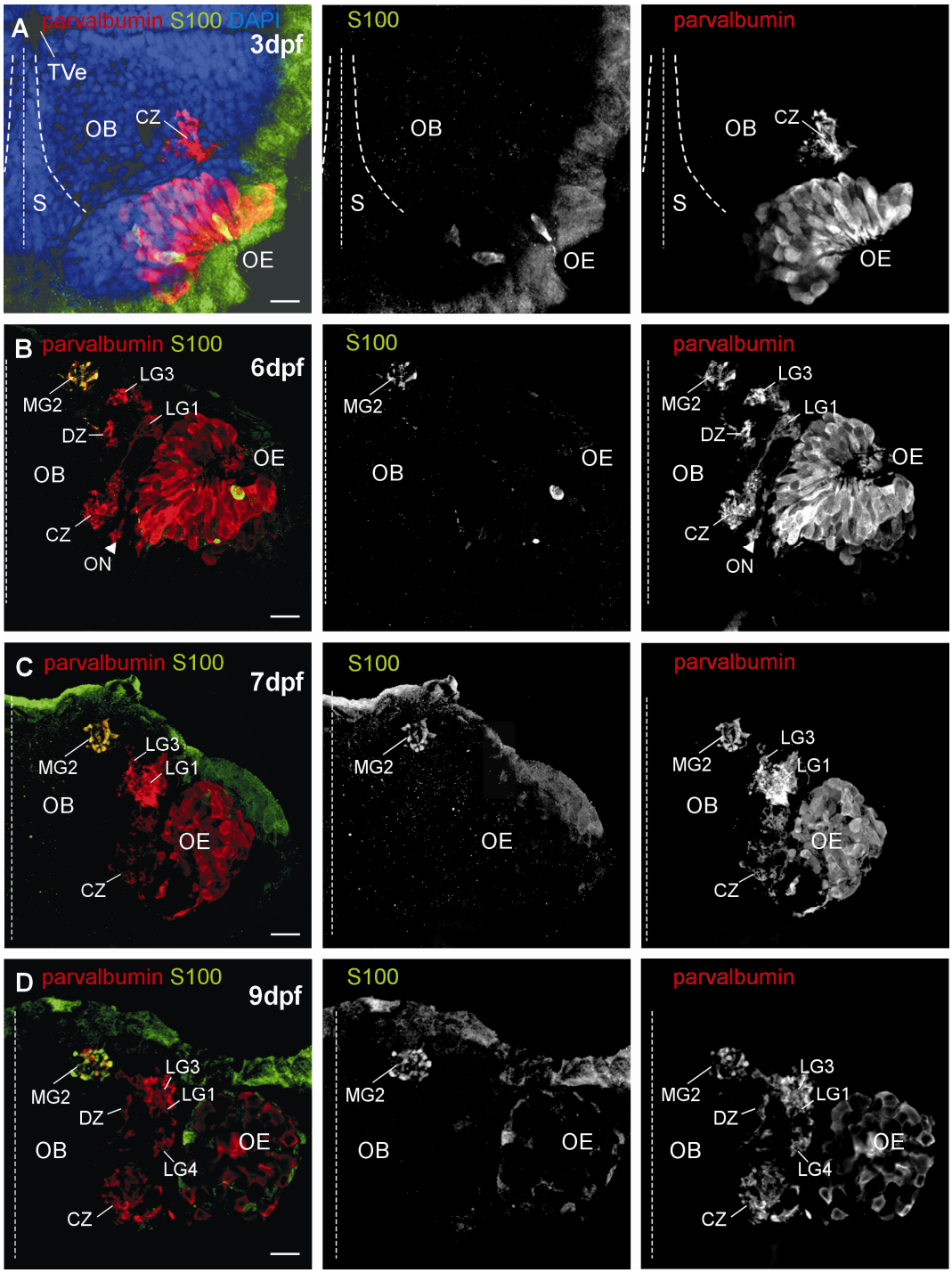

Fig. 35. Development of primary olfactory projections shown with CBPs. Transverse brain sections visualize expression of parvalbumin and S100 in olfactory sensory neurons (OSNs) in the olfactory epithelium (OE) and their projections in the olfactory bulb (OB) in 3 dpf (A), 6 dpf (B), 7 dpf (C) and in 9 dpf (D) larvae at comparable brain levels. Left panels demonstrate optical sections visualizing parvalbumin and S100 expression. Middle and right panels visualize S100 expression and parvalbumin expression, respectively, in monochromatic images. (A) transverse brain section of 3 dpf larva is counterstained with nuclear marker DAPI. Straight white dashed lines point out brain midline. Curved white dashed lines mark the boundary of subpallial proliferative zone (S). Strong expression of parvalbumin is visualized in OSNs and sparse projection in the central zone (CZ) in the OB at 3 dpf. S100 immunoreactive cells are visualized in OE. Note the absence of S100 projections in OB. (B), (C) and (D) Strong parvalbumin expression is visualized in OSNs and their projections to the central zone (CZ), lateral (LG) and medial (MG) glomeruli in OB. Expression of S100 is shown in scattered OSNs and S100 positive projections in the

medial glomerulus2 (MG2) of OB are evident. Note the double labeling of S100/parvalbumin projections to MG2 in the OB between 6 and 9 dpf. See list for abbreviations. Scale bars: 20 µm

The fact that the retarded S100 fibers develop increasingly in correlation with the olfactory imprinting process (6 to 7 dpf; see Introduction), prompted me to analyze the dynamics of crypt and microvillous OSN development in larval zebrafish from 3 to 9 dpf (Fig. 36). To this aim, I counted manually in ImageJ 1.37k the number of parvalbumin/S100 double labeled microvillous OSNs (purple bar graphs in Fig. 36) and S100 single positive crypt cells (magenta bar graphs in Fig. 36) in OE of larvae (8 animals per age; n = 8 for 3, 6, 7, 9 dpf in Fig. 36). The RGB stacks of optical sections were used for quantification. For statistical analyses I conducted a generalized linear model with Poisson error distribution and LSD (Least Significant Difference) post hoc tests. Statistical analyses revealed that the average number of microvillous OSNs in individual OEs increased significantly in the developing olfactory organ from 3 to 9 dpf (LSD post hoc test; **p < 0.01; purple bar graphs in Fig. 36). It starts with 10 microvillous OSNs at day 3 per OE on average and reaches more than 25 microvillous OSNs at day 9 per OE on average (Fig. 36). The number of crypt cells in OE is overall less in comparison to microvillous OSNs (magenta bar graphs in Fig. 36). The average number of crypt cells in OE increase from 3 to 6 dpf and decrease subsequently to a level similar to that observed at 3 dpf until 9 dpf. There are 4 crypt cells per animal on average in 3, 7 and 9 dpf, but 6 -7 crypt cells per OE on average in larvae at day 6.

Statistically pair-wise comparison revealed that number of crypt cells at 6 dpf is significantly different to 3 dpf (LSD post hoc test; *p = 0.022), to 7 dpf (LSD post hoc test; *p = 0.016) and also to 9 dpf (LSD post hoc test; *p = 0.040).

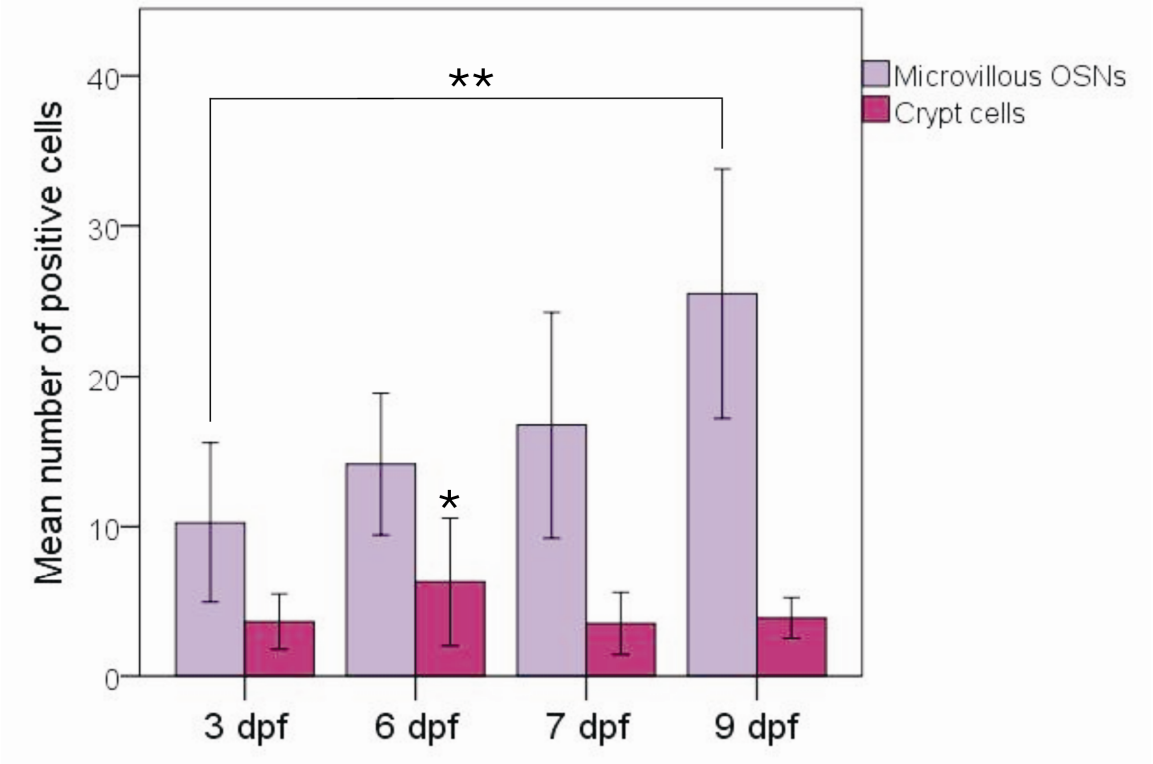

Fig. 36. Developmental dynamics of number of microvillous OSNs and crypt cells in the olfactory organ of larval zebrafish (3dpf, 6dpf, 7dpf and 9dpf)**.** Average number of parvalbumin/S100 positive cells (microvillous OSNs) and S100 single positive (crypt) cells in OE of larvae is shown on the y-axis. The purple bar graphs reveal a steady increase of microvillous OSNs from 3 to 9 dpf. The magenta bar graphs show an increase of crypt cells from 3 to 6 dpf and subsequent reduction at 7 dpf to a level similar to that observed at 3 dpf. 8 animals per age (n = 8 per 3, 6, 7, 9 dpf). Error bars: +/- 1 standard deviation (SD); *p < 0.05, **p < 0.01.

4.4.3. Adult Olfactory Bulb Projections

Combinatorial analyses of primary olfactory projections into the OB visualized with CBPs demonstrate even more subtle differences in projection patterns also in adult zebrafish (Fig. 37). For the adult morphology and identification of zebrafish glomeruli I use the proposal of Baier and Korsching (1994). Transverse brain sections of four levels from rostral to caudal of the same adult zebrafish olfactory bulb reveal in detail the different bulbar targets of calretinin, parvalbumin and S100 positive projections (Fig. 37A,B,C). Calretinin and parvalbumin positive projections show many overlapping glomeruli in OB. Strongly calretinin positive fibers are visualized in glomeruli of the dorsal cluster (dc), in the lateroventral posterior glomerulus (q) and in glomeruli of the ventral triplet (u-w) (Fig. 37A,D,D''). Glomeruli of the lateral chain (m and lc) receive more parvalbumin positive fibers in comparison to calretinin, excepting glomerulus 5 of the lateral chain (p in Fig. 37A, B). However, parvalbumin

positive fibers innervate additionally the anterior plexus (ap), the dorsal-cluster-associated glomeruli (a-e), gomeruli of the mediodorsal group (mdG) and the ventroposterior glomerulus (vpG) (Fig. 37B; white letters).

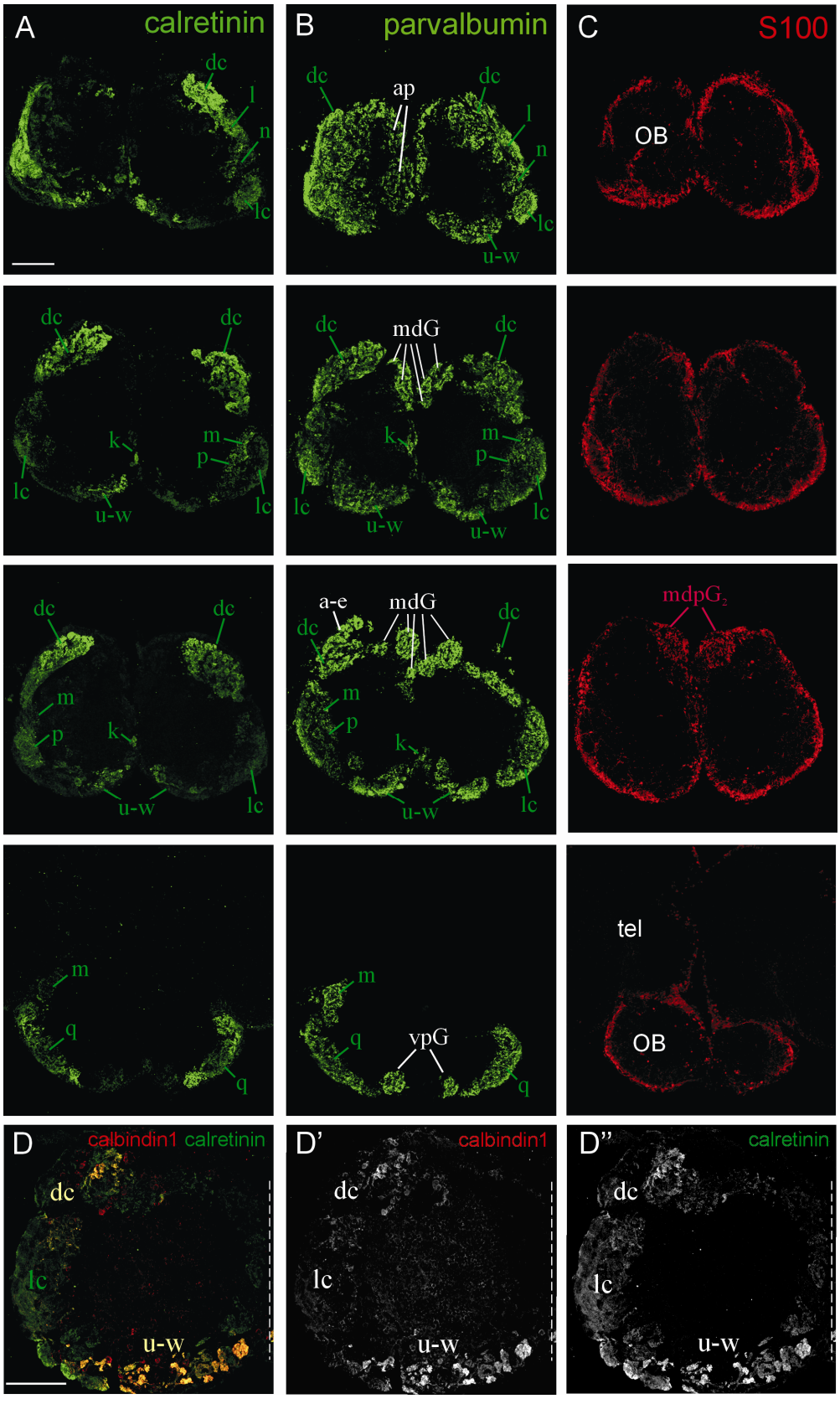

Fig. 37. Adult primary olfactory projections shown with CBPs. Transverse sections visualize expression of calcium binding proteins (CPBs) calretinin (A), parvalbumin (B), S100 (C) and double labeling of calbindin1 / calretinin (D) in olfactory bulb (OB) of adult zebrafish. (A), (B) and (C) Expression of CBPs is demonstrated in consecutive transverse brain sections of the same adult zebrafish brain from rostral (r) to caudal (c; see arrow on the left side) with every third section stained for a particular CBP. White letters in (B) point out glomeruli visualized by parvalbumin immunoreactive projections (ap, a-e, mdG, vpG), which are not visualized by calretinin expression (A). (C) Note that S100 immunoreactive projections are only visualized in the mediodorsal (posterior) glomerulus2 (md(p)G_2). (D) Optical section visualizes double labeling of calbindin1 and calretinin in olfactory bulb (OB). Straight white dashed line marks midline of brain. Yellow labeling marks calretinin and calbindin1 double labeled glomeruli of the dorsal cluster (dc) and of the ventral triplet (u-w). (D') and (D'') monochromatic images show calbindin1 and calretinin expression, respectively. Glomerular nomenclature after Baier & Korsching, 1994. See list for abbreviations. Scale bars: 100 µm.

The S100 positive projections only innervate the mediodorsal posterior glomerulus2 (mdpG_2) in adult zebrafish (Fig. 37C), as shown already above in larvae (see, MG2 in Fig. 34 and in Fig. 35). The designation of the S100 positive mediodorsal posterior glomerulus is mdpG2 of Baier and Korsching (1994), which was confirmed as mdG2 (of totally 5 mediodorsal glomeruli in a recent paper by Braubach and colleagues (2012; see Discussion).

Moreover, S100 immunoreactivity is also observed in some glial cell somata (mostly at the periphery of the bulb, but also some more centrally) and in numerous glial cell processes abutting the surface of the bulbs (for details see Fig. 38).

Thus, S100 positive projections in the adult zebrafish OB are restricted to the mediodorsal posterior glomerulus2 (mdpG_2; Fig. 38). Double labeling of S100 with the nuclear marker DAPI confirms S100 positive terminals in mdpG2, but in no other glomeruli of the mediodorsal group (Fig. 38A, A') and demonstrates that no S100 immunopositive cell bodies are present in the neuropil of both glomeruli. However, magnification of the boundary region of the OB dorsally or ventrally in the same brain section shows S100 immunoreactive astrocyte cell bodies and their processes at the surface of OB (Fig. 38C, C').

Analysis of glial fibrillary acidic protein (GFAP), a specific marker for astroglial cytoskeleton in glial fibers (but not for the somata), at the same section level of adult zebrafish OB reveals astrocytic processes of S100 positive cell bodies (Fig. 38B, B', B'' and C'). As expected, strong GFAP immunoreactive fibers are visualized at the entire surface of OB, but no

GFAP positive cell bodies. A comparison of GFAP with S100 reveals that astrocytes surround the OB and create a net of processes around it, with some less dense fibers extending into glomeruli (Fig. 38B-B''). In contrast, dense neuronal fibers seen in S100 immunoreactive mdpG2 are absent in GFAP stains (Fig. 38A', B').

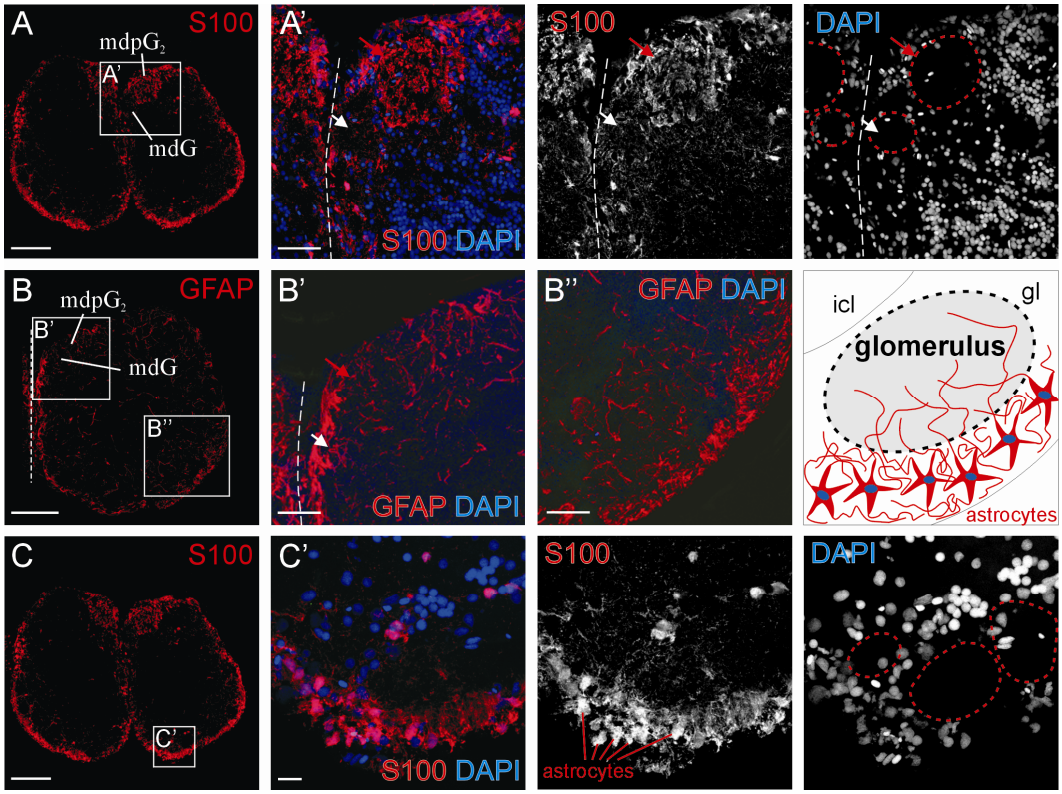

Fig. 38. S100 in mediodorsal OB. Transverse brain sections visualize expression of S100 and GFAP in olfactory bulb (OB) of adult zebrafish. (A) and (C) demonstrate expression of S100 in the same optical section. (B) visualizes expression of GFAP in optical section of OB. White boxes mark areas magnified in (A'), (B'), (B'') and (C') which visualize expression of S100 (A', C') and GFAP (B', B'') counterstained with nuclear marker DAPI. Right next to (A') and (C') monochromatic images visualize S100 and DAPI expression, respectively. Optical section and magnification in (A) and (A') point out S100 positive projections into one mediodorsal posterior glomerulus2 ($mdpG_2$) in OB. Red arrow mark S100 immunoreactive glomerulus and white arrow marks another mediodorsal glomerulus (mdG) without S100 positive projections. Straight white dashed lines indicate midline of adult OB in all panels. Red dashed circles in monochromatic image of DAPI mark boundaries of the two mediodorsal glomeruli in each OB. In (B) strong expression of GFAP is shown at the outer edge of glomerular layer (gl) around entire OB. (B') visualizes mediodorsal area of same brain level as shown in (A'). White and red arrows point to the two mediodorsal glomeruli. (B'') shows ventrolateral region of OB. Strong GFAP immunoreactive fibers are visualized also at the outer edge of (gl). Note strong GFAP immunoreactive fibers, but the absence of GFAP positive cell bodies. (C') Magnification of ventral area of OB visualizes S100 immunoreactive astroyctes at the outer edge of gl (pointed out in monochromatic image of S100 expression). Red dashed circles in monochromatic image of DAPI mark boundaries of glomerli in ventral area of OB. See list for abbreviations. Scale bars in (A), (B) and (C): 100 µm; in (A'), (B') and (C'): 50 µm.

Double labelings of calretinin and calbindin1 visualize largely overlapping bulbar targets (Fig. 37D-D' and Fig. 39), but in comparison, calbindin1 is less strongly expressed than calretinin in OE and OB, as shown above in larvae already (Fig. 34C-C''). Strongly calretinin immunoreactive fibers are represented in the dorsal cluster (dc) and in glomeruli of the ventral triplet (u-w), where also calbindin1 positive projections are shown. Detailed analysis of glomeruli in dc (Fig. 39 A_1) and the three glomeruli of the ventral triplet (Fig. 39 A_2) reveals more calretinin positive projections in comparison to restricted calbindin1 positive presynaptic terminals. Furthermore, calretinin positive projections are visualized in the plexus of lateral chain (lc), but calbindin1 positive projections seem absent there (Fig. 37D, D' and Fig. 39 A, C).

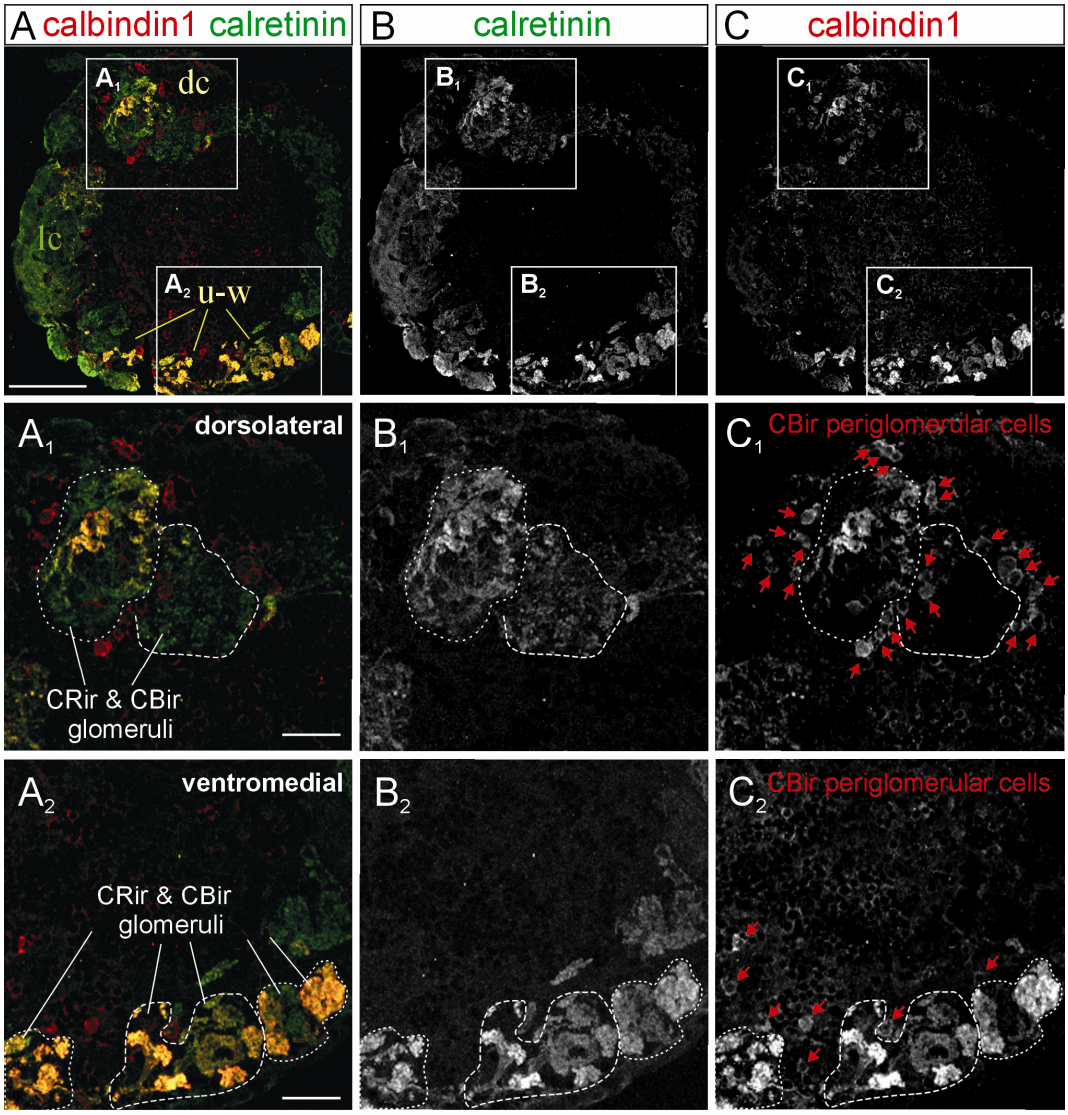

Fig. 39. Calbindin1/calretinin double label in OB. Transverse brain sections visualize expression of calretinin and calbindin1 in olfactory bulb (OB) of adult zebrafish. Left row

(A) demonstrates double labeling of calretinin and calbindin1 in optical section of OB. Middle (B) and right row (C) show expression of calretinin (B) and calbindin1 (C) in monochromatic images. White boxes mark dorsolateral area with calretinin and calbindin1 double labeled glomeruli of the dorsal cluster (dc) magnified in (A_1, B_1, C_1) and ventromedial area with double labeled glomeruli of the ventral triplet (u-w) magnified in (A_2, B_2, C_2). (A) Double labeling reveals calretinin (CRir) and calbindin1 immunoreactive (CBir) glomeruli in dorsolateral and ventromedial glomeruli. Strong calretinin expression is shown from dorsolateral to ventromedial involving all lateral glomeruli of OB. Calbindin1 positive projections are visualized only dorsolateral and ventromedial. Note that there are no CRir neurons visualized in OB, but CBir neurons surrounding glomeruli in dorsolateral and ventromedial areas of OB. (B) and (C) show monochromatic images of calretinin and calbindin1 in adult OB. (A_1 – C_1) demonstrate magnified dorsolateral area of OB. Strong expression of calretinin is visualized in glomeruli (B_1) and less calbindin1 positive projections in the same glomeruli (C_1 and A_1). Red arrows in (C_1) and C_2) point to CBir periglomerular neurons surrounding the glomeruli. (A_2 – C_2) show strong expression of calretinin and calbindin1 in the same ventromedial glomeruli. See list for abbreviations. Scale bar in (A): 100 µm; in (A_1) and (A_2): 50 µm.

Additionally, detailed analysis of calretinin/calbindin1 double labelings reveals calbindin1 immunoreactive periglomerular neurons in the OB of adult zebrafish (Fig. 39). As mentioned above, double labeled calretinin and calbindin1 immunoreactive terminals in glomeruli are seen in the dorsal cluster (dc) (Fig. 39 A_1) and in the ventral triplet (u-w) (Fig. 39A_2) of OB. In these glomerular clusters, calbindin1, but not calretinin positive cell somata surrounding the double labeled glomeruli (red arrows in Fig. 39B_1, C_1, B_2, C_2) are present.

Thus, my data on olfactory bulb projections visualized with antibodies against CBPs reveal the following: S100 positive projections, presumably originating from S100 positive crypt cells, are restricted to one glomerulus (mdpG2), whereas calretinin, calbindin1 and parvalbumin positive bulbar projections are extensive. Parvalbumin positive axons clearly have projection fields (i.e. mdG, vpG, ap, a-e) not shared with calretinin positive ones, which is in line with the fact, that most microvillous OSNs are parvalbumin positive in addition to ciliated cells. Also calbindin1 and calretinin positive fibers do not overlap completely despite the finding that both CBPs are expressed in the majority of, if not all, ciliated OSNs. For example, calbindin1 positive fibers do not project to the plexus of the lateral chain or to some glomeruli of the dorsal cluster and ventral triplet.

5. Discussion

5.1. Immediate Early Genes and pErk as Activity Markers in the Zebrafish Olfactory System

Zebrafish (*Danio rerio*) recognize kin vs. non - kin by olfactory and visual cues based on imprinting as larvae (see Introduction; Mann et al., 2003; Gerlach & Lysiak, 2006 Gerlach et al. 2008; Hinz et al., 2012; 2013). This distinguishes olfactory imprinting from other types of odor learning in which conditioned exposure to an odor stimulus is required for learning to occur (Dittmann and Quinn, 1996).

In my doctoral thesis I tried to identify the brain areas involved in olfactory imprinting in zebrafish. Therefore I used the Erk (Extracellular signal – regulated kinase) / MAPK (Mitogen – Activated Protein Kinase) signaling pathway and associated immediate early gene (IEG) expression to mark neuronal activity (see Fig. 40 and Materials and Methods for explanation of this signaling pathway). I studied basal expression patterns of these markers and tried to reveal subsequently the activation of neuronal circuitry involved in the processing of olfactory imprinting signals.

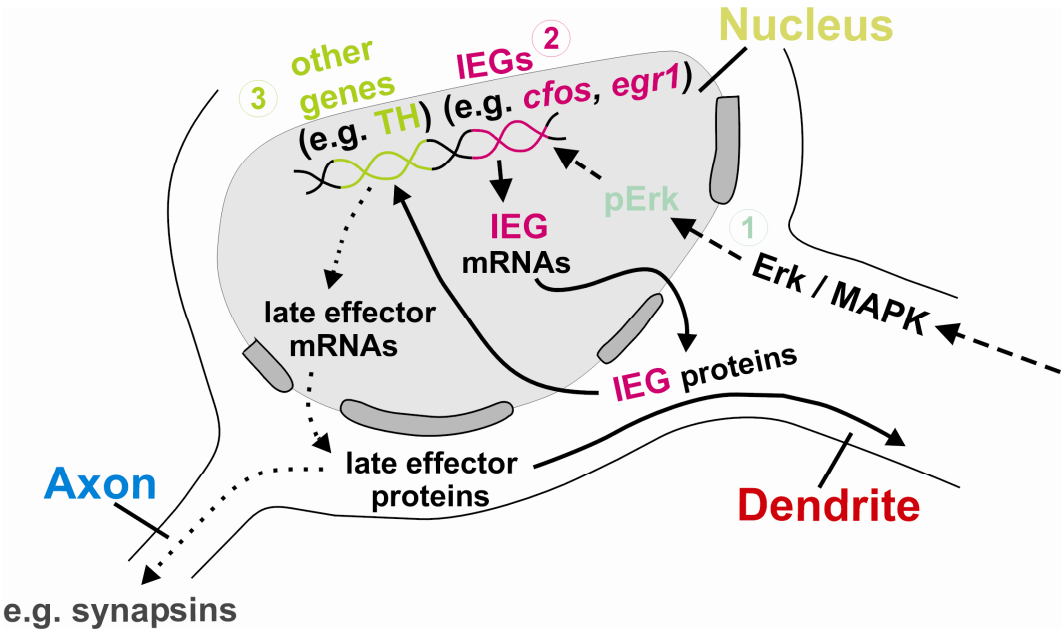

Fig. 40. The Erk / MAPK signaling pathway in neurons (as figure 7).

5.1.1. Experiments Involving the IEG *egr1*

Neurons respond to extra – cellular stimuli by engaging specific intracellular responses, like the signaling cascade that leads to the activation of MAPK. For example, in brains of male mouse phosporylated Erk – (pErk) positive cells increase after sexual odor stimulation (Taziaux et al., 2011). Moreover, in many groups of vertebrates IEGs have proven to be useful markers in the context of long term potentiation (LTP) and memory (Pinaud and Tremere, 2006). IEGs are also part of the cellular response mechanism that reacts to biochemical, electrical, pharmacological, and physiological stimuli as well as changes in behaviour (Pinaud and Tremere, 2006). The protein products of these regulatory genes are classified as inducible transcription factors and e.g., the IEGs cFos and Egr1 (Early growth response gene-1*;* also known as *krox-24, zif 268, ngfi-a* and *zenk*) are both implicated in brain plasticity and activated in the vertebrate brain by a variety of stimuli, including learning and memory (Pinaud and Tremere, 2006). Olfactory imprinting is a specialized form of unconditioned learning. It is possible that IEGs such as *egr1* and *cfos* are involved in the process of imprinting itself, but also in subsequent kin recognition, a form of learned long – term memory.

Hence, I expected by using sensory – driven gene expression that increased neuronal activity as basis of learning processes during olfactory imprinting can be shown. The IEG *egr1* has been used as neuronal activity marker in terms of LTP and memory in mammals (Akiba et al., 2009; Davis et al., 2003; Knapska and Kaczmarek, 2004), songbirds (Liu and Nottebohm, 2005; Mello and Clayton, 1994; Mello et al., 1992), frogs (Mangiamele and Burmeister, 2008), electric fish (Harvey-Girard et al., 2010) and cichlid fish (Burmeister and Fernald, 2005). Furthermore, in the mammalian olfactory system, *egr1* expression was used to map innervation of glomeruli by OSNs that are responsive to specific odorants (Alonso et al., 2006; Inaki et al., 2002; Johnson et al., 1995).

In zebrafish the homolog of the *egr1* gene was previously isolated and characterized (Drummond et al., 1994) and investigations showed via whole – mount *in situ* hybridization the brain regions of *egr1* expression

during zebrafish embryonic development up to 48 hours post – fertilization (hpf) (Close et al., 2002). Thus, the preconditions were given that *egr1* could be also functional as activity marker in zebrafish.

The proto – oncogene *cfos* is the earliest known and best characterized member of IEGs (Goelet et al., 1986; Kaczmarek, 1993; Kaczmarek and Kaminska, 1989; Kaczmarek and Nikolajew, 1990; Morgan and Curran, 1991; Sheng and Greenberg, 1990). Furthermore, *cfos,* and the Fos protein that it encodes, have been used extensively as markers of neuronal activity e.g. (Herdegen and Leah, 1998; Pinaud and Tremere, 2006), including processes associated with learning and memory (e.g. Pinaud and Tremere, 2006). Moreover, it was demonstrated that cFos can also be used as a neuronal activity marker in teleosts (Bosch et al., 1995; Okuyama et al., 2011).

However, both IEGs were not previously demonstrated as neuronal activity marker in zebrafish. Accordingly, I analyzed in my thesis for the first time the basal expression of the IEGs *cfos* and *egr1* in larval and adult zebrafish brains (Figs. 11, 12, 14, 21, 22) in order to provide background information for experiments involving olfactory activation or deprivation.

Furthermore, the protein products of IEGs return to the cell nucleus where they affect the transcription of other “late response” genes (Bolhuis and Gahr, 2006) (see Material & Methods Fig. 7), e.g. tyrosine hydroxylase (TH) which is the rate limiting enzyme for dopamine synthesis, catalyzing transformation of L-tyrosine to L-DOPA, a precursor of dopamine. In mammals, activity - dependent TH expression is induced by afferent input from OSNs and synaptic activity of mitral and tufted cells in the glomeruli (Baker et al., 1983; Baker et al., 1993). Furthermore, it has been shown that the IEG *egr1* mediates activity - dependent TH expression in OB of mice (Akiba *et al.* 2009). The TH proximal promoter contains IEG – transcription factor binding sites necessary for activity – dependent TH expression in the OB (Liu et al., 1999).

Thus, I analyzed *egr1*/TH and *cfos*/TH co – localization in the zebrafish brain in order to investigate correlation between the IEGs and TH gene regulation in an activity dependent way (Figs. 15, 16, 23, 24). The enzyme TH detects dopaminergic and noradrenergic positive neurons

based on its function in catecholaminergic biosynthesis. In the zebrafish, studies using antibodies against dopamine-beta-hydroxylase, which characterizes noradrenergic/adrenergic neurons, revealed that this enzyme is not present in the fore- and midbrain (Ma, 1997; Kaslin and Panula, 2001). Hence, it is safe to assume that in zebrafish all TH positive cells rostral to the hindbrain are dopaminergic.

In my doctoral thesis, I started with the analysis of basal *egr1* expression and established the developmental profile of basal *egr1* expression by *in situ* hybridization (ISH) beyond the known embryonic expression (Close et al., 2002) in larval and adult zebrafish (Figs. 11, 12, 14). The investigation of developmental *egr1* expression revealed a strong basal expression in untreated zebrafish larvae. The gene maintained its expression within the forebrain and alar plate mesencephalon and I confirmed essentially the reported embryonic domains of Close et al (2002) involving retina, telencephalon, hypothalamus, preoptic region, diencephalon and optic tectum. Whereas an embryonic expression had been reported by Close et al (2002) (probably erroneously), I did not see *egr1* expression in the basal plate midbrain tegmental domain at any larval stage and also not at adult stages. A comparison of early differentiated Hu – positive cells (Mueller and Wullimann, 2005) with *egr1* expression demonstrated that the larval midbrain tegmental cell masses were free of *egr1* expression (Fig. 12). In contrast, I could newly show that there is an *egr1* expression in the OB starting with 3 dpf, likely reflecting a correlation with onset of olfactory function, which was very important for my further analysis (Figs. 11A, 12A). In adult zebrafish, I observed a qualitatively very similar picture to the late larval situation and, thus, *egr1* is also highly expressed in the fore – and midbrain, whereas it is almost absent from the hindbrain with the exception of the cerebellum. The *egr1* expression in the cerebellum is only present in the adult zebrafish. The general relationships were nicely demonstrated in a comparison of an *egr1* stained sagittal section with a combined Bodian-silver/Cresyl stained sagittal section (Fig. 14). The majority of adult forebrain cell groups showed basal *egr1* expression, with negative cells only in some areas, e.g. Dp, the presumed homologue of the mammalian olfactory cortex. There is an impressive

similarity of basal *egr1* expression in the adult mouse (Christy et al., 1988; Schlingensiepen et al., 1991) and rat (Beckmann and Wilce, 1997; Herdegen et al., 1995; Herdegen et al., 1993; Herdegen et al., 1990) brain compared to my findings in the zebrafish brain. High *egr1* expression levels are found in all three species in the pallial and subpallial telencephalon, as well as in the diencephalon (pretectum, thalamus, hypothalamus) and (alar plate) mesencephalon (superior/inferior colliculus or optic tectum/torus semicircularis), but only restricted *egr1* expression domains are present in the basal plate midbrain and entire hindbrain. In summary, my investigations revealed in general a strong basal *egr1* expression in untreated larval and adult zebrafish.

Afterwards, I performed double labeling for TH (IHC) and *egr1* transcripts (ISH) in adult zebrafish in order to check for co – localization of both markers (see Materials & Methods). The double labeling revealed *egr1* and TH co – expressing cells in two candidate regions likely relevant for imprinting: the olfactory bulb (OB) and the supracommissural nucleus of the ventral telecephalic area (Vs), the suspected medial amygdala in zebrafish (Mueller et al., 2008; Northcutt, 2006; Northcutt and Braford, 1980; Wullimann and Mueller, 2004). As in all vertebrates, the OB in teleosts is the first brain center where odor information is processed and the medial amygdala (Vs) is essential for processing pheromonal signals (Fig. 15A, C).

However, the light microscopy may remain ambiguous and therefore, I established a new fluorescent in situ hybridization (FISH) protocol on zebrafish sections combined with immunofluorescence (see Materials & Methods). Using confocal microscopy for cellular detail allowed for an unambiguous identification of *egr1*/TH double labeled cells (Figs. 17, 18).

Thus, I established the adequate methodological tools to determine the dynamics of *egr1* and TH expression after various olfactory test procedures. However, the strong basal expression of *egr1* made it difficult for me to show the upregulation of *egr1* and TH. Since my work aims to demonstrate in the zebrafish brain that *egr1* and TH expression are susceptible to olfactory activity levels, I chose to visualize the

downregulation of *egr1* and TH expression via odor deprivation as a proof of principle (Fig. 19).

Odor deprivation through naris occlusion and other forms of olfactory epithelium deprivation experiments in rodents showed that TH is downregulated in periglomerular cells, whereas glutamic acid decarboxylase (GAD, marker for GABA cells) in these (and inner granule) cells is not downregulated (Baker et al., 1983, 1993). In all vertebrates, axons of OSNs synapse on dendrites of efferent glutamatergic mitral and tufted cells in glomeruli of OB. In mammals, periglomerular cells modulate this glutamatergic synaptic transmission by releasing both neurotransmitter GABA and dopamine (Cave and Baker, 2009), whereas the centrally lying small granule cells of the OB modulate mitral cell activity at the latter's secondary dendrites only via GABA. It has been shown that this modulatory network underlies plastic changes depending on olfactory experience (Mandairon and Linster, 2009). Moreover, immunohistochemical analysis of a naris – occluded mouse model of odor deprivation revealed a correlated downregulation of Egr1 and TH expression levels in a subset of dopaminergic periglomerular cells, but no Egr1 downregulation in inner granule cells (Akiba et al, 2009).

Therefore I tested whether olfactory deprivation through temporary loss of OSN's cilia / microvilli in the epithelium using the detergent Triton X-100 as lesion solution leads to downregulated expression of *egr1* and TH in periglomerular cells of the zebrafish OB. It had previously been shown that in zebrafish such treatment leads to temporary loss of cilia / microvilli without long – lasting effects on the olfactory epithelium (Friedrich and Korsching, 1997b) and that the olfactory epithelium recovers fully within 2 to 5 days (Iqbal and Byrd-Jacobs, 2010). I applied Triton X-100 over a period of 10 days once daily unilaterally into one olfactory epithelium of adult zebrafish and used the other untreated epithelium as control side (see Materials & Methods and Fig. 19).

Indeed, in my experiments, I could demonstrate a strong downregulation of TH enzyme and *egr1* transcripts in the OB ipsilateral to the treatment compared to the contralateral control, which was confirmed when quantified (Fig. 19). Furthermore, looking specifically at TH/egr1

double labeled cells, a strong reduction of these cells was shown on the treated side (Fig. 19M, N, O). Thus my investigations demonstrated activity dependent downregulation of *egr1* and TH in a subset of olfactory bulb periglomerular cells, possibly indicating the causal role of this immediate early gene in regulation of TH levels in zebrafish.

Nevertheless, one should be cautious to infer a simplistic causal relationship in activity – dependent plasticity between *egr1* expression and TH phenotype in teleostean OB periglomerular cells, because additional transcription factors such as fos-B and Nurr1 (NR42A) are also involved (as shown in rodents; Cave and Baker, 2009).

Additionally, *egr1* in non – dopaminergic GABAergic inner granule cells appears also diminished and this could reflect that *egr1* downregulation is also activity dependent in zebrafish inner granule cells (Fig. 19). This is different to what had been observed in mice (see above). However, the activity dependent function of *egr1* in the zebrafish olfactory bulb inner granular layer needs more investigation.

Moreover, visualization of OB histology with DAPI stain showed that the size and morphology of the OBs were unchanged on the deprived side, which was also confirmed when quantified (Fig. 19C, F, I, L). This indicated that there was no cell loss on the treated side. However, to ensure that *egr1*/ TH expression was downregulated without great cell loss in the OB on the treated side, I investigated adult neurogenesis in the Triton X-100 treated zebrafish. The great cell loss in the OB could cause faster turnover in the OB on the treated side and thus I visualized progenitor cells with the mitosis marker PH3 and checked for migrating cells along the rostral migratory stream (RMS) to the OB where they are known to differentiate into interneurons (März et al., 2010). Comparison of PH3 positive cells on the RMS in each telencephalic brain hemisphere of treated and control side demonstrated no difference (Fig. 20). This indicates that no increased cell replacement via the RMS was initiated by the lesion experiment. Thus, my investigations revealed a selective downregulation of *egr1* and TH expression in the same periglomerular cells in OB.

With regard to olfactory imprinting, the medial amygdala is a second area of immediate interest in this context and double labeling revealed *egr1* and TH co – expressing cells in Vs, the suspected medial amygdala in zebrafish (Fig. 15C). Moreover, in the mammalian medial amygdala co-expression of *egr1* and TH was also shown and in male prairie voles, *egr1* expression is modulated by social contact in medial amygdalar dopamine cells (Northcutt and Lonstein, 2009). The subpallial Vs is in receipt of secondary olfactory projections from the OB in teleosts (Nieuwenhuys and Meek, 1998; Northcutt, 2006). Furthmore in the zebrafish, Vs also receives extrabulbar projections directly from OSNs in the olfactory epithelium and the extrabulbar fibers contacting dendrites of TH immunoreactive neurons in Vs (Gayoso et al., 2011). Thus, *egr1* and TH co-expression cells in Vs are potentially also downregulated after odor deprivation treatment. However, my experiments were based on unilaterally application of lesion solution and as a result unilateral downregulation of *egr1*/TH co – expression, with the untreated side as control. The secondary olfactory terminal field in Vs consists of contralateral input and therefore processed odor information comes from both noses and olfactory bulbs (Nieuwenhuys and Meek, 1998). This fact made a comparison between treated side and control in Vs impossible and is therefore not elaborated in my deprivation experiments.

Thus, I could demonstrate selective downregulation of *egr1* and TH expression in the same olfactory bulb dopaminergic periglomerular cells via odor deprivation. These experiments I used as proof of principle since one aim of my thesis was the upregulation of *egr1* and TH expression after various olfactory test procedures via odor stimulation finally to identify the brain areas involved in olfactory imprinting in zebrafish. However, the strong basal expression of *egr1* made it difficult to measure its upreglation and thus I investigated the other immediate early gene *cfos* and phosphorylated Erk (pErk) as alternatives.

5.1.2. Experiments Involving the IEG *cfos*

Basal expression studies of *cfos* in larval (Fig. 21) and adult zebrafish brains (Figs. 22 – 24) revealed some overlapping expression

domains of *cfos* and *egr1*, but also significant differences. In larvae, weak basal *cfos* expression was demonstrated in OB corresponding with newly shown *egr1* expression in the larval OB (Fig. 21A). In adults, the general relationships were nicely demonstrated in a comparison of an *egr1* stained sagittal section with a *cfos* stained sagittal section (Fig. 22). Generally, the basal *cfos* expression was weaker in comparison to *egr1* in both zebrafish larvae (Figs. 21, as compared with Figs. 11 and 12) and adults (Fig. 22). Thus, my thesis shows for the first time basal *cfos* expression throughout the zebrafish brain. In a previous study Lau et al. (2011) compared *cfos* expression in the hypothalamus between untreated adult zebrafish and stressed adult testfish. This paper visualized basal *cfos* expression in hypothalamus (Lau et al., 2011; their Fig. S3*A*) and showed strong upregulation of *cfos* expressing hypothalamic cells after intense handling stress (Lau et al., 2011). In the zebrafish brain section visualizing basal *cfos* expression in the hypothalamus no *cfos* positive cells were shown (Lau et al., 2011; their Fig. S3*A*). In contrast, my extensive study of *cfos* basal expression visualized strong basal *cfos* expression in hypothalamus (H) of untreated larvae (Fig. 21G-I) and adult zebrafish (Figs. 22B, D; 24D, D'). The untreated larval and adult zebrafish in my study were also habituated to their environment for at least 24h and directly killed for comparison analysis without intense handling stress. Therefore, my extensive study of *cfos* basal expression could not confirm the results of Lau et al (2011).

Moreover, as was the case for *egr1* and TH, double labeling of *cfos* and TH revealed basal co – localization of *cfos* and TH in cells of the olfactory related brain areas OB (few) and Vs (many) (Fig. 23). Therefore the prerequisites were created to visualize *cfos* upregulation via odor stimulation. At first I compared *cfos* expression between imprinted and non – imprinted larvae (12 dpf) after short stimulation treatment with kin odor (see Materials and Methods), but no apparent qualitative differences between imprinted and non – imprinted larvae could be shown. The IEG expression is activated rapidly and transiently in response to a stimulus and thus the stimulus should be presented in repetitive cycles in order to avoid adaptation and return to its baseline level. Furthermore, it was

shown that it takes at least 60 min to obtain sufficient IEG mRNA induction and 90 min to visualize IEG protein induction for immunohistochemical detection of IEG upregulation (Chaudhuri, 1997; Watts et al., 2006). However, zebrafish larvae were unable to meet these requirements for this specified experimental procedure due to their physical constitution. Hence, I used the short stimulation treatment for visualization of IEG upregulation in the brain in the hope to demonstrate upregulation which was not successful. Future investigations must either establish new experimental setups which enable longer stimulation especially for larvae or do comparable experiments with adults to show IEG upregulation.

Secondly, I used *cfos* in order to show principally upregulation after olfactory stimulation with the amino acid L-alanin in adult zebrafish. In fish, amino acids have been identified as a class of natural odorants and it was shown that amino acids induced glomerular activity patterns in the OB by repeated application of amino acids (Friedrich and Korsching, 1998 and Rainer Friedrich, pers. comm). In zebrafish, the labeling of primary afferents using calcium – sensitive dye in conjunction with odor stimulation has previously shown that amino acids activate a chain of glomeruli located on the lateral side of the OB (Friedrich and Korsching, 1997). Therefore, I used amino acid L – alanine in the same concentration used for visualizing activation in lateral OB to show *cfos* upregulation after odor long stimulation treatment in a Mini – flume (see Figs. 9 and 10 in Materials & Methods). The Mini – flume allowed a fast replacement of stimulus to non – stimulus water (30 seconds) to provide a repetitive stimulation over time to reach enough detectable amount of IEGs in the tissue. Moreover to minimize the input of external stimuli such as light and noise there was little free moving space in the Mini – flume and the tests were performed almost in darkness and with silence.

In my analysis of L – alanine, as a class of natural odorants, the focus was directed to the olfactory related areas, OB and Dp, the presumed homologue of the mammalian olfactory cortex (Fig. 26). Although Friedrich and Korsching (1998) could demonstrate with the Calcium imaging a strong activation after alanin stimulation in zebrafish OB, the *cfos* expression was not upregulated in specific parts of the OB

after L - alanine exposure in my experiments. Furthermore, no differences in *cfos* expression could be shown in the olfactory pallium (Dp) which is responsible for general odor analyses. Thus, in both olfactory related areas (OB and Dp) in the adult zebrafish forebrain, no quantitative or qualitative differences could be shown in comparison to basal *cfos* expression or between L-alanine stimulated and non-stimulated fish. Since L- alanine is primarily a food related odor and maybe food odors do not lead to upregulation of *cfos* which was previously related to learning and memory processes in mammals (e.g. Pinaud and Tremere, 2006).

Unfortunately, it was neither possible for me to perform more long stimulation treatments to prove the upregulation of *cfos* with additional odor stimuli, nor to continue experiments with imprinted and non-imprinted fish (larval or adult). However, my extensive and detailed documentation of weaker basal expression of *cfos* in comparison to *egr1* basal expression in the larval and adult zebrafish brain lays important fundament and strongly indicates that *cfos* is potentially more useful as an activity marker in the zebrafish brain than *egr1*.

5.1.3. Experiments Involving pErk

I started my doctoral thesis with the use of IEGs as neuronal activity markers in zebrafish since in many groups of vertebrates IEGs have proven to be useful markers in the context of LTP and memory (Pinaud and Tremere, 2006). The IEGs are associated with the Erk / MAPK (Mitogen – Activated Protein Kinase) signaling pathway (see Material & Methods). In mammals, the phosphorylated Extra cellular – signal regulated kinase (pErk) as an indicator for the activation of the Erk / MAPK signaling pathway has been used as marker for neuronal activity including activity related to olfaction e.g. (Miwa and Storm, 2005; Taziaux et al., 2011). In male mice, sexual odor stimulation increased pErk – positive cells in most brain regions known to be involved in the processing of olfactory cues and in the control of copulatory behavior (the main and accessory OBs, amygdala and medial preoptic area) (Taziaux et al., 2011). Generally in vertebrates, protein phosphorylation plays a critical role in synaptic plasticity and learning and memory (Hawkins et al., 2006).

The pErk cascade in particular plays important roles in the modulation of LTP and is required for several forms of learning and memory (Sweatt, 2001). Thus I decided to visualize the expression of pErk in zebrafish as a further possibility to show neuronal activity related to olfactory imprinting.

Basal expression of pErk in zebrafish larvae revealed numerous pErk immunoreactive neurons and fibers in the forebrain including OB and terminal nerve (TN) cells (Fig. 27). Moreover triple labeling of the three activity markers pErk, *cfos* and TH revealed that pErk is co - expressed in TH positive periglomerular cells and co – expressed in *cfos* positive cells (Fig. 27) in OB and telencephalon. Additionally, pErk single labeled cells and fibers were visualized in the glomerular layer of OB.

Hence, basal pErk expression was visualized in olfactory related areas and as a next step I analyzed pErk expression of imprinted and non – imprinted larvae (10 dpf) after short stimulation with kin odor (Fig. 28).

After activation of the Erk / MAPK signaling pathway by a ligand or transmitter binding to receptors (e.g. GPCRs) on the neuron dendrite, the activated (p)Erk translocates to the nucleus and promotes the expression of immediate early genes (IEGs; e.g. *cfos* and *egr1*). Thus, the expression of IEGs like *cfos* or *egr1* is downstream of pErk, which also affects the time course of experimental procedure. It was shown in mice, that sexual odor stimulation increased pErk – positive cells in the male mouse brain within 10 minutes (Taziaux et al., 2011). Thus, no repeated stimulation seems necessary and I took a duration of 7 minutes in my odor stimulation experiments to visualize pErk – positive cells in the zebrafish brain, (short stimulation treatment, see Materials & Methods).

Qualitative analyses (Fig. 28) of pErk expression in OB and OE of imprinted and non – imprinted larvae revealed no dramatic differences but show a tendency of pErk upregulation in OB and OE in imprinted larvae (10 dpf). Additional analysis of pErk expression in the olfactory epithelium (OE) revealed pErk immunoreactive olfactory sensory neurons (OSNs) in imprinted and non - imprinted larvae, presumably representing ciliated OSNs (Fig. 28C, C').

In conclusion, my study revealed strong basal developmental pErk expression in OB and telencephalon and only small changes in pErk

expression after odor stimulation of imprinted and non – imprinted larvae in these areas. Thus, the duration of 7 minutes in my odor stimulation experiments may not have been long enough to visualize significant pErk expression differences in imprinted versus non – imprinted zebrafish larvae. In future investigations a precise temporal analysis of pErk upregulation in similar experiments seems useful.

Additionally, the detection of pErk as a potential activity marker in OSNs will be very helpful in future analyzes. The molecular processes during olfactory imprinting are not known so far. One possibility could be that specific OSNs possess receptors necessary for olfactory imprinting. Thus pErk could visualize the activation dynamics of olfactory sensory neurons during olfactory imprinting or reveal differences in OSN activation between imprinted versus non – imprinted larvae after odor stimulation with kin water. Since pErk is principally expressed in the olfactory epithelium, such investigations can be extended from the CNS to the OSNs in the periphery in order to visualize primary olfactory areas involved in olfactory imprinting. Thus, my initial investigations lead me to the assumption that pErk also is a useful activity marker in zebrafish larvae.

Basal expression of pErk in adult zebrafish revealed immunoreactive neurons and fibers surrounding glomeruli in the glomerular layer of OB and scattered pErk positive cells are also shown in the internal cellular layer of OB (Fig. 29A). Interestingly pErk immunoreactive cells are absent or very sparsely expressed in Dp (Fig. 29B, C), which is responsible for general odor analyses, but in Vs which is essential for processing pheromonal signals clearly defined pErk immunoreactive neurons were presented (Fig. 29C).

Based on these results of pErk basal expression in olfactory areas (OB, Dp and Vs) of adult zebrafish, I aimed to visualize pErk expression after an olfactory test procedure. It has been hypothesized that the chemical cue (ligand) involved in olfactory imprinting process has to closely match the receptor system of the recipient and suggested a genetic component similar to the innate immune system where cell – cell recognition and rejection of non – self ligands are based on the similarity

of the major histocompatibility complex (MHC) – derived surface proteins (Gerlach et al., 2008). In further studies of the Gerlach laboratory it had been revealed that imprinting on olfactory signals depends on MHC class II similarity in zebrafish and only larvae that share MHC class II alleles can imprint on each other (unpublished data; reviewed in Hinz et al., 2012). Thus adult zebrafish used in this experiment were offspring of the first generation of MHC peptide mix imprinted zebrafish (Hinz et al., 2012). In short stimulation treatments, MHC peptide mix imprinted adult zebrafish were used and half of them stimulated with MHC peptide mix for 7 minutes and the other half were stimulated with odorless water under same conditions.

However, triple labeling of pErk, TH and the nuclear marker DAPI in stimulated versus non – stimulated adult fish revealed no difference in expression patterns in olfactory related areas OB, Dp and Vs (Fig. 30). Furthermore, pErk expression patterns of both MHC peptide mix stimulated and non – stimulated fish showed also no differences to pErk basal expression (compare Figs. 29 and 30).

Thus, my investigations demonstrate for the first time the basal expression of pErk in larval and adult zebrafish, but upregulation of pErk expression after MHC peptide mix stimulation could not be shown. Again, the duration of short stimulation treatment (7 minutes) may not have been enough time to visualize significant pErk expression differences, as in kin water stimulation treatments of imprinted fish and their controls in larval zebrafish. Hence, future investigations regarding to experimental time course are also necessary in adult zebrafish.

In any case, basal pErk expression in olfactory epithelium OSNs is seen also in adult zebrafish. My initial analysis revealed presumably ciliated OSNs, but future investigations are necessary to exclude pErk immunoreactivity in the other two types of OSNs (microvillous OSNs and crypt cells). In future experiments, pErk expression may label activated OSNs after exposure to MHC peptide mix or kin water containing the ligand involved in olfactory imprinting process and discover one of the three different types of OSNs or a subpopulation of OSNs as the relevant pheromone sensory neurons in zebrafish.

In conclusion, in my doctoral thesis I visualized for the first time in the entire zebrafish larval and adult primary olfactory system the basal expression of the three activity markers *egr1*, *cfos* and pErk previously shown to be useful in mammals. I furthermore demonstrated activity dependent downregulation of *egr1*/TH expressing periglomerular cells after ipsilateral deprivation. Additionally, I laid groundwork for continuing experiments using imprinted and non-imprinted larval and adult zebrafish to test for upregulation of activity markers (in particular pErk and *cfos*) after exposure to imprinting or kin cues (MHC peptides, kin water).

5.2. Combinatorial Analysis of Calcium Binding Proteins (CBPs) in Zebrafish Primary Olfactory System

5.2.1. Combinatorial Analysis of CBPs in Zebrafish Olfactory Epithelium Reveals Differential Relationships to OSNs

The analysis of the four calcium binding proteins parvalbumin, calretinin, calbindin1 and S100 combinatorially defines subpopulations of olfactory sensory neurons (OSNs) and shows differential primary projections in larval and adult zebrafish. Teleostean olfactory epithelium consists of the two distinct types of OSNs also seen in mammals (ciliated and microvillous OSNs) and as a special feature, a third type of OSNs (the crypt cells) which is absent in mammals (Hansen & Zeiske, 1998).

Table 8 summarizes expression of these CBPs in the three OSN types in zebrafish (ciliated OSNs, microvillous OSNs and crypt cells) used in my combinatorial analysis and complemented with data from the literature. Blue and red indicate weak CBP expression in a small subpopulation of OSNs or main and strong expression, respectively. One circle after reference relates to results in embryos (48h) and two circles to results in larvae. Question marks indicate uncertain identifications.

Table 8. Summary of CBP expressions in the three zebrafish OSNs

	ciliated OSNs 	microvillous OSNs 	crypt cells 
parvalbumin	**data**	**data**	**---**
calretinin	**data** **data°°** **Braubach et al., 2012** **Castro et al., 2006** **Gayoso et al., 2011** **Germana et al., 2007** **Koide et al., 2009°°**	**data°°** **Braubach et al., 2012** **?** **Koide et al., 2009°°** **Duggan et al., 2008°**	**---**
calbindin1	**data** **data°°**	**data°°**	**---**
S100	**?** **?**	**data** **?** **?**	**data** **Braubach et al., 2012** **Gayoso et al., 2011** **Germana et al., 2004** **Germana et al., 2007** **Oka et al., 2012** **Sandulescu et al., 2011** **Sato et al., 2005**

small subpopulation (and weakly stained)
main expression

° in embryos [48 h]
°° in larvae

The summary shows that there is no complete agreement on CBP expression patterns in the three different types of OSNs. For example, Braubach and colleagues (2012) reported that S100 is mainly expressed in crypt cells (Braubach et al., 2012). Gayoso and colleagues observed some “round to ovoid S100 immunoreactive OSNs in the upper third of the zebrafish OE” (presumably crypt cells), but most S100 positive OSNs were interpreted as “plump, spindle – shaped cells with a short dendrite protruding in the surface of the lamella” (presumably microvillous OSNs) (Gayoso et al., 2011, 2012). In contrast, other immunohistochemical reports on the distribution of S100 “specifically recognize crypt cells” (Sandulescu et al., 2011) or conclude that “specific S100 protein-like

immunostaining was detected exclusively in crypt neurons, whereas ciliated and microvillous neurons were not reactive, and the supporting glial cells as well“, therefore S100 protein “represents an excellent marker to identify crypt olfactory neurons in zebrafish” (Germana et al., 2004).

Moreover table 8 demonstrates differences in calretinin expression between larval and adult zebrafish. Analysis of developmental calretinin expression showed a small subpopulation of calretinin positive ciliated OSNs in larvae and main expression of calretinin in microvillous OSNs (Koide et al., 2009). In adult zebrafish main expression or even exclusive expression of calretinin was visualized in ciliated OSNs (Braubach et al., 2012; Castro et al., 2006; Gayoso et al., 2011; Germana et al., 2007).

Using combinatorial analysis of CBPs, my doctorial thesis extends previous results of CBP expressions and reveals for the first time data of parvalbumin - and calbindin1 expressions in olfactory subsystems of larval and adult zebrafish. My investigations reveal that calbindin1 and calretinin are strongly expressed both in ciliated and microvillous OSNs of larvae (Fig. 34), but restricted to ciliated OSNs in adult zebrafish (Fig. 33). In larvae calbindin1 expression is shown in less ciliated and microvillous OSNs in comparison to calretinin (Fig. 34). Parvalbumin is strongly expressed both in microvillous and ciliated OSNs in larvae and adult zebrafish.

Thus, these three CBPs are not visualized in crypt cells, which comprise only a minor population in the teleostean OE. Instead, my investigations confirm that S100 is mainly expressed in crypt cell OSNs in larvae and adult zebrafish (Figs. 32, 33). Interestingly S100 is also visualized in a small subpopulation of microvillous OSNs (Figs. 32, 33). Further investigations with double labeling of parvalbumin and S100 revealed that the microvillous OSNs are divided at least in solely parvalbumin positive and parvalbumin/ S100 double positive subpopulations in larval and adult zebrafish (Figs. 32, 33). Thus, I was able to detect and differentiate between the three types of OSNs and even define subpopulations of microvillous OSNs by using CBPs expression in larval and adult zebrafish.

5.2.2. Combinatorial Analysis of CBPs in Zebrafish Primary Olfactory System Reveals New Differential Projections to OB

These combinatorial analyses of CBPs not only define OSNs in epithelium but also reveal new differential relationships of OSN projections to the olfactory bulb (OB) in larval and adult zebrafish.

Nomenclature of Olfactory Bulb Glomeruli. For detection and evaluation of OSN axonal projections in the developing (larval) OB, two different approaches were previously used to detect larval glomerular clusters (Dynes and Ngai, 1998; Miyasaka et al., 2009). Whereas Dynes & Ngai (1998) traced axonal projections of 3 dpf zebrafish larvae, Miyasaka and colleagues (2009) used transgenic visualization of axonal projections in 7 dpf larvae which resulted in recognition of additional two medial glomeruli (mG5 - 6). Myasaka et al furthermore renamed dorsal and central zone (DZ and CZ, respectively) as dorsal and anteroventral glomerular cluster (dG and avG), respectively and combined four previously recognized separate lateral glomeruli (LG1-4) to glomeruli of lateral glomerular cluster (lG). Both papers separated the bulbar glomerular fields in dorsal, medial, anterior, lateral and ventral groups which were already designated by Baier and Korsching (1994) in adult zebrafish (see Introduction).

Using CBP labeling, a comparison of the two different solutions for bulbar representation of larval axonal projections revealed that the glomerular groups described by Dynes & Ngai (1998) more precisely fit my data (Fig. 41). Furthermore, their designations also reflect the nomenclature in adult zebrafish (Baier and Korsching, 1994). Dynes & Ngai's (1998) coronal larval sections offer designations for many separate glomeruli and this allows clear analysis of glomerular clusters and comparison with axonal projections visualized with CPB immunohistochemistry and is more easily to be compared with the adult zebrafish situation. In contrast, Miyasaka and colleagues (2009) present schematic drawings of glomerular clusters in frontal view of whole – mount zebrafish larvae which makes a comparison more difficult, although developmental stage of 7dpf is more similar to zebrafish larvae used in my

study. Thus, in my doctoral thesis I use the terminology of larval glomeruli after Dynes and Ngai (1998).

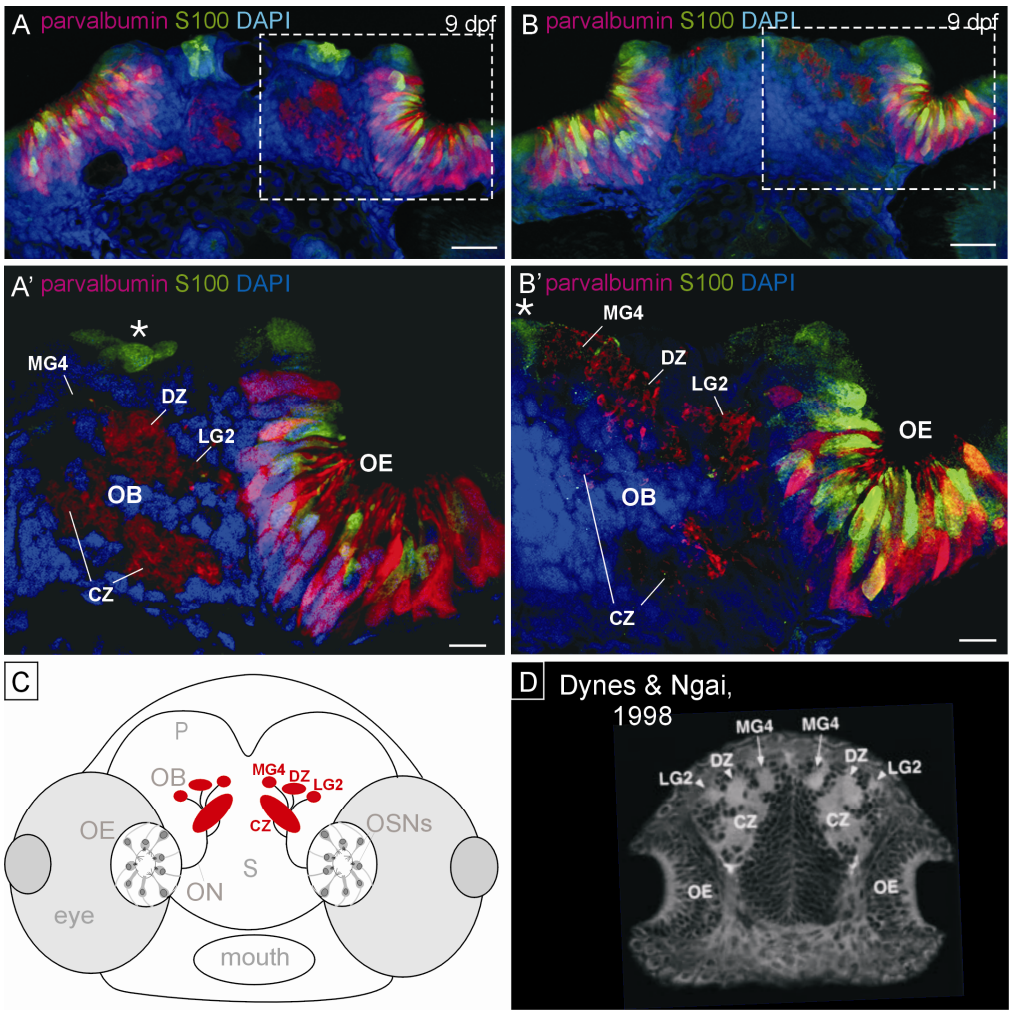

Fig. 41. Detection and evaluation of OSN projections in the developing olfactory bulb. (A), (B) Transverse sections visualize in two different larvae (9 dpf) as examples expression of parvalbumin and S100 counterstained with nuclear marker DAPI in olfactory epithelium and OB at the slightly different brain levels. White box marks area magnified in (A') and (B'). White stars point out S100 immunoreactive neuromasts. (C) Schematic drawing of larval zebrafish head with olfactory sensory neurons and projections into OB gives an interpretation of parvalbumin immunoreactive glomerular targets of the optical sections shown in (A') and (B') following glomerular nomenclature of Dynes & Ngai, 1998 (see Discussion). Parvalbumin expressing projections are detected in dorsal zone (DZ), central zone (CZ), in lateral glomerulus 2 (LG2) and in medial glomerulus 4 (MG4). No S100 expressing projections are visualized in OB at these levels. (D) Shows for comparison with sections in (A) and (B) a section taken from the tracing study by Dynes and Ngai (1998). See list for abbreviations. Scale bars in (A) and (B): 50µm and in (A') and (B'): 20 µm.

In adult zebrafish, the Braubach and colleagues (2012) expanded the study of adult glomeruli distribution by Baier & Korsching (1994) and detected new glomeruli by whole – mount immunohistochemistry combined with confocal imaging of all OB surfaces (see Introduction). They presented views of whole – mount adult zebrafish OBs but a

comparison with transverse sections of OB used in my study is difficult similar to the situation described for larvae above (see Miyasaka et al., 2009, Dynes and Ngai; 1998). Thus, the glomerular nomenclature used here is based on previous schemes used in adult zebrafish (Baier and Korsching, 1994) as the new glomeruli detected by Braubach could not be differentiated in my immunohistochemically study in transverse sections of the OB. Thus, the glomerular nomenclature used here is based on previous schemes used in developing (Dynes and Ngai, 1998) and adult zebrafish (Baier and Korsching, 1994).

Primary Projection Patterns to OB. The primary olfactory projection patterns to the OB visualized by analysis of different CBPs show subtle differences:

In larvae double labeling of calretinin and calbindin1 reveals that calbindin1 positive projections are less strongly expressed in bulbar targets in comparison to calretinin. Thus, in comparison to calretinin calbindin1 is expressed in less microvillous and ciliated OSNs in the OE and this is reflected in expanded bulbar targets of calretinin positive fibers in the larval OB. Furthermore, both of these CBP positive projections are not visualized in medial glomeruli.

In adult zebrafish strongly calretinin positive projections are visualized in glomeruli of the dorsal cluster (dc) and posteriorly in the ventral region of the OB (q and u – w) (Figs. 37, 39). Moreover less strong calretinin positive fibers are visualized in the plexus of the lateral chain (lc), excepting glomerulus 5 of the lateral chain (p) where strong calretinin positive projections are seen (Fig. 37). Double labeling of calretinin and calbindin1 in adult zebrafish reveals that both CBP positive projections overlap in numerous glomeruli, but calbindin1 positive fibers are more restricted in overlapping glomeruli and seem absent in lateral regions of OB (Figs. 37, 39). However, no obvious differences of calretinin - and calbindin1 expressing OSNs in OE could be demonstrated (Figs. 33, 34). Detailed analyses are necessary to proof whether there are less calbindin1 expressing OSNs in adult as it was shown in larvae (Fig. 34).

In any case, in adult zebrafish calretinin and calbindin1 are visualized only in ciliated OSNs. This type of OSNs express the large olfactory receptor gene families ORs and trace amine – associated receptors (TAARs; Alioto and Ngai, 2005; Niimura and Nei, 2005; Gloriam et al, 2005) corresponding to large specific olfactory bulb targets (Fig. 37). Interestingly, no calretinin or calbindin1 positive fibers are visualized in medial glomeruli of larval and adult zebrafish.

Future investigations will have to show in more detail where calbindin1 and calretinin positive projections overlap in the bulb and where there are subtle intensity differences in particular glomeruli as shown in these initial analyses. Moreover, differences in projections involving in particular more calretinin positive/calbindin1 negative glomeruli are likely to be visualized. Because the analysis of calretinin/calbindin1 double labelings also revealed calbindin1 immunoreactive neurons surrounding glomeruli in the OB of adult zebrafish (see Fig. 39), it must be established whether they include other cells than periglomerular cells, as is the case in mice (Kosaka and Kosaka, 2011). Furthermore, it should be investigated whether both calretinin and calbindin1 positive fibers are absent at all anteroposterior levels in the medial glomeruli.

Parvalbumin positive projections are visualized in almost all glomeruli in larval and adult OB (Figs. 34, 37). Calretinin positive and parvalbumin positive fibers largely overlap in the OB, but parvalbumin positive projections achieve additionally the anterior plexus (ap), the dorsal –cluster – associated glomeruli (a-e), the ventroposterior glomerulus (vpG) and glomeruli of the mediodorsal group (mdG; Fig. 37).

The axonal projections from ciliated and microvillous OSNs were previosly visualized in adult transgenic zebrafish lines (Sato et al., 2005). One of these transgenic lines labels cells expressing the transient receptor potential channel2 (Trpc2), a VNO – specific member of the transient receptor potential family of calcium channels associated with V2R – like receptors exclusively expressed in microvillous OSNs. The second line labels transgencially cells expressing the olfactory marker protein (OMP) associated with ORs and $G\alpha_{olf2}$ in ciliated OSNs (Sato et al., 2005; see Introduction). According to Sato et al (2005), most ciliated OSNs project to

the dorsal part of the OB, including the dorsal cluster (dc) and the dorsal – cluster – associated glomeruli and to the medial region of the OB, including the anterior plexus (ap) and medial glomeruli, excepting the mediodorsal posterior glomeruli ($mdpG_{1,2}$). Moreover ventromedial glomeruli (presumably glomeruli of the ventral triplet 1 – 3; u – w) and the medioventral posterior glomerulus are innervated by axonal projections of the ciliated OSNs. However, only one lateral glomerulus at the most posterior position of the lateral chain (p) received projections from ciliated OSNs (Sato et al., 2005).

In my CBP analysis, calretinin is shown to be expressed in ciliated OSNs and the calretinin positive projections mostly confirm the axonal projections from ciliated OSNs shown in the transgenic zebrafish line discussed aboves. Thus, strongly calretinin positive projections are visualized in glomeruli of the dorsal cluster (dc) (but no in dorsal cluster-associated glomeruli a-e), in glomerulus 5 of the lateral chain (p) and in the ventromedial region of the OB (u – w) (Fig. 39). In contrast, weak to no calretinin positive label is seen in lateral glomeruli (except for glomerulus p).

The axonal projections of microvillous OSNs in the adult transgenic zebrafish line innervated only the lateral and ventrolateral glomeruli of the OB but not the medial regions (Sato et al., 2005).Thus, these ventrolateral transgenically labeled Trpc2 expressing microvillous OSN projections did not overlap with the OMP labeled ciliated OSN projections.

My combinatorial analysis of CBPs revealed that parvalbumin is strongly expressed both in microvillous and ciliated OSNs (Figs. 32, 33). Parvalbumin and calretinin positive projections largely overlap in the OB consistent with the fact that both CBPs are expressed in ciliated OSNs. Moreover, it can be concluded from this, that the non – overlapping projections in the OB are innervated by microvillous OSNs expressing parvalbumin only, for example the ventrolateral olfactory bulb regions (lc,m). However, many of the non – overlapping glomeruli are present in the medial region of the OB (ap, $mdpG_1/_2$ and vpG) not innervated by the Trpc2-related axonal projections of microvillous OSNs in zebrafish

transgenic lines (Sato et al., 2005). This speaks for two subpopulations of microvillous cells, one expressing Trpc2 and the other not.

Furthermore, my CBP analysis revealed that S100 positive fibers only target one mediodorsal glomerulus in larval (MG2) and adult ($mdpG_2$) zebrafish OB (Figs. 34, 35, 37, 38; Poster: Daniela Biechl, Sigrid. Kress, Mario F. Wullimann, 2013, ECRO meeting, Leuwen, Belgium). Double labeling of S100 with the nuclear marker DAPI demonstrates periglomerular cell somata and confirms S100 positive terminals in mdpG2, but in no other glomeruli of the mediodorsal group. Moreover, many S100 immunoreactive glial cell bodies and their processes were visualized at the surface of OB and in lower numbers within the olfactory bulb (Fig. 38). Immunohistochemical analysis of glial fibrillary acidic protein (GFAP) revealed astrocytic processes of these superficial S100 positive cell bodies. Gayoso et al (2011) also observed S100 immunoreactivity in some glial cells and in numerous glial cell processes abutting the surface of the zebrafish OB (Gayoso et al., 2011). A comparison of GFAP with S100 reveals that astrocytes surround the OB and create a net of processes around it, with some less dense fibers extending into glomeruli (Fig. 38). However, dense neuronal S100 immunoreactive fibers are seen only in one glomerulus (mdpG2) and these are absent in GFAP stains. Thus, detailed investigations of S100 positive glomerulus in OB confirmed mdpG2 as the only target glomerulus of S100 immunoreactive fibers.

Braubach et al (2012) also showed the S100 projections only into mdpG2 (their mdG2). This paper reported in addition to two mediodorsal posterior glomeruli also shown in my study ($mdpG_1$ and $mdpG_2$), four more, adding up to six mediodorsal glomeruli (mdG1-6) arranged in a cluster on the dorsomedial OB surface (Braubach et al., 2012). Moreover, Gayoso et al (2012) demonstrated the restricted projection of S100 fibers primarily in crypt cells, but also in microvillous OSNs by DiI tracing. A recent study by Korsching and colleagues (2013) confirmed axonal projections of crypt cells to the same single gomerulus (mdG2) by using TrkA antibody restricted to crypt cells in zebrafish (Ahuja et al., 2013).

Thus, the $mdpG_2$ is innervated by parvalbumin - and S100 positive projections and the other mediodorsal glomeruli (mdG) only receive

parvalbumin positive fibers. According to my combinatorial analysis, the restricted projections to adult mdpG2/larval MG2 arise in S100 positive crypt cells and microvillous OSNs and projections to other mdG arise in parvalbumin positive microvillous OSNs.

Teleost Receptor Proteins and OSN Projections. In contrast to mammals which have a main and accessory olfactory epithelium, teleosts are equipped with only one olfactory organ containing three distinct types of OSNs (see Introduction). Possibly, the three different types of OSNs respond to different classes of odorants with different receptors and use different signal transduction machineries for odor information processing.

The odorant receptors ORs, TAARs and the vomeronasal receptor – types V1R – like *oras*, and V2R – like *olfC* receptors have been identified in zebrafish (see Introduction). Considering expression of teleost V2R – like receptors indicates that these molecules are phylogenetically older than the VNO itself (Hansen et al., 2004).

Moreover, in teleosts it has been shown that microvillous OSNs detect amino acids through V2R – like olfactory receptors (Speca et al., 1999; Hansen et al., 2003; Luu et al., 2004; reviewed in Yoshihara, 2009). Labeling of primary afferents with calcium – sensitive dye visualized that amino acids activate a chain of glomeruli located on the lateral side of the OB (Friedrich and Korsching, 1997) in accordance with transgenic zebrafish line visualizing Trpc2 related labeled projections of microvillous OSNs also in lateral region of the OB (Sato et al., 2005).

Ciliated OSNs express ORs and TAAR receptors (Alioto and Ngai, 2005; Niimura and Nei, 2005; Gloriam et al, 2005) detecting bile acids which elicit strong responses in the anteromedial and lateroposterior part of the OB (Friedrich and Korsching, 1997). The transgenic zebrafish line visualized OMP labeled projections of ciliated OSNs in the same parts of the OB in accordance with activation by bile acids (Sato et al., 2005).

Recent studies in salmonids and cyprinids have shown that both ciliated OSNs and microvillous OSNs respond to amino acids, but bile acids stimulate ciliated OSNs, and nucleotides activate microvillous OSNs (Hansen and Zielinski, 2005). Hansen and colleagues (2003) suggested

that amino acids activate both ciliated and microvillous OSNs but via different transduction pathways in the two types of OSNs.

The third OSN type in teleosts, the crypt cells, only expresses the V1R – like *ora4* gene (Oka et al., 2012). This type of OSNs bears apical microvilli as well as cilia extending into a crypt at the apex of the cell and the crypt cells have unknown odorant ligands (Hansen and Zielinski, 2005). Different laboratories used also an antibody against the CBP S100 to label crypt cells and their axons (Germana et al., 2004, 2007; Gayoso et al., 2011; Sandulescu et al., 2011; Braubach et al., 2012; Oka et al., 2012).

My combinatorial analysis revealed that the morphologies of anti S100 labeled OSN types are consistent with previous descriptions of crypt cells and microvillous OSNs supporting the results of Braubach and colleagues (2012). Interestingly, my analysis also confirms that S100 positive projections only innervate one mediodorsal posterior glomerulus in larval and adult zebrafish OB. In contrast, it has been shown in the crucian carp (Hamdani and Doving, 2006) and in the channel catfish (Hansen et al., 2003) that in these species crypt cells project to glomeruli in the ventral glomerular field. Moreover, in the crucian carp the secondary neurons located in the ventral part of the OB receiving crypt cell projections are stimulated by specific sex pheromones (Lastein et al., 2006). Korsching and colleagues (2013) supposed that a distinctly different position of crypt cell innervated glomeruli in OB could reflect differences in the subsequent circuits and therefore possibly differences in function of crypt cells between species (Ahuja et al., 2013).

However, in teleosts several morphological, biochemical and functional subsets of OSNs exist (Hamdani and Doving, 2000; Hamdani et al., 2001; Hansen et al., 2003, 2004; reviewed in Hansen and Zielinski, 2005). These subsets of OSNs project axons to specific targets (glomeruli) in the OB and may relate to the different odorant ligands (Friedrich and Korsching, 1998; Hansen et al., 2003, 2004; reviewed in Hansen and Zielinski, 2005).

In mammals putative pheromones induced responses in only a particular subset of microvillous OSNs in the epithelium of vomeronasal

organ (Leinders-Zufall et al., 2000). In zebrafish, double labeling of parvalbumin and S100 revealed that the microvillous OSNs are divided at least in solely parvalbumin positive and parvalbumin/ S100 double positive subpopulations in zebrafish (Fig. 32). Sato et al. (2005) used immunohistochemical analysis of S100 to demonstrate that no crypt cells were labeled in either of the transgenic lines labeling microvillous and ciliated OSNs in adult zebrafish (their Figure 4). However, in their Trpc2 line, next to strongly S100 labeled crypt cells (revealed by S100 positivity and their morphology), morphologically different more weakly S100 labeled cells were visualized. The additionally S100 labeled OSNs were plump, short OSNs in superficial – middle location of the OE and represent presumably microvillous OSNs. However, although the Trpc2 transgenic line of Sato and colleagues (2005) showed a limited possible subpopulation of microvillous OSNs labeled by S100, their corresponding primary projections in the OB were not visualized. The Sato group (2005) suggested that microvillous OSNs projected their axons exclusively to the (ventro-) lateral region of the OB. Maybe subpopulations of parvalbumin positive and parvalbumin/S100 positive microvillous OSNs visualized in my study innervate the glomeruli presented in the medial region of the OB (ap, mdpG_1/$_2$) not innervated by axonal projections of Trpc2 – expressing microvillous OSNs in zebrafish transgenic lines (Sato et al., 2005; Fig. 37).

In zebrafish, microvillous OSNs express the V2R – like receptors (Sato et al., 2005) and crypt cells express only one member of V1R – like *ora* genes (Oka et al., 2012). Pfister and Rodriguez (2005) demonstrated V1R – like receptors in zebrafish for the first time and suggested that the V1R - expressing OSNs are either microvillous OSNs or crypt cells identified by their position of somata in the epithelium (Pfister and Rodriguez, 2005). Definitive evidence for V1R – like receptors in microvillous OSNs of zebrafish was not obtained so far.

However, the results of my CBP combinatorial analysis lead me to the hypothesis that a subpopulation of parvalbumin positive microvillous OSNs possibly expresses V1R – like *ora* receptors and project axons to dorsomedial glomeruli in zebrafish. Saraiva and Korsching (2007) demonstrated six V1R – like *ora* genes in zebrafish and there are six

glomeruli in dorsomedial region of OB detected by the expanded tudy of glomeruli distribution of Braubach et al (2012). Although the new glomeruli detected by Braubach could not be differentiated in my immunohistochemically study, I reveal parvalbumin positive projections of microvillous OSNs to glomeruli dorsomedial in the OB not innervated by microvillous OSN axons in transgenic lines (Sato et al., 2005). The OSN types expressing the other 5 V1R – like *ora* genes are not known but at least *ora1* and *ora2* are might be expressed in microvillous OSNs identified by their morphology and position of soma in the epithelium (Oka et al., 2012). The mammalian V1R family, which is derived entirely from the *ora1*/*ora2* subfamily (Saraiva and Korsching 2007; reviewed in Oka et al., 2012), is expressed in a subgroup of microvillous OSNs (Mombaerts, 2004; reviewed in Oka et al., 2012) Thus, the assumption that *ora1* and *ora2* are might be expressed in microvillous OSNs would constitute a conserved feature across the teleost / tetrapod divide (Oka et al., 2012).

Moreover, backtracing via injection of DiI at the mediodorsal Glomerulus3 (mdG_3) supports my hypothesis and labeled OSNs with non – crypt morphology, presumably microvillous OSNs (Ahuja et al., 2013). In the same study, axonal projections of TrkA – positive crypt cells to the single gomerulus mdG_2 has been shown, confirming my results of CBP analysis (Ahuja et al., 2013). Backtracing via injection of DiI into the mdG_2 labeled crypt cells as well as microvillous OSNs. Korsching and colleagues (2013) argued that the homogenous labeling of one glomerulus by the TrkA antibody speaks against the small number of additionally backtraced cells reflecting collateral innervation to the mdG_2 glomerulus and supposed that some diffusion of DiI from the injection site into neighboring glomeruli is the cause (Ahuja et al., 2013). However, my CBP analysis revealed additional parvalbumin positive projection to mdG_2 arising from microvillous OSNs.

Sato and colleagues generated transgenic zebrafish lines which labeled Trpc2 together with V2R – like receptors exclusively in microvillous OSNs (Sato et al., 2005). It was reported that the gene that codes for the ion channel Trpc2 is essential for VNO function in mice (Dulac and Torello, 2003; Leypold et al., 2002; Stowers et al., 2002).

Teleosts have for many genes two paralogous copies, where only one ortholog is present in tetrapods (Hoegg et al., 2004). These duplicated paralogs originate in the whole genome duplication early in teleost evolution (Hoegg et al., 2004).

Thus it is possible, that in zebrafish a subpopulation of microvillous OSNs expressing V1R – like receptors exhibit a paralog of t*rpc2* gene. If so, the axonal projections of this microvillous OSNs subpopulation would not be shown in the transgenic zebrafish line by Sato et al (2005). Indeed, the axonal projections of microvillous OSNs in adult transgenic zebrafish lines innervated only the lateral and ventrolateral glomeruli of the OB but not the medial region (Figure 6 of Sato et al., 2005). These gaps of glomerular targets in the medial OB support the assumption that in zebrafish a subpopulation of microvillous OSNs expressing V1R – like receptors and a paralog of *trpc2* gene innervates the six glomeruli in dorsomedial region of OB detected by the enlarged study of glomeruli distribution of Braubach et al (2012). However, further studies are needed to support this hypothesis.

My combinatorial analysis detected another ventromedial glomerulus only receiving parvalbumin positive projections, the ventroposterior glomerulus (vpG, see in Fig. 37). This vpG is also likely weakly labeled in Trpc2 transgenic zebrafish line (Figure 6 O/W of Sato et al., 2005), although Sato et al (2005) did not identify this glomerulus as vpG but instead was assigned to the ventrolateral glomeruli. Moreover Sato et al (2005) visualized S100 expression in OSNs of Trpc2 associated transgenic zebrafish line (Figure 4 in Sato et al., 2005). Some of the S100 positive OSNs in superficial – middle position (presumably microvillous OSNs) appeared to exhibit also Trpc2. On the other hand some S100 positive OSNs in superficial – middle position (presumably microvillous OSNs) are not co - labeled in Trpc2 associated transgenic zebrafish line (Figure 4 F, H of Sato et al., 2005). It is possible that these differently labeled microvillous OSNs might also reflect different subpopulations: S100/Trpc2 positive microvillous OSNs and S100 positive (Trpc2 negativ) microvillous OSNs. Furthermore it is also possible that the axons of S100/Trpc2 subpopulation of microvillous OSNs project exclusively to vpG

weakly labeled in Trpc2 associated transgenic zebrafish line. In mammals deficiency of Trpc2 markedly impairs the sensory activation of VNO neurons by urine pheromones reflecting the crucial role of Trpc2 in the VNO signaling transduction cascade (Dulac and Torello, 2003). Thus the subpopulations could represent two functionally different microvillous OSNs.

In conclusion, I assume that there are different molecular and functional subpopulations of microvillous OSNs in zebrafish: One subpopulation of microvillous OSNs was visualized in Trpc2 associated transgenic zebrafish line projecting axons to the (ventro-) lateral region of the OB. Another subpopulation could be the S100/Trpc2 subpopulation of microvillous OSNs projecting axons exclusively to vpG which is weakly labeled in Trpc2 associated transgenic zebrafish line. The third subpopulation of microvillous OSNs could express V1R – like receptors and S100, and, possibly, a paralog of t*rpc2* gene and innervate the glomeruli presented in the medial region of the OB (mdG) not visualized in Trpc2 associated transgenic zebrafish line. According to this, in my study parvalbumin labeled all microvillous OSNs, but my combinatorial analysis of OSNs and their primary projections shown with several calcium binding proteins revealed subpopulations of microvillous OSNs.

In a recent study Korsching and colleagues (2013) also demonstrated the restricted axonal projections of crypt cells into only one target glomerulus (mdG2) (Ahuja et al., 2013). Previously the same group revealed that crypt cells express only one member of V1R – like *ora* genes (*ora4*) (Oka et al., 2012). These two discoveries led them to the hypothesis that crypt cells show a novel “one cell type – one receptor – one glomerulus” concept, distinct from the “one neuron – one receptor” mode of expression established for ciliated OSNs in zebrafish (Barth et al., 1997; Sato et al., 2007) reviewed in Ahuja et al., 2013). Thus, while ciliated and microvillous OSNs are thought to comprise a combinatorial code of odorants represented by the activation of different glomerular clusters, all crypt cells would send the information to one glomerulus in the OB. This coding strategy could enable crypt cells to be dedicated to a particular innate behavioral response, which was designated as ‘‘labeled lines’’ for

pheromone perception in insects (Touhara and Vosshall, 2009; reviewed in Oka et al., 2012). In insects, pheromones in general appear to activate a “labeled line pathway” in which pheromone input leads to a direct behavioral or physiological output (Touhara and Vosshall, 2009). My thesis work supports this hypothesis because my analysis revealed only one target glomerulus (mdG2) to receive crypt cell projections in larval and adult zebrafish (Figs. 34, 35, 37, 38; Poster: Daniela Biechl, Sigrid. Kress, Mario F. Wullimann, 2013, ECRO meeting, Leuwen, Belgium).

Higher Olfactory Brain Centers. Moreover, I would like to extend the hypothesis of “labeled line” for crypt cells to higher brain centers in zebrafish based on the following discussion. Miyasaka et al.(2009) reported transgenically visualized mitral cell populations (MCs) associated with different glomerular clusters tend to send axons to different target regions in the telencephalon which partly overlap. Thus, the odor information converging into glomeruli is relayed by axons of MCs to multiple brain areas in parallel and might be processed in different ways to execute distinct output responses (Miyasaka et al., 2009). However, in addition, Miyasaka and colleagues (2009) detected MCs innervating particular medial glomerular cluster displaying axon convergence to common target regions in higher brain centers. In detail, a large subpopulation of MCs innervating the medial glomeruli (MG1-6 in larvae, mdG1-6 in adult) projects their axons directly and asymmetrically to the right habenula (Miyasaka et al., 2009), whereas the majority of MCs innervating glomeruli outside the medial glomeruli cluster project their axons to different target regions in higher brain centers. Moreover, the odor information coming from different medial glomeruli appears to be integrated onto a specific population of habenular neurons (Miyasaka et al., 2009). Miyasaka and colleagues (2009) suggested that the neurons in the medial compartment of the right habenula may receive and process some particular odor information to elicit a specific behavioral response supporting the extended hypothesis of “labeled line” of crypt cells. Two studies revealed a role for the habenula in experience – dependent modulation of fear responses (Agetsuma et al., 2010; Lee et al., 2010) and

another recent study indicated the medial habenula as a regulator of anxiety in zebrafish (Mathuru and Jesuthasan, 2013).

Additionally, retrograde and anterograde labeling following application of DiI to the dorsomedial glomerular field in zebrafish OB supported the results of axonal projections of crypt cells and microvillous OSNs into dorsomedial glomeruli and visualized secondary olfactory projections arising from the dorsomedial glomerular field to telencephalic areas (Vv, Vs and Dp; Gayoso et al., 2012). Dp is homologous to the olfactory (lateral) pallium (piriform cortex) and the strongest pallial recipient of secondary olfactory projections in all teleosts (Wullimann and Mueller, 2004). Yaksi et al (2007) demonstrated that neurons responding to different combinations of odors are intermingled in Dp and neurons responding to different odors are intermingled in Vv (Yaksi et al., 2007). It has been hypothesized that Vs represent part of the subpallial (medial) amygdala (Mueller et al., 2008; Northcutt, 2006; Northcutt & Braford, 1980; Wullimann and Mueller, 2004).

Interestingly, only projections from MCs in the dorsomedial glomerular field innervate Vs (Gayoso et al., 2012). In teleosts, the medial amygdala (Vs) is possibly related to socially relevant olfactory signals (Mueller et al., 2008; Northcutt, 2006; Northcutt & Braford, 1980; Wullimann and Mueller, 2004). In mammals the amygdala is recipient of vomeronasal information, often involved with processing of pheromones (Martinez-Garcia et al., 2009).

Therefore Vs could also be another candidate for a target region in higher brain centers involved in a “labeled line” of pheromone processing in zebrafish. It is also possible that the dorsomedial glomerular field (including all 6 mdG) represents an intersection of two parallel “labeled lines” with odorants that trigger fear behavior or pheromones as ligands (“activators”). This hypothesis is supported by the fact that two different types of OSNs (subpopulation of microvillous OSNs and crypt cells) innervate the six dorsomedial glomeruli in OB. Thus, it is also possible that crypt cells show a novel “one cell type – one receptor – one glomerulus – one target region in higher brain centers” concept, as well as a

subpopulation of microvillous OSNs may complete the requirements for this "labeled line".

Furthermore, in adult zebrafish axons of MCs project to either the medial olfactory tract (MOT) or lateral olfactory tract (LOT), due to the location of the cell on the medial or lateral side of the OB, respectively (Fuller et al., 2006). Thus axonal projections of MCs in dorsomedial region of OB (including mdG) extend into the telencephalon via the medial olfactory tract (MOT). Several studies in fish supported that the MOT plays a significant role in processing of pheromonal information, thus mediates reproductive behavior (Demski and Dulka, 1984; Fuller et al., 2006; Hamdani et al., 2001; Sorensen et al., 1991; Stacey and Kyle, 1983; Weltzien et al., 2003).

Moreover in the crucian carp alarm reaction is mediated by the medial bundle of the MOT (Hamdani et al., 2000) and a recent study in zebrafish revealed activity of mitral cells in the dorsomedial region of OB after stimulation with an odorant that trigger fear behavior (Mathuru et al., 2012). Both facts also support my hypothesis of two different parallel “labeled lines” in zebrafish.

The hypothesis of “labeled line” for crypt cell, “one cell type – one receptor – one glomerulus”, is based on results shown by Korsching and colleagues (Oka et al., 2012; Ahuja et al., 2013) as well as in my combinatorial analysis of calcium binding proteins (Figs. 34, 35, 37, 38; Poster: Daniela Biechl, Sigrid Kress, Mario F. Wullimann, 2013, ECRO meeting, Leuwen, Belgium). But to confirm the expanded hypothesis of “labeled line”, one cell type – one receptor – one glomerulus – one target region in higher brain centers”, further studies are needed. All in all, the dorsomedial region of zebrafish OB seems to be the preferred starting point for further investigations.

Further Molecular Details. The morphologically different types of OSNs utilize different families of olfactory receptors coupled to different G protein α – subunits (Hansen et al, 2004). **I**n mammals the VNS consists of subclasses of vomeronasal receptor neurons distinguished by differential expression of G proteins ($G\alpha_{i2}$ and $G\alpha_{o}$) and segregated projections to the

accessory olfactory bulb (Jia and Halpern, 1996) (see Introduction Fig. 1). The microvillous OSNs of the vomeronasal organ express, segregated from each other, V1R receptors as well as the G protein $G\alpha_{i2}$ and the V2R receptors together with the G protein $G\alpha_o$ (Dulac and Torello, 2003).

In zebrafish, ciliated OSNs express ORs and TAARs associated with $G\alpha_{olf2}$, microvillous OSNs express V2R – like *olfC* receptors associated with the paralog pair *Gα$_{o1}$* and *Gα$_{o2}$* and crypt cells express only V1R – like *ora4* associated with $G\alpha_{i1b}$ (see Introduction).

Therefore the expression of Gα proteins in teleosts seems to be very similar to the expression of Gα proteins in mammals but some differences should be considered. For instance, the teleost Gα protein family is larger than the mammalian families due to the partial retention of duplicate genes, which may have been generated in a whole – genome duplication early in the teleost lineage (Oka and Korsching, 2011).

For many paralog pairs (e.g. $G\alpha_{i1a}$ /$G\alpha_{i1b}$) only one member is expressed in the chemosensory organs and the other member thus may have acquired new functions in other tissues (Oka and Korsching, 2011). Possibly, different paralogous genes may also be expressed in the olfactory epithelium, but associated with different receptors and/or different odorant ligands activating different signal transduction cascades (see below). This needs further investigation in teleosts.

Braubach et al (2012) showed a restricted projection of $G\alpha_o$ positive fibers into one small dorsomedial glomerulus (mdG_5) close to mdG_2 in the OB (mdG_5). In that study the $G\alpha_o$ immunoreactive OSNs in OE were identified by their morphology. $G\alpha_o$ positive OSNs exhibit elongated perikarya and a single short dendrite and small apical processes were often visible at the tips of these dendrites, thus, these OSNs are presumably microvillous OSNs (Figure1 F of Braubach et al., 2012). Right next to the described OSNs another $G\alpha_o$ positive cell type is imaged showing ovoid perikarya with acentric nuclei located near the epithelial surface, presumably crypt cells (Figure1 F of Braubach et al., 2012). In catfish anti - $G\alpha_o$ labeled crypt cells and in goldfish anti - $G\alpha_o$ labeled microvillous OSNs were reported (Hansen et al., 2003, 2005). Both genes of the paralog pair *Gα$_{o1}$* and *Gα$_{o2}$* are expressed in the zebrafish OE,

presumably in microvillous OSNs expressing the V2R – like *olfC* genes, like the single mammalian *Gα$_o$* gene which is co – expressed with *v2r* genes (Oka and Korsching, 2011). However, if two different microvillous OSN subpopulations should express *Gα$_o$*, then it is even less understandable that only one single glomerulus receives Gα$_o$ positive projections. The *Gα$_o$* targeted glomerulus is one of the six glomeruli in dorsomedial region of OB detected by the expanded study of glomeruli distribution of Braubach et al (2012). I hypothesized above that in zebrafish a subpopulation of microvillous OSNs expressing V1R – like receptors and another paralog of *trpc2* gene innervates the six glomeruli in dorsomedial region of OB (mdG$_{1-6}$). But, what we know so far is, that the V2R – like *olfC* receptors are associated with *Gα$_o$* in zebrafish. Thus, I have to expand my hypothesis and propose that the one glomerulus mdG$_5$ receives projections from a separate subpopulation of microvillous OSNs expressing V2R – like *olfC* receptors associated with *Gα$_o$* and a paralog of *trpc2* gene not visualized in the transgenic zebrafish line by Sato et al (2005). Another possibility is that a subpopulation of crypt cells expresses V2R – like *olfC* receptors associated with *Gα$_o$*. Both possibilities assume a subpopulation of OSNs not shown so far which project to only one target glomerulus (mdG$_5$.) in the OB.

The third type of OSNs, the crypt cells, which is absent in mammals, is a special feature in teleosts. The most striking characteristic of crypt cells is the fact that they bear cilia as well as microvilli, which is remarkable because the other two OSNs types only bear one of the cellular membrane protrusions and functionally differ from each other. In goldfish only crypt cells exhibit reactivity for more than one G protein (Hansen et al., 2004). Hansen and Zeiske (1998) visualized crypt cells in an ultrastructural study for the first time. In the same year Cao et al (1998) analyzed V2R receptors in OSNs in goldfish. In Figure 5 of Cao et al (1998) V2R receptors are shown via *in situ* analysis in superficial OSNs that may include crypt cells. Perhaps they were not able to distinguish between the different types of OSNs due to their knowledge at this time and visualized nesciently V2R receptors in crypt cells. This would match with the results of Braubach et al (2012) visualizing Gα$_o$ positive crypt

cells. By this crypt cells may also express V2R – like *olfC* receptors associated with the G protein $G\alpha_o$ supporting one of my stated possibilities (see above).

Moreover, another possibility is that the cilia of crypt cells possess ORs and TAAR receptors coupled to a paralog of $G\alpha_{olf}$ or another undetected Gα protein as another special feature in teleosts. It was revealed that the crypt cells in zebrafish express a single V1R – like gene, *ora4*, and no evidence for expression of other V1R – like *ora* genes, V2R – like *olfC* or *taar* genes in crypt cells was found (Ahuja et al., 2013; Oka and Korsching, 2011). However, there may be a reason why these cells feature two different protrusions (cilia and microvilli) which are usually in different OSNs equipped with specific receptors and associated with specific Gα proteins. Thus it is also possible that crypt cells utilize different receptors coupled to different G proteins at their cilia and microvilli not revealed so far. The microvillous OSNs in teleosts appear to respond feeding cues, whereas microvillous OSNs in the VNO of rodents respond preferentially to pheromones (Sato et al., 2005). Moreover, in crucian carp reproductive pheromones have been revealed as activators of crypt cells by Hamdani and Doving (2006) who supposed that crypt cells express olfactory receptors for sex pheromones. According to this the function of microvilli - , as well as cilia - bearing crypt cells in (VNO – lacking) teleosts is unknown and provides plenty of opportunity for speculation.

With regard to the two transduction pathway active in ciliated versus microvillous OSNs in mammals (see Introduction), it was demonstrated in teleosts that there are biochemical and physiological evidence for both, cAMP and IP_3 dependent transduction mechanisms. In channel catfish amino acids and bile acids are apparently detected predominantly by $G\alpha_{olf}$ expressing ciliated OSNs relying on cAMP transduction cascade (Hansen et al, 2003). In contrast, evidence for an IP_3 mediated pathway for amino acid stimulation has been shown in salmon (Hansen and Zielinski, 2005; Lo et al., 1993) and in zebrafish (Ma and Michel, 1998). It could be shown that two drugs affecting IP_3 / phospholipase C – mediated transduction cascade block the cyclic nucleotide – gated channels (CNC) in a voltage – dependent and reversible manner in adult zebrafish (Ma and Michel,

1998). Therefore, teleosts also exhibit the two types of odor – activated transduction pathways with the second messengers cAMP or IP_3. However the signal transduction steps in crypt neurons and their subsequent neuronal network are not known so far (Oka and Korsching, 2011).

In conclusion, teleost fish lack a morphologically separate VNS but they are able to detect and discriminate several structurally different classes of odorants and pheromones. Additionally the crypt cells, which are absent in mammals, are a special feature in teleosts and their specific function is not known so far. However, teleosts and mammals share many molecular characteristics necessary for pheromone perception and obviously the teleostean olfactory system is not less complex compared with the mammalian olfactory system. The current state of knowledge leads me to the assumption that crypt cells and likely different subpopulations of microvillous OSNs could functionally replace the VNS in teleosts. My combinatorial analyses of CBPs in zebrafish reveal new differential relationships of OSN projections to OB and thereby display subpopulations of microvillous OSNs. Future investigations are necessary in order to support my hypotheses. In any case, my combinatorial analyses of different CBPs provide new insight about differential olfactory zebrafish subsystems.

5.3. Analysis of Parvalbumin/S100 Positive Axonal Projections in the Developing OB Reveals Different Time Course of Different Primary Projections

My analysis of parvalbumin versus S100 positive axonal projections in the developing OB reveals different time course of different primary projections between 3 to 9 dpf (Fig. 35). According to my analysis, the restricted projections to the mediodorsal glomerulus (MG2) arise in S100 positive crypt cells and microvillous OSNs. The S100 terminals develop after day 3 and are only seen in MG2 whereas parvalbumin positive projections into MG2 and many other glomeruli appear earlier (at the latest at day 3).

Previously Sandulescu et al (2011) analysed the dynamics of number of S100 positive cells in the developing zebrafish olfactory organ up to 12 dpf. This study is based on immunoreactivity of OSNs to the same S100 antibody used in my combinatorial analyses. However, Sandulescu et al (2011) identified S100 positive OSNs only as crypt cells. They revealed a significant increase of numbers of S100 positive crypt cells in olfactory rosettes in the first few days after hatching up to 7 dpf and subsequent significant reduction to a level similar to that observed at the onset of S100 expression by 12 dpf again (Sandulescu et al., 2011).

Possibly, the retarded S100 fibers develop in correlation with the olfactory imprinting process between day 6 to 7 dpf (Gerlach et al. 2008; see Introduction). Moreover, in zebrafish kin recognition is based on phenotype matching of olfactory cues which is caused by imprinted effects on urinary odor during development (Gerlach and Lysiak, 2006). As mentioned, microvillous OSNs and crypt cells express members of the V1R/V2R receptor superfamily similar to the situation for the VNO of mammals in the context of pheromone detection. Thus I utilized the different expression patterns of parvalbumin and S100 to separate crypt cells and microvillous OSNs in larval OE (Fig. 32) and analyzed the dynamics of crypt cells and microvillous OSN development in larval zebrafish from 3 to 9 dpf (Fig. 36). Statistical analyses revealed that the average number of microvillous OSNs in OEs increased significantly in the developing olfactory organ between 3 to 9 dpf, but the average number of crypt cells in OE increased significantly only from 3 to 6 dpf and decrease subsequently to a level similar to that observed at 3 dpf until 9 dpf (Fig. 36). Hence, my analysis confirmed only to a small extent the results of Sandulescu et al (2011). My counts demonstrated only an increase in numbers of crypt cells in the olfactory rosettes at day 6. In detail, there are 4 crypt cells per animal on average in 3, 7 and 9 dpf, but 6 - 7 crypt cells per animal on average in larvae at day 6 (Fig. 36). Sandulescu et al (2011) revealed a steady increase of S100 positive crypt cells and showed the highest number at day 7 and subsequent significant reduction of numbers at day 8. However, a comparison with my data is difficult because the

mentioned study identified and counted all S100 positive OSNs as crypt cells.

In contrast, using the morphology of the different OSNs and their position in the epithelium, I utilized the different expression patterns of parvalbumin and S100 to separate crypt cells and microvillous OSNs. The steady rise of microvillous OSNs reflects the expected increase in the volume of OE and numbers of cells during development in general. The number of crypt cells behaves differently than expected in terms of the dynamic during development. It is possible that on day 6 a specific “event” leads to an increase in crypt cells compatible with the imprinting process in larvae. Crypt cells are suspected to be important for the detection of urinary odors (pheromones) in zebrafish. These results in turn would confirm the assumption and explained by an increase of the crypt cells on the day of imprinting. In contrast, although microvillous OSNs also express pheromone receptors (V2R – like olfC and presumably V1R – like oras), no specific increase of microvillous OSNs was visualized.

In order to further increase the unambiguous identification of crypt cells in future investigations, a specific antibody for crypt cells, e.g. TrkA antibody should be used because it is a robust and sensitive marker for crypt cells (Ahuja et al., 2013). Moreover the specific time window from day 6 to 7 dpf of olfactory imprinting in zebrafish larvae leaves much room for speculations. It is possible that the V1R – like ora4 receptors in crypt cells as well as other V1R - like ora and V2R – like olfC receptors in microvillous OSNs are more strongly expressed in this phase – sensitive process. However, currently, no specific antibodies are commercially available to test this more specific hypothesis of involvement of V1R-like ora receptors in this process. Additionally, in Trpc2$^{-/-}$mammals the sensory activation of VNO neurons by urine pheromones is markedly impaired (Dulac and Torello, 2003). Thus, the Trpc2 associated transgenic zebrafish line of Sato et al (2005) or specific antibodies against olfactory receptors in zebrafish, could help to visualize dynamics of other olfactory related parts possibly involved in the imprinting process.

5.4. Role of Terminal Nerve in Olfaction

As mentioned in the Introduction, zebrafish olfactory kin recognition depends on an imprinting process that requires a two – step learning process involving olfactory as well as visual cues of kin (Hinz et al., 2012, 2013). Thus, olfactory or visual cues alone are not sufficient for successful imprinting.

The neurobiological link between visual and olfactory sensory system in zebrafish could be represented by the olfactoretinal centrifugal pathway (Fig. 42B). Terminal nerve (TN) fibers containing the neuropeptide FMRFamide, project to telencephalon and tectal targets and, importantly, to the contralateral retina (Maaswinkel and Li, 2003).

Odor information reaches the OB as first central processing center from which projection neurons (mostly mitral cells) send axons to different target regions in the forebrain as secondary olfactory pathway (Fig. 42). One of the main targets of secondary olfactory projections in zebrafish is the posterior zone of dorsal telencaphalic area (Dp), the presumed homologue of mammalian olfactory cortex (Wullimann and Mueller, 2004, Mueller and Wullimann, 2009). In the olfactoretinal centrifugal pathway the TN cells play a key role: They receive input from Dp and pass on the information to the supracommissural nucleus of the ventral telencephalic area (Vs), the hypothetical medial amygdala in zebrafish (Mueller et al., 2008; Northcutt, 2006; Northcutt and Braford, 1980; Wullimann and Mueller, 2004), as well as back to Dp, and project in the periphery to OSNs most likely representing a modulatory circuit. Additionally, the contralateral retina and the ipsilateral optic tectum as central visual target region both also receive input from TN cells.

Moreover, in the zebrafish TN input to the retina upon olfactory stimulation has an effect on behavioural visual sensitivity (Maaswinkel and Li, 2003; Whitlock et al. 2003). Thus, Maaswinkel and Li (2003) suggested that TN is the prime candidate for olfactory modulation of visual sensitivity. Furthermore the TN cell bodies themselves receive input from brain areas involved in sensory functions such as olfaction and vision (Yamamoto and Ito, 2000). Thus, rather than being a sensory nerve, the TN is in a position to initiate olfactoretinal modulation. TN cell bodies may integrate olfactory

and visual information and through its modulatory outputs described above represent an important link in the imprinting process in zebrafish.

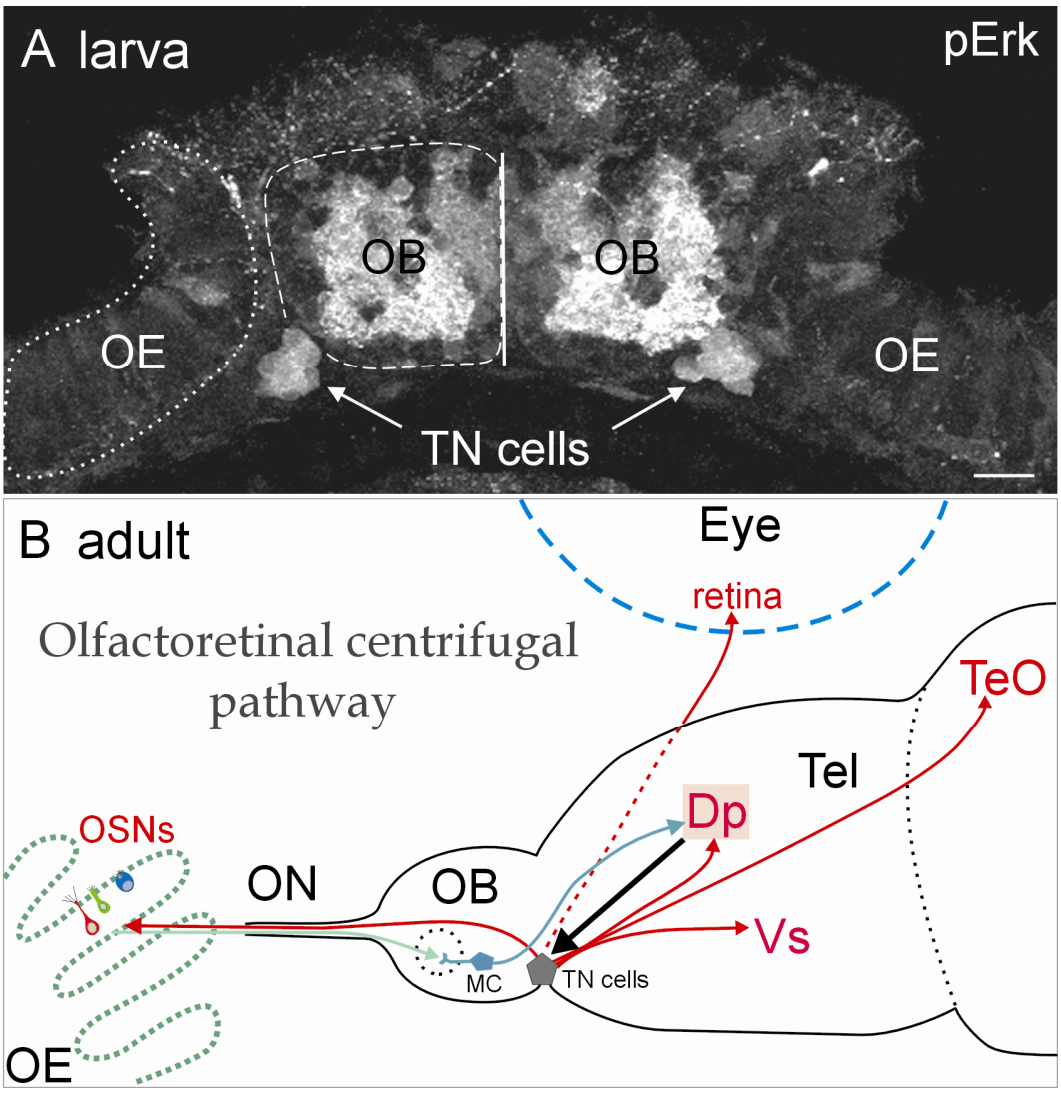

Fig. 42. Olfactoretinal centrifugal pathway in zebrafish. Visualization of terminal nerve (TN) cells in larval zebrafish (9dpf) via pErk expression (A) and circuitry of TN cells in olfactoretinal centrifugal pathway in adult zebrafish (B). (A) Transverse section of zebrafish larva shows pErk positive TN cells (arrows) and olfactory bulb cells (OB, surrounded by dashed line) Straight white line: shows brain midline. Dotted line indicates boundary of olfactory epithelium (OE). (B) Schematic drawing of olfactoretinal centrifugal pathways (red) in adult zebrafish.

In conclusion, my characterization of the zebrafish olfactory epithelium using Ca-binding protein (CBP) immunohistochemistry showed differential expression of calretinin, calbindin1, parvalbumin and S100 in the three olfactory sensory neuronal cell types (OSNs). While calretinin and calbindin1 are predominantly, if not exclusively, expressed in adult ciliated OSNs, parvalbumin is expressed equally abundantly in microvillous and ciliated OSNs. Whereas these three CBPs are absent in crypt cells, S100 is strongly expressed in crypt cells and weakly in a

subpopulation of microvillous cells. During larval development, calbindin1 and calretinin are also expressed in microvillous cells, but become increasingly restricted to ciliated cells in the adult. Primary projections of OSNs were also revealed in CBP immunohistochemistry and show calretinin/calbindin1 positive fibers in dorsolateral and ventrolateral glomeruli. Parvalbumin positive fibers are present in various additional mediodorsal, lateral and ventroposterior glomeruli, consistent with the expression of this CBP in microvillous cells in addition. Only one mediodorsal glomerulus (mdpG_2) exhibits S100 positive fibers, indicating that it contains all crypt cell plus the S100 positive microvillous OSN projections. The study of the temporal development of projections in larvae indicates a retardation of S100 positive projections compared to parvalbumin and a peak of crypt cell numbers around 6 dpf. Whether or not, this correlation with the known imprinting process has a functional context, must be further investigated.

6. References

Agetsuma M, Aizawa H, Aoki T, Nakayama R, Takahoko M, Goto M, Sassa T, Amo R, Shiraki T, Kawakami K, Hosoya T, Higashijima S, Okamoto H. 2010. The habenula is crucial for experience-dependent modification of fear responses in zebrafish. Nat Neurosci 13(11):1354-1356.

Ahuja G, Ivandic I, Salturk M, Oka Y, Nadler W, Korsching SI. 2013. Zebrafish crypt neurons project to a single, identified mediodorsal glomerulus. Sci Rep 3:2063.

Akiba N, Jo S, Akiba Y, Baker H, Cave JW. 2009. Expression of EGR-1 in a subset of olfactory bulb dopaminergic cells. J Mol Histol 40(2):151-155.

Alioto TS, Ngai J. 2005. The odorant receptor repertoire of teleost fish. BMC Genomics 6:173.

Alioto TS, Ngai J. 2006. The repertoire of olfactory C family G protein-coupled receptors in zebrafish: candidate chemosensory receptors for amino acids. BMC Genomics 7:309.

Allison AC. 1953. The structure of the olfactory bulb and its relationship to the olfactory pathways in the rabbit and the rat. J Comp Neurol 98(2):309-353.

Alonso M, Viollet C, Gabellec MM, Meas-Yedid V, Olivo-Marin JC, Lledo PM. 2006. Olfactory discrimination learning increases the survival of adult-born neurons in the olfactory bulb. J Neurosci 26(41):10508-10513.

Anadon R, Manso MJ, Rodriguez-Moldes I, Becerra M. 1995. Neurons of the olfactory organ projecting to the caudal telencephalon and hypothalamus: a carbocyanine-dye labelling study in the brown trout (Teleostei). Neurosci Lett 191(3):157-160.

Araneda RC, Kini AD, Firestein S. 2000. The molecular receptive range of an odorant receptor. Nat Neurosci 3(12):1248-1255.

Aroniadou-Anderjaska V, Ennis M, Shipley MT. 1999. Dendrodendritic recurrent excitation in mitral cells of the rat olfactory bulb. J Neurophysiol 82(1):489-494.

Baier H, Korsching S. 1994. Olfactory glomeruli in the zebrafish form an invariant pattern and are identifiable across animals. J Neurosci 14(1):219-230.

Baier H, Rotter S, Korsching S. 1994. Connectional topography in the zebrafish olfactory system: random positions but regular spacing of sensory neurons projecting to an individual glomerulus. Proc Natl Acad Sci U S A 91(24):11646-11650.

Baker H. 1990. Unilateral, neonatal olfactory deprivation alters tyrosine hydroxylase expression but not aromatic amino acid decarboxylase or GABA immunoreactivity. Neuroscience 36(3):761-771.

Baker H, Cummings DM, Munger SD, Margolis JW, Franzen L, Reed RR, Margolis FL. 1999. Targeted deletion of a cyclic nucleotide-gated channel subunit (OCNC1): biochemical and morphological consequences in adult mice. J Neurosci 19(21):9313-9321.

Baker H, Kawano T, Margolis FL, Joh TH. 1983. Transneuronal regulation of tyrosine hydroxylase expression in olfactory bulb of mouse and rat. J Neurosci 3(1):69-78.

Baker H, Morel K, Stone DM, Maruniak JA. 1993. Adult naris closure profoundly reduces tyrosine hydroxylase expression in mouse olfactory bulb. Brain Res 614(1-2):109-116.

Bally-Cuif L, Vernier P. 2010. Organization and Physiology of the Zebrafish Nervous System. In: Perry SF, Ekker M, Farrell AP, Brauner CJ, editors. Zebrafish: Elsevier.

Barth AL, Dugas JC, Ngai J. 1997. Noncoordinate expression of odorant receptor genes tightly linked in the zebrafish genome. Neuron 19(2):359-369.

Barth AL, Justice NJ, Ngai J. 1996. Asynchronous onset of odorant receptor expression in the developing zebrafish olfactory system. Neuron 16(1):23-34.

Baxi KN, Dorries KM, Eisthen HL. 2006. Is the vomeronasal system really specialized for detecting pheromones? Trends Neurosci 29(1):1-7.

Bayer SA. 1983. 3H-thymidine-radiographic studies of neurogenesis in the rat olfactory bulb. Exp Brain Res 50(2-3):329-340.

Beckmann AM, Wilce PA. 1997. Egr transcription factors in the nervous system. Neurochem Int 31(4):477-510; discussion 517-476.

Belluscio L, Lodovichi C, Feinstein P, Mombaerts P, Katz LC. 2002. Odorant receptors instruct functional circuitry in the mouse olfactory bulb. Nature 419(6904):296-300.

Berghard A, Buck LB. 1996. Sensory transduction in vomeronasal neurons: evidence for G alpha o, G alpha i2, and adenylyl cyclase II as major components of a pheromone signaling cascade. J Neurosci 16(3):909-918.

Birnbaumer L. 2007. Expansion of signal transduction by G proteins. The second 15 years or so: from 3 to 16 alpha subunits plus betagamma dimers. Biochim Biophys Acta 1768(4):772-793.

Boehm T, Zufall F. 2006. MHC peptides and the sensory evaluation of genotype. Trends Neurosci 29(2):100-107.

Bolhuis JJ, Gahr M. 2006. Neural mechanisms of birdsong memory. Nat Rev Neurosci 7(5):347-357.

Bosch TJ, Maslam S, Roberts BL. 1995. A polyclonal antibody against mammalian FOS can be used as a cytoplasmic neuronal activity marker in a teleost fish. J Neurosci Methods 58(1-2):173-179.

Bradbury JW, Vehrencamp SL. 2011. Chemical Signals. Principles of animal communication. Second Edition ed: Sinauer Associates, Inc.

Braubach OR, Fine A, Croll RP. 2012. Distribution and functional organization of glomeruli in the olfactory bulbs of zebrafish (Danio rerio). J Comp Neurol 520(11):2317-2339, Spc2311.

Breer H. 2001. Introduction: molecular mechanism of olfaction. CMLS, Cell Mol Life Sci 58:501-502.

Breer H, Fleischer J, Strotmann J. 2006. The sense of smell: multiple olfactory subsystems. Cell Mol Life Sci 63(13):1465-1475.

Brennan PA. 2001. The vomeronasal system. CMLS, Cell Mol Life Sci 58:546-555.

Brennan PA, Keverne EB. 1997. Neural mechanisms of mammalian olfactory learning. Prog Neurobiol 51(4):457-481.

Buck L, Axel R. 1991. A novel multigene family may encode odorant receptors: a molecular basis for odor recognition. Cell 65(1):175-187.

Buck LB. 2000. The molecular architecture of odor and pheromone sensing in mammals. Cell 100(6):611-618.

Bundschuh ST, Zhu P, Scharer YP, Friedrich RW. 2012. Dopaminergic modulation of mitral cells and odor responses in the zebrafish olfactory bulb. J Neurosci 32(20):6830-6840.

Burmeister SS, Fernald RD. 2005. Evolutionary conservation of the egr-1 immediate-early gene response in a teleost. J Comp Neurol 481(2):220-232.

Byrd CA. 2000. Deafferentation-induced changes in the olfactory bulb of adult zebrafish. Brain Res 866(1-2):92-100.

Byrd CA, Brunjes PC. 1995. Organization of the olfactory system in the adult zebrafish: histological, immunohistochemical, and quantitative analysis. J Comp Neurol 358(2):247-259.

Cao Y, Oh BC, Stryer L. 1998. Cloning and localization of two multigene receptor families in goldfish olfactory epithelium. Proc Natl Acad Sci U S A 95(20):11987-11992.

Carleton A, Petreanu LT, Lansford R, Alvarez-Buylla A, Lledo PM. 2003. Becoming a new neuron in the adult olfactory bulb. Nat Neurosci 6(5):507-518.

Castro A, Becerra M, Manso MJ, Anadon R. 2006. Calretinin immunoreactivity in the brain of the zebrafish, Danio rerio: distribution and comparison with some neuropeptides and neurotransmitter-synthesizing enzymes. I. Olfactory organ and forebrain. J Comp Neurol 494(3):435-459.

Cave JW, Baker H. 2009. Dopamine systems in the forebrain. Adv Exp Med Biol 651:15-35.

Chamero P, Leinders-Zufall T, Zufall F. 2012. From genes to social communication: molecular sensing by the vomeronasal organ. Trends Neurosci 35(10):597-606.

Chao TI, Kasa P, Wolff JR. 1997. Distribution of astroglia in glomeruli of the rat main olfactory bulb: exclusion from the sensory subcompartment of neuropil. J Comp Neurol 388(2):191-210.

Chaudhuri A. 1997. Neural activity mapping with inducible transcription factors. NeuroReport 8(3).

Christy BA, Lau LF, Nathans D. 1988. A gene activated in mouse 3T3 cells by serum growth factors encodes a protein with "zinc finger" sequences. Acad Sci USA 85:7857-7861.

Close R, Toro S, Martial JA, Muller M. 2002. Expression of the zinc finger Egr1 gene during zebrafish embryonic development. Mech Dev 118(1-2):269-272.

Davis S, Bozon B, Laroche S. 2003. How necessary is the activation of the immediate early gene zif268 in synaptic plasticity and learning? Behav Brain Res 142(1-2):17-30.

De Marchis S, Bovetti S, Carletti B, Hsieh YC, Garzotto D, Peretto P, Fasolo A, Puche AC, Rossi F. 2007. Generation of distinct types of periglomerular olfactory bulb interneurons during development and in adult mice: implication for intrinsic properties of the subventricular zone progenitor population. J Neurosci 27(3):657-664.

Demski LS, Dulka JG. 1984. Functional-anatomical studies on sperm release evoked by electrical stimulation of the olfactory tract in goldfish. Brain Res 291(2):241-247.

Didier A, Carleton A, Bjaalie JG, Vincent JD, Ottersen OP, Storm-Mathisen J, Lledo PM. 2001. A dendrodendritic reciprocal synapse provides a recurrent excitatory connection in the olfactory bulb. Proc Natl Acad Sci U S A 98(11):6441-6446.

Dittmann AH, Quinn TP. 1996. Homing in pacific salmon: mechanisms and ecological basis. The Journal of Experimental Biology 199:83-91.
Doving KB, Trotier D. 1998. Structure and function of the vomeronasal organ. J Exp Biol 201(Pt 21):2913-2925.
Downes GB, Gautam N. 1999. The G protein subunit gene families. Genomics 62(3):544-552.
Drummond IA, Rohwer-Nutter P, Sukhatme VP. 1994. The zebrafish egrl gene encodes a highly conserved, zinc-finger transcriptional regulator. DNA and Cell Biology 13(9):953-961.
Dryer L, Graziadei PP. 1994. Influence of the olfactory organ on brain development. Perspect Dev Neurobiol 2(2):163-174.
Dulac C, Axel R. 1995. A novel family of genes encoding putative pheromone receptors in mammals. Cell 83(2):195-206.
Dulac C, Torello AT. 2003. Molecular detection of pheromone signals in mammals: from genes to behaviour. Nat Rev Neurosci 4(7):551-562.
Dulac C, Wagner S. 2006. Genetic analysis of brain circuits underlying pheromone signaling. Annu Rev Genet 40:449-467.
Dynes JL, Ngai J. 1998. Pathfinding of olfactory neuron axons to stereotyped glomerular targets revealed by dynamic imaging in living zebrafish embryos. Neuron 20(6):1081-1091.
Edwards JG, Michel WC. 2002. Odor-stimulated glutamatergic neurotransmission in the zebrafish olfactory bulb. J Comp Neurol 454(3):294-309.
Egger V, Urban NN. 2006. Dynamic connectivity in the mitral cell-granule cell microcircuit. Semin Cell Dev Biol 17(4):424-432.
Eisthen HL. 1992. Phylogeny of the vomeronasal system and of receptor cell types in the olfactory and vomeronasal epithelia of vertebrates. Microsc Res Tech 23(1):1-21.
Eisthen HL. 1997. Evolution of Vertebrate Olfactory Systems. Brain, Behavior and Evolution 50(4):222-233.
Eisthen HL. 2004. The goldfish knows: olfactory receptor cell morphology predicts receptor gene expression. J Comp Neurol 477(4):341-346.
Eisthen HL, Wyatt TD. 2006. The vomeronasal system and pheromones. Curr Biol 16(3):R73-74.
Eyre MD, Antal M, Nusser Z. 2008. Distinct deep short-axon cell subtypes of the main olfactory bulb provide novel intrabulbar and extrabulbar GABAergic connections. J Neurosci 28(33):8217-8229.
Farbman AI. 1994. The cellular basis of olfaction. Endeavour 18(1):2-8.
Ferstl R, Eggert F, Muller-Ruchholtz W. 1998. Major histocompatibility complex-associated odours. Nephrol Dial Transplant 13(5):1117-1119.
Firestein S. 2001. How the olfactory system makes sense of scents. Nature 413(6852):211-218.
Firestein S, Beauchamp GK. 2008. Architecture of the Olfactory Bulb. The Senses: A comprehensive reference: Academic Press.
Fleischer J, Schwarzenbacher K, Besser S, Hass N, Breer H. 2006. Olfactory receptors and signalling elements in the Grueneberg ganglion. J Neurochem 98(2):543-554.
Freitag J, Krieger J, Strotmann J, Breer H. 1995. Two classes of olfactory receptors in Xenopus laevis. Neuron 15(6):1383-1392.
Friedman D, Strowbridge BW. 2000. Functional role of NMDA autoreceptors in olfactory mitral cells. J Neurophysiol 84(1):39-50.

Friedrich RW, Habermann CJ, Laurent G. 2004. Multiplexing using synchrony in the zebrafish olfactory bulb. Nat Neurosci 7(8):862-871.

Friedrich RW, Jacobson GA, Zhu P. 2010. Circuit neuroscience in zebrafish. Curr Biol 20(8):R371-381.

Friedrich RW, Korsching SI. 1997a. Combinatorial and chemotopic odorant coding in the zebrafish olfactory bulb visualized by optical imaging. Neuron 18(5):737-752.

Friedrich RW, Korsching SI. 1997b. Combinatorial and chemotopic odorant coding in the zebrafish olfactory bulb visualized by optical imaging. Neuron 18(5):737-752.

Friedrich RW, Korsching SI. 1998. Chemotopic, combinatorial, and noncombinatorial odorant representations in the olfactory bulb revealed using a voltage-sensitive axon tracer. J Neurosci 18(23):9977-9988.

Friedrich RW, Laurent G. 2001. Dynamic optimization of odor representations by slow temporal patterning of mitral cell activity. Science 291(5505):889-894.

Friedrich RW, Laurent G. 2004. Dynamics of olfactory bulb input and output activity during odor stimulation in zebrafish. J Neurophysiol 91(6):2658-2669.

Fuller CL, Byrd CA. 2005. Ruffed cells identified in the adult zebrafish olfactory bulb. Neurosci Lett 379(3):190-194.

Fuller CL, Yettaw HK, Byrd CA. 2006. Mitral cells in the olfactory bulb of adult zebrafish (Danio rerio): morphology and distribution. J Comp Neurol 499(2):218-230.

Gaillard I, Rouquier S, Giorgi D. 2004. Olfactory receptors. Cell Mol Life Sci 61(4):456-469.

Gayoso J, Castro A, Anadon R, Manso MJ. 2012. Crypt cells of the zebrafish Danio rerio mainly project to the dorsomedial glomerular field of the olfactory bulb. Chem Senses 37(4):357-369.

Gayoso JA, Castro A, Anadon R, Manso MJ. 2011. Differential bulbar and extrabulbar projections of diverse olfactory receptor neuron populations in the adult zebrafish (Danio rerio). J Comp Neurol 519(2):247-276.

Gerlach G. 2006. Pheromonal regulation of reproductive success in female zebrafish: female suppression and male enhancement. Animal Behaviour 72:1119 - 1124.

Gerlach G, Hodgins-Davis A, Avolio C, Schunter C. 2008. Kin recognition in zebrafish: a 24-hour window for olfactory imprinting. Proc Biol Sci 275(1647):2165-2170.

Gerlach G, Hodgins-Davis A, MacDonald B, Hannah R. 2007. Benefits of kin association: related and familiar zebrafish larvae (Danio rerio) show improved growth. Behav Ecol Sociobiol 61:1765-1770.

Gerlach G, Lysiak N. 2006. Kin recognition and inbreeding avoidance in zebrafish, Danio rerio, is based on phenotype matching. Animal Behaviour 71:1371–1377.

Germana A, Montalbano G, Laura R, Ciriaco E, del Valle ME, Vega JA. 2004. S100 protein-like immunoreactivity in the crypt olfactory neurons of the adult zebrafish. Neurosci Lett 371(2-3):196-198.

Germana A, Paruta S, Germana GP, Ochoa-Erena FJ, Montalbano G, Cobo J, Vega JA. 2007. Differential distribution of S100 protein and calretinin in mechanosensory and chemosensory cells of adult zebrafish (Danio rerio). Brain Res 1162:48-55.

Gloriam DE, Bjarnadottir TK, Yan YL, Postlethwait JH, Schioth HB, Fredriksson R. 2005. The repertoire of trace amine G-protein-coupled receptors: large expansion in zebrafish. Mol Phylogenet Evol 35(2):470-482.

Goelet P, Castellucci VF, Schacher S, Kandel ER. 1986. The long and the short of long-term memory--a molecular framework. Nature 322(6078):419-422.

Gracia-Llanes FJ, Crespo C, Blasco-Ibanez JM, Marques-Mari AI, Martinez-Guijarro FJ. 2003. VIP-containing deep short-axon cells of the olfactory bulb innervate interneurons different from granule cells. Eur J Neurosci 18(7):1751-1763.

Greer CA. 1987. Golgi analyses of dendritic organization among denervated olfactory bulb granule cells. J Comp Neurol 257(3):442-452.

Grus WE, Zhang J. 2006. Origin and evolution of the vertebrate vomeronasal system viewed through system-specific genes. BioEssays 28:709-718.

Halasz N, Johansson O, Hokfelt T, Ljungdahl A, Goldstein M. 1981. Immunohistochemical identification of two types of dopamine neuron in the rat olfactory bulb as seen by serial sectioning. J Neurocytol 10(2):251-259.

Halpern M. 1987. The organization and function of the vomeronasal system. Annu Rev Neurosci 10:325-362.

Halpern M, Shapiro LS, Jia C. 1995. Differential localization of G proteins in the opossum vomeronasal system. Brain Res 677(1):157-161.

Hamdani EH, Alexander G, Doving KB. 2001. Projection of sensory neurons with microvilli to the lateral olfactory tract indicates their participation in feeding behaviour in crucian carp. Chem Senses 26(9):1139-1144.

Hansen A, Anderson KT, Finger TE. 2004. Differential distribution of olfactory receptor neurons in goldfish: structural and molecular correlates. J Comp Neurol 477(4):347-359.

Hansen A, Rolen SH, Anderson K, Morita Y, Caprio J, Finger TE. 2003. Correlation between olfactory receptor cell type and function in the channel catfish. J Neurosci 23(28):9328-9339.

Hansen A, Zeiske E. 1993. Development of the olfactory organ in the zebrafish, Brachydanio rerio. J Comp Neurol 333(2):289-300.

Hansen A, Zeiske E. 1998. The peripheral olfactory organ of the zebrafish, Danio rerio: an ultrastructural study. Chem Senses 23(1):39-48.

Hansen A, Zielinski BS. 2005. Diversity in the olfactory epithelium of bony fishes: development, lamellar arrangement, sensory neuron cell types and transduction components. J Neurocytol 34(3-5):183-208.

Hansen A, Zippel HP, Sorensen PW, Caprio J. 1999. Ultrastructure of the olfactory epithelium in intact, axotomized, and bulbectomized goldfish, Carassius auratus. Microsc Res Tech 45(4-5):325-338.

Harteneck C, Plant TD, Schultz G. 2000. From worm to man: three subfamilies of TRP channels. Trends Neurosci 23(4):159-166.

Harvey-Girard E, Tweedle J, Ironstone J, Cuddy M, Ellis W, Maler L. 2010. Long-term recognition memory of individual conspecifics is associated with telencephalic expression of Egr-1 in the electric fish Apteronotus leptorhynchus. J Comp Neurol 518(14):2666-2692.

Hashiguchi Y, Nishida M. 2007. Evolution of trace amine associated receptor (TAAR) gene family in vertebrates: lineage-specific expansions and degradations of a second class of vertebrate chemosensory receptors expressed in the olfactory epithelium. Mol Biol Evol 24(9):2099-2107.

Hawkins RD, Kandel ER, Bailey CH. 2006. Molecular mechanisms of memory storage in Aplysia. Biol Bull 210(3):174-191.

Hayar A, Karnup S, Ennis M, Shipley MT. 2004. External tufted cells: a major excitatory element that coordinates glomerular activity. J Neurosci 24(30):6676-6685.

Herdegen T, Kovary K, Buhl A, Bravo R, Zimmermann M, Gass P. 1995. Basal expression of the inducible transcription factors c-Jun, JunB, JunD, c-Fos, FosB, and Krox-24 in the adult rat brain. J Comp Neurol 354(1):39-56.

Herdegen T, Leah JD. 1998. Inducible and constitutive transcription factors in the mammalian nervous system: control of gene expression by Jun, Fos and Krox, and CREB/ATF proteins. Brain Res Brain Res Rev 28(3):370-490.

Herdegen T, Sandkuhler J, Gass P, Kiessling M, Bravo R, Zimmermann M. 1993. JUN, FOS, KROX, and CREB transcription factor proteins in the rat cortex: basal expression and induction by spreading depression and epileptic seizures. J Comp Neurol 333(2):271-288.

Herdegen T, Walker T, Leah JD, Bravo R, Zimmermann M. 1990. The KROX-24 protein, a new transcription regulating factor: expression in the rat central nervous system following afferent somatosensory stimulation. Neurosci Lett 120(1):21-24.

Hildebrand JG, Shepherd GM. 1997. Mechanisms of olfactory discrimination: converging evidence for common principles across phyla. Annu Rev Neurosci 20:595-631.

Hinz C, Gebhardt K, Hartmann AK, Sigman L, Gerlach G. 2012. Influence of kinship and MHC class II genotype on visual traits in zebrafish larvae (Danio rerio). PLoS One 7(12):e51182.

Hinz C, Kobbenbring S, Kress S, Sigman L, Mueller A, Gerlach G. 2013. Kin recognition in zebrafish, Danio rerio, is based on imprinting on olfactory and visual stimuli. Animal Behaviour 85(5):925-930.

Hoegg S, Brinkmann H, Taylor JS, Meyer A. 2004. Phylogenetic timing of the fish-specific genome duplication correlates with the diversification of teleost fish. J Mol Evol 59(2):190-203.

Hofmann MH, Meyer DL. 1995. The extrabulbar olfactory pathway: primary olfactory fibers bypassing the olfactory bulb in bony fishes? Brain Behav Evol 46(6):378-388.

Honkanen T, Ekstrom P. 1990. An immunocytochemical study of the olfactory projections in the three-spined stickleback, Gasterosteus aculeatus, L. J Comp Neurol 292(1):65-72.

Hu J, Zhong C, Ding C, Chi Q, Walz A, Mombaerts P, Matsunami H, Luo M. 2007. Detection of near-atmospheric concentrations of CO2 by an olfactory subsystem in the mouse. Science 317(5840):953-957.

Huesa G, Anadon R, Yanez J. 2000. Olfactory projections in a chondrostean fish, Acipenser baeri: an experimental study. J Comp Neurol 428(1):145-158.

Huh GS, Boulanger LM, Du H, Riquelme PA, Brotz TM, Shatz CJ. 2000. Functional requirement for class I MHC in CNS development and plasticity. Science 290(5499):2155-2159.

Hussain A, Saraiva LR, Korsching SI. 2009. Positive Darwinian selection and the birth of an olfactory receptor clade in teleosts. Proc Natl Acad Sci U S A 106(11):4313-4318.

Imai T, Sakano H. 2008. Odorant Receptor Gene Choice and Axonal Projections in the Mouse Olfactory System. In: Meyerhof W, Korsching S, editors. Chemosensory Systems in Mammals, Fishes, and Insects: Springer.

Imai T, Sakano H, Vosshall LB. 2010. Topographic mapping--the olfactory system. Cold Spring Harb Perspect Biol 2(8):a001776.

Imamura F, Nagao H, Naritsuka H, Murata Y, Taniguchi H, Mori K. 2006. A leucine-rich repeat membrane protein, 5T4, is expressed by a subtype of granule cells with dendritic arbors in specific strata of the mouse olfactory bulb. J Comp Neurol 495(6):754-768.

Inaki K, Takahashi YK, Nagayama S, Mori K. 2002. Molecular-feature domains with posterodorsal-anteroventral polarity in the symmetrical sensory maps of the mouse olfactory bulb: mapping of odourant-induced Zif268 expression. Eur J Neurosci 15(10):1563-1574.

Iqbal T, Byrd-Jacobs C. 2010. Rapid degeneration and regeneration of the zebrafish olfactory epithelium after triton X-100 application. Chem Senses 35(5):351-361.

Iwema CL, Fang H, Kurtz DB, Youngentob SL, Schwob JE. 2004. Odorant receptor expression patterns are restored in lesion-recovered rat olfactory epithelium. J Neurosci 24(2):356-369.

Jia C, Halpern M. 1996. Subclasses of vomeronasal receptor neurons: differential expression of G proteins (Gi alpha 2 and G(o alpha)) and segregated projections to the accessory olfactory bulb. Brain Res 719(1-2):117-128.

Johnson BA, Woo CC, Duong H, Nguyen V, Leon M. 1995. A learned odor evokes an enhanced Fos-like glomerular response in the olfactory bulb of young rats. Brain Res 699(2):192-200.

Juilfs DM, Fuller HJ, Zhao AZ, Houslay MD, Garbers DL, Beavo JA. 1997. A subset of olfactory neurons that selectively express cGMP-stimulated phosphodiesterase (PDE2) and guanylyl cyclase-D define a unique olfactory signal transduction pathway. Proc Natl Acad Sci U S A 94:3388-3395.

Kaczmarek L. 1993. Molecular biology of vertebrate learning: is c-fos a new beginning? J Neurosci Res 34(4):377-381.

Kaczmarek L, Kaminska B. 1989. Molecular biology of cell activation. Exp Cell Res 183(1):24-35.

Kaczmarek L, Nikolajew E. 1990. c-fos protooncogene expression and neuronal plasticity. Acta Neurobiol Exp (Wars) 50(4-5):173-179.

Kaslin J, Panula P. 2001. Comparative anatomy of the histaminergic and other aminergic systems in zebrafish (Danio rerio). J Comp Neurol 440(4):342-377.

Kasowski HJ, Kim H, Greer CA. 1999. Compartmental organization of the olfactory bulb glomerulus. J Comp Neurol 407(2):261-274.

Kent PF, Mozell MM, Murphy SJ. 1996. The interaction of imposed and inherent olfactory mucosal activity patterns and their composite representation in a mammalian species using voltage-sensitive dyes. J Neurosci 16:345-353.

Kiyokage E, Pan YZ, Shao Z, Kobayashi K, Szabo G, Yanagawa Y, Obata K, Okano H, Toida K, Puche AC, Shipley MT. 2010. Molecular identity of periglomerular and short axon cells. J Neurosci 30(3):1185-1196.

Knapska E, Kaczmarek L. 2004. A gene for neuronal plasticity in the mammalian brain: Zif268/Egr-1/NGFI-A/Krox-24/TIS8/ZENK? Prog Neurobiol 74(4):183-211.

Koide T, Miyasaka N, Morimoto K, Asakawa K, Urasaki A, Kawakami K, Yoshihara Y. 2009. Olfactory neural circuitry for attraction to amino acids revealed by transposon-mediated gene trap approach in zebrafish. Proc Natl Acad Sci U S A 106(24):9884-9889.

Korsching S. 2008. The Molecular Evolution of Teleost Olfactory Receptor Gene Families. In: Meyerhof W, Korsching S, editors. Chemosensory Systems in Mammals, Fishes, and Insects: Springer.

Korsching SI, Argo S, Campenhausen H, Friedrich RW, Rummrich A, Weth F. 1997a. Olfaction in zebrafish: what does a tiny teleost tell us? Semin Cell Dev Biol 8(2):181-187.

Korsching SI, Argo S, Campenhausen H, Friedrich RW, Rummrich A, Weth F. 1997b. Olfaction in zebrafish: What does a tiny teleost tell us? Seminars in Cell & Developmental Biology 8(2):181-187.

Kosaka K, Aika Y, Toida K, Kosaka T. 2001. Structure of intraglomerular dendritic tufts of mitral cells and their contacts with olfactory nerve terminals and calbindin-immunoreactive type 2 periglomerular neurons. J Comp Neurol 440(3):219-235.

Kosaka K, Kosaka T. 2005a. synaptic organization of the glomerulus in the main olfactory bulb: compartments of the glomerulus and heterogeneity of the periglomerular cells. Anat Sci Int 80(2):80-90.

Kosaka K, Kosaka T. 2007a. Chemical properties of type 1 and type 2 periglomerular cells in the mouse olfactory bulb are different from those in the rat olfactory bulb. Brain Res 1167:42-55.

Kosaka K, Toida K, Aika Y, Kosaka T. 1998. How simple is the organization of the olfactory glomerulus?: the heterogeneity of so-called periglomerular cells. Neurosci Res 30(2):101-110.

Kosaka K, Toida K, Margolis FL, Kosaka T. 1997. Chemically defined neuron groups and their subpopulations in the glomerular layer of the rat main olfactory bulb--II. Prominent differences in the intraglomerular dendritic arborization and their relationship to olfactory nerve terminals. Neuroscience 76(3):775-786.

Kosaka T, Hama K. 1979. Ruffed cell: a new type of neuron with a distinctive initial unmyelinated portion of the axon in the olfactory bulb of the goldfish (Carassius auratus) I. Golgi impregnation and serial thin sectioning studies. J Comp Neurol 186(3):301-319.

Kosaka T, Hama K. 1981. Ruffed cell: a new type of neuron with a distinctive initial unmyelinated portion of the axon in the olfactory bulb of the goldfish (Carassius auratus). III. Three-dimensional structure of the ruffed cell dendrite. J Comp Neurol 201(4):571-587.

Kosaka T, Hama K. 1982. Synaptic organization in the teleost olfactory bulb. J Physiol (Paris) 78(8):707-719.

Kosaka T, Kosaka K. 2003. Neuronal gap junctions in the rat main olfactory bulb, with special reference to intraglomerular gap junctions. Neurosci Res 45(2):189-209.

Kosaka T, Kosaka K. 2004. Neuronal gap junctions between intraglomerular mitral/tufted cell dendrites in the mouse main olfactory bulb. Neurosci Res 49(4):373-378.

Kosaka T, Kosaka K. 2005b. Intraglomerular dendritic link connected by gap junctions and chemical synapses in the mouse main olfactory bulb: electron microscopic serial section analyses. Neuroscience 131(3):611-625.

Kosaka T, Kosaka K. 2005c. Structural organization of the glomerulus in the main olfactory bulb. Chem Senses 30 Suppl 1:i107-108.

Kosaka T, Kosaka K. 2007b. Heterogeneity of nitric oxide synthase-containing neurons in the mouse main olfactory bulb. Neurosci Res 57(2):165-178.

Kosaka T, Kosaka K. 2008a. Heterogeneity of parvalbumin-containing neurons in the mouse main olfactory bulb, with special reference to short-axon cells and betaIV-spectrin positive dendritic segments. Neurosci Res 60(1):56-72.

Kosaka T, Kosaka K. 2008b. Tyrosine hydroxylase-positive GABAergic juxtaglomerular neurons are the main source of the interglomerular connections in the mouse main olfactory bulb. Neurosci Res 60(3):349-354.
Kosaka T, Kosaka K. 2009. Two types of tyrosine hydroxylase positive GABAergic juxtaglomerular neurons in the mouse main olfactory bulb are different in their time of origin. Neurosci Res 64(4):436-441.
Kosaka T, Kosaka K. 2010. Heterogeneity of calbindin-containing neurons in the mouse main olfactory bulb: I. General description. Neurosci Res 67(4):275-292.
Kosaka T, Kosaka K. 2011. "Interneurons" in the olfactory bulb revisited. Neurosci Res 69(2):93-99.
Kress S, Wullimann MF. 2012. Correlated basal expression of immediate early gene egr1 and tyrosine hydroxylase in zebrafish brain and downregulation in olfactory bulb after transitory olfactory deprivation. J Chem Neuroanat 46(1-2):51-66.
Kuhn E, Koster RW. 2010. Analysis of gene expression by in situ hybridization on adult zebrafish brain sections. Cold Spring Harb Protoc 2010(2):pdb prot5382.
Laberge F, Hara TJ. 2001a. Neurobiology of fish olfaction: a review. Brain Res Brain Res Rev 36(1):46-59.
Laberge F, Hara TJ. 2001b. Neurobiology of fish olfaction: a review. Brain Research Reviews 36(1):46-59.
Lastein S, Hamdani el H, Doving KB. 2006. Gender distinction in neural discrimination of sex pheromones in the olfactory bulb of crucian carp, Carassius carassius. Chem Senses 31(1):69-77.
Lau BY, Mathur P, Gould GG, Guo S. 2011. Identification of a brain center whose activity discriminates a choice behavior in zebrafish. Proc Natl Acad Sci U S A 108(6):2581-2586.
Laurent G. 2002. Olfactory network dynamics and the coding of multidimensional signals. Nat Rev Neurosci 3(11):884-895.
Lee A, Mathuru AS, Teh C, Kibat C, Korzh V, Penney TB, Jesuthasan S. 2010. The habenula prevents helpless behavior in larval zebrafish. Curr Biol 20(24):2211-2216.
Leinders-Zufall T, Brennan P, Widmayer P, S PC, Maul-Pavicic A, Jager M, Li XH, Breer H, Zufall F, Boehm T. 2004. MHC class I peptides as chemosensory signals in the vomeronasal organ. Science 306(5698):1033-1037.
Leinders-Zufall T, Cockerham RE, Michalakis S, Biel M, Garbers DL, Reed RR, Zufall F, Munger SD. 2007. Contribution of the receptor guanylyl cyclase GC-D to chemosensory function in the olfactory epithelium. Proc Natl Acad Sci U S A 104(36):14507-14512.
Leinders-Zufall T, Ishii T, Mombaerts P, Zufall F, Boehm T. 2009. Structural requirements for the activation of vomeronasal sensory neurons by MHC peptides. Nat Neurosci 12(12):1551-1558.
Leinders-Zufall T, Lane AP, Puche AC, Ma W, Novotny MV, Shipley MT, Zufall F. 2000. Ultrasensitive pheromone detection by mammalian vomeronasal neurons. Nature 405(6788):792-796.
Levai O, Breer H, Strotmann J. 2003. Subzonal organization of olfactory sensory neurons projecting to distinct glomeruli within the mouse olfactory bulb. J Comp Neurol 458(3):209-220.

Leypold BG, Yu CR, Leinders-Zufall T, Kim MM, Zufall F, Axel R. 2002. Altered sexual and social behaviors in trp2 mutant mice. Proc Natl Acad Sci U S A 99(9):6376-6381.

Li W, Scott AP, Siefkes MJ, Yan H, Liu Q, Yun SS, Gage DA. 2002. Bile Acid secreted by male sea lamprey that acts as a sex pheromone. Science 296(5565):138-141.

Liberles SD, Buck LB. 2006. A second class of chemosensory receptors in the olfactory epithelium. Nature 442(7103):645-650.

Liberles SD, Horowitz LF, Kuang D, Contos JJ, Wilson KL, Siltberg-Liberles J, Liberles DA, Buck LB. 2009. Formyl peptide receptors are candidate chemosensory receptors in the vomeronasal organ. Proc Natl Acad Sci U S A 106(24):9842-9847.

Liman ER, Buck LB. 1994. A second subunit of the olfactory cyclic nucleotide-gated channel confers high sensitivity to cAMP. Neuron 13(3):611-621.

Linder ME, Ewald DA, Miller RJ, Gilman AG. 1990. Purification and characterization of Go alpha and three types of Gi alpha after expression in Escherichia coli. J Biol Chem 265(14):8243-8251.

Liu N, Cigola E, Tinti C, Jin BK, Conti B, Volpe BT, Baker H. 1999. Unique regulation of immediate early gene and tyrosine hydroxylase expression in the odor-deprived mouse olfactory bulb. J Biol Chem 274(5):3042-3047.

Liu S, Shipley MT. 2008a. Intrinsic conductances actively shape excitatory and inhibitory postsynaptic responses in olfactory bulb external tufted cells. J Neurosci 28(41):10311-10322.

Liu S, Shipley MT. 2008b. Multiple conductances cooperatively regulate spontaneous bursting in mouse olfactory bulb external tufted cells. J Neurosci 28(7):1625-1639.

Liu WC, Nottebohm F. 2005. Variable rate of singing and variable song duration are associated with high immediate early gene expression in two anterior forebrain song nuclei. Proc Natl Acad Sci U S A 102(30):10724-10729.

Liu WL, Shipley MT. 1994. Intrabulbar associational system in the rat olfactory bulb comprises cholecystokinin-containing tufted cells that synapse onto the dendrites of GABAergic granule cells. J Comp Neurol 346(4):541-558.

Lo YH, Bradley TM, Rhoads DE. 1993. Stimulation of Ca(2+)-regulated olfactory phospholipase C by amino acids. Biochemistry 32(46):12358-12362.

Loconto J, Papes F, Chang E, Stowers L, Jones EP, Takada T, Kumanovics A, Fischer Lindahl K, Dulac C. 2003. Functional expression of murine V2R pheromone receptors involves selective association with the M10 and M1 families of MHC class Ib molecules. Cell 112(5):607-618.

Lodovichi C, Belluscio L, Katz LC. 2003. Functional topography of connections linking mirror-symmetric maps in the mouse olfactory bulb. Neuron 38(2):265-276.

Lucas P, Ukhanov K, Leinders-Zufall T, Zufall F. 2003. A diacylglycerol-gated cation channel in vomeronasal neuron dendrites is impaired in TRPC2 mutant mice: mechanism of pheromone transduction. Neuron 40(3):551-561.

Luo Y, Lu S, Chen P, Wang D, Halpern M. 1994. Identification of chemoattractant receptors and G-proteins in the vomeronasal system of garter snakes. J Biol Chem 269(24):16867-16877.

Luu P, Acher F, Bertrand HO, Fan J, Ngai J. 2004. Molecular determinants of ligand selectivity in a vertebrate odorant receptor. J Neurosci 24(45):10128-10137.

Ma L, Michel WC. 1998. Drugs affecting phospholipase C-mediated signal transduction block the olfactory cyclic nucleotide-gated current of adult zebrafish. J Neurophysiol 79(3):1183-1192.
Ma M. 2012. Odor and pheromone sensing via chemoreceptors. Adv Exp Med Biol 739:93-106.
Ma PM. 1997. Catecholaminergic systems in the zebrafish. III. Organization and projection pattern of medullary dopaminergic and noradrenergic neurons. J Comp Neurol 381(4):411-427.
Maaswinkel H, Li L. 2003. Olfactory input increases visual sensitivity in zebrafish: a possible function for the terminal nerve and dopaminergic interplexiform cells. J Exp Biol 206(Pt 13):2201-2209.
Malnic B, Hirono J, Sato T, Buck LB. 1999. Combinatorial receptor codes for odors. Cell 96(5):713-723.
Mandairon N, Linster C. 2009. Odor perception and olfactory bulb plasticity in adult mammals. J Neurophysiol 101(5):2204-2209.
Mangiamele LA, Burmeister SS. 2008. Acoustically evoked immediate early gene expression in the pallium of female tungara frogs. Brain Behav Evol 72(3):239-250.
Mann KD, Turnell ER, Atema J, Gerlach G. 2003. Kin recognition in juvenile zebrafish (Danio rerio) based on olfactory cues. Biol Bull 205(2):224-225.
Margrie TW, Sakmann B, Urban NN. 2001. Action potential propagation in mitral cell lateral dendrites is decremental and controls recurrent and lateral inhibition in the mammalian olfactory bulb. Proc Natl Acad Sci U S A 98(1):319-324.
Martinez-Garcia F, Martinez-Ricos J, Agustin-Pavon C, Martinez-Hernandez J, Novejarque A, Lanuza E. 2009. Refining the dual olfactory hypothesis: pheromone reward and odour experience. Behav Brain Res 200(2):277-286.
Marz M, Chapouton P, Diotel N, Vaillant C, Hesl B, Takamiya M, Lam CS, Kah O, Bally-Cuif L, Strahle U. 2010. Heterogeneity in progenitor cell subtypes in the ventricular zone of the zebrafish adult telencephalon. Glia 58(7):870-888.
Mathuru AS, Jesuthasan S. 2013. The medial habenula as a regulator of anxiety in adult zebrafish. Front Neural Circuits 7:99.
Matsunami H, Buck LB. 1997. A multigene family encoding a diverse array of putative pheromone receptors in mammals. Cell 90(4):775-784.
Mello CV, Clayton DF. 1994. Song-induced ZENK gene expression in auditory pathways of songbird brain and its relation to the song control system. J Neurosci 14(11 Pt 1):6652-6666.
Mello CV, Vicario DS, Clayton DF. 1992. Song presentation induces gene expression in the songbird forebrain. Proc Natl Acad Sci U S A 89(15):6818-6822.
Menini A, Lagostena L, Boccaccio A. 2004. Olfaction: from odorant molecules to the olfactory cortex. News Physiol Sci 19:101-104.
Merkle FT, Mirzadeh Z, Alvarez-Buylla A. 2007. Mosaic organization of neural stem cells in the adult brain. Science 317(5836):381-384.
Mezler M, Fleischer J, Breer H. 2001. Characteristic features and ligand specificity of the two olfactory receptor classes from Xenopus laevis. J Exp Biol 204(Pt 17):2987-2997.
Miwa N, Storm DR. 2005. Odorant-induced activation of extracellular signal-regulated kinase/mitogen-activated protein kinase in the olfactory bulb promotes survival of newly formed granule cells. J Neurosci 25(22):5404-5412.

Miyamichi K, Serizawa S, Kimura HM, Sakano H. 2005. Continuous and overlapping expression domains of odorant receptor genes in the olfactory epithelium determine the dorsal/ventral positioning of glomeruli in the olfactory bulb. J Neurosci 25(14):3586-3592.

Miyasaka N, Morimoto K, Tsubokawa T, Higashijima S, Okamoto H, Yoshihara Y. 2009. From the olfactory bulb to higher brain centers: genetic visualization of secondary olfactory pathways in zebrafish. J Neurosci 29(15):4756-4767.

Miyasaka N, Wanner AA, Li J, Mack-Bucher J, Genoud C, Yoshihara Y, Friedrich RW. 2013. Functional development of the olfactory system in zebrafish. Mech Dev 130(6-8):336-346.

Mombaerts P. 1999. Seven-transmembrane proteins as odorant and chemosensory receptors. Science 286(5440):707-711.

Mombaerts P. 2004. Genes and ligands for odorant, vomeronasal and taste receptors. Nat Rev Neurosci 5(4):263-278.

Mombaerts P, Wang F, Dulac C, Chao SK, Nemes A, Mendelsohn M, Edmondson J, Axel R. 1996. Visualizing an olfactory sensory map. Cell 87(4):675-686.

Moorman S, Mello CV, Bolhuis JJ. 2011. From songs to synapses: Molecular mechanisms of birdsong memory. Bioessays 33:377-385.

Morgan JI, Curran T. 1991. Stimulus-transcription coupling in the nervous system: involvement of the inducible proto-oncogenes fos and jun. Annu Rev Neurosci 14:421-451.

Mori K, Kishi K, Ojima H. 1983. Distribution of dendrites of mitral, displaced mitral, tufted, and granule cells in the rabbit olfactory bulb. J Comp Neurol 219(3):339-355.

Mori K, Nagao H, Yoshihara Y. 1999. The olfactory bulb: coding and processing of odor molecule information. Science 286(5440):711-715.

Mori K, Sakano H. 2011. How Is the Olfactory Map Formed and Interpreted in the Mammalian Brain? Annu Rev Neurosci 34:467-499.

Mueller T, Wullimann MF. 2005. Atlas of early zebrafish brain development: a tool for molecular neurogenetics. Amsterdam: Elsevier Publishing Company.

Mueller T, Wullimann MF. 2009. An evolutionary interpretation of teleostean forebrain anatomy. Brain Behav Evol 74(1):30-42.

Mueller T, Wullimann MF, Guo S. 2008. Early teleostean basal ganglia development visualized by zebrafish Dlx2a, Lhx6, Lhx7, Tbr2 (eomesa), and GAD67 gene expression. J Comp Neurol 507(2):1245-1257.

Murphy LO, Blenis J. 2006. MAPK signal specificity: the right place at the right time. Trends Biochem Sci 31(5):268-275.

Murthy VN. 2011. Olfactory maps in the brain. Annu Rev Neurosci 34:233-258.

Ngai J, Dowling MM, Buck L, Axel R, Chess A. 1993. The family of genes encoding odorant receptors in the channel catfish. Cell 72(5):657-666.

Nicoll RA, Jahr CE. 1982. Self-excitation of olfactory bulb neurones. Nature 296(5856):441-444.

Niessing J, Friedrich RW. 2010. Olfactory pattern classification by discrete neuronal network states. Nature 465(7294):47-52.

Nieuwenhuys R, Meek J. 1998. Holostean and Teleosts. The Central Nervous System of Vertebrates: Springer.

Niimura Y. 2009. Evolutionary dynamics of olfactory receptor genes in chordates: interaction between environments and genomic contents. Hum Genomics 4(2):107-118.

Niimura Y, Nei M. 2005. Evolutionary dynamics of olfactory receptor genes in fishes and tetrapods. Proc Natl Acad Sci U S A 102(17):6039-6044.
Northcutt KV, Lonstein JS. 2009. Social contact elicits immediate-early gene expression in dopaminergic cells of the male prairie vole extended olfactory amygdala. Neuroscience 163(1):9-22.
Northcutt RG. 2006. Connections of the lateral and medial divisions of the goldfish telencephalic pallium. J Comp Neurol 494(6):903-943.
Northcutt RG, Braford MFJ. 1980. New observations on the organization and evolution of the telencephalon of actinopterygian fishes. New York: Plenum Press.
Nowycky MC, Mori K, Shepherd GM. 1981. GABAergic mechanisms of dendrodendritic synapses in isolated turtle olfactory bulb. J Neurophysiol 46(3):639-648.
Oka Y, Korsching SI. 2011. Shared and unique G alpha proteins in the zebrafish versus mammalian senses of taste and smell. Chem Senses 36(4):357-365.
Oka Y, Saraiva LR, Korsching SI. 2012. Crypt neurons express a single V1R-related ora gene. Chem Senses 37(3):219-227.
Oka Y, Saraiva LR, Kwan YY, Korsching SI. 2009. The fifth class of Galpha proteins. Proc Natl Acad Sci U S A 106(5):1484-1489.
Okuyama T, Suehiro Y, Imada H, Shimada A, Naruse K, Takeda H, Kubo T, Takeuchi H. 2011. Induction of c-fos transcription in the medaka brain (Oryzias latipes) in response to mating stimuli. Biochem Biophys Res Commun 404(1):453-457.
Orona E, Scott JW, Rainer EC. 1983. Different granule cell populations innervate superficial and deep regions of the external plexiform layer in rat olfactory bulb. J Comp Neurol 217(2):227-237.
Parrish-Aungst S, Kiyokage E, Szabo G, Yanagawa Y, Shipley MT, Puche AC. 2011. Sensory experience selectively regulates transmitter synthesis enzymes in interglomerular circuits. Brain Res 1382:70-76.
Pfister P, Rodriguez I. 2005. Olfactory expression of a single and highly variable V1r pheromone receptor-like gene in fish species. Proc Natl Acad Sci U S A 102(15):5489-5494.
Pinaud R, Tremere L. 2006. Immediate Early Genes: Springer.
Pinching AJ, Powell TP. 1971. The neuropil of the glomeruli of the olfactory bulb. J Cell Sci 9(2):347-377.
Poo C, Isaacson JS. 2009. Odor representations in olfactory cortex: "sparse" coding, global inhibition, and oscillations. Neuron 62(6):850-861.
Pressler RT, Strowbridge BW. 2006. Blanes cells mediate persistent feedforward inhibition onto granule cells in the olfactory bulb. Neuron 49(6):889-904.
Price JL, Powell TP. 1970a. The mitral and short axon cells of the olfactory bulb. J Cell Sci 7(3):631-651.
Price JL, Powell TP. 1970b. The morphology of the granule cells of the olfactory bulb. J Cell Sci 7(1):91-123.
Price JL, Powell TP. 1970c. The synaptology of the granule cells of the olfactory bulb. J Cell Sci 7(1):125-155.
Ressler KJ, Sullivan SL, Buck LB. 1994. Information coding in the olfactory system: evidence for a stereotyped and highly organized epitope map in the olfactory bulb. Cell 79(7):1245-1255.

Rhein LD, Cagan RH. 1980. Biochemical studies of olfaction: isolation, characterization and odorant binding activity of cilia from rainbowtrout olfactory rosettes. Proc Natl Acad Sci USA 77:4412-4416.
Rink E, Wullimann MF. 2001. The teleostean (zebrafish) dopaminergic system ascending to the subpallium (striatum) is located in the basal diencephalon (posterior tuberculum). Brain Res 889(1-2):316-330.
Rink E, Wullimann MF. 2004. Connections of the ventral telencephalon (subpallium) in the zebrafish (Danio rerio). Brain Res 1011(2):206-220.
Riviere S, Challet L, Fluegge D, Spehr M, Rodriguez I. 2009. Formyl peptide receptor-like proteins are a novel family of vomeronasal chemosensors. Nature 459(7246):574-577.
Rodriguez I, Boehm U. 2008. Pheromone Sensing in Mice. In: Meyerhof W, Korsching S, editors. Chemosensory Systems in Mammals, Fishes, and Insects: Springer.
Ronnett GV, Moon C. 2002. G proteins and olfactory signal transduction. Annu Rev Physiol 64:189-222.
Salin PA, Lledo PM, Vincent JD, Charpak S. 2001. Dendritic glutamate autoreceptors modulate signal processing in rat mitral cells. J Neurophysiol 85(3):1275-1282.
Sandulescu CM, Teow RY, Hale ME, Zhang C. 2011. Onset and dynamic expression of S100 proteins in the olfactory organ and the lateral line system in zebrafish development. Brain Res 1383:120-127.
Saraiva LR, Korsching SI. 2007. A novel olfactory receptor gene family in teleost fish. Genome Res 17(10):1448-1457.
Sato Y, Miyasaka N, Yoshihara Y. 2005. Mutually exclusive glomerular innervation by two distinct types of olfactory sensory neurons revealed in transgenic zebrafish. J Neurosci 25(20):4889-4897.
Sato Y, Miyasaka N, Yoshihara Y. 2007. Hierarchical regulation of odorant receptor gene choice and subsequent axonal projection of olfactory sensory neurons in zebrafish. J Neurosci 27(7):1606-1615.
Satou M. 1990. Synaptic organization, local neuronal circuitry, and functional segregation of the teleost olfactory bulb. Prog Neurobiol 34(2):115-142.
Schlingensiepen KH, Luno K, Brysch W. 1991. High basal expression of the zif/268 immediate early gene in cortical layers IV and VI, in CA1 and in the corpus striatum--an in situ hybridization study. Neurosci Lett 122(1):67-70.
Schneider SP, Scott JW. 1983. Orthodromic response properties of rat olfactory bulb mitral and tufted cells correlate with their projection patterns. J Neurophysiol 50(2):358-378.
Schoenfeld TA, Clancy AN, Forbes WB, Macrides F. 1994. The spatial organization of the peripheral olfactory system of the hamster. Part I: Receptor neuron projections to the main olfactory bulb. Brain Res Bull 34(3):183-210.
Schoenfeld TA, Cleland TA. 2005. The anatomical logic of smell. Trends Neurosci 28(11):620-627.
Schoppa NE, Urban NN. 2003. Dendritic processing within olfactory bulb circuits. Trends Neurosci 26(9):501-506.
Schoppa NE, Westbrook GL. 2001. Glomerulus-specific synchronization of mitral cells in the olfactory bulb. Neuron 31(4):639-651.
Schoppa NE, Westbrook GL. 2002. AMPA autoreceptors drive correlated spiking in olfactory bulb glomeruli. Nat Neurosci 5(11):1194-1202.

Schwob JE. 2002. Neural regeneration and the peripheral olfactory system. Anat Rec 269(1):33-49.
Serizawa S, Miyamichi K, Sakano H. 2004. One neuron-one receptor rule in the mouse olfactory system. Trends Genet 20(12):648-653.
Sheng M, Greenberg ME. 1990. The regulation and function of c-fos and other immediate early genes in the nervous system. Neuron 4(4):477-485.
Shepherd GM, Chen WR, Greer CA. 2004. Olfactory bulb. In: Shepherd GM, editor. The Synaptic Organization of the Brain: Oxford, New York. p 165-216.
Shepherd GM, Chen WR, Willhite D, Migliore M, Greer CA. 2007. The olfactory granule cell: from classical enigma to central role in olfactory processing. Brain Res Rev 55(2):373-382.
Shepherd GM, Greer CA. 2004. The Synaptic Organization of the Brain. In: Shepherd GM, editor. New York: Oxford University Press.
Shi P, Zhang J. 2007. Comparative genomic analysis identifies an evolutionary shift of vomeronasal receptor gene repertoires in the vertebrate transition from water to land. Genome Res 17(2):166-174.
Shi P, Zhang J. 2008. Extraordinary Diversity of Chemosensory Receptor Gene Repertoires Among Vertebrates. In: Meyerhof W, Korsching S, editors. Chemosensory Systems in Mammals, Fishes, and Insects: Springer.
Shipley MT, Ennis M. 1996. Functional organization of olfactory system. J Neurobiol 30(1):123-176.
Shipley MT, Ennis M, Puche A. 2004. Olfactory System. In: Paxinos G, editor. The Rat Nervous System. San Diego: Elsevier Academic Press.
Sorensen PW, Caprio J. 1998. Chemoreception in fish. In: Evans RE, editor. The Physiology of Fishes: CRC Press. p 375-406.
Sorensen PW, Fine JM, Dvornikovs V, Jeffrey CS, Shao F, Wang J, Vrieze LA, Anderson KR, Hoye TR. 2005. Mixture of new sulfated steroids functions as a migratory pheromone in the sea lamprey. Nat Chem Biol 1(6):324-328.
Sorensen PW, Hara TJ, Stacey NE. 1991. Sex pheromones selectively stimulate the medial olfactory tracts of male goldfish. Brain Res 558(2):343-347.
Speca DJ, Lin DM, Sorensen PW, Isacoff EY, Ngai J, Dittman AH. 1999. Functional identification of a goldfish odorant receptor. Neuron 23(3):487-498.
Spehr M, Hatt H, Wetzel CH. 2002. Arachidonic acid plays a role in rat vomeronasal signal transduction. J Neurosci 22(19):8429-8437.
Spehr M, Leinders-Zufall T. 2005. One neuron--multiple receptors: increased complexity in olfactory coding? Sci STKE 2005(285):pe25.
Stacey NE, Kyle AL. 1983. Effects of olfactory tract lesions on sexual and feeding behavior in the goldfish. Physiol Behav 30(4):621-628.
Stacey NE, Sorensen PW. 2005. Hormones, pheromones, and reproductive behaviors. In: Hoar WS, Randall DJ, Farrell AP, editors. Fish Physiology. New York: Academic Press.
Stettler DD, Axel R. 2009. Representations of odor in the piriform cortex. Neuron 63(6):854-864.
Stowers L, Holy TE, Meister M, Dulac C, Koentges G. 2002. Loss of sex discrimination and male-male aggression in mice deficient for TRP2. Science 295(5559):1493-1500.
Strotmann J. 2001. Targeting of olfactory neurons. Cell Mol Life Sci 58(4):531-537.

Sweatt JD. 2001. The neuronal MAP kinase cascade: a biochemical signal integration system subserving synaptic plasticity and memory. J Neurochem 76(1):1-10.

Tabor R, Friedrich RW. 2008. Pharmacological analysis of ionotropic glutamate receptor function in neuronal circuits of the zebrafish olfactory bulb. PLoS One 3(1):e1416.

Tang-Martinez Z. 2001. The mechanisms of kin discrimination and the evolution of kin recognition in vertebrates: a critical re-evaluation. Behavioural Processess 53:21-40.

Taylor SJ, Chae HZ, Rhee SG, Exton JH. 1991. Activation of the beta 1 isozyme of phospholipase C by alpha subunits of the Gq class of G proteins. Nature 350(6318):516-518.

Taziaux M, Keller M, Balthazart J, Bakker J. 2011. Rapid activation of phosphorylated MAPK after sexual stimulation in male mice. NeuroReport 22(6):294-298.

Thompson RJ, Roberts B, Alexander CL, Williams SK, Barnett SC. 2000. Comparison of neuregulin-1 expression in olfactory ensheathing cells, Schwann cells and astrocytes. J Neurosci Res 61(2):172-185.

Thompson RN, Napier A, Wekesa KS. 2006. Attenuation of the production of inositol 1,4,5-trisphosphate in the mouse vomeronasal organ by antibodies against the alphaq/11 subfamily of G-proteins. Chem Senses 31(7):613-619.

Tirindelli R, Dibattista M, Pifferi S, Menini A. 2009. From pheromones to behavior. Physiol Rev 89(3):921-956.

Tirindelli R, Mucignat-Caretta C, Ryba NJ. 1998. Molecular aspects of pheromonal communication via the vomeronasal organ of mammals. Trends Neurosci 21(11):482-486.

Toida K. 2008. Synaptic organization of the olfactory bulb based on chemical coding of neurons. Anat Sci Int 83(4):207-217.

Toida K, Kosaka K, Aika Y, Kosaka T. 2000. Chemically defined neuron groups and their subpopulations in the glomerular layer of the rat main olfactory bulb--IV. Intraglomerular synapses of tyrosine hydroxylase-immunoreactive neurons. Neuroscience 101(1):11-17.

Toida K, Kosaka K, Heizmann CW, Kosaka T. 1998. Chemically defined neuron groups and their subpopulations in the glomerular layer of the rat main olfactory bulb: III. Structural features of calbindin D28K-immunoreactive neurons. J Comp Neurol 392(2):179-198.

Touhara K, Vosshall LB. 2009. Sensing odorants and pheromones with chemosensory receptors. Annu Rev Physiol 71:307-332.

Treloar HB, Feinstein P, Mombaerts P, Greer CA. 2002. Specificity of glomerular targeting by olfactory sensory axons. J Neurosci 22(7):2469-2477.

Vassar R, Chao SK, Sitcheran R, Nunez JM, Vosshall LB, Axel R. 1994. Topographic organization of sensory projections to the olfactory bulb. Cell 79(6):981-991.

Vielma A, Ardiles A, Delgado L, Schmachtenberg O. 2008. The elusive crypt olfactory receptor neuron: evidence for its stimulation by amino acids and cAMP pathway agonists. J Exp Biol 211(Pt 15):2417-2422.

Wachowiak M, Shipley MT. 2006. Coding and synaptic processing of sensory information in the glomerular layer of the olfactory bulb. Semin Cell Dev Biol 17(4):411-423.

Watts AG, Khan AM, Sanchez-Watts G, Salter D, Neuner CM. 2006. Activation in neural networks controlling ingestive behaviors: what does it mean, and how do we map and measure it? Physiol Behav 89(4):501-510.

Weiler E, McCulloch MA, Farbman AI. 1999. Proliferation in the vomeronasal organ of the rat during postnatal development. Eur J Neurosci 11(2):700-711.

Weltzien FA, Hoglund E, Hamdani el H, Doving KB. 2003. Does the lateral bundle of the medial olfactory tract mediate reproductive behavior in male crucian carp? Chem Senses 28(4):293-300.

Weth F, Nadler W, Korsching S. 1996. Nested expression domains for odorant receptors in zebrafish olfactory epithelium. Proc Natl Acad Sci U S A 93(23):13321-13326.

Whitman MC, Greer CA. 2007. Adult-generated neurons exhibit diverse developmental fates. Dev Neurobiol 67(8):1079-1093.

Wiechert MT, Judkewitz B, Riecke H, Friedrich RW. 2010. Mechanisms of pattern decorrelation by recurrent neuronal circuits. Nat Neurosci 13(8):1003-1010.

Wilkie TM, Gilbert DJ, Olsen AS, Chen XN, Amatruda TT, Korenberg JR, Trask BJ, de Jong P, Reed RR, Simon MI, et al. 1992. Evolution of the mammalian G protein alpha subunit multigene family. Nat Genet 1(2):85-91.

Wilson RI, Mainen ZF. 2006. Early events in olfactory processing. Annu Rev Neurosci 29:163-201.

Wullimann MF. 1997. The Central Nervous System. In: Evans DH, editor. Physiology of Fishes: CRC Press. p 245-282.

Wullimann MF. 2009. Secondary neurogenesis and telencephalic organization in zebrafish and mice: a brief review. Integr Zool 4(1):123-133.

Wullimann MF, Mueller T. 2004. Teleostean and mammalian forebrains contrasted: Evidence from genes to behavior. J Comp Neurol 475(2):143-162.

Wullimann MF, Rupp B, Reichert H. 1996. Neuroanatomy of the Zebrafish Brain. A Topological Atlas Basel: Birkhäuser Verlag.

Yaksi E, Judkewitz B, Friedrich RW. 2007. Topological reorganization of odor representations in the olfactory bulb. PLoS Biol 5(7):e178.

Yaksi E, von Saint Paul F, Niessing J, Bundschuh ST, Friedrich RW. 2009. Transformation of odor representations in target areas of the olfactory bulb. Nat Neurosci 12(4):474-482.

Yamamoto K, Ruuskanen JO, Wullimann MF, Vernier P. 2011. Differential expression of dopaminergic cell markers in the adult zebrafish forebrain. J Comp Neurol 519(3):576-598.

Yamamoto N, Ito H. 2000. Afferent sources to the ganglion of the terminal nerve in teleosts. J Comp Neurol 428(2):355-375.

Yoshihara Y. 2008. Molecular Genetic Dissection of the Zebrafish Olfactory System. In: Meyerhof W, Korsching S, editors. Chemosensory Systems in Mammals, Fishes, and Insects: Springer.

Zeiske E, Theisen B, Bruecker H. 1992. Structure, development, and evolutionary aspects of the peripheral olfactory system In: Hara TJ, editor. Fish Chemoreception. London: Chapman and Hall. p 13-39.

Zhang JJ, Okutani F, Inoue S, Kaba H. 2003. Activation of the mitogen-activated protein kinase/extracellular signal-regulated kinase signaling pathway leading to cyclic AMP response element-binding protein phosphorylation is required for the long-term facilitation process of aversive olfactory learning in young rats. Neuroscience 121(1):9-16.

Zhang X, Firestein S. 2002. The olfactory receptor gene superfamily of the mouse. Nat Neurosci 5(2):124-133.

Zhang X, Firestein S. 2008. Genomics of Olfactory Receptors. In: Meyerhof W, Korsching S, editors. Chemosensory Systems in Mammals, Fishes, and Insects: Springer.

Zou Z, Horowitz LF, Montmayeur JP, Snapper S, Buck LB. 2001. Genetic tracing reveals a stereotyped sensory map in the olfactory cortex. Nature 414(6860):173-179.

Zou Z, Li F, Buck LB. 2005. Odor maps in the olfactory cortex. Proc Natl Acad Sci U S A 102(21):7724-7729.

Zufall F. 2005. The TRPC2 ion channel and pheromone sensing in the accessory olfactory system. Naunyn Schmiedebergs Arch Pharmacol 371(4):245-250.

Zufall F, Munger SD. 2010. Receptor guanylyl cyclases in mammalian olfactory function. Mol Cell Biochem 334(1-2):191-197.

Publications

Kress S, Wullimann MF, J Chem Neuroanat. 2012 Dec;46(1-2):51-66
“Correlated basal expression of immediate early gene *egr1* and tyrosine hydroxylase in zebrafish brain and downregulation in olfactory bulb after transitory olfactory deprivation”

Hinz C, Kobbenbring S, Kress S, Sigman L, Mueller A, Gerlach G, Animal Behaviour 2013 May;85(1-6)
“Kin recognition in zebrafish, *Danio rerio*, is based on imprinting on olfactory and visual stimuli”

Kress S, Biechl D, Wullimann MF, Brain Struct Funct. 2014 Apr;13
“Combinatorial analysis of calcium-binding proteins in larval and adult zebrafish primary olfactory system identifies differential olfactory bulb glomerular projection fields”

Eidesstattliche Erklärung

Ich versichere hiermit an Eides statt, dass die vorliegende Dissertation von mir selbstständig und nur mit den angegebenen Hilfsmitteln angefertigt wurde.

München, den……..... ……..

(Unterschrift)